AHMED, TAREK HUSSEIN

AN EXPERIMENTAL STUDY OF CRUDE OIL RECOVERY BY HIGH PRESSURE NITROGEN INJECTION

The University of Oklahoma PH.D. 1980

THE UNIVERSITY OF OKLAHOMA

GRADUATE COLLEGE

AN EXPERIMENTAL STUDY OF CRUDE OIL RECOVERY BY HIGH PRESSURE NITROGEN INJECTION

A DISSERTATION

SUBMITTED TO THE GRADUATE FACULTY

in partial fulfillment of the requirements for the

degree of

DOCTOR OF PHILOSOPHY

BY

TAREK H. AHMED

Norman, Oklahoma

1980

AN EXPERIMENTAL STUDY OF CRUDE OIL RECOVERY

BY HIGH PRESSURE NITROGEN INJECTION

APPROVED BY

D E Menzie

DISSERTATION COMMITTEE

AN EXPERIMENTAL STUDY OF CRUDE OIL RECOVERY

BY HIGH PRESSURE NITROGEN INJECTION

BY: Tarek H. Ahmed

MAJOR PROFESSOR: Dr. Donald E. Menzie

ABSTRACT

AN EXPERIMENTAL STUDY OF CRUDE OIL RECOVERY

BY HIGH PRESSURE NITROGEN INJECTION

The objectives of this study were to investigate the:

1. Compositional changes taking place during the displacing of crude oil by continuous high pressure nitrogen injection.

2. Changes in the properties of the liquid and vapor phases.

3. Miscible pressures for nitrogen displacement.

4. Distance from the injection point at which the miscibility will be achieved.

The experiments were conducted in a low permeability, consolidated, sand-packed, stainless steel tube 125 feet long and 0.45 inches in diameter. Five sampling points were located at equal intervals along the length of the linear core. Vapor samples were collected periodically from the sampling valves and analyzed by the gas chromatograph.

The results of this experimental investigation showed the compositional distribution of the vapor phase throughout the core during the nitrogen injection process. The mechanism of the nitrogen displacement process was analyzed and the fronts formed during the oil recovery experiments were recorded and studied in order to better understand the overall recovery mechanism.

ACKNOWLEDGEMENTS

The author wishes to express his sincere appreciation to the many people who helped make this work possible. Special appreciation is given to Dr. D. E. Menzie, who served as an advisor in this research, for his continued support, interest and guidance in the completion of this effort.

Appreciation is also extended to the members of my doctoral committee; Dr. H. B. Crichlow, Dr. F. M. Townsend, Dr. B. Foote, and Dr. A. W. McCray.

Special thanks is extended to Mr. N. S. Knight for his help and superb craftsmanship in the design and construction of certain specialized equipment.

I also wish to express my thanks to Mrs. Carol Wedel for her superb typing ability.

Thanks is given to Patrick, Susan and Shanna for their help, and appreciation is also expressed to the Egyptian Government, Tenneco Oil Company, and the E.R.C.

Finally, and most importantly, I would like to express my appreciation to my Father, General Hussein Ahmed, for his continued encouragement, understanding and support throughout the entire program of advanced study leading to this work.

TABLE OF CONTENTS

TABLE OF CONTENTS (continued)

TABLE OF CONTENTS (continued)

LIST OF TABLES

LIST OF FIGURES

LIST OF FIGURES (continued)

LIST OF FIGURES (continued)

LIST OF FIGURES (continued)

LIST OF FIGURES (continued)

LIST OF FIGURES (continued)

LIST OF FIGURES (continued)

AN EXPERIMENTAL STUDY OF CRUDE OIL RECOVERY BY HIGH PRESSURE NITROGEN INJECTION

CHAPTER I

INTRODUCTION

Petroleum engineers are frequently faced with the problem of predicting what will happen if a dry or rich gas is injected into a reservoir. One aspect of this problem is predicting the phase changes taking place during the displacing process.

The high pressure gas injection process was first proposed by Whorton, et al.,[1] and was one of several miscible displacement processes developed for the purpose of displacing all of the oil contained within the contacted area of a reservoir.

One method which has been used to increase oil recovery is the maintenance of reservoir pressure by the injection of gas. Part of the beneficial effect resulting from this gas injection was to prevent evolution of the gas which was disolved in the reservoir oil. This evolution would cause the oil to shrink and become more viscous, thereby adversely affecting oil recovery. In dealing with multiphase systems, it is necessary to consider the effect of the forces acting

at the interface when two immiscible fluids are in contact. When these two fluids are liquid and gas, the interface is normally referred to as the liquid surface.[2] All molecules are attracted one to the other in proportion to the product of their masses and inversely as the square of the distance between them. Considering water and oil, fluids commonly found in petroleum reservoirs, it is found that an interfacial tension always exists between the fluids. A molecule at the interface has a force acting upon it from the oil lying immediately above the interface and water molecules lying below the interface. The resulting forces are unbalanced and give rise to interfacial tension. A certain amount of work is required to move a water molecule from within the body of the liquid through the interface. This work is frequently referred to as the free surface energy of the liquid. Free surface energy may be defined as the work necessary to create a unit area of new surface.

The interfacial tension is the force per unit length required to create a new surface. The combination of all the active surface forces determines the wettability and capillary pressure of a porus rock. The distribution of the liquid in a porous system is dependent upon the wetting characteristics. The wetting fluid tends to occupy the smaller interstics of the rock and the nonwetting fluid occupies the more open channels. Reservoir engineers and scientists have long recognized the importance of the role that capillary and interfacial forces play in controlling the efficiency of

recovery mechanisms. These forces cause the retention of oil in the reservoir matrix and they control fluid movement.

A residual oil saturation remains in the rock during displacement by water or gas was studied in detail by Clark, et al.[2] They showed that water drive recovery is expected to be greater than gas drive recovery when reservoir conditions are the same. The expected recovery by water drive ranges from 60 to 80 per cent while recovery by gas drive ranges from 30 to 80 per cent. Displacement of oil by gas differs considerably from displacement by water. Gas has a lower viscosity than oil and exists in pore spaces as a nonwetting phase. It tends to move ahead of the oil in the center of the pore channel, leaving behind droplets of oil as residual saturation. The wide range of gas drive recovery expectancy results from variations in such factors as sand permeability, oil viscosity, and injection pressure.

Recognizing that 100 per cent displacement efficiency requires the elimination of the interfacial forces between the displacing and displaced fluids, researchers studied various approaches to the achievement of miscible displacement. One can group the various miscible displacement processes into two natural divisions: those processes in which miscibility already exists between the displaced and displacing fluids and those in which the injected fluid is not miscible with the oil, but by some process in the reservoir it develops the required miscible displacement. The propane or miscible slug process[3,4] is an

example of the former.

Propane as a liquid is already miscible with the reservoir oil. The high pressure gas process[5-9] and the enriched gas drive[10,11] are members of the second class of processes. In these latter processes the gas injected is not miscible with the reservoir oil, but when it is brought into intimate contact with the oil in the reservoir pores, a miscible displacement will be developed under certain injection pressure.

The object of this study was to conduct an experimental investigation directed toward a relatively new process of oil recovery by high pressure nitrogen injection.

CHAPTER II

STATEMENT OF THE PROBLEM

Miscible displacement processes have generally been recognized by the petroleum industry as an important enhanced oil recovery method. Very recently,[7,8] nitrogen flooding has become an attractive material for economically enhancing oil recovery. No previous studies have been undertaken to directly observe miscibility conditions during their development in an oil reservoir. The primary objective of this work was to initiate an experimental investigation of the mechanisms through which miscibility could be achieved in a reservoir model undergoing high pressure nitrogen injection.

Other objectives of this study were to investigate the:

1. Compositional changes taking place during displacing of crude oil by continuous high pressure nitrogen injection.

2. Change in properties of the liquid and vapor phases during the nitrogen injection.

3. Miscible pressures for nitrogen displacement.

4. Distance from the injection point at which the miscibility would be achieved.

In order to accomplish these objectives, the experiments were conducted in a low permeability, consolidated, sand-packed

stainless steel tube 125 feet long and .435 inches in diameter. Five sampling points were located at equal intervals along the length of the linear core. The design of these sampling points enables one to take samples of vapor under high pressure for analysis by the gas chromatograph.

The results of this experimental investigation showed the compositional distribution of the vapor phase throughout the core during the nitrogen injection process. The mechanism of the nitrogen displacement process was analyzed and the fronts formed during the oil recovery experiments were recorded and studied in order to better understand the overall recovery mechanism.

CHAPTER III

LITERATURE REVIEW

High Pressure Gas Injection

Laboratory Studies

The reinjection of natural gas was probably the first process suggested for improving the recovery of oil. There are records indicating that gas injection was employed for this purpose prior to 1900.[12,13]

These early applications were designed to increase the immediate productivity and so should be classified as pressure maintenance projects. Growth in the technology of gas injection has relied on developments in miscible flooding by high pressure gas displacement.

Slobod, et al.,[5] divided the high-pressure gas sweeps into two basic processes:

i) Displacement in which the phases in equilibrium at the front were essentially immiscible (type I).

ii) Displacement in which the injected gas became sufficiently enriched that, at the front, it was completely miscible with the reservoir fluid (type M).

Whether a given case was type I or type M would depend mainly upon the composition of reservoir fluid and the injection

pressure. They concluded that the intermediates (largely C_2 through C_6) were the main materials involved in this exchange of hydrocarbon between the injected gas and the reservoir fluid, which in turn worked in the direction of making the displacing and displaced phase more alike, and results in a more efficient displacement.

Whorton, et al.,[1] conducted an experimental investigation on sandstone cores to study the mechanism of displacing reservoir fluids by high pressure gas injection. The authors reported a recovery up to approximately 90 percent of the oil in place could be obtained. The authors illustrated that recoveries were improved by:

1. high injection pressures,

2. high concentration of intermediates in the injected gas or the displaced oil, and

3. undersaturation of the reservoir oil at the pressure of displacement.

The authors concluded that the displacement mechanism was controlled by the higher mutual solubility of the phases at the higher pressures with the attendant effect of reduction in the difference in viscosity between the displaced and the displacing phase.

Koch, et al.,[14] investigated the misible flooding by high pressure gas injection. The authors discussed the process in which miscibility was developed at the displacement front by the evaporation of intermediates from the oil phase into the

gas phase. The authors also reached the conclusion that the recovery at breakthrough was a function of pressure only up to the miscibility pressure. Once miscibility was reached, no noticeable increase in breakthrough recovery was achieved by increasing the pressure. They also stated that the high pressure miscible gas process was applicable only with reservoir fluids which contain a high concentration of intermediates.

Rutherford[20] pointed out that asphaltene deposition had no important effect on the result of his experimental displacement of oil by light hydrocarbons.

Koch[15] indicated that reservoir fluids having over 30 percent (C_2-C_6) and a C_{7+} fraction whose molecular weight is less than 240 should be a good prospect for high pressure miscible gas displacement. The author also pointed out that the reservoir fluid should be undersaturated in order to achieve a proper exchange of C_2-C_6 components with the injected gas.

Cook, et al.,[18] conducted an experimental investigation on the recovery of oil by the cycling of natural gas. The authors stated that the amount of oil vaporized during the injection process was a function of the pressure, temperature, volatility of the oil (as indicated by oil gravity), and the amount of gas cycled. They also found that any increase in each of these conditions was accompanied by an increase in the volume of the vaporized oil, and concluded that vaporization could play an important role in a high percentage of oil recovery.

Blackwell, et al.,[17] studied the factors influencing the efficiency of miscible displacement. They found the formation of channels in their reservoir models was mainly due to viscous fingering, gravity segregation, and variation in permeability. The authors also pointed out that with adverse mobility ratios, the diffusion would not be effective in preventing the channels and growth of fingers, even in homogeneous sand.

High Pressure Gas Projects

Two of the largest field applications of high pressure gas injection have been at University Block 31, in Texas, and the Hassi-Messaoud in Algeria.

A high-pressure miscible injection project was initiated in the Block 31 field, Texas, in 1949.[24,25] In 1969, it was estimated that 60 per cent of the oil-in-place would be recovered by this project. Several factors contributed to the success of the project:

1. The project was begun early in the life of the reservoir.
2. The formation rock was continuous and homogeneous.
3. Close engineering control over the project ensured miscible displacement and maximum sweep efficiency.

The Hassi-Messaoud[26] high-pressure gas injection project in Algeria is the only reported miscible flood outside North America. The project commenced in 1964 and entails maintaining the reservoir pressure at about 4500 psi in part of the pool

by the injection of produced solution gas which was found to be miscible with the reservoir oil when contacted with it at a pressure above 3700 psi.

By January 1970, 330 x 10^9 scf of gas was injected, sweeping an estimated 13 per cent pore volume of the pool and 20 per cent pore volume of the area enclosed by drilled wells.

The significance of this project is the successful use of high pressure gas miscibility to improve recovery from a very complex reservoir of highly variable permeability.

Condensing Gas-Drive Process (Enriched Gas Drive)

Laboratory Studies

Laboratory studies have shown that extremely high recoveries, sometimes approaching 100 per cent, can be obtained by using a condensing gas as the injected fluid. A condensing gas is defined as a gas which is appreciably soluble in the reservoir oil. The reservoir oil volume is increased considerably by the condensing gas phase going into solution in the oil, which materially increases the effective oil permeability.

Stone and Crump[16] studied the effect of gas composition upon oil recovery while holding the reservoir pressure constant. Their experimental results are shown in Figure 3-1. Stone and Crump[3] stated that the use of a condensing gas drive to displace oil from a reservoir would result in a greater oil recovery than an equilibrium gas drive. The authors believed that the

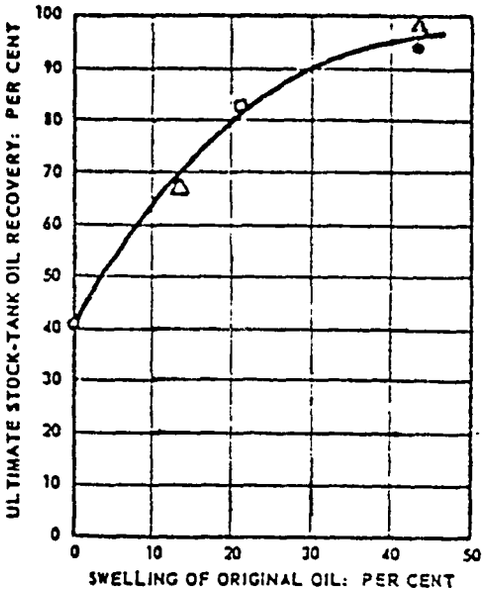

Figure 3-1. EFFECT OF OIL SWELLING ON OIL RECOVERY
(After Stone, et al.,[16] courtesy of the SPE of AIME)

increased recovery was a result of a solution of the injected gas both at the invading gas front and behind this front. They explained that the gas condensation at the front tends to retard invasion of the oil-saturated portion of the reservoir by the displacing gas, since it swells the oil phase at that point, and also dissolves the leading fingers of the gas phase. At the same time the swelling of the oil lowers the viscosity of that phase, and this effect favors more efficient displacement of the oil.

Benham, et al.,[3] found that the controlling factors for attainment of miscibility were the C_{2+} content of the reservoir fluid and the C_{5+} content of the displacing fluid.

Wilson[19] conducted a combination of flow experiments and equilibrium phase-behavior measurements on miscible displacement by enriched gas. The author concluded that the ternary phase diagram was a reliable guide for predicting the conditions required for miscibility in a flowing system of considerable complexity.

Arnold, et al.,[21] reported that a small bank of an oil-miscible gas driven by methane could displace all of the oil contacted in a piston-like manner. The authors concluded that the displacement with an oil-miscible bank offered the following advantages over displacement oil with an immiscible bank: (a) oil recovery was greater, (b) total gas injection for ultimate recovery was less, and (c) in long flow systems, smaller minimum bank size and smaller quantities of enriching materials were required.

Condensing Gas Drive Projects

The Seeligson (Zone 20B-07)[28] enriched gas project was intiated in 1957. The pool is a thin stratified sand encountered at approximately 6,000 feet. It contains approximately 877 productive acres and has 16 wells. The average sand thickness is about 12 feet with a maximum thickness of 42 feet in the center of the field.

Reservoir oil was saturated at the original reservoir pressure of 3,010 psi. Gravity of the produced crude oil is 40° API. The field originally contained 7.4 million STB. The injected gas is composed of 44.5% methane, 4% ethane, and 50.5% propane with the rest being butane and heavier components. The mobility ratio was twelve. About 50% of the original oil was recovered, compared with an expected 22% for primary and about 45% for a water flood.

It was concluded that the displacement efficiency was 100% in the swept zones but the vertical and areal conformance was below that expected owing to reservoir heterogeneity, gravity override and viscous fingering.

The Ante Creek Field in Alberta,[29] Canada, is an 11,000 foot deep pool containing originally 37 million STB of oil. The most notable reservoir properties are a low viscosity of 0.13 cp and a high initial pressure of 5170 psi.

A miscible recovery project was initiated in June 1968. Plant residue gas containing approximately 67 per cent methane plus nitrogen and 33 per cent (C_2-C_6) fraction was injected

into three wells, essentially all components were miscible at pressures above 3900 psi. The estimated recovery was 61 per cent.

Liquid Petroleum Gas (LPG) Slug Drive

Laboratory Studies

In miscible slug injection, a slug or bank of LPG or propane is driven by dry gas or water through the reservoir. This slug miscibly displaces the reservoir oil from the swept portions of the reservoir. At pressures above 1100 psi, the LPG is also miscible with the driving gas.[30]

The quantity of LPG required to maintain miscibility conditions is an important factor in the economics of miscible flooding. In the case of low solvent (LPG) content, miscibility is lost when the bank of LPG deteriorates. At that point, the displacement will become immiscible rather than miscible, and recovery will drop accordingly.

Hutchinson, et al.,[6] stated that miscibility cannot be regenerated once it is lost through the breakdown of the slug from dispersion.

Craig, et al.,[30] found that factors such as: (1) rock permeability, (2) displacement rate, (3) reservoir viscosity, (4) distance between the injection and producing well, and (5) diffusion rate would determine the extent of mixing at solvent-crude oil interface and the solvent-driving gas interface. The authors also stated that the mixing would tend to occur longitudinally in the direction of flow.

Koch, et al.,[31] pointed out that factors controlling the size of the LPG slug were: (1) reservoir length, (2) reservoir fluid composition, and (3) reservoir pressure at the displacement front.

Lacey, et al.,[32] claimed that small banks of LPG (5 per cent HPV or less) were not effective in increasing oil recovery in horizontal reservoirs. Instead, where small banks were used, the driving gas quickly penetrates the LPG bank because of fingering and channeling, and from this point on, the process behaved essentially as an immiscible gas-injection project. The authors also claimed that their conclusion was substantiated by: (1) laboratory studies of the effect of rate, model size and mobility ratio on miscible displacement in areal models, and (2) calculation of field recovery, which compared closely with actual field recovery.

LPG Slug Drive Projects

In 1957, a miscible slug project was started in Parks Field, Texas, in the Pennsylvanian Bend reservoir.[33] A slug of propane (4 per cent of the total hydrocarbon pore volume) was injected followed by dry gas. In 1961, Marrs[35] estimated that 17 per cent by primary means would be increased to 55 per cent.

Carbon Dioxide Injection

Laboratory Studies

Carbon dioxide is known to be highly soluble in crude oils, and in water at reservoir pressures and temperatures,

which causes a (1) reduction in oil viscosities, and (2) an appreciable swelling of crude oil. Both of these factors will increase oil recovery.

Carbon dioxide flooding can be carried out in one of three ways:

1. injection of carbonated water,

2. injection of a small slug of pure liquid CO_2 followed by water, and

3. miscible CO_2 flooding.

Holm[34] showed that water driven CO_2 banks or carbonated water could improve the oil recovery by a factor of 50 per cent to 100 per cent when compared to water flood and immiscible gas injection. Holm concluded from long core displacement tests that a CO_2 bank of about 5 per cent HPV followed by water would give a more favorable oil recovery than would the same volume of CO_2 dissolved in a water bank.

Simon, et al.,[35] claimed that injection of CO_2 with a pressure of 800 psi in their reservoir model caused 20 to 90 per cent reduction in oil viscosities and swelling up to 50 per cent of the crude oil.

Menzie, et al.,[37] found that the injected carbon dioxide could reach equilibrium conditions within a short time and that condensate was recovered by vaporization.

Holm[34] reported that a bank of light hydrocarbons (vaporization of crude oil) was formed by the CO_2-carbonated water flood. Beeson[36] and Holm[34] claimed that significant

swelling and viscosity reduction would not be achieved unless the injection pressure was above 800 psi.

Carbon Dioxide Injection Projects

The Mead-Strawn Field[38] pilot project was conducted to test the effectiveness of carbon dioxide as an oil recovery agent in a primary-depleted reservoir. The process consisted of injection of a small slug of CO_2 (4 per cent p.v), followed by a slug of carbonated water (12 per cent p.v), and then brine. Prior to CO_2 injection, water was injected to raise the reservoir pressure in the test area from about 115 to 850 psi; the objective was to maintain the average reservoir pressure at a minimum of 850 psi throughout the test to ensure maximum effectiveness of the CO_2.. The formation volume factor and oil viscosity were 1.12 and 1.3 cp, respectively, at the start of the CO_2 flood. Carbonation changed these values to 1.25 and 0.58 cp.

The Mead-Strawn test flood showed that over 50 per cent more oil was produced by the CO_2-carbonated water flood than by the conventional water flood, confirming results obtained from laboratory studies of the oil-recovery process.

CHAPTER IV

MISCIBILITY RELATIONSHIPS IN THE DISPLACEMENT OF OIL BY NITROGEN

Miscibility exists when two fluids are able to mix in all proportions without any interface forming between them. Miscibility is controlled by the pressure and temperature, the composition of the oil, and the composition of the displacing fluid. The triangular phase diagram is often used as an aid in understanding the miscibility process for complex hydrocarbon mixtures.

Representation of Miscible Displacement by Nitrogen on Triangular Diagram

A triangular diagram was first proposed by J. Willard Gibbs[39] to present phase relations of a three pure-component system. Since then, it has been used extensively for liquid-liquid, liquid-solid, and gas-liquid systems.

As it was reviewed by Slobod, et al.,[5] let us examine briefly the information which is given on a triangular diagram such as shown in Figure 4-1. Any point within the triangle represents a system with a specific composition made up of definite amounts of N_2 (nitrogen), C_m (intermediates, mainly methane through hexane), and C_{7+} (heptanes and heavior hydrocarbons).

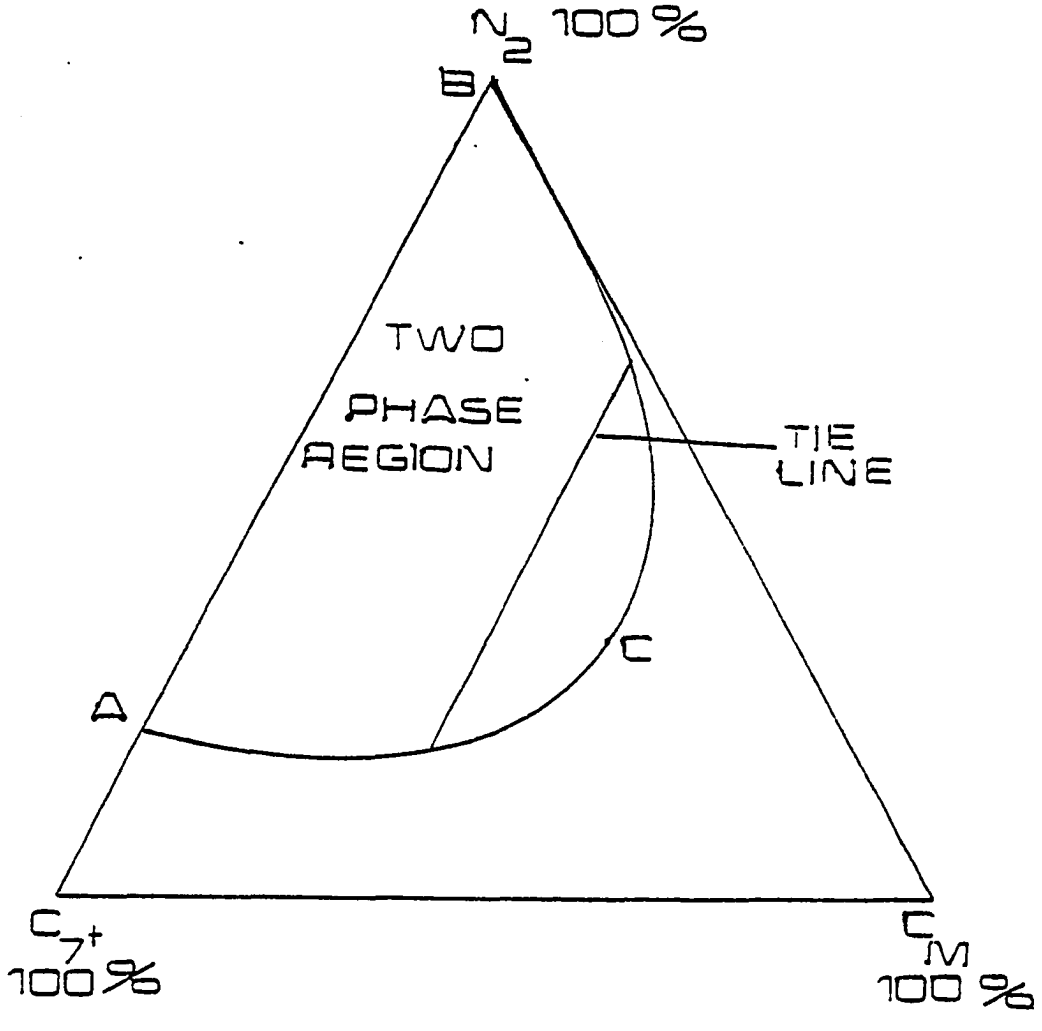

Figure 4-1. THREE-COMPONENT PRESENTATION OF MULTI-COMPONENT SYSTEM, TEMPERATURE AND PRESSURE CONSTANT

The phase boundary curve ACB on the diagram separates the single-phase and two-phase regions. At the pressure and temperature given, any system of the three components whose composition is inside this curve will form two phases. Any system outside this curve will be in a single phase at equilibrium.

The lower part of the curve is the bubble point line AC and gives the liquid phase composition of any two phase system. The upper part of the curve is a dew-point line CB and gives the gas phase composition of the two-phase system.

The lines that connect gas- and liquid-phase composition that are in equilibrium with each other are called tie lines. Any system composition along a tie line will break into two phase with composition given by the ends of that tie line. The bubble and dew points meet at the plait point, C, where the liquid and gas phases become identical.

With this diagram one needs only to know the compositions of the displacing and the displaced phase to define the initial type of displacement. If a line is drawn between the points representing the composition of the two phases and passes through the two phase region, the gas and reservoir oil will not be miscible.

Available published information on oil displacement by nitrogen injection is limited to five papers.[7-9,14,40]

Figures 4-2 through 4-5 show ternary composition diagrams from the work of Rushing, et al.[7-9] The three-

component system shown consists of nitrogen (N_2), the intermediates (C_1 through C_6) and all hydrocarbons heavier than C_6 (C_{7+}).

The stepwise process of oil displacement by continuous nitrogen injection can be shown in Figure 4-2. As nitrogen is injected and comes in contact with crude oil, a mass exchange of components in the gas and oil occurs as the two phases tend to come to equilibrium (point R_1) in the presence of each other.

This point which is lying in the two phase region represents the overall composition of the liquid and gas phase in contact. Assuming equilibrium occurs, the oil composition changes to composition L_1, and the gas composition changes to composition G_1. It can be seen that crude oil has lost both in intermediate components (C_1-C_6) and heavy components (C_{7+}) while nitrogen has absorbed these components. More nitrogen, coming from behind, contacts the remaining oil (with composition L_1) in the displacement process, and, when equilibrium occurs, at point R_2, this oil-L_1 composition changes to L_2 composition and the displacing phase to G_2 composition.

After several consecutive steps of nitrogen contacting the remaining oil, additional oil components vaporize until the oil composition becomes L_5 and the displacing nitrogen becomes G_5 when equilibrium occurs.

Because of the high mobility of gas, gas of composition G_1 (which is rich in the intermediate components) formed by

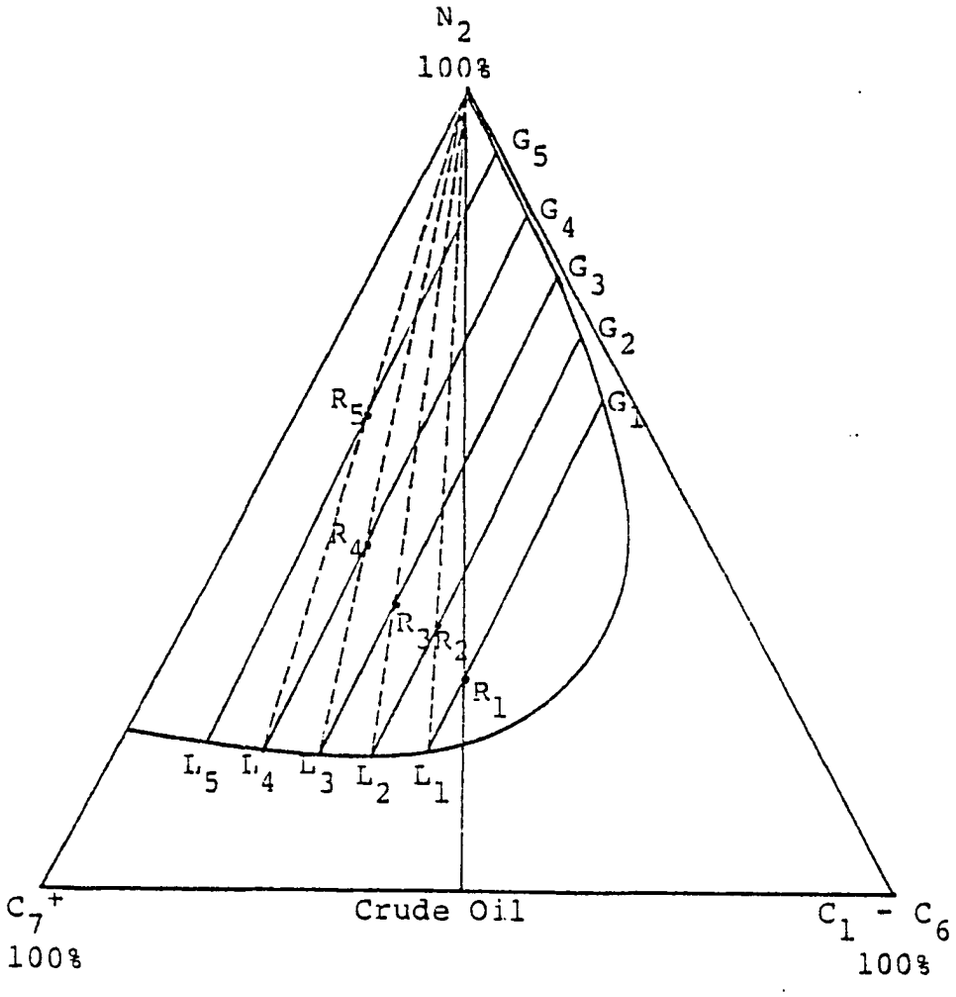

Figure 4-2. TRIANGULAR GRAPH SHOWING CHANGES IN COMPOSITION OF CRUDE OIL (After Rushing, et al.,[7-9] courtesy of the SPE of AIME)

contact of nitrogen and virgin oil, moves ahead and contacts more of the original oil in place. As it is seen in Figure 4-3, an equilibrium point R_2 is established. Again, gas with composition G_2 moves faster than the formed oil of composition L_2 and contacts more virgin oil, as a result, a new equilibrium point R_3 is established. The quantity of intermediate and heavy components in the gas varies and gets greater as the gas moves further into the oil in the displacement process. This enrichening process causes the oil to get leaner of intermediates in the areas through which most gas has moved.

Figure 4-4 is similar to Figure 4-3 but contains a family of curves representing the effect of pressure on miscibility in high pressure nitrogen injection. Phase boundary curves for pressures P_1, P_2, and P_3 are labeled. As shown in Figure 4-3, at higher pressures, the boundary curves move to the left so that at pressure P_3 the composition of crude oil is such that a miscible displacement will occur.

The importance of the crude oil composition can be shown in Figure 4-5. Crude B is more favorable for miscible type displacement than crude A since it contains more intermediate components and is closer to the critical point. A faster establishment of miscible displacement occurs with crude B than with crude A.

It is important now to review briefly the results of the experiments conducted by Rushing, et al.,[7-9] McNeese,[40] and Koch, et al.[14]

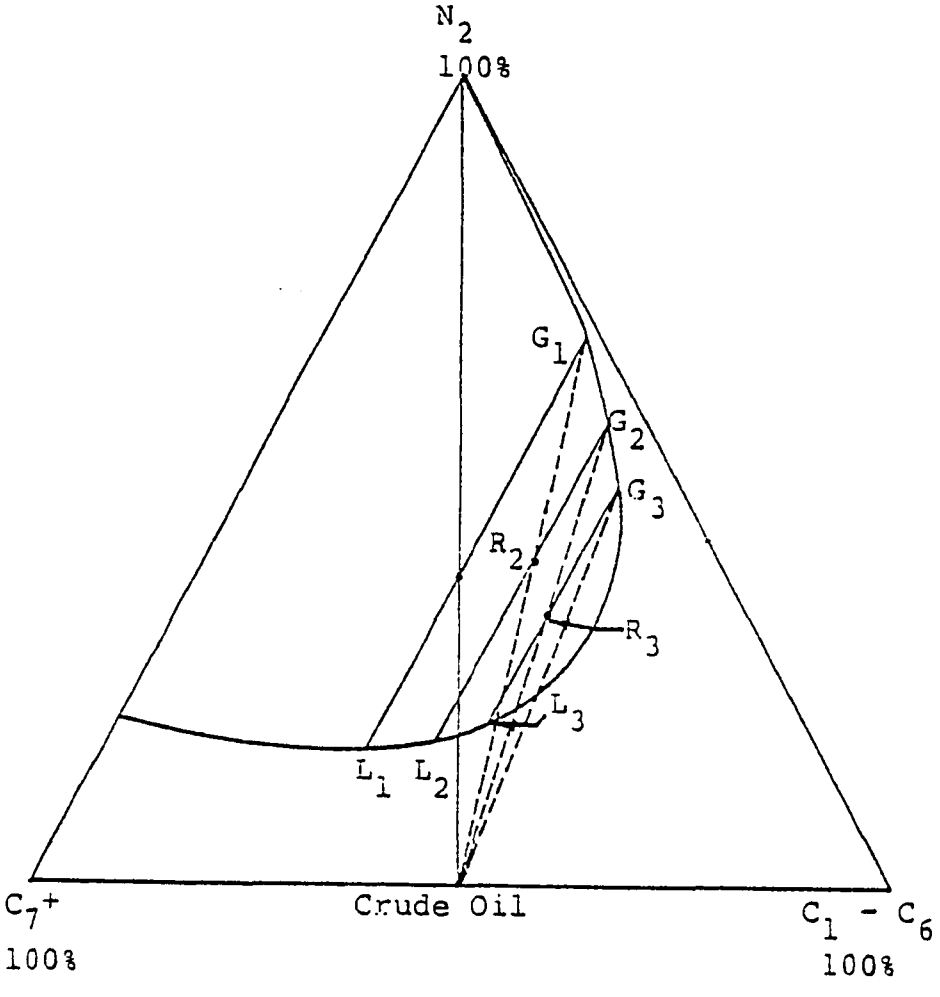

Figure 4-3. TRIANGULAR GRAPH SHOWING CHANGES IN COMPOSITION OF NITROGEN (After Rushing, et al.,[7-9] courtesy of the SPE of AIME)

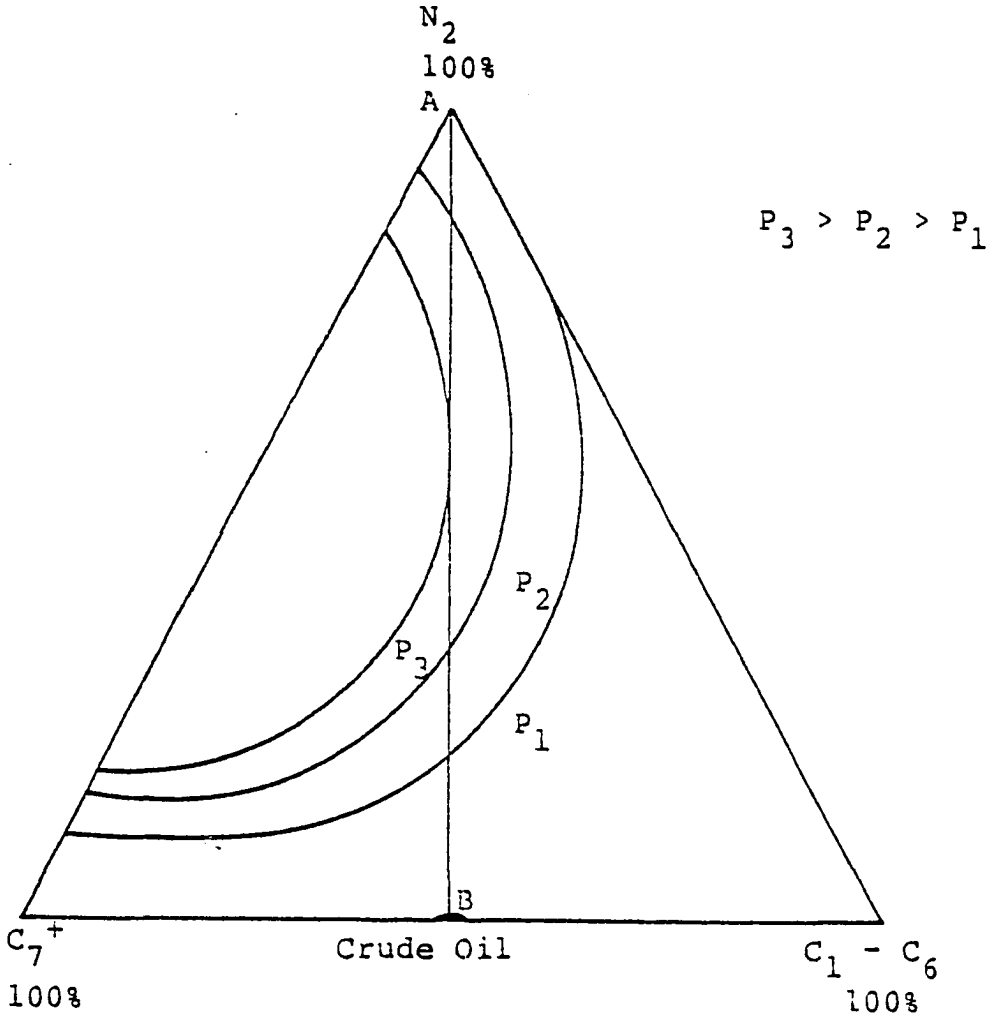

Figure 4-4. TRIANGULAR DIAGRAM SHOWING THE EFFECT OF PRESSURE ON THE PHASE ENVELOPE (After Rushing, et al.,[7-9] courtesy of the SPE of AIME)

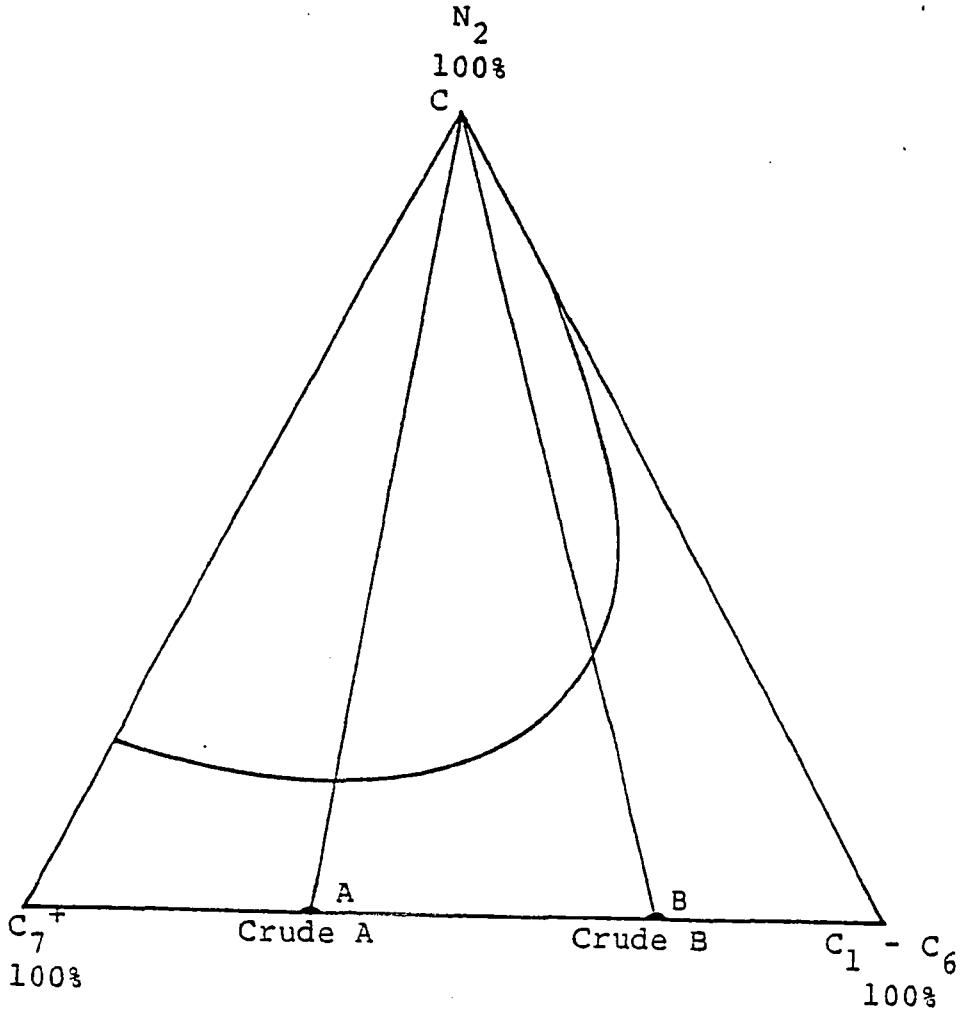

Figure 4-5. INITIAL CRUDE COMPOSITION VS. PHASE ENVELOPE
(After Rushing, et al.,[7-9] courtesy of the SPE of AIME)

Research of Rushing, et al.[7-9]

The authors conducted an experimental investigation to study mainly the pressure on oil recovery by nitrogen flooding. Their reservoir model was a 40 foot stainless steel tube of 0.2 inch inside diameter. The coiled tube was packed with 140-200 mesh sieved manufactured glass beads. Tests were made on a 54.4 gravity crude containing 700 scf/bbl. Oil recovery ranged from 65 per cent of oil originally in place at 3000 psig to 92.8 per cent of oil originally in place at a run pressure of 5000 psig. They concluded that nitrogen could be used for miscible displacement in oil reservoirs.

Research of Koch and Hutchinson

Koch and Hutchinson[14] reported a number of laboratory tests on displacement of oil by nitrogen, natural gas and some mixtures of nitrogen and natural gas. Table 4-1 shows the results of Koch, et al.[14]

The authors conducted their experiments on a 143 foot unconsolidated sand packed column as their reservoir model. Four gases of different composition were used, mainly 100 per cent nitrogen, 100 per cent lean gas (85 per cent C_1, 15 per cent C_2), and two mixtures of the foregoing gases (one 15 per cent nitrogen, the other 66 per cent nitrogen). They reported the miscibility pressure for 100 per cent nitrogen was found to be 3,870 psi. This was only 370 psi greater than the 3,500 psi miscibility pressure determined for 100 per cent lean gas. They also claimed that the miscibility pressure only increased

TABLE 4-1

THE EXPERIMENTAL RESULTS OF KOCH, et al.[14]

Run No.	Injection Gas Composition % N_2	Injection Pressure Psi	Stock Tank Oil Recovery % of OIP Initially	
			At Breakthrough	Ultimate
L-44	15	3500	68.0	77.5
L-45	15	3600	74.0	82.9
L-46	15	3700	80.4	86.0
L-42	66	3500	67.3	76.5
L-41	66	3700	77.9	87.3
L-40	100	2900	49.2	59.6
L-38	100	3500	67.2	69.4
L-37	100	3800	77.6	83.6
L-39	100	4000	80.6	83.2
L-32	100	4300	80.6	84.7

from 3,700 psi to 3,730 psi when the nitrogen content of the injected gas was increased from 15 per cent to 66 per cent. Their data suggests that dilution of nitrogen with relatively small amounts of hydrocarbon gas could be helpful in reducing the miscibility pressure.

They[14] also found that the displacement efficiency in the first 123 feet of this column was 83.2 per cent for nitrogen sweep as compared to 95 per cent for lean gas sweep. In the final 20 feet of the 143 foot sand column the ultimate displacement efficiency had increased to 94 per cent with nitrogen injection, which compares favorably to the 95.3 per cent obtained by use of lean gas in this length core.

Research of McNeese

McNeese[40] conducted four (I, II, III, and IV) tests on a reservoir model 143 feet long. All four tests were performed at pressures in excess of that required to achieve a miscible displacement using flue gas (88 per cent nitrogen). His results, as reproduced and shown in Figure 4-6, indicated that miscibility was obtained during all tests except number I. The author concluded that the miscibility pressure was essentially independent of the composition of the displacing phase and that some finite displacement length was required before miscibility could be achieved.

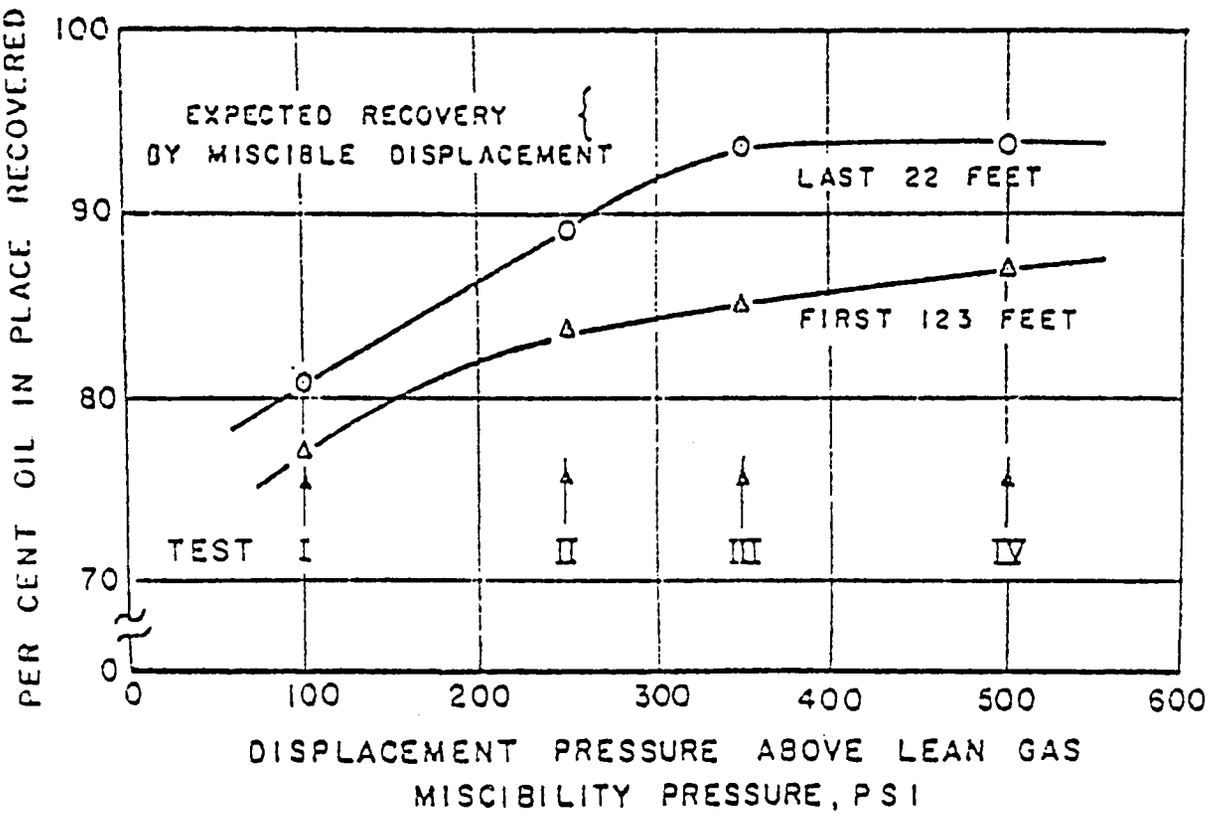

Figure 4-6. EFFECT OF PRESSURE ON RECOVERY
(After McNeese[40])

CHAPTER V

CALCULATION OF FLUID PROPERTIES

In a displacement of crude oil by nitrogen, there will be a continuous change in the composition of both the displaced and the displacing phase as a result of an exchange of components between the oil and gas.

Liquid and vapor phase properties such as surface tension, viscosity and density are considered to be a function of composition, temperature, as well as pressure in each phase.

There are several published techniques for calculating viscosities, densities, molecular weights, and surface tensions of hydrocarbon mixtures from their compositional information. From these techniques, we have selected those methods which have been most widely used by other investigators.

Densities of Gas and Oil

Gas Density

The density of the vapor phase is found by using the law of corresponding stated as follows:

$$\rho_v = \frac{\bar{M} \cdot P}{ZRT} \quad lb/ft^3 \tag{5-1}$$

where:

$\bar{M}$ = average molecular weight, and can be defined mathematically as:

$$\bar{M} = \sum_{i=1}^{n} y_i M_i \qquad (5\text{-}2)$$

y_i = mole fraction of ith component in vapor phase

M_i = molecular weight of ith component

P = absolute pressure of the system, psi

T = absolute temperature °R

R = gas constant = 10.72 psi·ft^3/lb mole °R

The gas deviation factor, Z, is a function of the reduced pressure and reduced temperature.

$$Z = f(P_r, T_r) \qquad (5\text{-}3)$$

The pseudo-reduced pressure and temperature are defined mathematically as:

$$P_r = \frac{P}{\sum_{i=1}^{n} y_i P_{c_i}} \qquad (5\text{-}4)$$

$$T_r = \frac{T}{\sum_{i=1}^{n} y_i T_{c_i}} \qquad (5\text{-}5)$$

where:

P_{c_i} = critical pressure of the ith component in the vapor phase, psi

T_{c_i} = critical temperature of ith component, °R

P = current pressure, psi

T = prevailing temperature, °R

The gas derivation factor for natural gas was correlated[49] using pseudo-reduced properties, and may be obtained from Brown, et al.[49]

Liquid Density

The density of any complex mixtures in the liquid state can be computed from the composition of the mixtures and the density of their components.

The procedure for calculating the liquid densities follows the method published by Standing.[50]

$$\rho_L = \frac{\sum_{\substack{i=1 \\ i \neq c_{6+}}}^{n} x_i M_i + x_{c_{6+}} M_{c_{6+}}}{\sum_{\substack{i=1 \\ i \neq c_{6+}}}^{n} x_i M_i V_i + x_{c_{6+}} M_{c_{6+}} V_{c_{6+}}} \qquad (5\text{-}6)$$

ρ_L = liquid density at standard pressure and temperature, lb/ft^3

x_i = mole fraction of ith component in the mixture

$x_{c_{6+}}$ = mole fraction of hexane and heavier in the liquid phase

$M_{c_{6+}}$ = molecular weight of hexane and heavier

V_i = specific volume of the ith component, ft^3/lb

$V_{c_{6+}}$ = specific volume of hexane and heavier, ft^3/lb

The specific volumes and molecular weights of any component can be obtained from NGAA data book.[49] For hexane and heavier, $V_{c_{6+}}$ and $M_{c_{6+}}$ can be determined in the laboratory.

Extensive data are available in the literature on the effects of pressure and temperature on the density of hydrocarbon mixtures. Standing and Katz,[50] correlated the available data in the form of "density-correction curves." These curves, reproduced here in Figure 5-1 and Figure 5-2, can be used to correct the density of mixture to our desired pressure and temperature. (For more details consult Standing.[50])

Molecular Weight of Liquid Hydrocarbon Mixtures

The molecular weight of any hydrocarbon mixture can easily be calculated by a method developed by McLeod.[52] His excellent experimental investigation showed that the Eykman Molecular Refraction (EMR) bears a linear relationship with molecular weight for any complex hydrocarbon mixture.

The straight line equation for the EMR-molecular weight relationship is:

$$M = -2.97 + 1.3591\ EMR \qquad (5\text{-}7)$$

where, M = molecular weight of the hydrocarbon mixture. Knowing the density of the mixture, the Eykman Molecular Refraction (EMR) can be estimated by utilizing Figure 5-3. For further details see McLeod.[52]

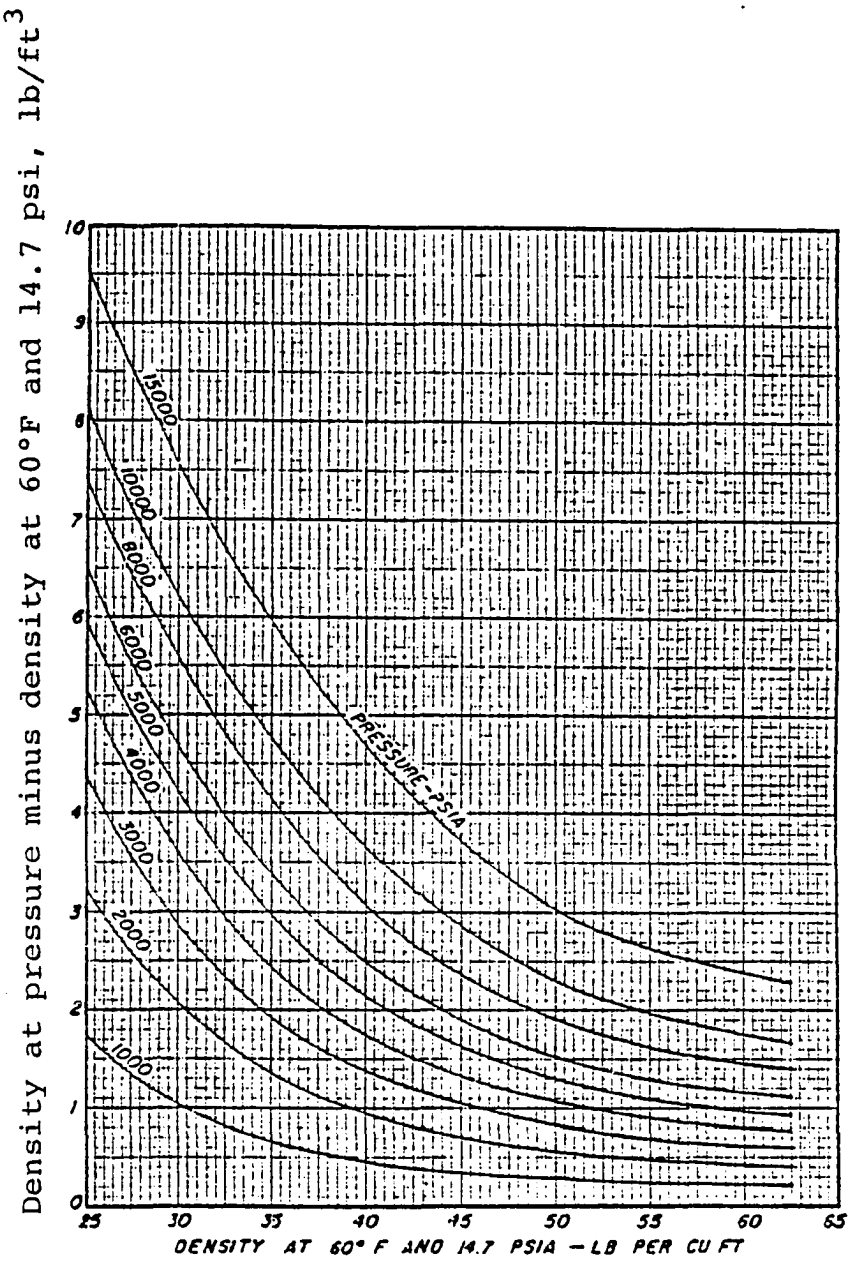

Figure 5-1. DENSITY CORRECTION FOR COMPRESSIBILITY OF LIQUIDS (From Standing[50])

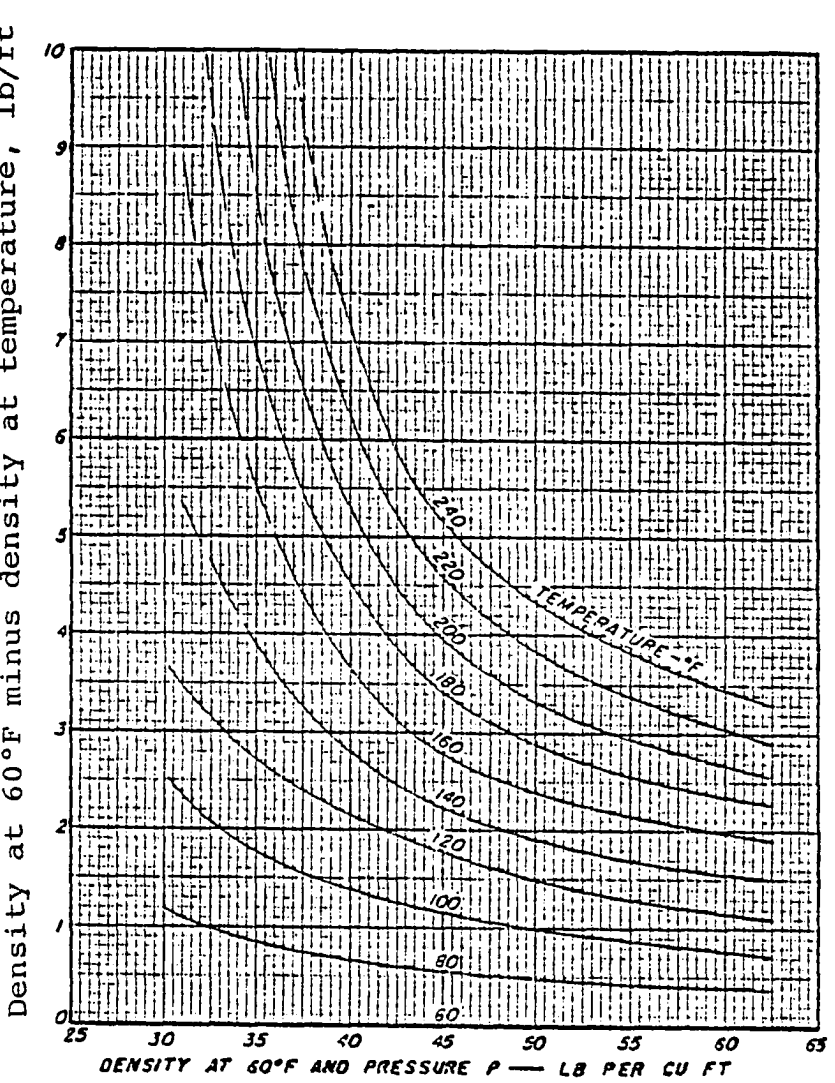

Figure 5-2. DENSITY CORRECTION FOR THERMAL EXPANSION OF LIQUIDS (From Standing[50])

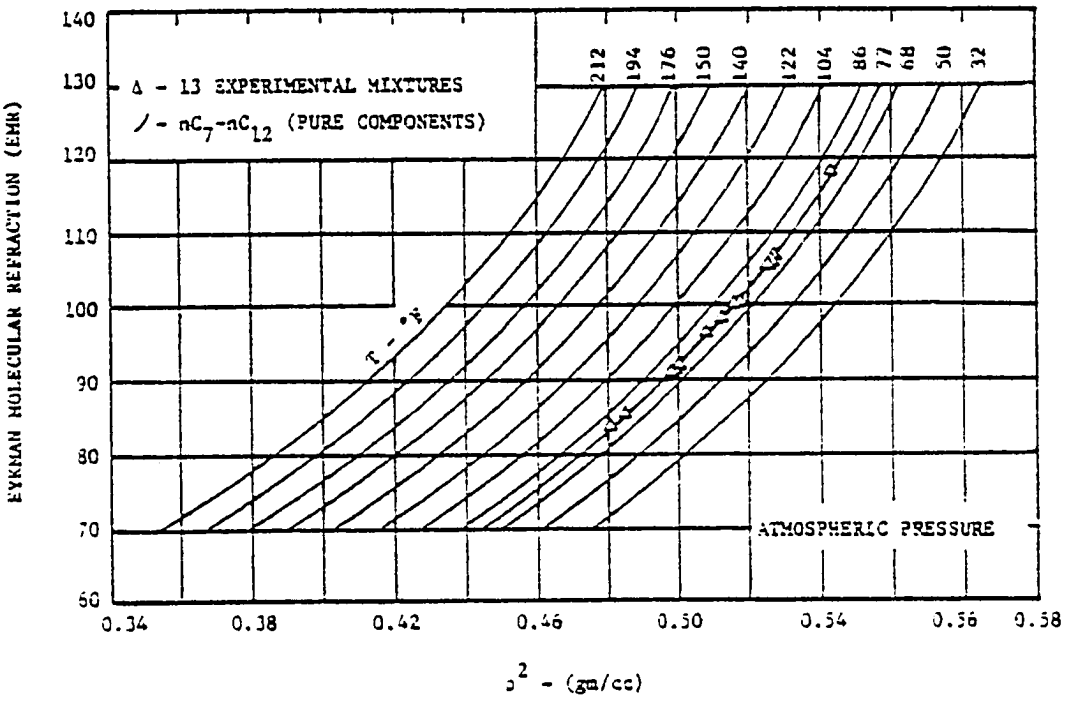

Figure 5-3. EYKMAN MOLECULAR REFRACTION (EMR) VERSUS ρ^2 (From the work of McLeod[52])

Surface Tension

Surface tension is the stress at the surface between a liquid and a vapor caused by the differences between the molecular forces in the vapor and those in the liquid and by the imbalance of these forces at the interface.

Early work on the surface tension of mixtures of hydrocarbons was investigated experimentally by Katz, et al.[53] who, from the experimental data, developed a procedure for calculating surface tension. The method based on the parachor and the equation proposed by Sugden[54] related the surface tension to the properties of the liquid and vapor phases.

Parachors for pure hydrocarbons, nitrogen, and carbon dioxide are given in Table 5-1. A correlation of the parachor with molecular weight is presented in Figure 5-4. For a mixture the surface tension is defined[53] by the following relation:

$$\sigma^{\frac{1}{4}} = \sum_{i=1}^{n} P_{chi} \left(x_i \frac{\rho_L}{M_L} - y_i \frac{\rho_v}{M_v}\right) \qquad (5\text{-}8)$$

where P_{chi} = parachor of ith component

x_i and y_i = mole fractions of ith component in liquid and vapor phase respectively

ρ_L and M_L = density in gm/cm^3 and molecular weight, respectively, of liquid phase

ρ_v and M_v = density in gm/cm^3 and molecular weight, respectively, of vapor phase.

TABLE 5-1

PARACHORS OF PURE SUBSTANCES
(From Katz, et al.[53])

COMPONENT	PARACHOR
Methane	77.0
Ethane	108
Propane	150.3
i-Butane	181.5
n-Butane	190.0
i-Pentane	225
n-Pentane	232
n-Hexane	271
Nitrogen	41
Carbon Dioxide	78

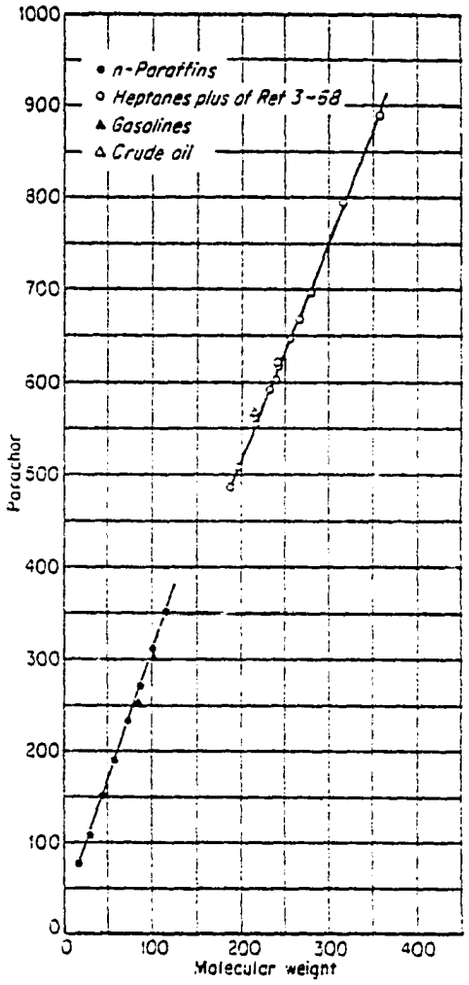

Figure 5-4. PARACHORS FOR HYDROCARBONS VS. MOLECULAR WEIGHT (From Katz, et al.[53])

Physical and Critical Properties of Hexane and Heavier Fraction

The critical pressure, temperature, and boiling point of hexane and heavier used in this study was estimated from the published charts developed by Standing[50] and Clark.[58]

One of the problems which the author faced was to estimate the critical volume (V_c) for hexane-plus. We found that a plot of log ($M_i \cdot V_{c_i}$) versus $b(\frac{1}{T_b} - \frac{1}{T})$ is a reasonably smooth curve which permits $(V_c)_{C_{6+}}$ to be correlated as shown in Figure 5-5. The value for the constant b for each component is determined by the following relation:

$$b = \frac{(\log P_c - \log 14.7)}{(\frac{1}{T_b} - \frac{1}{T_c})} \qquad (5\text{-}9)$$

where:

b = constant characteristic of the particular hydrocarbon

P_c = critical pressure, psia

T_c = critical temperature, °R

T_b = boiling point, °R

T = prevailing temperature of the system, °R

Values for b for the various pure components through decane are given in Table 5-2.

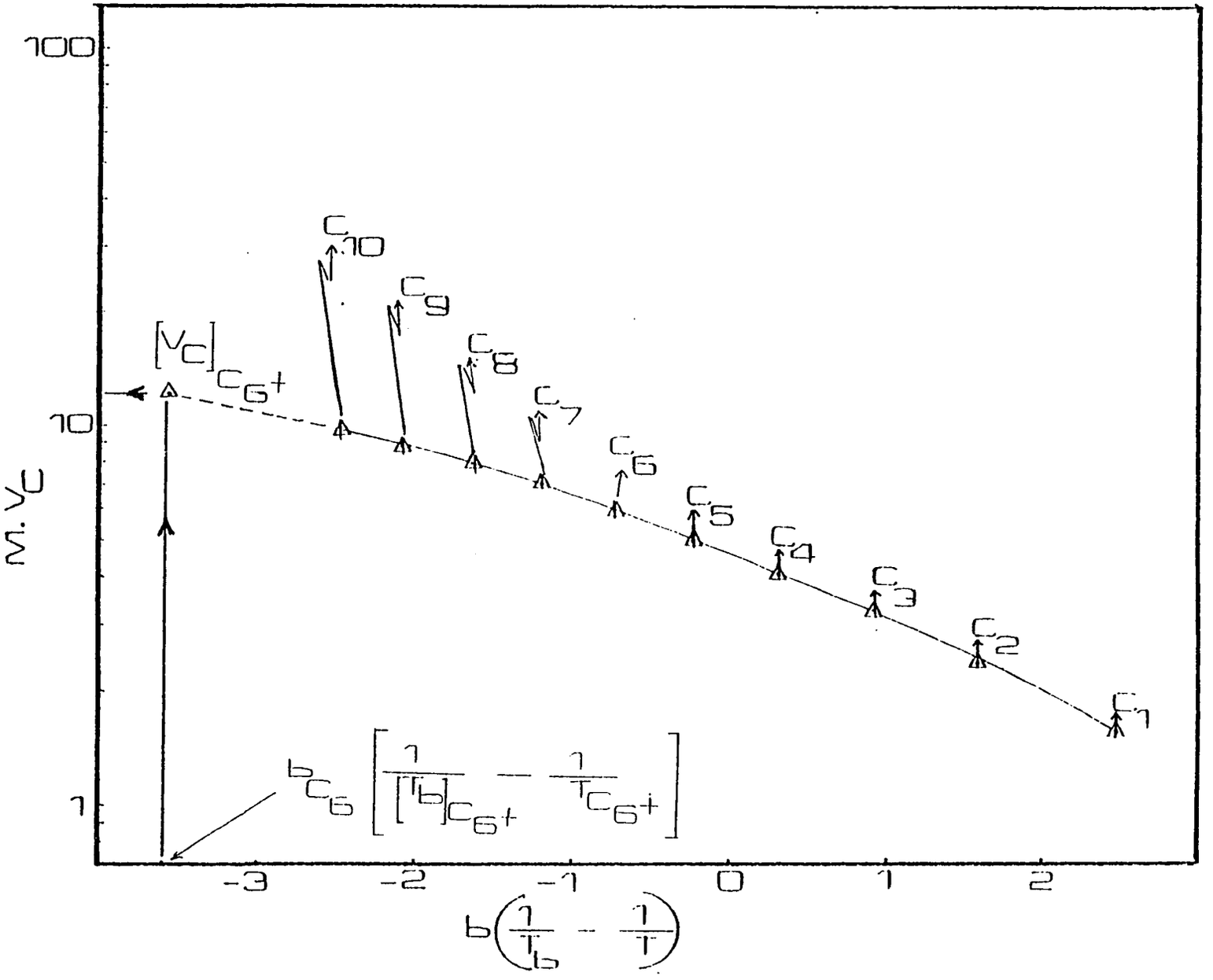

Figure 5-5. CORRELATION OF $M \cdot V_c$ vs. $b(\frac{1}{T_b} - \frac{1}{T})$ TO DETERMINE V_c VALUES FOR HEAVIER COMPONENTS

TABLE 5-2

VALUES FOR b FUNCTION FOR PURE HYDROCARBON COMPONENTS
(After Clark[58])

Component	b-value	Component	b-value
Methane	808	N-Pentane	2473
Ethane	1415	Hexane	2780
Propane	1792	Heptane	3061
I-Butane	2045	Octane	3333
N-Butane	2129	Nonane	3602
I-Pentane	2375	Decane	3847

Viscosities of Gas and Oil

Gas Viscosity

Herning and Zipperer[55] proposed the following mixture rule for the viscosity of a mixture of gases under atmospheric pressure and the temperature of interest:

$$U_l = \frac{\sum_{i=1}^{n} (y_i U_i^* M_i^{\frac{1}{2}})}{\sum_{i=1}^{n} (y_i M_i^{\frac{1}{2}})} \qquad (5\text{-}10)$$

where:

U_i^* = viscosity of component i at atmospheric pressure, cp

Y_i = mole fraction of i component in vapor phase

M_i = molecular weight of i component

U_l = viscosity of gas mixture at atmospheric pressure, cp

Values of U_i^* and M_i may be obtained from NGAA Data Book.[48]

Carr and coworkers[56] presented an experimentally established correlation, Figure 5-6, for correcting the atmospheric viscosity of hydrocarbons to the desired pressure. The correlation of Carr was based on the association of the viscosity ratio $\frac{U}{U_l}$ with pseudo-reduced pressure and temperature, where U is the viscosity of the mixture at the prevailing conditions and U_l is the viscosity of the mixture at atmospheric pressure and system temperature.

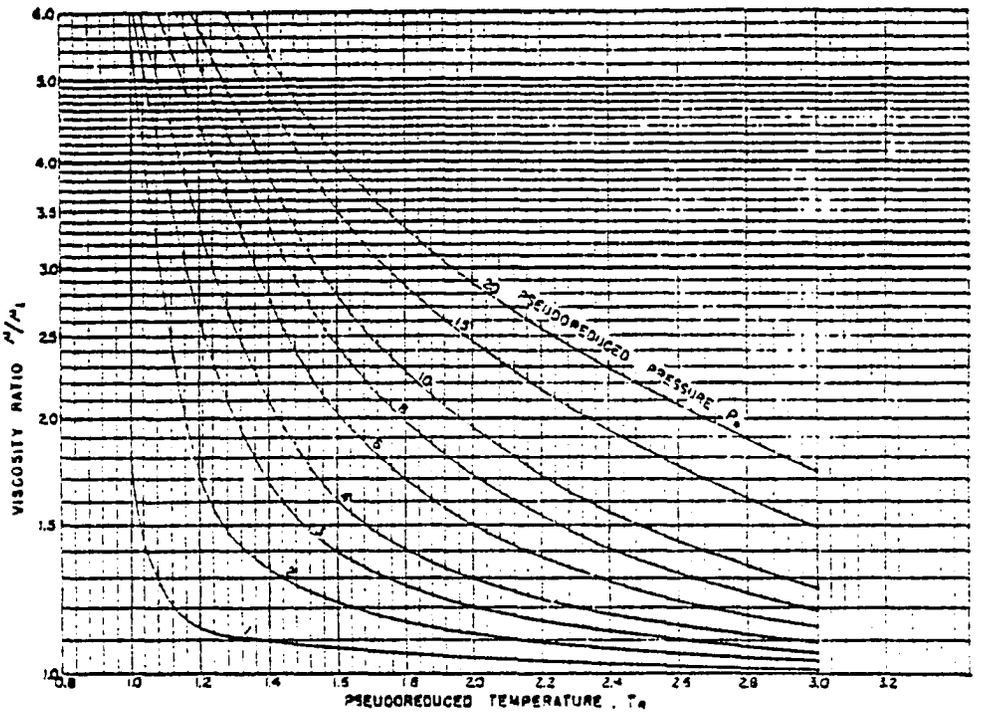

Figure 5-6. VISCOSITY RATIO VERSUS PSEUDO-REDUCED TEMPERATURE (From Carr, et al.[56])

The pseudo-reduced pressure and temperature required for entry into Figure 5-6 can be obtained through the use of Equations (5-4) and (5-5). For more details see Carr, et al.[56]

Liquid Viscosity

The procedure for calculating the liquid viscosity follows the method proposed by Lohrenz, et al.[57] The technique is illustrated in the following steps.

a) Calculate the atmospheric viscosity at the composition and temperature of the phase

$$U_l = \frac{\sum_{\substack{i=1 \\ i\neq c_{6+}}}^{n} [x_i U_i^* M_i^{1/2}] + [x_{c_{6+}} U^*_{c_{6+}} M^{1/2}_{c_{6+}}]}{\sum_{\substack{i=1 \\ i\neq c_{6+}}}^{n} (x_i M_i^{1/2}) + x_{c_{6+}} M^{1/2}_{c_{6+}}} \qquad (5\text{-}11)$$

where U_l is the atmospheric viscosity of liquid phase, cp. The other parameters were defined in the previous sections.

b) Calculate the reduced density as it was defined by Lohrenz:

$$\rho_r = \frac{\rho_L}{\sum_{\substack{i=1 \\ i\neq c_{6+}}}^{n} x_i V_{c_i} + x_{c_{6+}} V_{c_{c_{6+}}}} \qquad (5\text{-}12)$$

where:

ρ_r = reduced density

$V_{c_{6+}}$ = critical volume of c_{6+}, ft^3/lb-mole

ρ_L = liquid density, lb/ft^3

x_i = mole fraction of i component

v_{c_i} = critical volume of i component, ft^3/lb-mole

c) Estimate the mixture viscosity parameter:[57]

$$E = \frac{\left[\sum_{\substack{i=1 \\ i\neq c_{6+}}}^{n} x_i T_{c_i} + x_{c_{6+}} T_{c_{c_{6+}}}\right]^{1/6}}{\left[\sum_{\substack{i=1 \\ i\neq c_{6+}}}^{n} x_i M_i + x_{c_{6+}} M_{c_{6+}}\right]^{1/2} \left[\sum_{\substack{i=1 \\ i\neq c_{6+}}}^{n} x_i Pc_i + x_{c_6+} P_{c_{c_{6+}}}\right]^{2/3}} \qquad (5\text{-}13)$$

where:

E = mixture viscosity parameter

p_{c_i}, $P_{c_{c_{6+}}}$ = critical pressure of i component and hexane-plus respectively, psi

T_{c_i}, $T_{c_{c_{6+}}}$ = critical temperature of i component and hexane-plus respectively, °R

d) Solve the following equation for the viscosity U.

$$[(U-U_l)E + 10^{-4}]^{1/4} = 0.1023 + 0.023364\ \rho_r + 0.058533\ \rho_r^2 - 0.040758\ \rho_r^3 + 0.009332\ \rho_r^4 \qquad (5\text{-}14)$$

where, U = liquid viscosity at the prevailing pressure and temperature, cp.

K-Values and Convergence Pressures in Equilibrium Calculations

K-Values for Light Hydrocarbon Components

The idea of using the equilibrium constant K in phase behavior calculations is sound, requiring only that appropriate K-values be known for components of the material within the range of temperatures and pressures covered by the particular investigation. Equilibrium ratios which are sometimes called vaporization equilibrium constants can be defined as:

$$K_i = \frac{y_i}{x_i}$$

where:

y_i = mole fraction of any component in the vapor phase

x_i = mole fraction of the same component in the liquid phase

However, the difficulty in obtaining the proper K-values for any individual component arises from the fact that the values vary not only with temperature and pressure changes, but also with changes in the composition of the mixture; thus, a K-value for a given component actually changes each time the mixture in which the component exists changes.

The K-values used in this study were obtained from the published correlation in NGAA Engineering Data Book.[59]

K-values for Heaviest Fraction

The K-values of hexane and heavier used in this study were calculated by the method developed by Clark.[58] In this

procedure, the best K-values obtainable for the light components, together with their b-values from Table 5-2, are first plotted as log K vs. b. The line is extrapolated to a b-value calculated by Equation (5-9) for hexane-plus.

Convergence Pressure

The problem of incorporating composition into general K correlations has been an arduous one. The most common approach has been the use of the "convergence pressure" concept. Convergence pressure, P_k, is that pressure at which the K values of all components in the system converge at a value of K = 1.0, at system temperature. For multicomponent systems, convergence pressure depends on both temperature and system composition.

NGPA[59] proposed a method for calculating the convergence pressure which embodies the following main steps:

Step 1 - Assume a convergence pressure.

Step 2 - Read K-values from the charts for the convergence pressure close to the assumed value.

Step 3 - Calculate the flash liquid using these K-values $\frac{y_i}{K_i}$

Step 4 - For the computed liquid phase omit the lightest component (in this study, nitrogen was considered to be the lightest component).

Step 5 - Calculate the weight average critical temperature and pressure for the remaining material.

$$\text{Weight average } T_c = \frac{\sum_{\substack{i=2 \\ i \neq c_{6+}}}^{n} x_i M_i T_{c_i} + x_{c_{6+}} M_{c_{6+}} T_{c_{6+}}}{\sum_{\substack{i=2 \\ i \neq c_{6+}}}^{n} x_i M_i + x_{c_{6+}} M_{c_{6+}}}$$

$$\text{Weight average } P_c = \frac{\sum_{\substack{i=2 \\ i \neq c_{6+}}}^{n} x_i M_i P_{c_i} + x_{c_{6+}} M_{c_{6+}} P_{c_{6+}}}{\sum_{\substack{i=2 \\ i \neq c_{6+}}}^{n} x_i M_i + x_{c_{6+}} M_{c_{6+}}}$$

This is the critical point of the hypothetical heavy component.

Step 6 - Locate this critical point in Figure 5-7. Sketch the binary critical locus for a binary mixture consisting of the lightest component (nitrogen) and the hypothetical heavy component. The intersection of the system temperature and the interpolated curve is the convergence pressure.

Step 7 - Repeat steps 2 through 7 until the assumed and calculated convergence pressures check within an acceptable tolerance.

The previous method was used throughout this study.

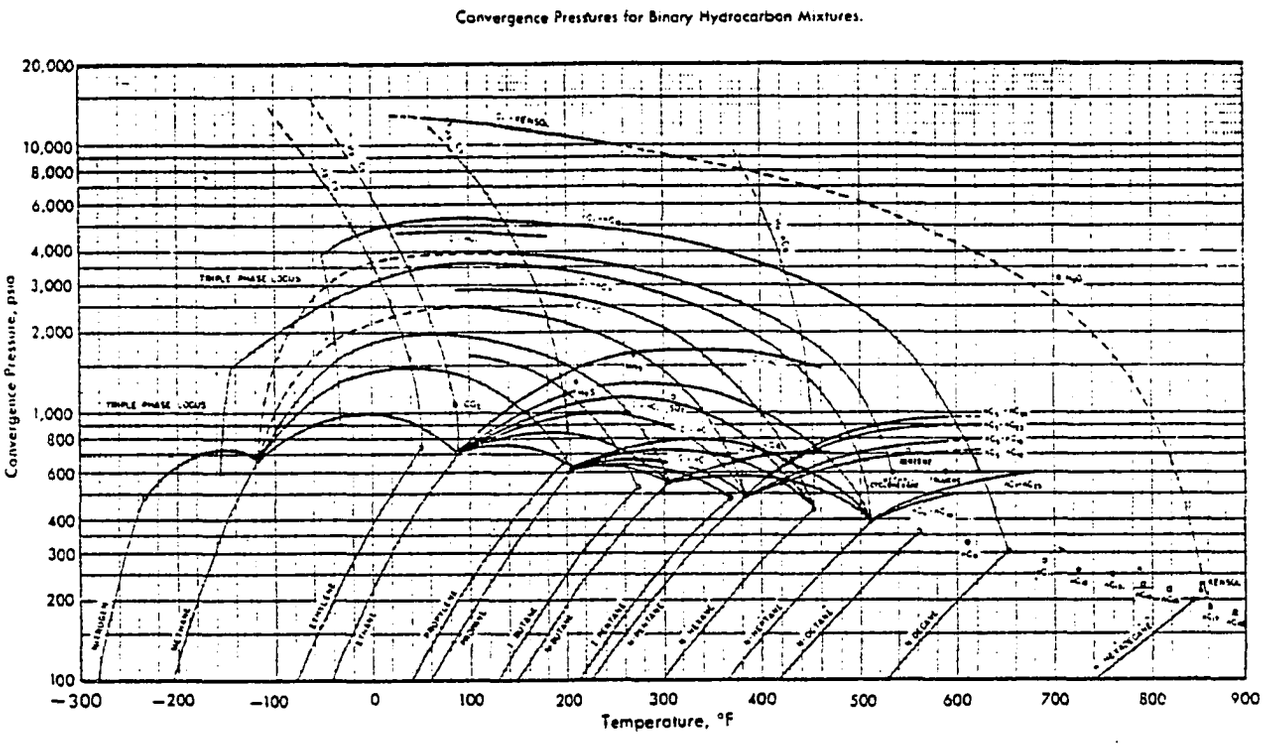

Figure 5-7. CONVERGENCE PRESSURE FOR BINARY HYDROCARBON MIXTURE (Engineering Date Book[59] 9th Edition, NPGA, 1972)

CHAPTER VI

TECHNIQUES OF CHROMATOGRAPHIC ANALYSES

This chapter is meant to assist anyone, who in the future, may work with the techniques of gas chromatography.

Chromatography is the physical process of separating the components of a mixture in which the materials to be separated are partitioned between two phases. One phase is stationary and the other (mobile phase) is passed through the stationary phase.

If the stationary phase is a solid, we speak of Gas-Solid Chromatography. This depends upon the adsorptive properties of the column packing to separate samples, primarily gases. Common packing used are silica gel, molecular sieve, and charcoal.

If the stationary phase is a liquid, we speak of Gas-Liquid Chromatography.

The liquid is spread as a thin film over an inert solid and the basis for separation is the partitioning of the sample in and out of the liquid film. Several articles have been written on the subject.[41-43]

Apparatus

The chromatograph consists of three basic sections: flow system, column, and dectector. See Figure 6-1.

Flow System

- Carrier Gas: The mobile phases or carrier gases, such as helium, hydrogen, nitrogen, and carbon dioxide, are supplied to the chromatograph by a high pressure gas cylinder. A two stage pressure regulator is used to assure a uniform pressure to the column inlet.
- Injection Part: The sample injection system provides a means of introducing the sample, as a "plug" into the carrier gas upstream of the column. Gases are usually introduced by gas-tight syringes.

Columns

The columns, on which the samples are to be separated, constitute the heart of chromatographic processing. There are two general classifications for columns, the "filled" or packed column and the "open tubular" column.

- Packed columns usually consist of 1/4" or 1/8" tubing filled with some type of granular adsorption material. The separations performed are determined by the proper selection of stationary placed in the column; thus, two variations of packed columns are the adsorption and partitioning. Adsorption columns use silica gel, charcoal, or mole sieve which are materials having the ability to adsorb gases on their

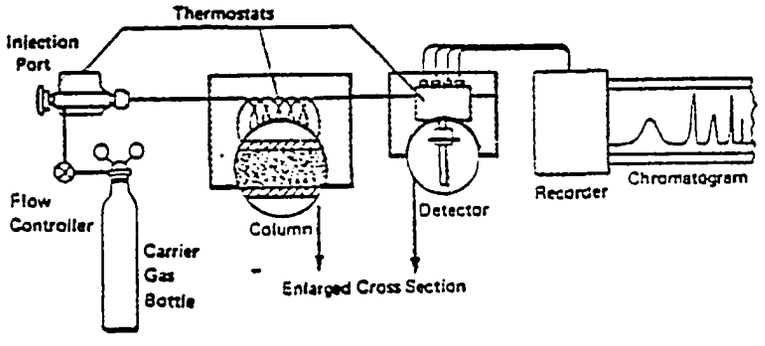

Figure 6-1. SCHEMATIC DRAWING OF A GAS CHROMATOGRAPH SYSTEM (After Hendricks[41])

surfaces. These columns separate light gases such as oxygen, nitrogen, helium, and methane. Partition columns are packed with inert granular support solids which are coated with a liquid (stationary) phase. Two prominent partition columns are the silicon 200/500 and the BMEE. Both give a good separation of hydrocarbons, through pentanes and have a long life relative to their usage.

- Open tubular columns, referred to as capillary columns, are constructed of a very long tube having a capillary size internal diameter. These columns may or may not be coated with a stationary liquid phase. The mechanics of separation are essentially the same as packed columns.

The ability of a column to separate or resolve the components of a mixture is affected by the following column conditions:

. Column length
. Operating temperature
. Gas flow rate

These parameters should be held constant during sample and corresponding standard reference runs. In order to keep the columns at a constant temperature, they are housed in chromatographic ovens where a temperature variation of no more than 0.3 degrees centigrade is maintained.

Detectors

After the separations have been made by the column, each pure component is passed to a detector where a

quantitative measure is made of the amount in the carrier gas. The most widely used detector for gas chromatography is thermal conductivity (TC), since it meets almost all the characteristics of the ideal detector. Characteristics desirable in a detector are stability, sensitivity, and rapid response to changes. Basically the TC cell is a hot wire filament suspended inside a metal block or tube through which gas is passing. An electrical current is applied to the filament causing its temperature to rise to some constant value. At the same time, the detector block housing the filament is held at a constant temperature below that of the filament. The temperature attained by the filament is now dependent not only on the current, but also the block temperature and the thermal conductivity of the passing gaseous medium surrounding the filament. As a result, filament resistance and subsequently the current through-put is related to the rate at which heat is conducted away from the filament through the gas medium to the cell block.

Placing the cell block in a constant temperature detector oven eliminates significant temperature variations. Assuming the flow rate is constant, any change in current out-put of the filament is dependent only on the thermal conductivity of the gas in the cell.

Expanding the single filament detector theory, it is quite simple to construct a thermal conductivity differential detector. A metal block containing two pairs of filaments,

(each pair isolated in a separate gas chamber) one pair of filaments constitutes a reference side, seeing only the carrier gas, while the other filaments serving as the sample side, see any effluents in the carrier gas eluted from the separation column.

A 1 millivolt strip chart recorder is connected to the detector output. When pure carrier gas is passing through both sides of the detector, the output of the bridge is constantly giving a baseline recording on the chart. As effluents from the column are detected, the bridge output will drive the chart pen from the baseline. A strip chart recording of the components in the sample is obtained.

There are many things about the process of gas chromatography that can only be learned by working with a gas chromatograph instrument.

The gas chromatograph is an essential and valuable part of any experimental gas injection research. One must become familiarized with the instrument before using it. The following section deals with the observations and procedures used in this investigation.

Before attempting to use the instrument, one must be able to:

1. Choose the right column for the purpose of gas components separations.
2. Identify the various separated peaks (each peak represents a different gas component).

3. Determine column temperature.
4. Estimate detector temperature.
5. Calculate the flow rate of the carrier gas.
6. Magnitude of the bridge current.
7. Estimate the size of gas sample to be analyzed.
8. Calibrate the gas chromatograph.

The column is the heart of the chromatograph. The actual separation of sample components is achieved in the column. Consequently, the success or failure of a particular separation will depend to a large extent upon the choice of column (consult Dewar, et al.[45] and Bendnas, et al.[46] for column selection).

One of the problems currently facing chromatographic workers is the positive identification of the numerous peaks emerging from gas chromatograph columns. Under constant pressure conditions, the flow rate is linear with time and one could also speak of retention time.* This retention time is characteristic of the sample and the liquid phase, and can therefore be used to identify the sample. Identification is then based on a comparison of the rentention time of the unknown component with that obtained from a known compound analyzed under identical conditions.

The column temperature should be high enough so that the analysis is accomplished in a reasonable length of time.

---

*The time required to elute a compound from the G. C. Column is called the retention time.

According to a simple approximation made by Giddings,[47] the retention time doubles for every 30° decrease in column temperature. For more details consult Giddings.[47]

The influence of temperature on the detector depends considerably upon the type of detector employed. As a general rule, however, it can be said that the detector and connections from the column exit to detector must be hot enough so that condensation of the sample does not occur. Peak broadening and loss of component peaks are characteristic of condensation.

Column efficiency depends upon choosing the proper flow rate of carrier gas. The optimum flow rate can be easily determined experimentally by making a simple Van Deemter[47] plot of HETP vs. gas flow rate (see Figure 6-2). The most efficient flow-rate is at the minimum of HETP. The height equivalent to a theoretical plate (HETP), is defined by the following equation:

$$HETP = L/N$$

where L is the length of the chromatographic column, cm. and N = number of theoretical plates = $16(\frac{x}{y})^2$, where "y" is the length of the baseline cut by the two tangents (Figure 6-3), and "x" is the distance from injection to peak maximum.

Figure 6-4 shows the maximum bridge current for specific cell temperature (detector temperature) and carrier gases helium, nitrogen and argon. These should not be exceeded.

The sample should be introduced instantaneously as a "plug" onto the column. Gases are usually introduced by gas-

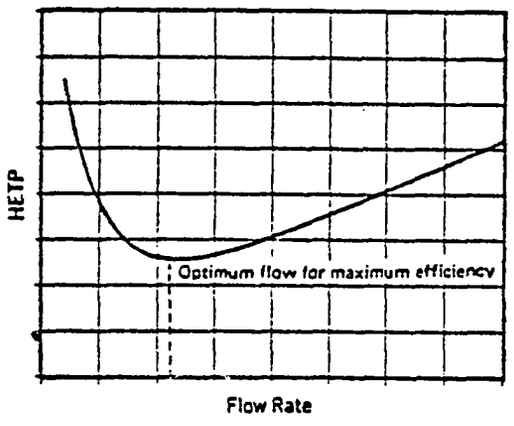

Figure 6-2. FLOW RATE vs. HETP (After McNair, et al.[42])

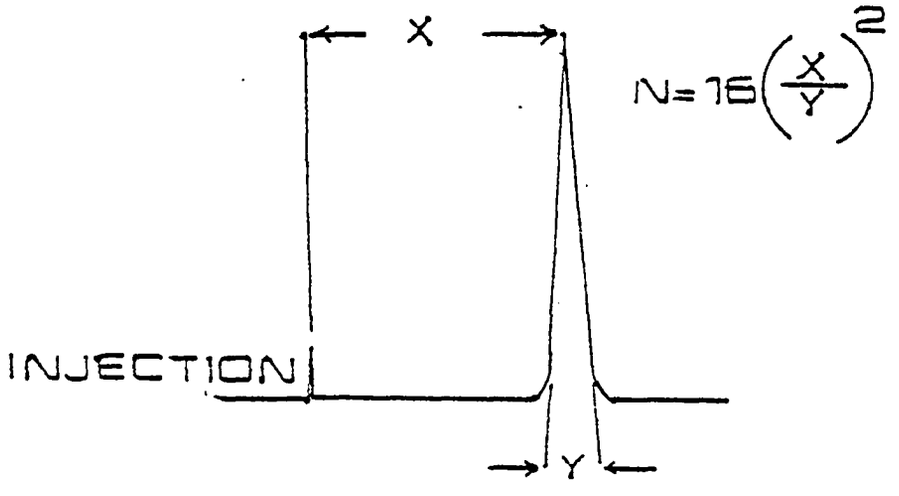

Figure 6-3. CALCULATION OF THE THEORETICAL PLATES

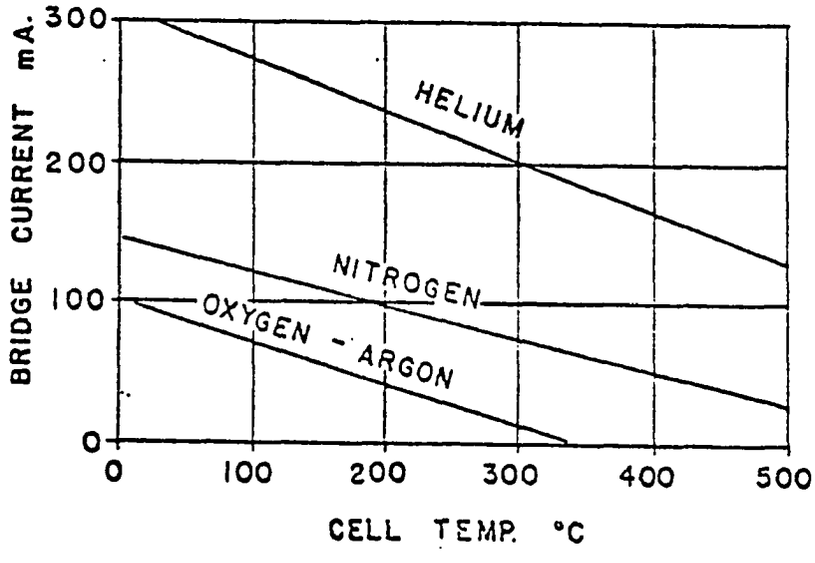

Figure 6-4. CELL TEMPERATURE vs. BRIDGE CURRENT (After Miller[43])

tight syringes. Table 6-1 shows sample sizes for different columns.

TABLE 6-1

SAMPLE VOLUMES FOR DIFFERENT COLUMNS

Column Type	Sample Sizes	
	Gas	Liquid
Regular Analytical, 1/4" O.D.	0.5-50 ml	.02-2 ml
High Efficiency, 1/8" O.D.	.1-1 ml	0.04-4 ul
Capillary, 1/16" O.D.	0.1-10 ul	0.004-0.5 ul

From the work of McNair and Bonelli[42]

The area produced for each peak is proportional to that peak's concentration. This can be used to determine the exact concentration of each component. Once the numbers representing the area are obtained, they must be related to the composition of the sample. This is discussed separately in the next section.

Calibration of Gas Chromatograph

The following standard procedure is proposed by the Natural Gas Processors Association (NGPA).[48]

1. Response factors for each component are calculated from the reference standard chromatogram using the peak height or peak area. The response factor (RF) is determined by the

relationship:

$$RF = M/H$$

where:

M = mole per cent of each component in the reference standard.

H = corresponding peak height or area.

2. Peak heights or areas are measured on the chromatogram of the unknown sample.

3. The mole per cent of unknown is calculated by the relationship:

$$\text{mole \% of unknown} = RF \times A$$

where:

RF = response factor for each component

A = corresponding peak height or area of unknown

Gas Analysis

In this investigation, a Gow-Mac temperature programmable gas chromatograph, model 550P (thermal conductivity), was used to analyze the following gases: Nitrogen, Methane, Ethane, Propane, Butane, Pentane, and Hexane-plus. The output from the thermal conductivity was monitored on Gow-Mac integrating strip chart recorder, model 70-750. Figure 6-5 shows a pictorial representation of the instruments.

The column used on the gas chromatograph was: stainless-steel 30' x 1/8" 30% DC-200/500 on Chromosorb P.A.W. 60-80. The gas chromatograph was fitted with "Backflush to Detector Valve." The instrument was operated under the following conditions:

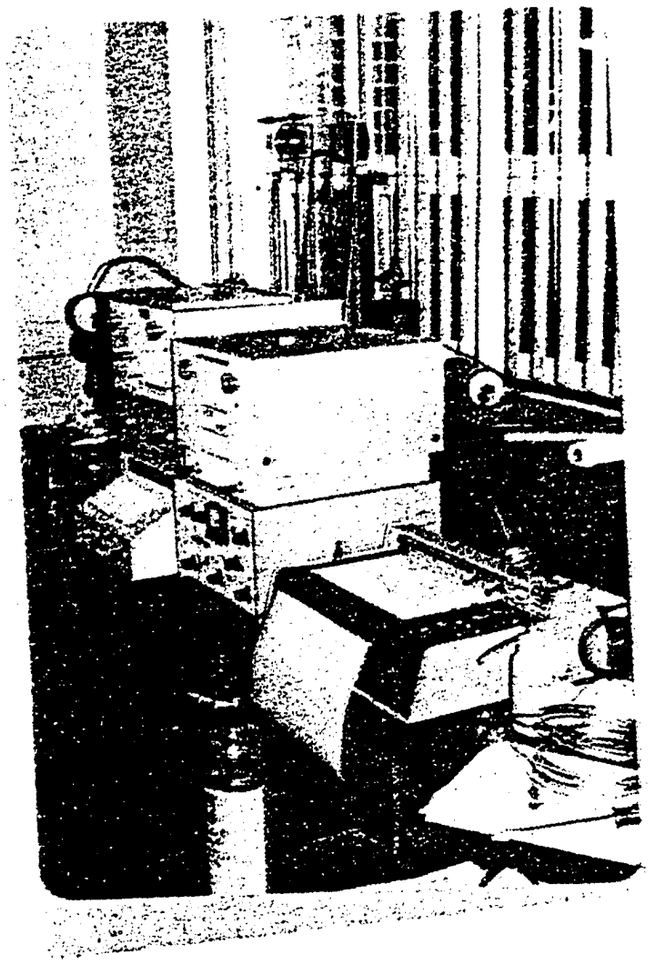

Figure 6-5. SIDE VIEW OF THE GAS CHROMATOGRAPH AND STRIP CHART RECORDER

Helium flow rate	50 cc/min
Column temperature	70 °C
Detector temperature	250 °C
Bridge current	170 MA
Sample size	4 cc
Recorder	1 mv

The calibration gas used in this study was a Scott analyzed gas with the following volume percentage composition:

N_2 =	10%
CH_4	69%
$C_2 H_6$	9%
$C_3 H_8$	6%
$C_4 H_{10}$	3%
$C_5 H_{12}$	2%
$C_6 H_{14}$	1%

CHAPTER VII

EXPERIMENTAL APPARATUS AND MATERIALS

Apparatus

The laboratory equipment was designed to study:

1. vaporization of oil by high pressure nitrogen injection,

2. mechanisms of nitrogen multiple contact miscibility displacement, and

3. compositional changes which take place between nitrogen and oil-in-place during the test.

A schematic diagram and pictorial representation of the equipment used to perform the experimental study are shown in Figures 7-1 and 7-2 respectively. For purposes of description, the experimental apparatus may be divided into three main parts: an injection system, a simulated one-dimensional oil reservoir and a production and analytical system.

Injection System

The injection system consisted of:

1. Constant rate positive displacement mercury pump. The mercury pump (Figure 7-3) was connected through 1/8 inch stainless-steel tubing to the bottom of a recombine cell

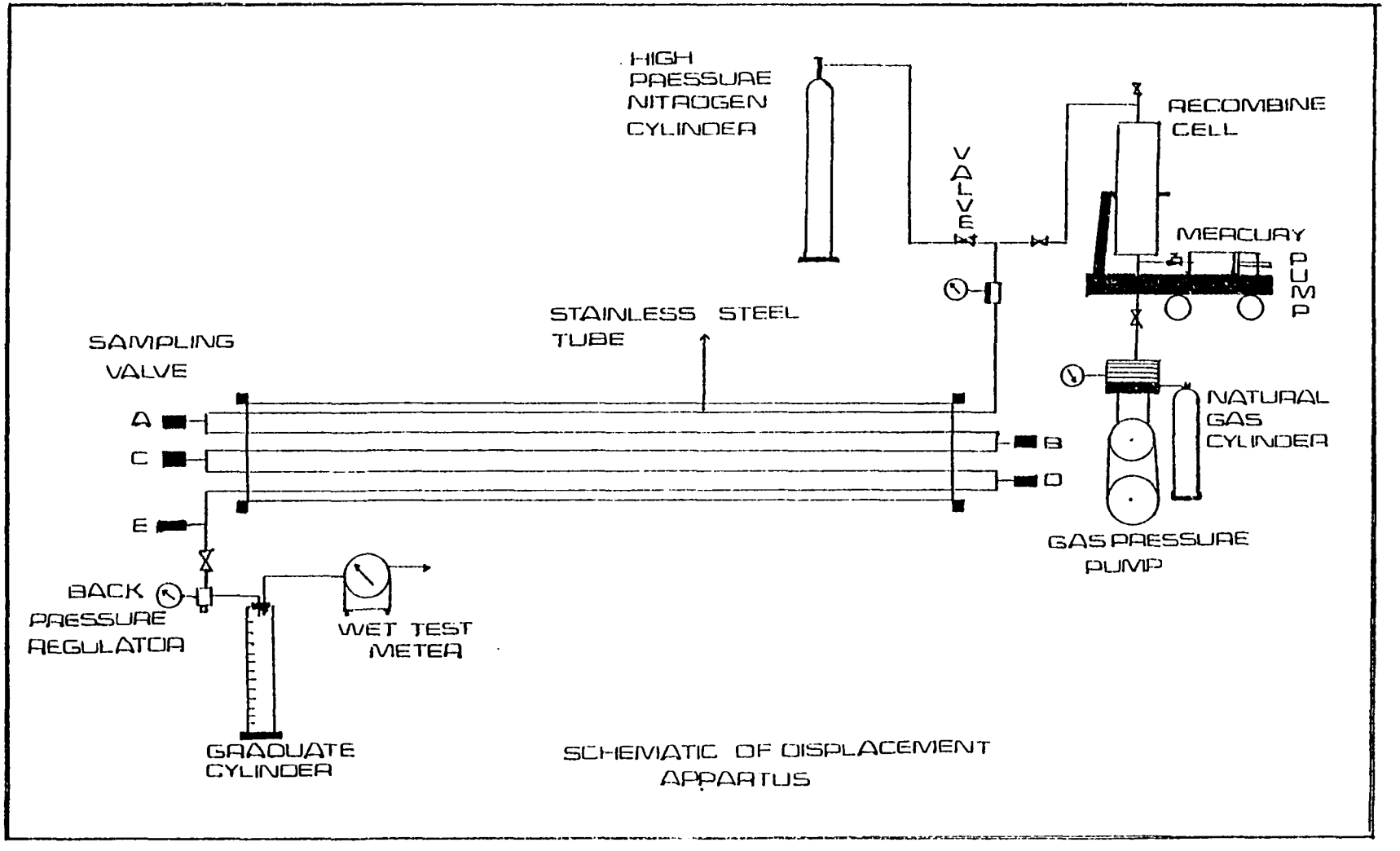
HIGH
PRESSURE
NITROGEN
CYLINDER
VALVE
RECOMBINE
CELL
MERCURY
PUMP
STAINLESS STEEL
TUBE
SAMPLING
VALVE
A
C
E
B
D
NATURAL
GAS
CYLINDER
GAS PRESSURE
PUMP
BACK
PRESSURE
REGULATOR
WET TEST
METER
GRADUATE
CYLINDER
SCHEMATIC OF DISPLACEMENT
APPARATUS

FIGURE 7-1

Figure 7-2. EXPERIMENTAL EQUIPMENT USED IN THE INVESTIGATION

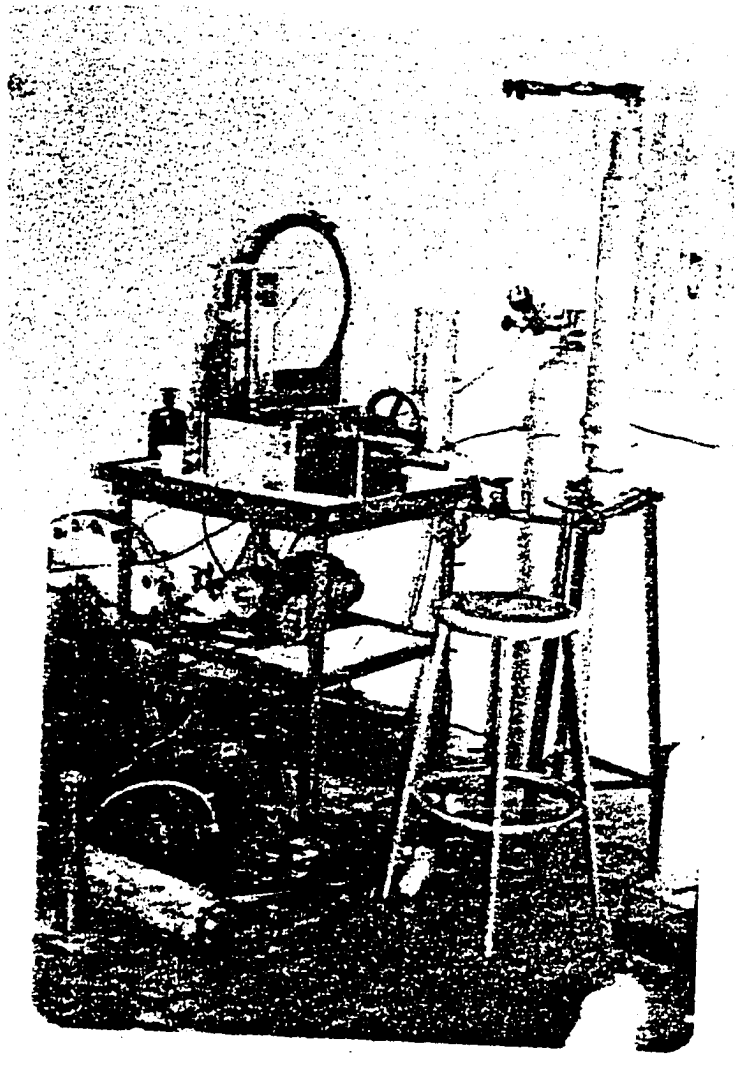

Figure 7-3. FRONT VIEW OF THE MERCURY PUMP

(Figure 7-4). The top of the cell was in turn connected to a sand-packed stainless-steel tube representing an oil-reservoir model.

2. Natural gas pump. For the recombining purpose, a high pressure natural gas pump (Figure 7-5) was utilized. The inlet was connected to a natural gas cylinder, and the outlet to the bottom of the recombine cell through 1/8 inch stainless-steel tubing. Various valves were placed between the pump and the recombine cell to facilitate the recombing process.

3. High pressure nitrogen cylinder. A special high pressure nitrogen cylinder (Figure 7-6) was used for the displacement process. The cylinder contained 494 $ft.^3$ nitrogen of purity 99.999 per cent under 6000 psi. A high pressure stainless-steel regulator with high load needle bearing was used to achieve excellent pressure selection sensitivity. The regulator was connected to the reservoir inlet (Figure 7-7) through 1/4 inch stainless-steel tubing.

Laboratory Oil Reservoir Model

A one-dimensional oil reservoir was represented by a loop of stainless-steel tubes packed with consolidated sand.

The tube was approximately 125 feet long and had an inside diameter of .435 inch. The sand contained approximately 900 ml of voids, had a porosity of 29 per cent, and an average permeability to nitrogen of 0.93 darcies.

Five sampling valves (Figure 7-8) were located at equal intervals along the length of the reservoir model. The design

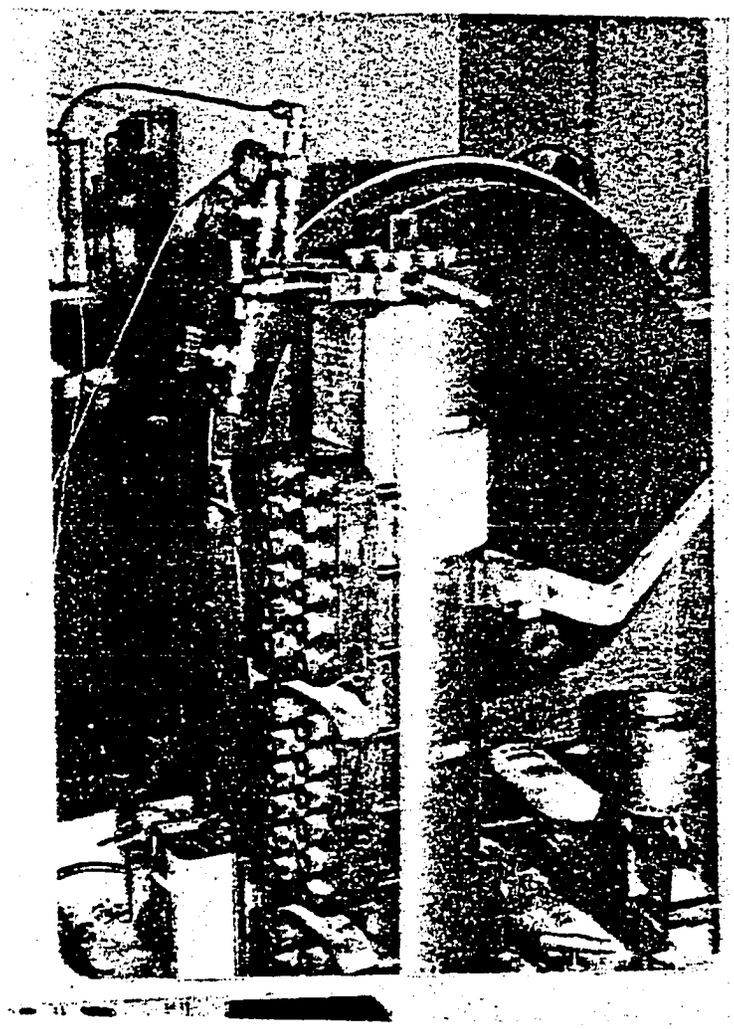

Figure 7-4. SIDE VIEW OF THE RECOMBINE CELL

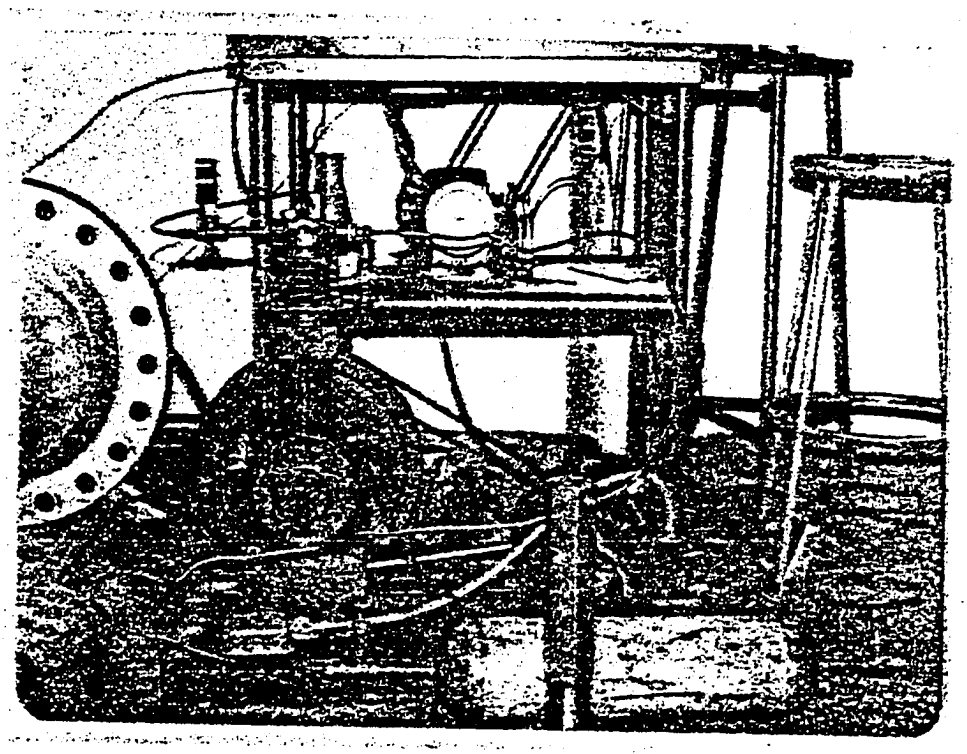

Figure 7-5. SIDE VIEW OF THE NATURAL GAS PUMP

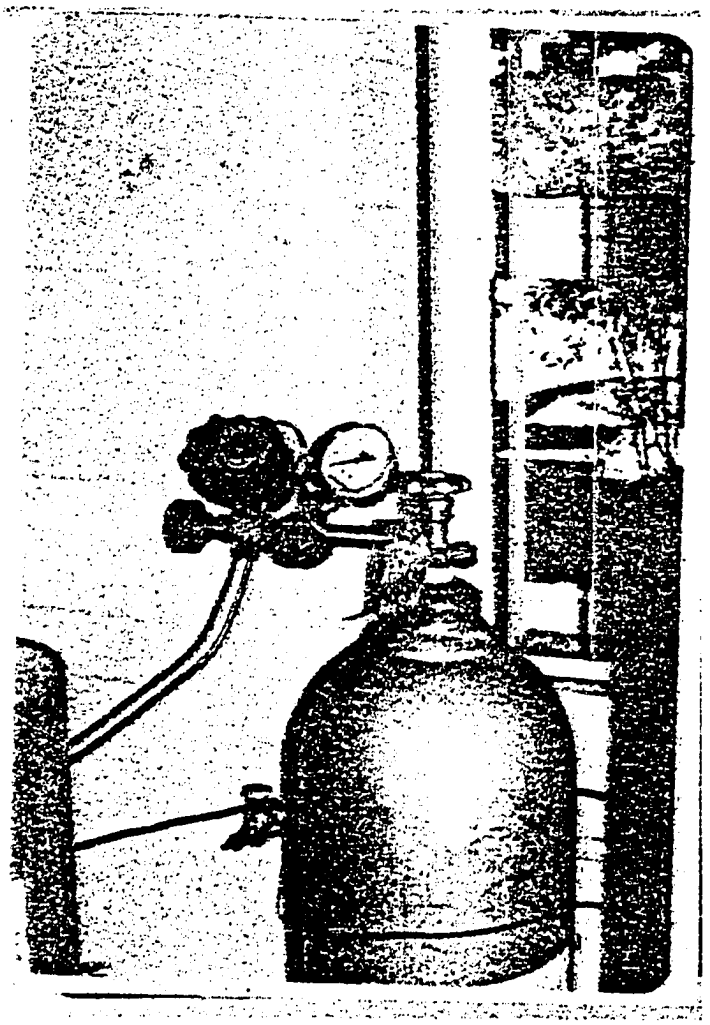

Figure 7-6. FRONT VIEW OF THE HIGH PRESSURE NITROGEN CYLINDER

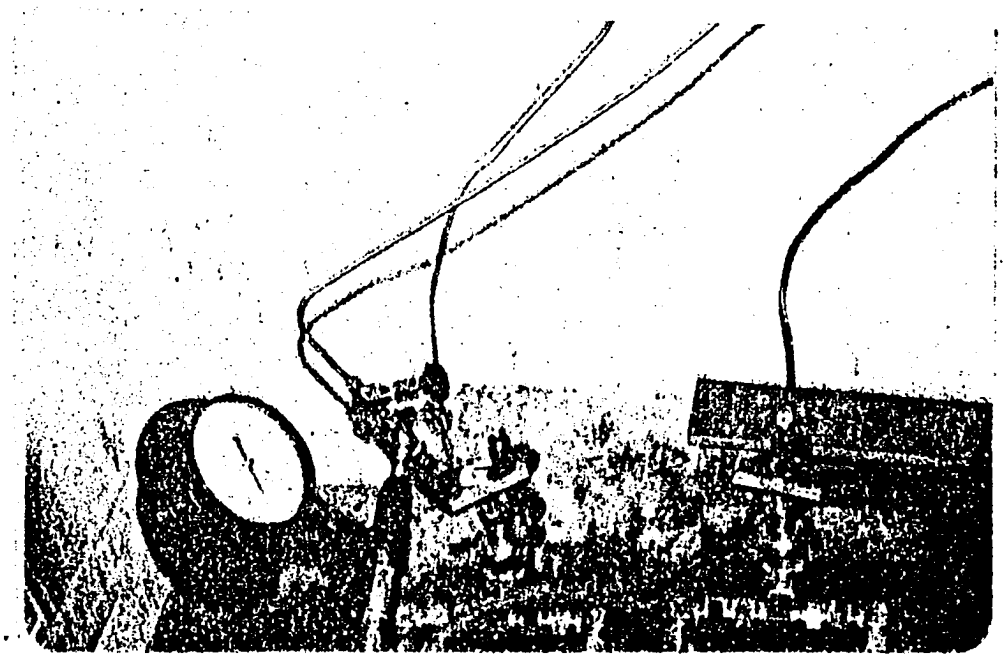

Figure 7-7. SIDE VIEW OF THE INLET OF THE CORE

of these sampling points enable one to take samples of vapor under pressure during the displacement process.

Various valves and gages were placed in the reservoir model system at appropriate points to allow pressure measuring, flow control, sampling, etc.

Production and Analytical System

Figure 7-9 shows the outlet flow arrangement of the reservoir model. Back pressure on the system was held constant by the use of a spring controlled back pressure regulator (Figure 7-10).

The produced liquid was collected in a graduated cylinder. Produced gas was metered by a wet test gas meter after passing through a silica gel.

Analysis of the collected vapor samples was facilitated by the use of temperature programmable gas chromatograph (Figure 7-11). A 5 cc sample was injected (using helium as a carrier gas) into a 30' x 1/8" column packed with 30% DC - 200/500 on Chromosorb P.A.W. 60-80.

Materials

The porous medium was clean Oklahoma sand number 1 with 100 mesh size. The oil utilized on each of the experiment runs was a light crude oil with a stock tank gravity of 40° API. The natural gas and crude oil used in this investigation was produced from South Lone Elm Cleveland Sand Unit, Nobel County, Oklahoma, operated by Tenneco Oil Company

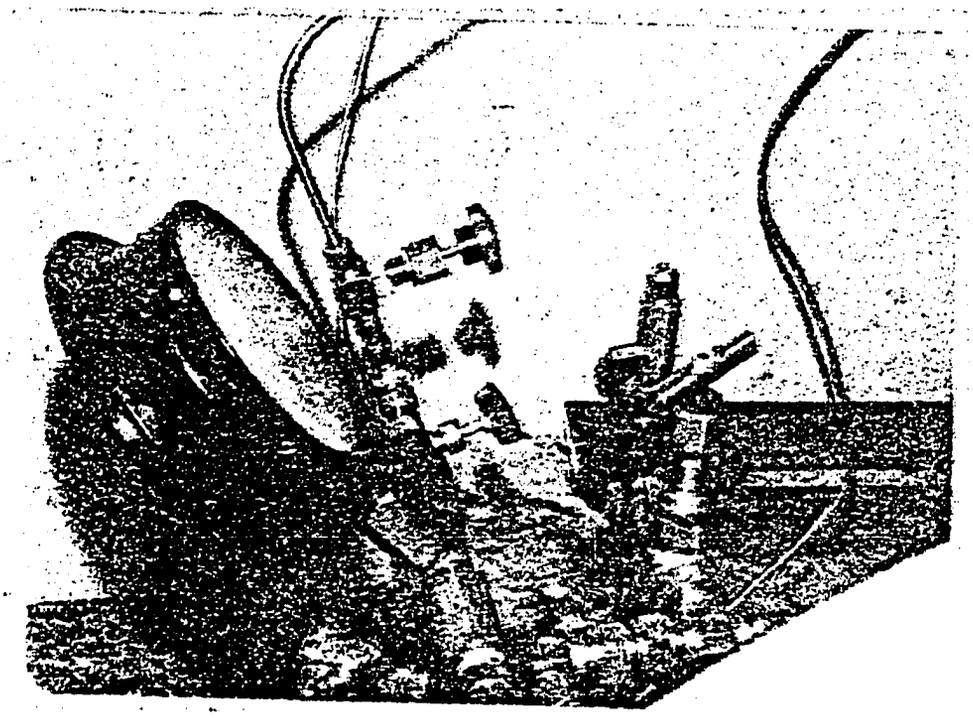

Figure 7-8. BACK VIEW OF THE SAMPLING VALVE

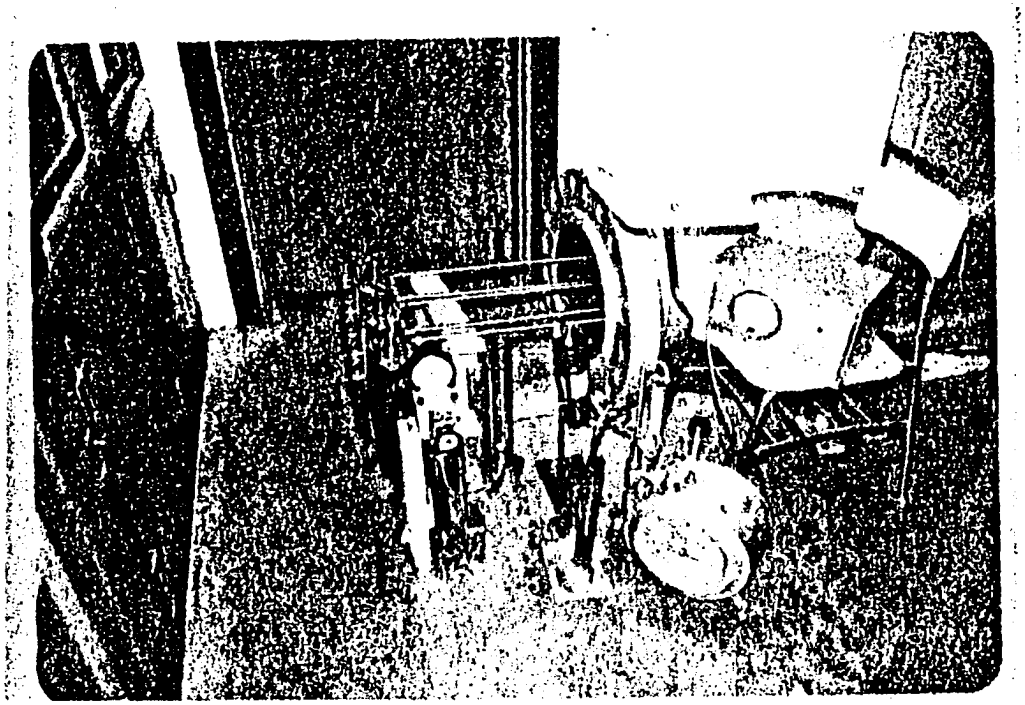

Figure 7-9. SIDE VIEW OF THE OUTLET END OF THE CORE

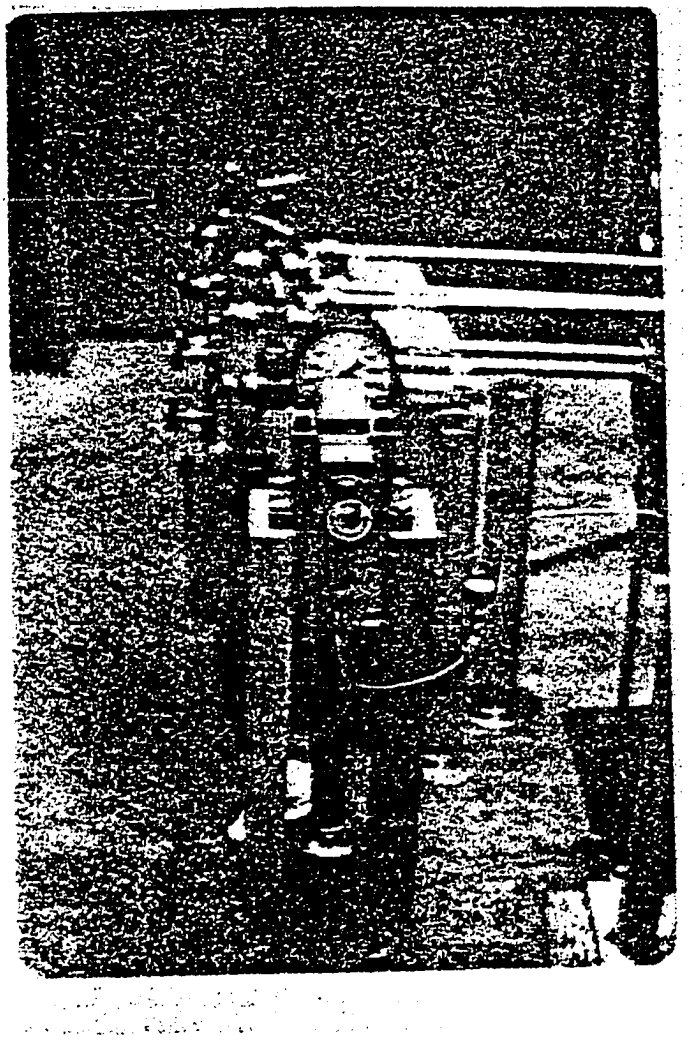

Figure 7-10. FRONT VIEW OF THE BACK PRESSURE REGULATOR

Figure 7-11. FRONT VIEW OF THE GAS CHROMATOGRAPH

(Figure 7-12). Other pertinent properties of this oil and analysis of natural gas used are shown in Table 7-1 and Table 7-2, respectively.

TABLE 7-1

PROPERTIES OF OIL

1.	Stock Tank Oil Gravity	43° API
2.	Viscosity of Oil at 70°F and 14.7 psi	3.0 cp
3.	Saturation Pressure	1700 psi
4.	Solution Gas-Oil Ratio	575 scf/STB
5.	Formation Volume Factor at 2000 psi and 70°F	1.32 bbl/STB
6.	Molecular Weight of Stock Tank Oil	214.5

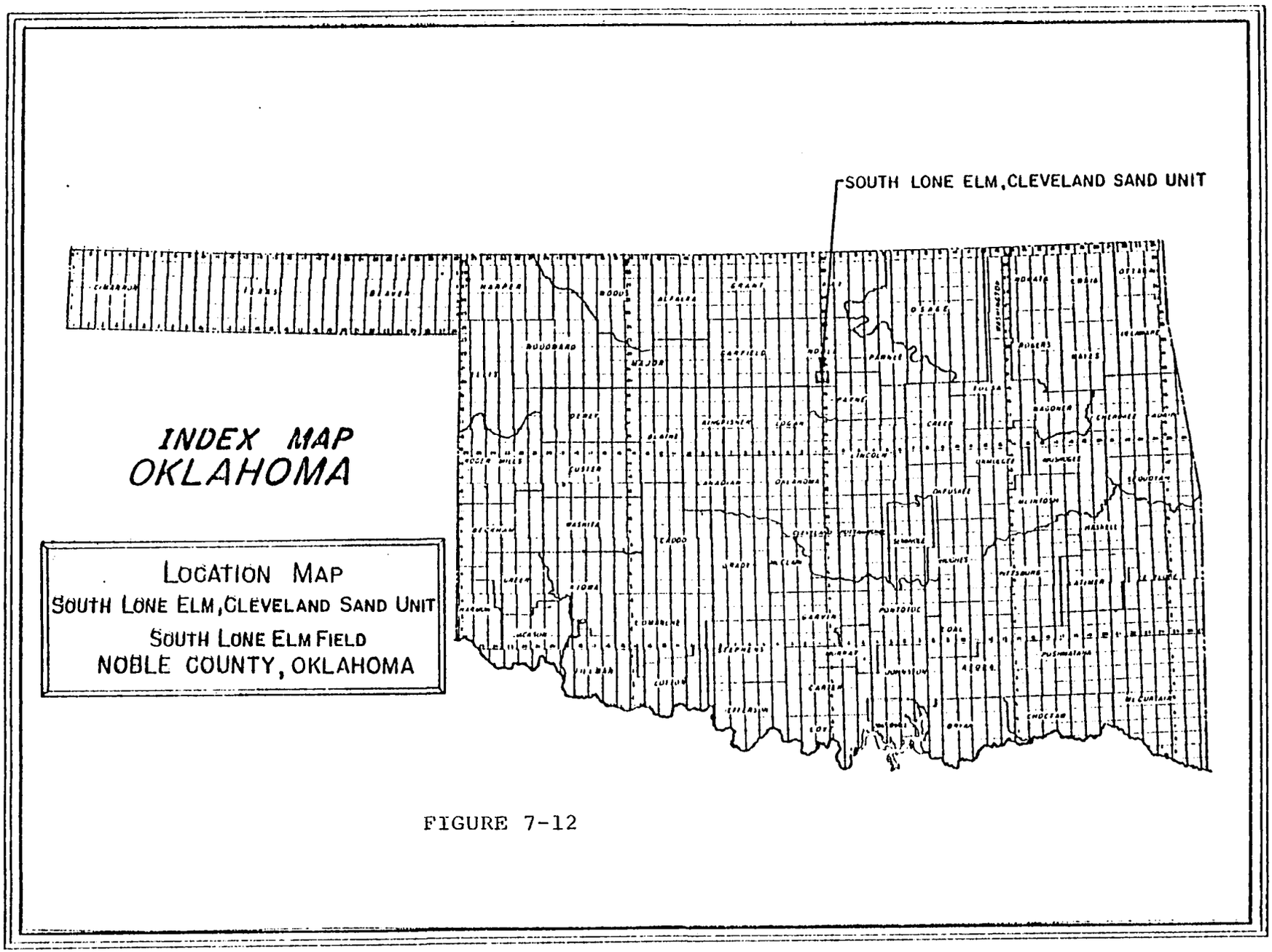
SOUTH LONE ELM, CLEVELAND SAND UNIT
INDEX MAP
OKLAHOMA
LOCATION MAP
SOUTH LONE ELM, CLEVELAND SAND UNIT
SOUTH LONE ELM FIELD
NOBLE COUNTY, OKLAHOMA

FIGURE 7-12

TABLE 7-2

ANALYSIS OF NATURAL GAS[1]

Component	Mole %
Methane	.656
Ethane	.155
Propane	.133
Butane	.024
Pentane	.035

Mol. wt. of gas = 24.97

Gas gravity = .862

[1]South Lone Elm Field

CHAPTER VIII

EXPERIMENTAL PROCEDURE

For purposes of illustration, the experimental procedure may be divided into the three steps:

- Recombination process
- Saturating and displacing process, and
- Recording and sampling analysis process

Recombination Process

The preparation of reservoir oil samples used in this experimental investigation began with the recombination of the stock tank oil with a natural gas sample. A high pressure cell (Figure 8-1) of 400 cm^3 was used to facilitate the recombination. In reference to Figure 8-1, the top of the recombine cell was connected to the water pump, oil graduated cylinder, and the inlet of the reservoir model through 1/8 inch stainless-steel tubing. The tubing was fitted with three (A, B, C) 1/8 inch Hoke needle valves.

The bottom of the recombine cell was connected to a mercury, vacuum, and gas pumps through 1/8" stainless-steel tubing fitted with three 1/8" valves (D, E, F).

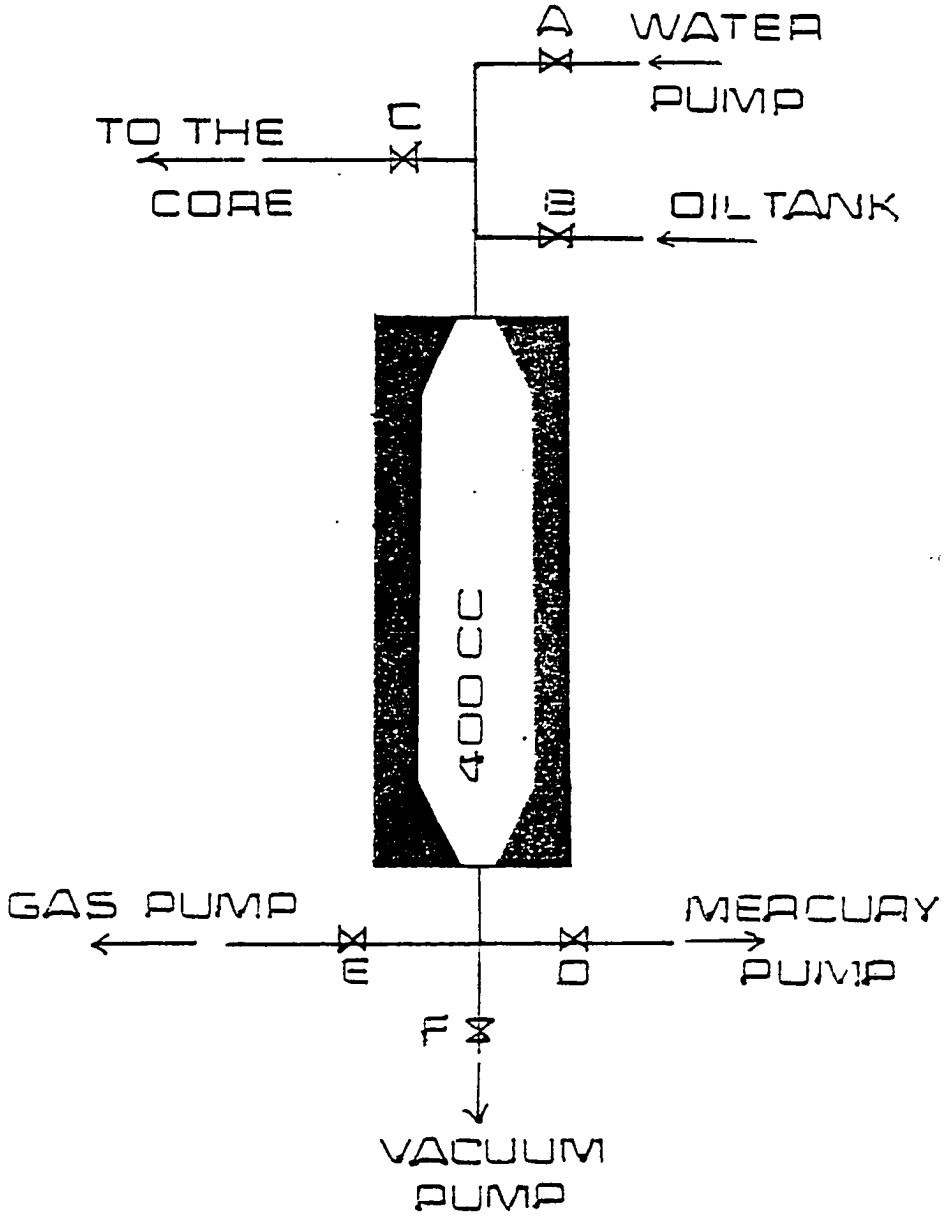

Figure 8-1. SCHEMATIC DIAGRAM OF THE RECOMBINE CELL

As standard procedure, the recombination was accomplished as follows:

1. Before each recombination run, a vacuum was pulled in the cell for 20 minutes, after which the bottom valve, F, was closed and the vacuum pump turned off.

2. The top valve, B, was then opened until the cell was charged with 120 cc stock tank oil.

3. The natural gas was then injected into the cell by turning on the gas pump and opening the bottom valve, E.

4. Valve E was then closed and the gas pump turned off when the pressure inside the cell reached 600 psi.

5. Oil and gas mixture was then pressurized by mercury to 2000 psi from the mercury pump (notice that the saturation pressure was 1700 psi). By following the previous standard procedure, the estimated initial solution gas-oil ratio was 575 scf/STB.

Saturating and Displacing Process

Saturation Procedure

In preparation for each run, the reservoir was thoroughly cleaned and then charged with water followed by the recombined sample at the desired displacement pressure. The following standard steps (proposed by Rushing[7-9] and modified by the author) were used:

1. The oil reservoir model was cleaned by injection of naphtha into the core.

2. The naphtha was then displaced from the core by nitrogen injection.

3. The core placed on a vaccum for 24 hours. The core was considered clean after these previous steps.

4. Prior to injection of the recombined sample into the reservoir, the recombine cell was charged with water.

5. Water was then displaced into the core by means of mercury pump at the desired run pressure.

6. Pore volume was calculated.

7. With the core now saturated with water, the recombine sample was compressed to run pressure by injected mercury into the base of the recombine cell.

8. The recombine sample was then charged slowly into the reservoir through a valve, H, located at the core inlet (Figure 8-2).

9. Water was bled from the outlet end of the tube as the recombine oil was admitted into the model.

10. The amount of water collected after saturating the core with oil would indicate the valve of the residual water saturation as well as the oil saturation of the core

Displacement Process

Nitrogen, contained in a special high pressure cylinder under 6000 psi, was used for the displacement process. The desired injection pressure for each run was regulated and held constant by a special high pressure gas regulator. The displacement procedure was as follows:

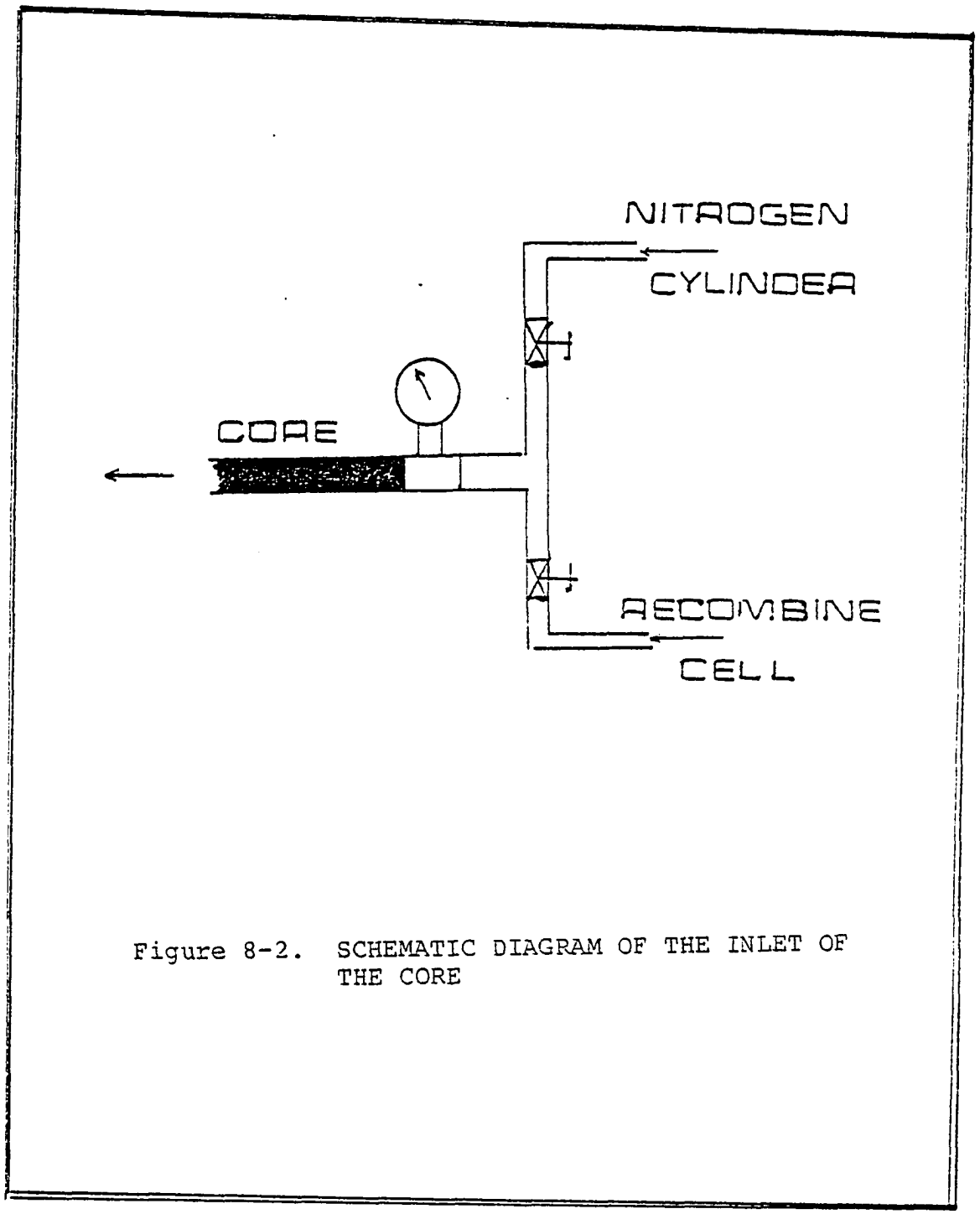

Figure 8-2. SCHEMATIC DIAGRAM OF THE INLET OF THE CORE

1. By setting the nitrogen cylinder regulator to the desired displacing pressure, the nitrogen was injected into the core through valve, G, placed at the inlet of the core (Figure 8-2).

2. A back pressure of 2000 psi was held constant by the backpressure regulator placed at the outlet end of the core.

3. The produced liquid was collected in a graduated cylinder.

4. Nitrogen injection into the reservoir was continued until breakthrough.

Recording and Sampling Analysis Process

The following parameters were recorded during each run:

- Initial oil saturation
- Residual water saturation
- Injection pressure
- Temperature
- Barometric pressure
- Pressure drop
- Time and amount of liquid collected
- Time of breakthrough
- Frontal advance

During the displacement process, vapor samples were taken from five sampling valves located at equal intervals of 24 feet along the length of the reservoir.

The samples were analyzed by means of temperature programmable gas chromatograph. Chapter VI contains a discussion of chromatographic analysis techniques used in this study.

CHAPTER IX

PRESENTATION AND DISCUSSION OF RESULTS

A total of seven runs were conducted primarily to establish and study the compositional changes which take place during the displacing of crude oil by continuous high pressure nitrogen injection.

The results of the flow studies are summarized in Table 9-1. This table identifies the injection pressure, types of displacing fluid, fluid saturations at the start of the runs, and a summary of the production data are also indicated.

First Run

This run was performed at an injection pressure of 4000 psi. During the displacement process, samples of the displacing phase were collected periodically from five sampling points (designated by A, B, C, D and E) and located at equal intervals (24 feet) along the length of the linear core. These samples were analyzed by means of a gas chromatograph. Summary of the analysis is given in Table 9-2.

1) Experimental Composition Profiles

Figures 9-1 through 9-4 show the compositional profiles

TABLE 9-1

RESULTS OF OIL DISPLACEMENT BY NITROGEN AND WATER INJECTION

Run No.	Type of Displ. Fluid	Injection Pressure, psi	Solution G.O.R. SCFISTB	Initial Oil Saturation	Initial Water Saturation	Initial Stock Tank Oil in Place CC	Oil Recovery at B.T., % of Stock Tank I.O.I.P.
1	N_2	4000	575	.756	.244	698	80
2	N_2	5000	575	.75	.25	692	86
3	N_2	3000	575	.732	.268	676	54
4	N_2	3700	575	.743	.257	686	72
5	H_2O	variable	575	.76	.24	702	65
6	N_2	4000	575	.266	.734	246	13
7	N_2	5000	0	.75	.25	900	59

TABLE 9-2

MOLAR COMPOSITION OF THE COLLECTED SAMPLES

P.V.N_2 inj. → / Comp. ↓	Sampling Point A		Sampling Point B				Sampling Point C					Sampling Point D			
	.14	.29	.33	.42	.46	.57	.53	.57	.62	.64	.70	.72 to .8	.815	.83	.9
N_2	50.5	85	35.8	47	56	96.2	20.5	22.8	26.04	38.8	88.8	7.2	21	34.05	85.35
C_1	35.2	10.8	40.0	30.6	23	3.0	45.5	44	41.6	35	5	55	47	40	9.5
C_2	5.4	1.6	10.2	9.8	9.55	.5	11.9	11.8	11.68	9.9	3.75	13	11.45	9.7	2.95
C_3	3.9	1.3	6.95	6.9	6.8	.1	9.45	9.38	9.3	7.7	1.7	10.9	9.25	7.7	1.6
C_4	.9	.1	1.15	6.9	.25	0	2.0	1.7	1.42	.7	0	2.1	1.45	.8	0
C_5	1.5	.3	1.9	1.1	.5	0	2.6	2.35	2.1	1.4	0	2.9	2.3	1.65	0
C_{6+}	2.6	.9	4.0	3.9	3.9	.2	8.05	7.97	7.86	6.5	.75	8.9	7.55	6.1	0

RUN #1

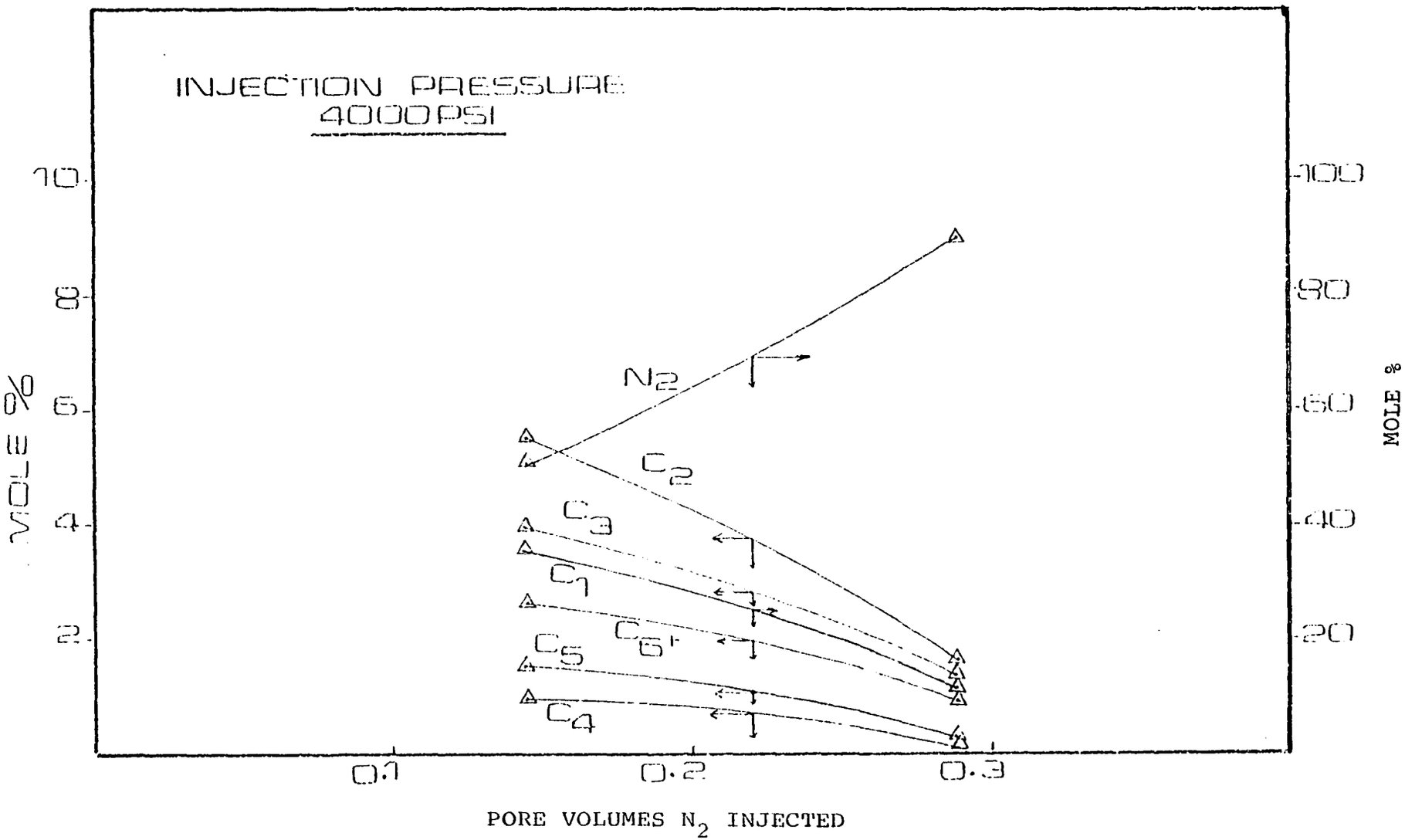

Figure 9-1. Composition of vapor phase samples taken from sampling point "A" vs. pore volumes N_2 injected

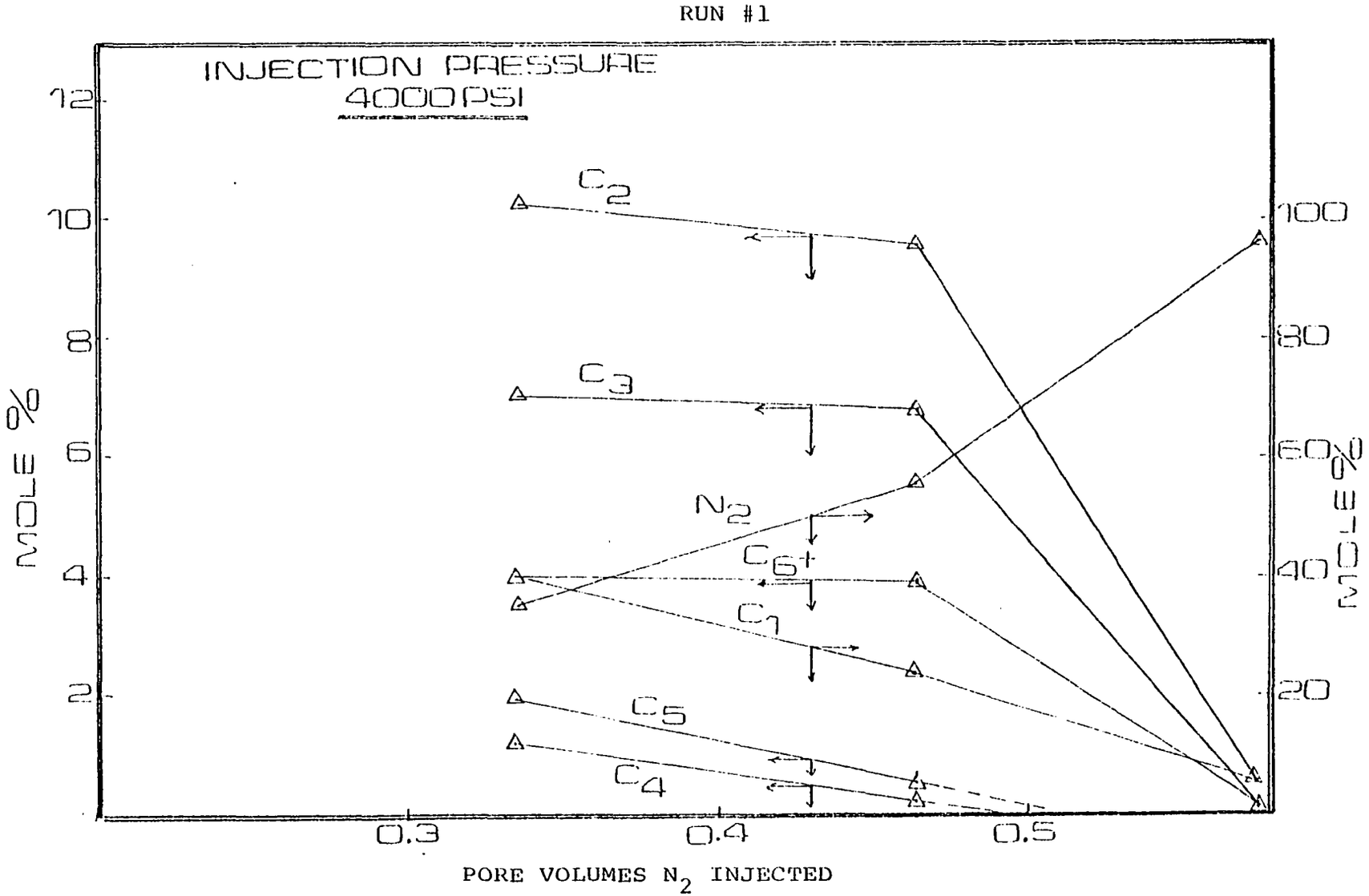

Figure 9-2. Composition of vapor phase samples taken from sampling point "B" vs. pore volumes N_2 injected

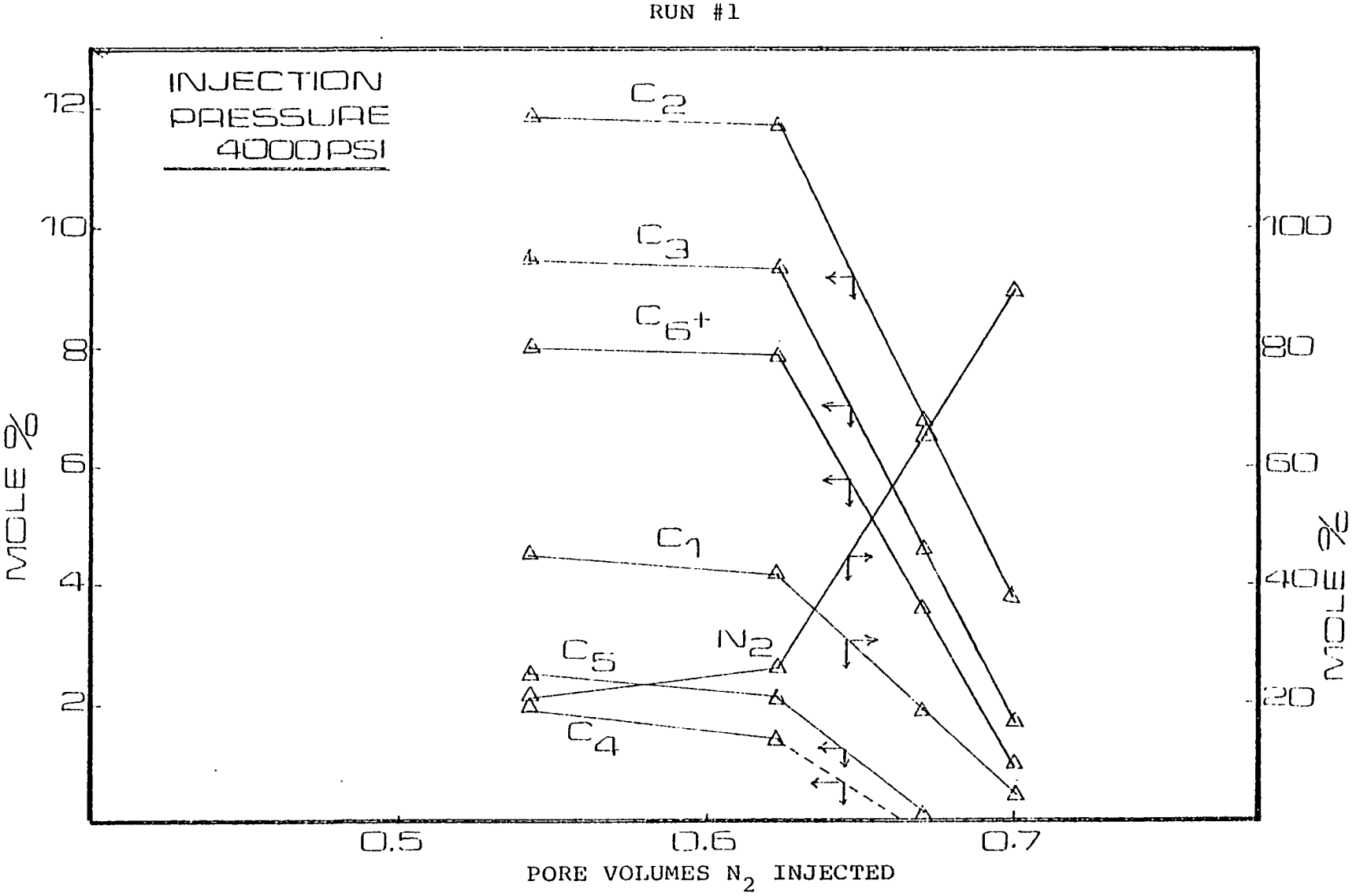

Figure 9-3. Composition of vapor phase samples taken from sampling point "C" vs. pore volumes N_2 injected

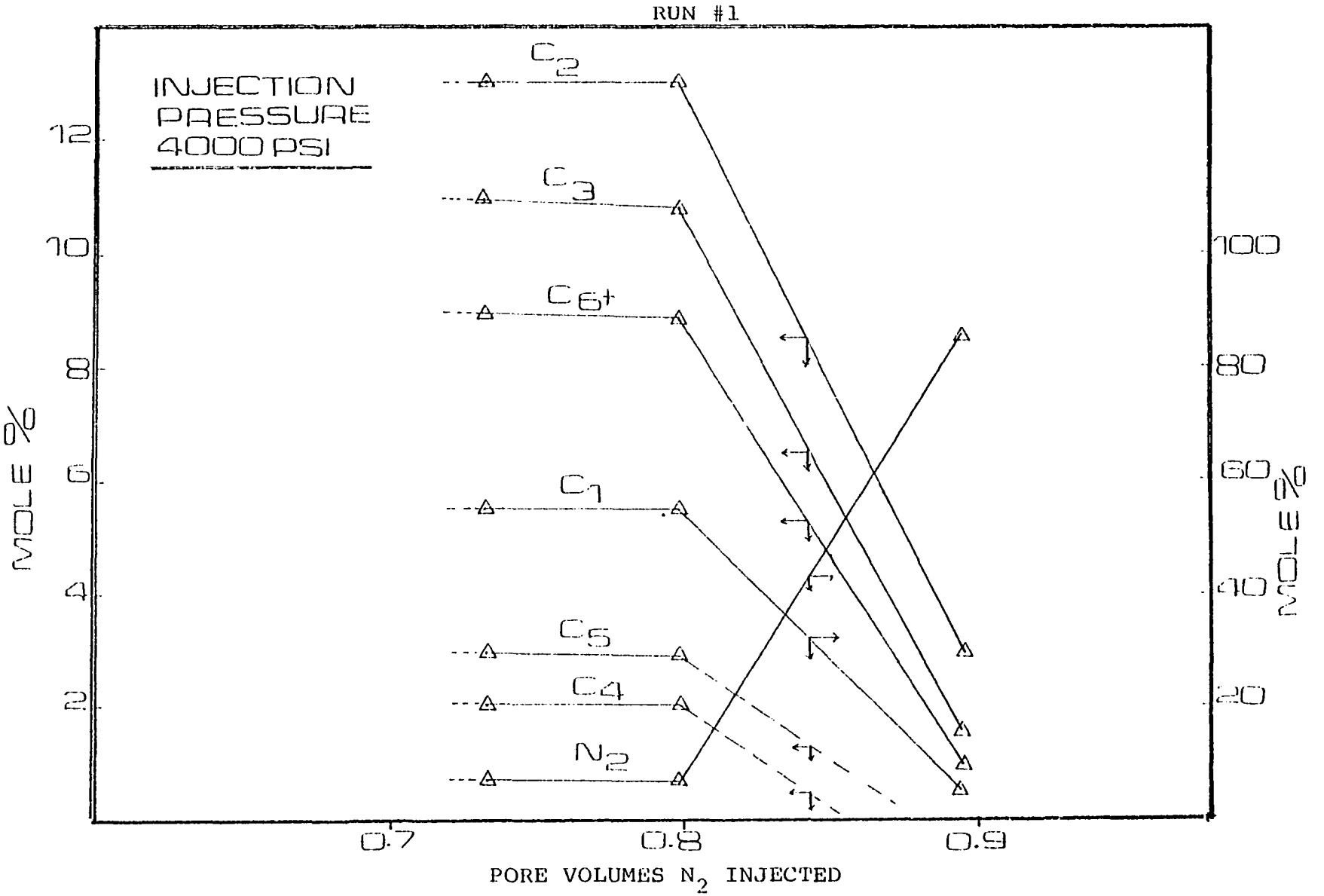

Figure 9-4. Composition of vapor phase samples taken from sampling point "D" vs. pore volumes N_2 injected

for each component of the displacing phase as a function of the distance from the injection point and pore volumes nitrogen injected.

Analysis of the figures show that:

a) The primary displacement mechanism or mass transfer was a stripping (vaporization) process. A clear indication of vaporization can be obtained by observing the continuous enrichment of nitrogen with the intermediate components (C_1-C_5) and C_{6+} .

b) The maximum composition of these components occurred at the flood front, which indicated that if miscibility was to develop it would do so at this point.

c) By the time the injected nitrogen reached sampling point "D" at a distance of 96 feet from the injection point, it developed a "SLUG" of enriched gas (as it is shown in Figure 9-4). The total volume of this slug was approximately 8 percent of the pore volume with the composition shown in Table 9-3.

d) All curves of the compositional profiles are characterized by two distinct phases:

i) The initial phase is indicated by the section of the plots with a lower slope. This phase represented a "slug build-up process." This process was continued until there was no change in the composition of the slug as it reached sampling point D at a distance of 96 feet from the injection point.

ii) The second phase is the steep section of the

TABLE 9-3

MOLAR COMPOSITION OF THE GENERATED SLUG

COMPONENT	COMPOSITION MOLE %
N_2	8.6
C_1	55
C_2	12.8
C_3	10.7
C_4	2.0
C_5	2.8
C_{6+}	8.9

curves. This section represented a "transition zone" which consisted of gases ranging from very rich gas to pure nitrogen.

Figure 9-5 shows the compositional distribution of the displacing phase throughout the core. It is recognizable by examining this figure that the displacing phase (nitrogen) was continually enriched by stripping intermediate components from the liquid phase. This enrichment of the vapor continued until miscibility (critical composition) was reached. This critical composition was formed in the region of 72% to 80% N_2 (as it is indicated by the flat section of the curves).

Figure 9-6 shows the total enrichment process of the vapor phase with (C_2-C_{6+}) components as it progressed in the reservoir. Notice that the rate of enrichment decreased as the composition of the displacing phase moved closer to the critical composition.

2) Composite Ternary Diagram

One purpose of this investigation was to see if the ternary phase diagram could be used to predict with reasonable accuracy the conditions necessary for miscible displacements with actual reservoir systems.

In this study the complex, multicomponent hydrocarbon systems were arbitrarily divided into three groups: N_2, C_1 through C_5, and C_{6+}. This division was practical from an analytical point of view and also showed the importance of the intermediate components C_1 through C_5, and C_{6+} in the high pressure nitrogen injection process.

RUN #1

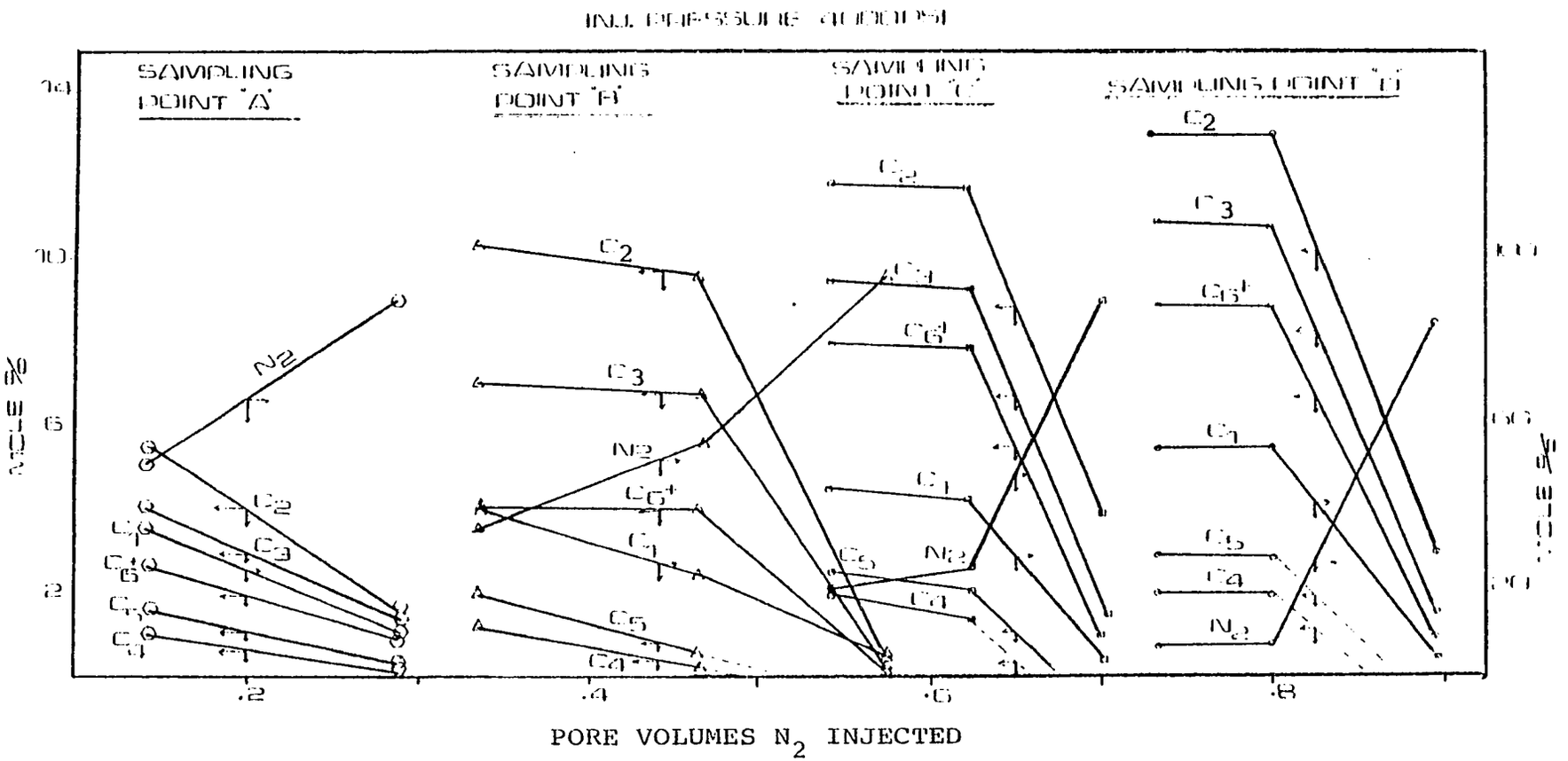

Figure 9-5. Compositional distribution of vapor phase throughout the core vs. pore volumes N_2 injected

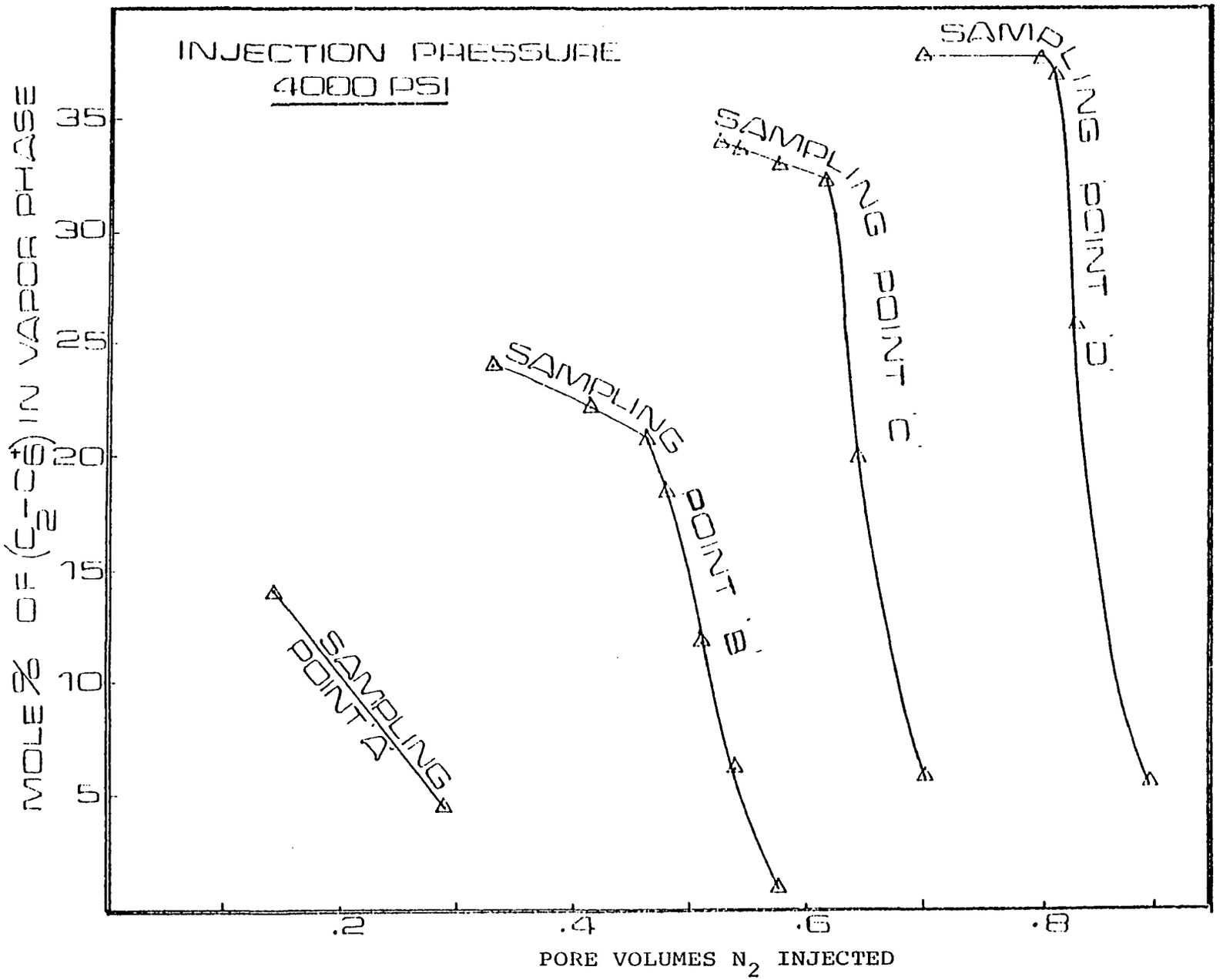

Figure 9-6. Overall composition of (C_2-C_{6+}) in vapor phase throughout the core vs. pore volumes N_2 injected

Through the repeated contacts of the displacing phase and native reservoir fluid, the equilibrium properties of these two phases were continually changed. Since the change in the composition of the displacing phase was regularly monitored, it was possible to determine the composition of the liquid phase by using the K-values.

To construct the ternary diagrams (figures 9-7 through 9-10), three types of data were needed.

(i) Compositions of the displacing phase as a function of: location from the injection point, pressure, and cumulative injected volume of N_2.

(ii) Equilibrium vaporization constants (K-values).

(iii) Compositions of the equilibrium liquid (in contact with the displacing phase).

The first type of data was obtained by collecting and analyzing vapor samples from the five different sampling locations.

The second type of data (K-values) was determined by the method described in Chapter V.

The third type of data (composition of liquid phase) needed to construct the ternary diagrams was estimated by utilizing the following equilibrium relation:

$$x_i = \frac{y_i}{K_i} \qquad (9\text{-}1)$$

where, y_i = mole fraction of ith component in the gas phase.

K_i = equilibrium ratio for ith component.

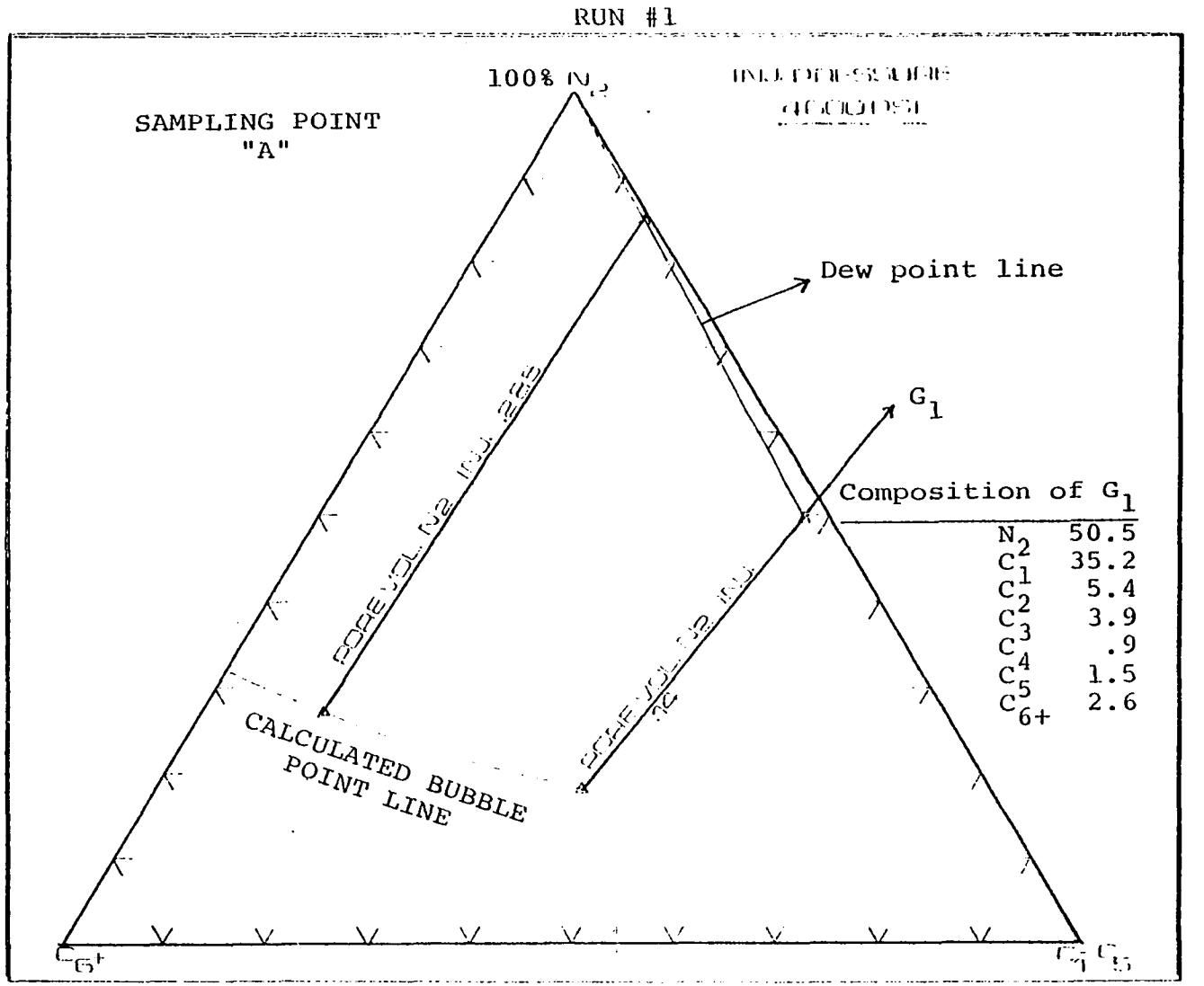

Figure 9-7. Triangular diagram showing changes in composition of vapor and liquid phase

RUN #1

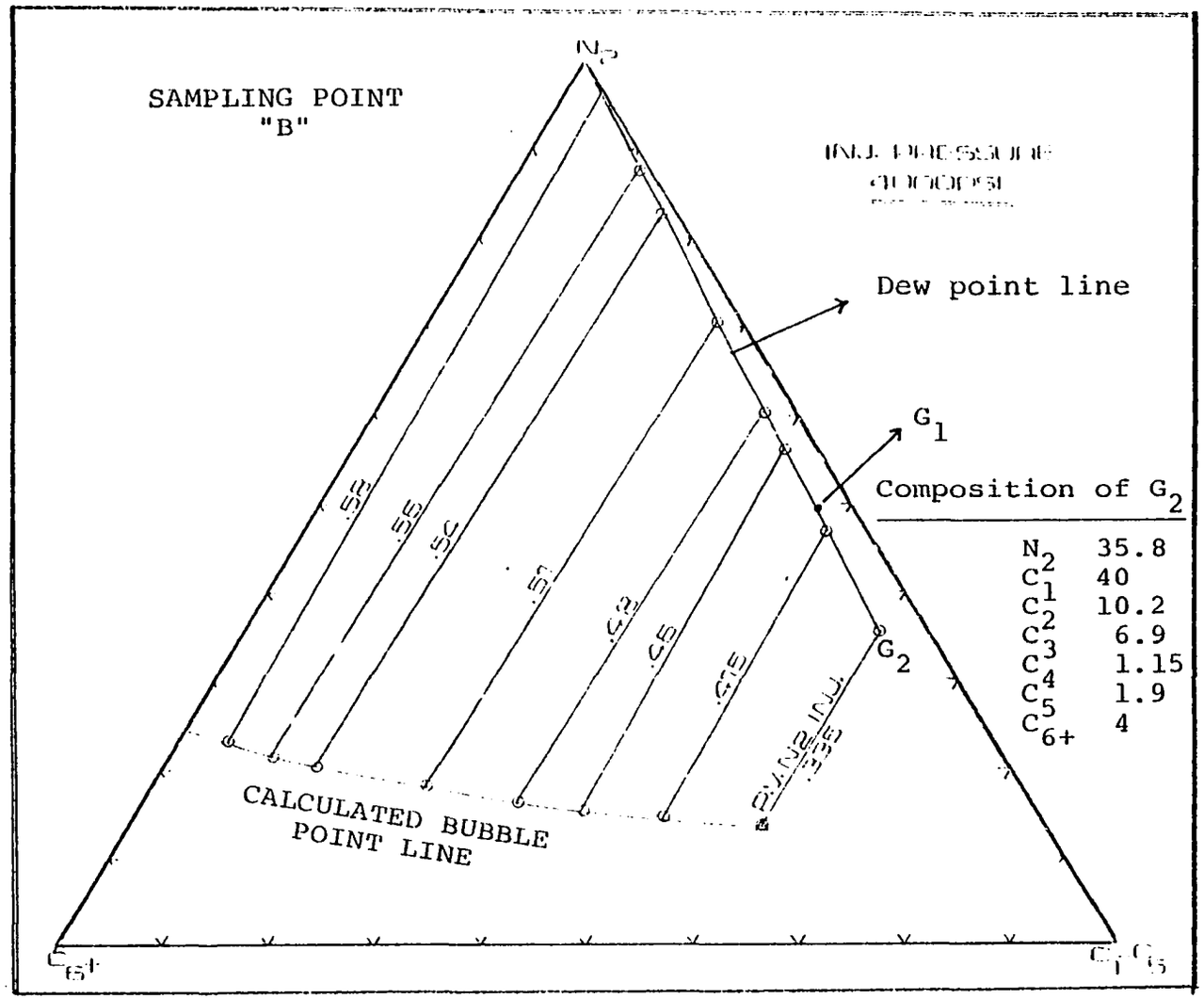

Figure 9-8. Triangular diagram showing changes in composition of vapor and liquid phase

RUN #1

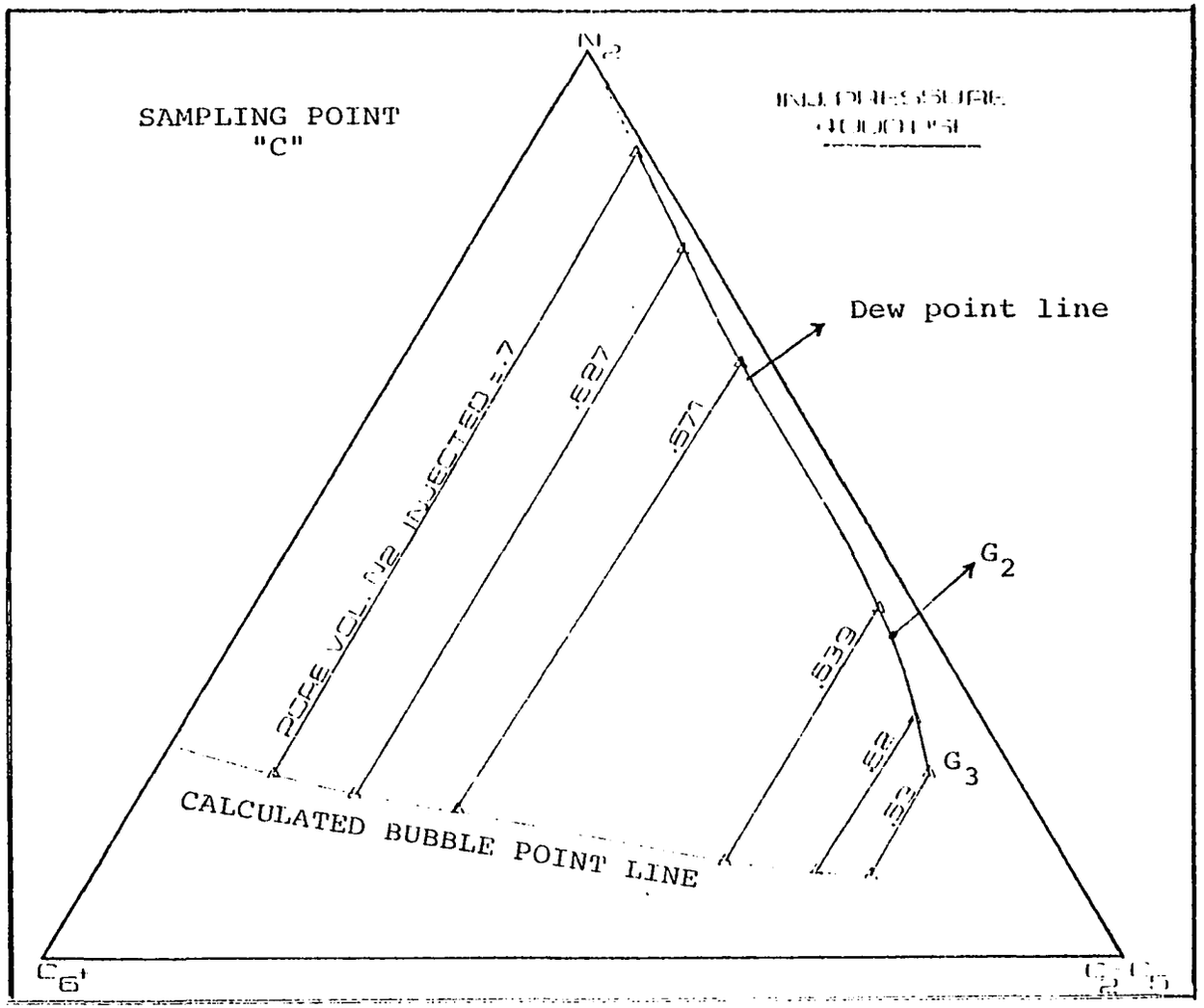

Figure 9-9. Triangular diagram showing changes in composition of vapor and liquid phase

RUN #1

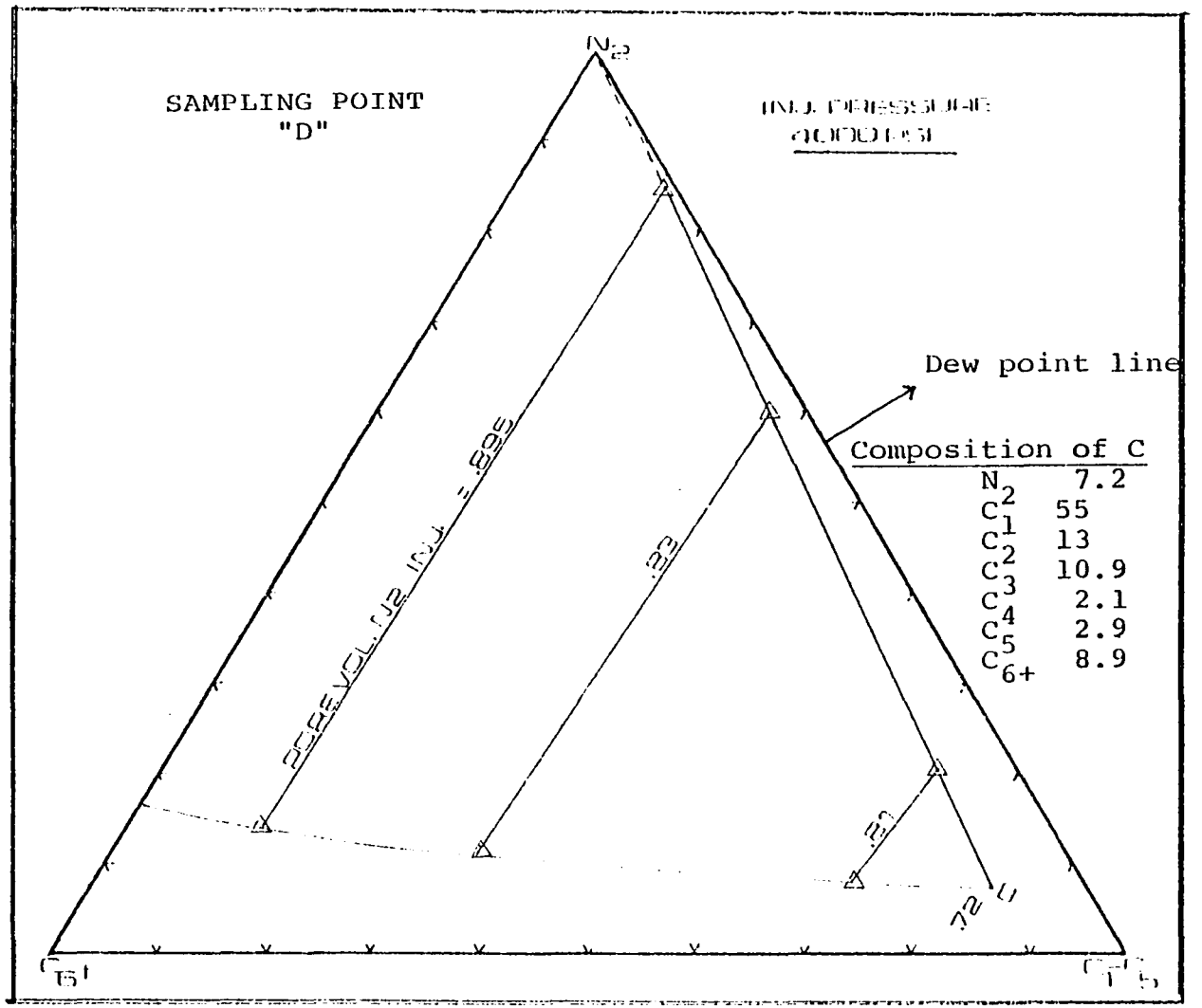

Figure 9-10. Triangular diagram showing changes in composition of vapor and liquid phase

x_i = mole fraction of ith component in the liquid phase.

After repeating several vapor phase sample analyses, a series of equilibrium vapor and liquid compositions were obtained (summary of the results are given in tables A-59 through A-64, Appendix A) and each resultant equilibrium composition was plotted on the ternary diagram as a point. By joining the points representing the equilibrium liquids, the calculated bubble point line was obtained. Then by connecting the points representing the equilibrium gas, the dew point line was constructed.

Point G_1, in Figure 9-7, shows the composition of the vapor phase at the leading edge as it approached sampling point A. As the leading edge, G_1, progressed toward sampling point B, an exchange of the intermediate components between the leading edge and the virgin oil occurred, causing a change in the vapor phase composition (see point G_2 in Figure 9-8).

The previous process was continued until the compositions of the phases in equilibrium at the front approached each other (Figure 9-10) at the critical point* C. At this point a miscible phase displacement was achieved.

3) Vapor and Liquid Phase Properties

With liquid and vapor composition data available, methods discussed in Chapter V were used to calculate the density and viscosity profiles of the displacing and displaced phase.

---

*Critical point is defined as the point at which the vapor and liquid phases become continuously identical.

With the density of the liquid and vapor phase being dependent upon their compositions, it was expected that at every step when a change in composition occurred, the density of the two phases would also change.

Results of density calculations are given in tables A-1 through A-27, Appendix A, and shown in figures 9-11 through 9-15. By examining the figures closely, the author proposes that two processes would occur during the displacement mechanism:

(i) In the generated slug, which has a higher concentration of the intermediate components, it is possible that a phase transfer of the light end components from the slug to the liquid (causing a decrease in the liquid density) can occur. On the other hand, the slug becomes richer in condensable ends which causes an increase in the density of the displacing phase.

(ii) Behind the generated slug, a stripping process could occur in which intermediate components of the liquid phase are transferred to the gas phase. This process was characterized by a sharp break in the liquid and vapor density curves.

The previous process was continued as the slug advanced in the reservoir model until the liquid and vapor density converged at the critical point C (figures 9-14 and 9-15). Figures 9-16 and 9-17 are plots of the calculated liquid and vapor densities as a function of the distance from the injection

RUN #1

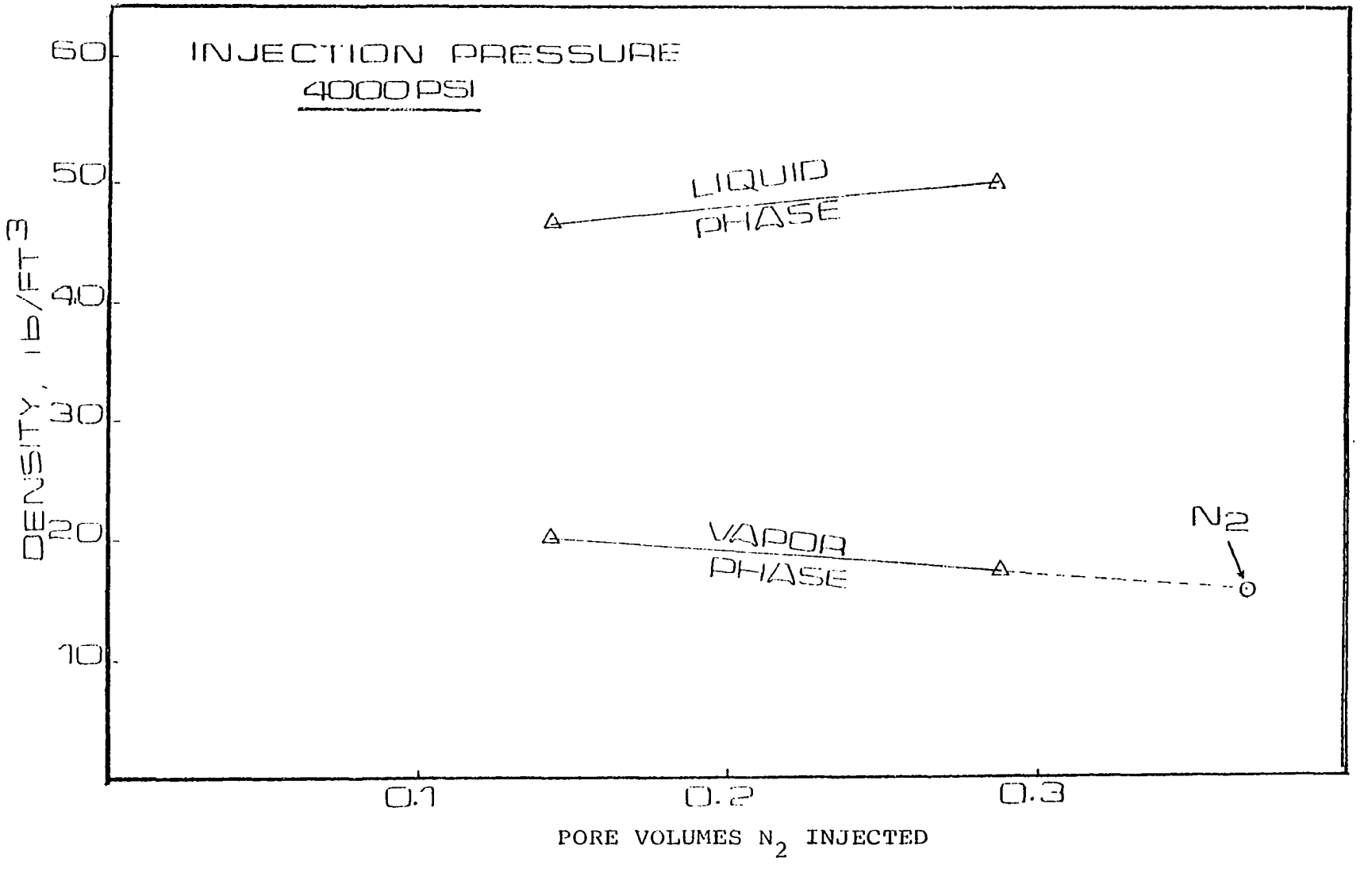

Figure 9-11. Calculated vapor and liquid phase density of samples taken from sampling point "A" vs. pore volumes N_2 injected

RUN #1

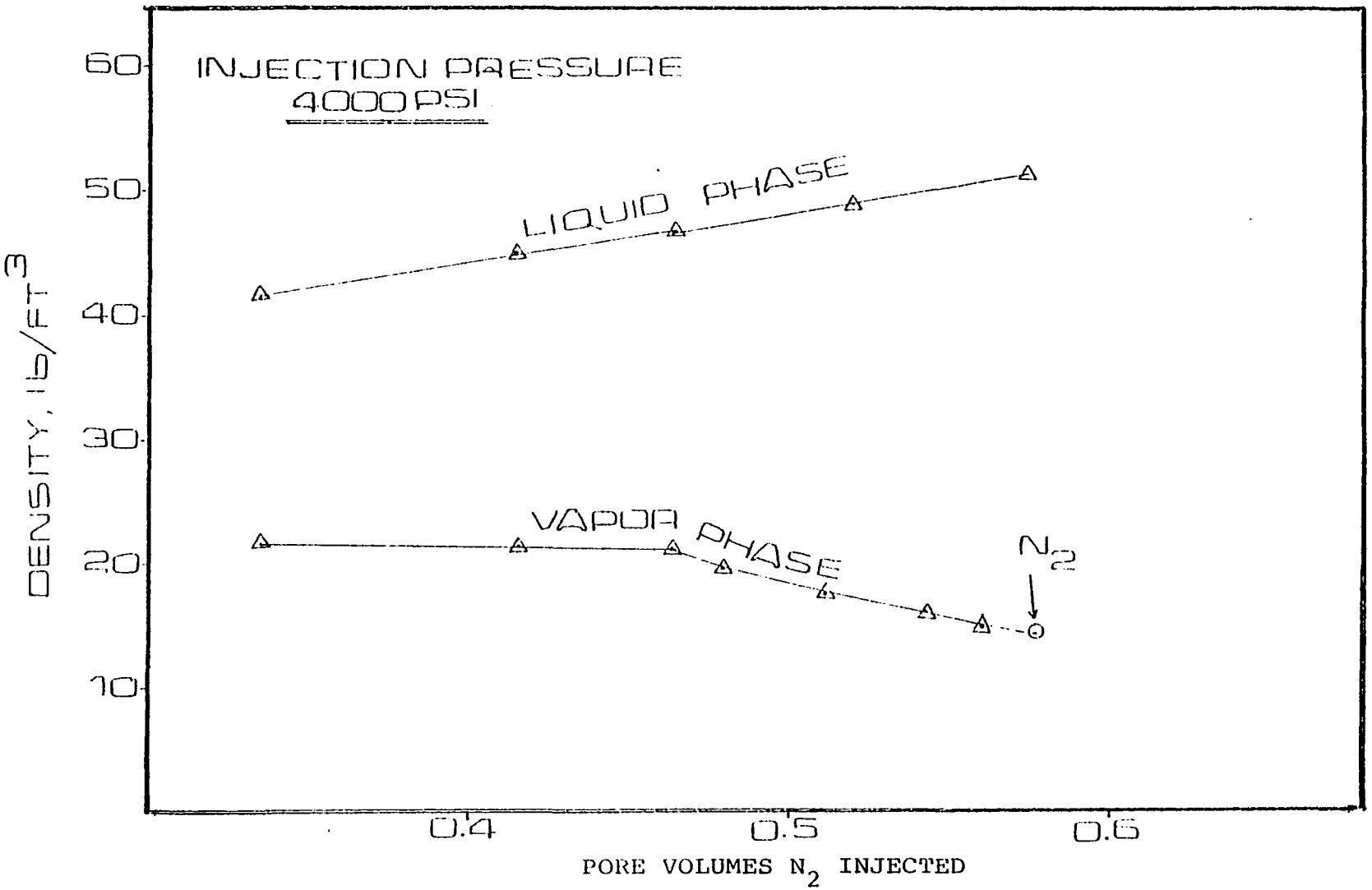

Figure 9-12. Calculated vapor and liquid phase density of samples taken from sampling point "B" vs. pore volumes N_2 injected

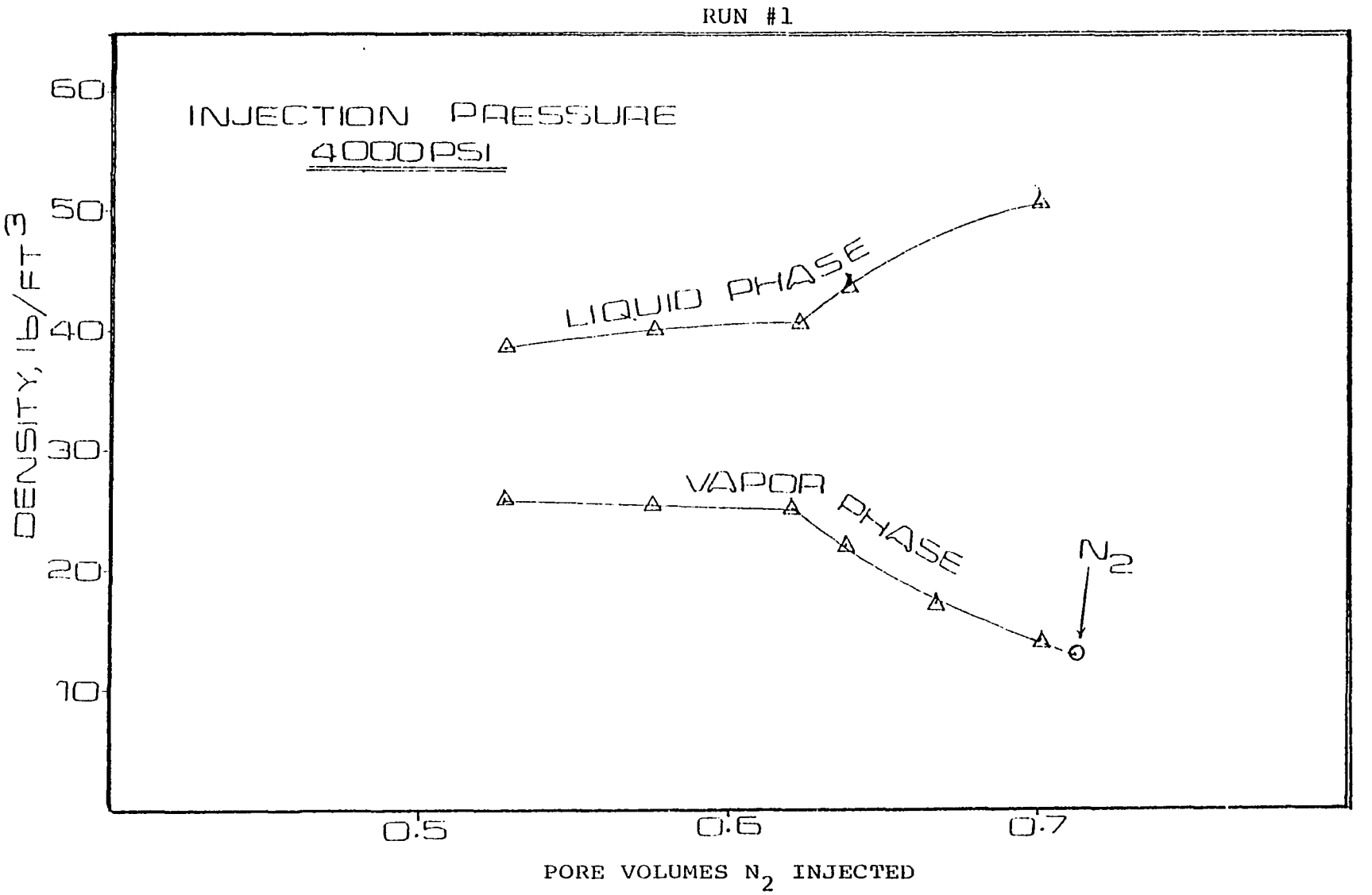

Figure 9-13. Calculated vapor and liquid density of samples taken from sampling point "C" vs. pore volumes N_2 injected

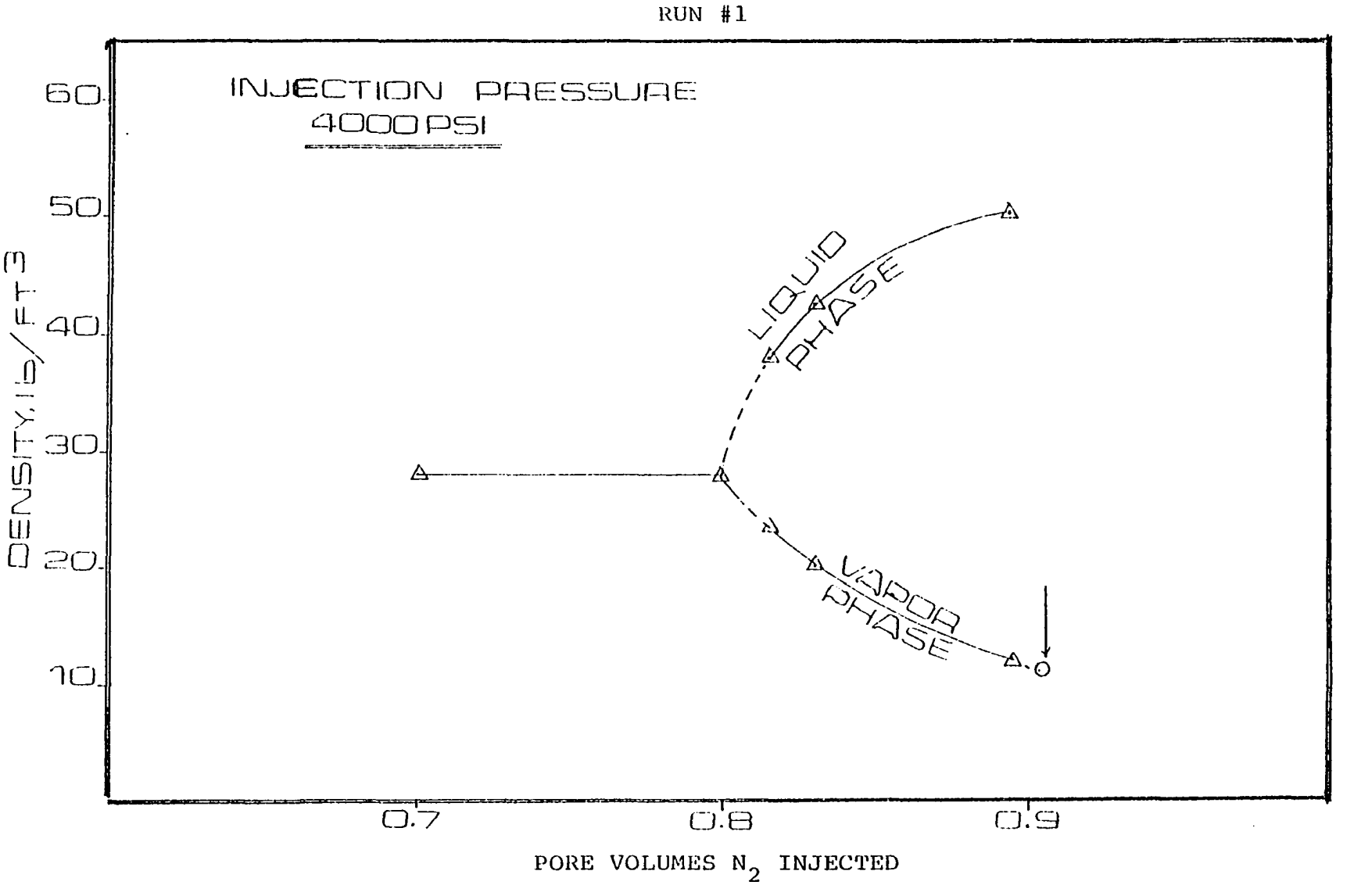

Figure 9-14. Calculated vapor and liquid phase density of samples taken from sampling point "D" vs. pore volumes N_2 injected

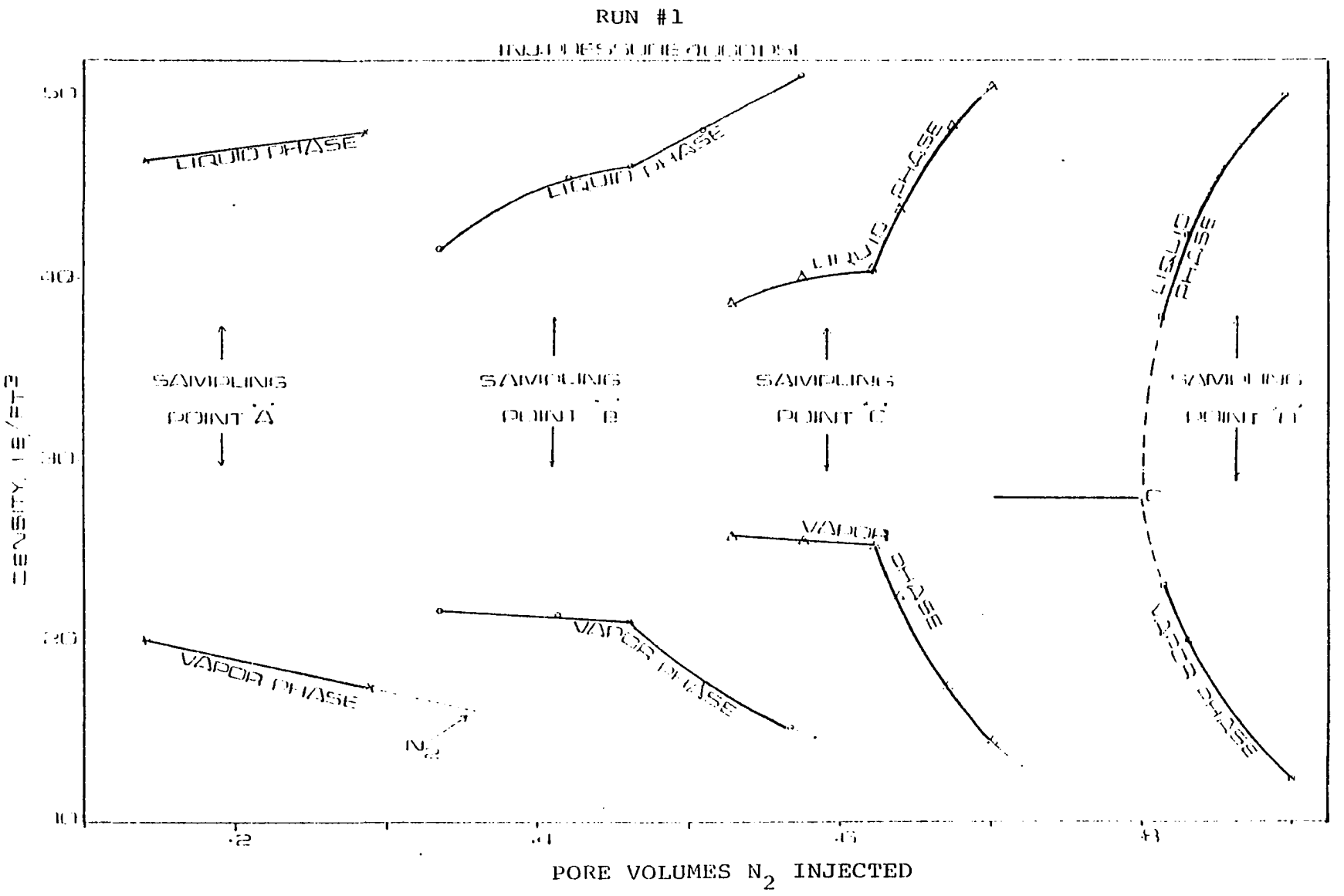

Figure 9-15. Calculated liquid and vapor phase density distribution throughout the core vs. pore volumes N_2 injected

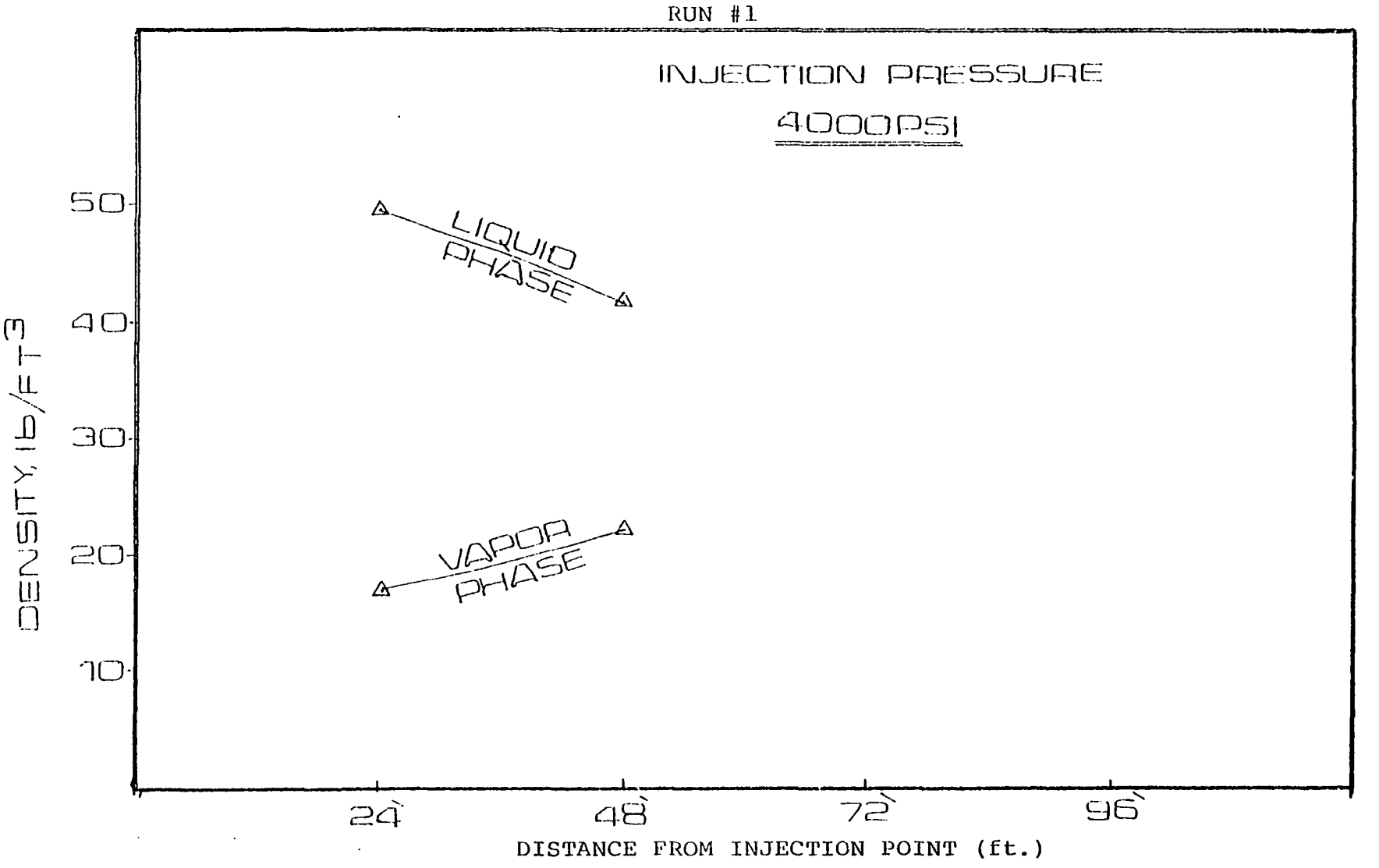

Figure 9-16. Liquid and vapor density profile throughout the core after injection of 0.335 P.V. N_2

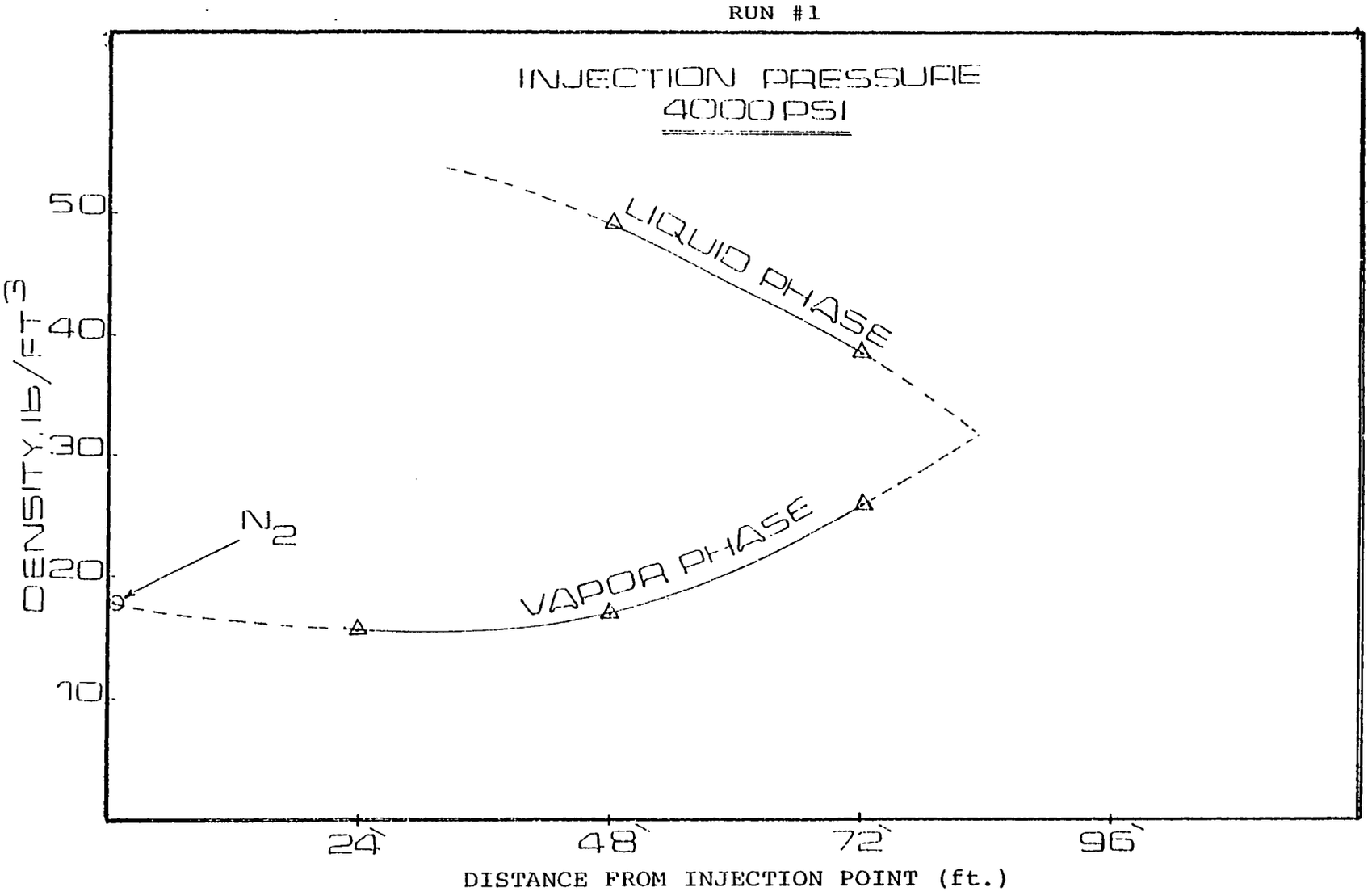

Figure 9-17. Liquid and vapor density profile throughout the core after injection of 0.53 P.V. N_2

point. It shows that miscibility was achieved at approximately 82 feet from the injection point.

The density calculations were followed by a calculation of the viscosity for each composition of the displacing and displaced phase. Methods discussed in Chapter V were used to estimate the viscosities on the basis of knowledge of the composition of the oil and gas phase. Results of the viscosity calculations are given in Table 9-4 and shown in figures 9-18 to 9-22, while a summary of all their results is given in Table A-28 through Table A-54, Appendix A.

Analysis of figures 9-18 to 9-22 show that:

(i) As the critical point was approached along the dew-point curve, the viscosity of the displacing phase was progressively increasing.

(ii) As the critical point was approached along the bubble-point curve, the viscosity of the liquid was continually decreasing, approaching the same value as the displacing phase at the critical point.

These observations again support the author's claim that there exists two combined mechanisms by which the miscibility could be achieved:

(a) In the generated slug, a mutual phase transfer process will occur between the displacing and displaced phase.

(b) Behind the generated slug, a stripping process takes place where the intermediate components are transferred from the liquid phase to the vapor phase.

TABLE 9-4

CALCULATED LIQUID AND GAS VISCOSITY

SAMPLING POINT	A		B				C					D		
N_2 Volume Injected, %p.v.	.14	.29	.33	.42	.46	.57	.53	.57	.62	.64	.7	.815	.83	.9
Gas Viscosity, cp	.03	.016	.034	.033	.0316	.026	.049	.039	.385	.38	.024	.042	.04	.0231
Liquid Viscosity, cp	3.12	2.79	2.36	2.8	2.82	3.09	1.44	1.7	1.86	2.64	3.1	1.06	1.98	3.12

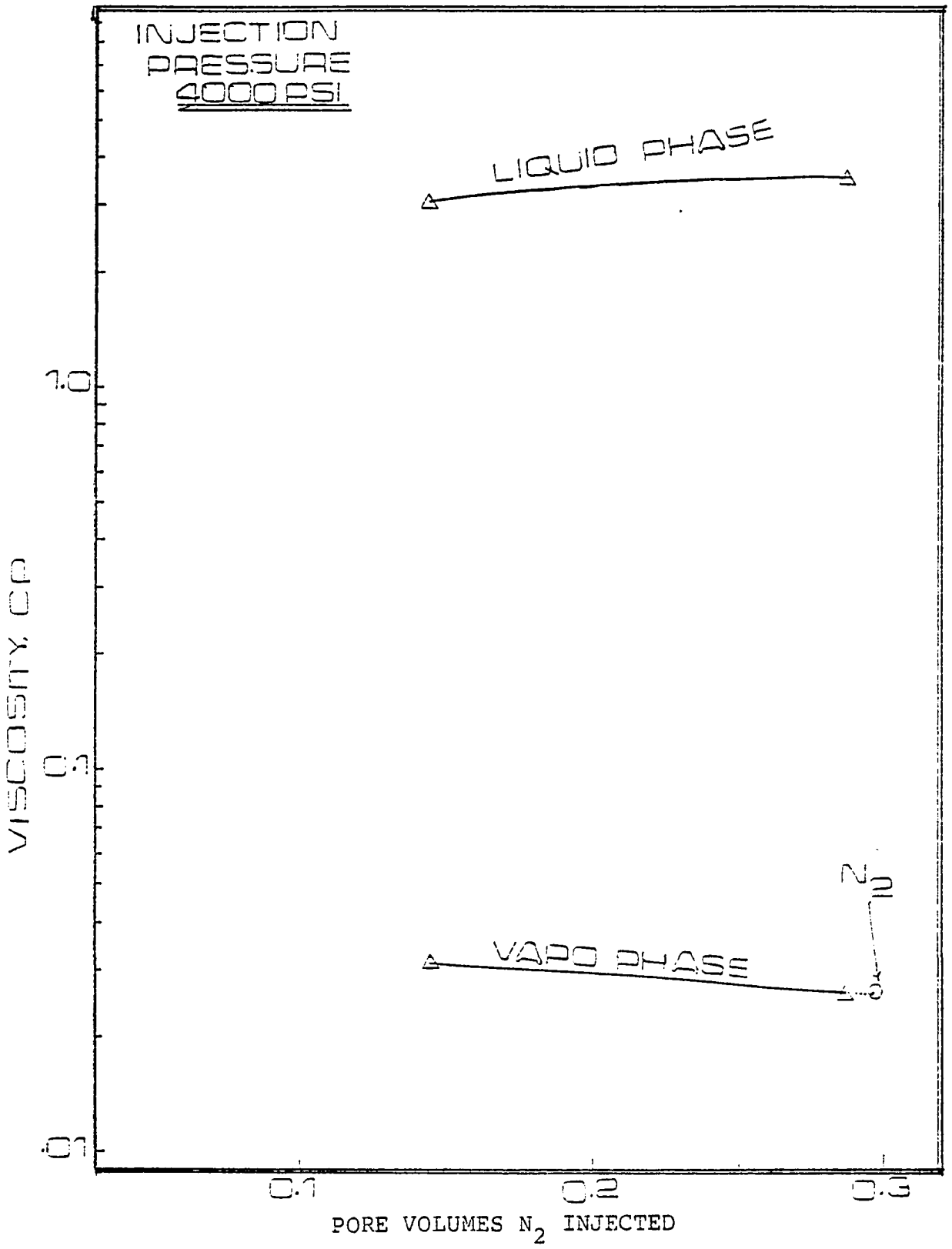

Figure 9-18. Calculated liquid and vapor phase viscosity of samples taken from sampling point "A" vs. pore volumes N_2 injected

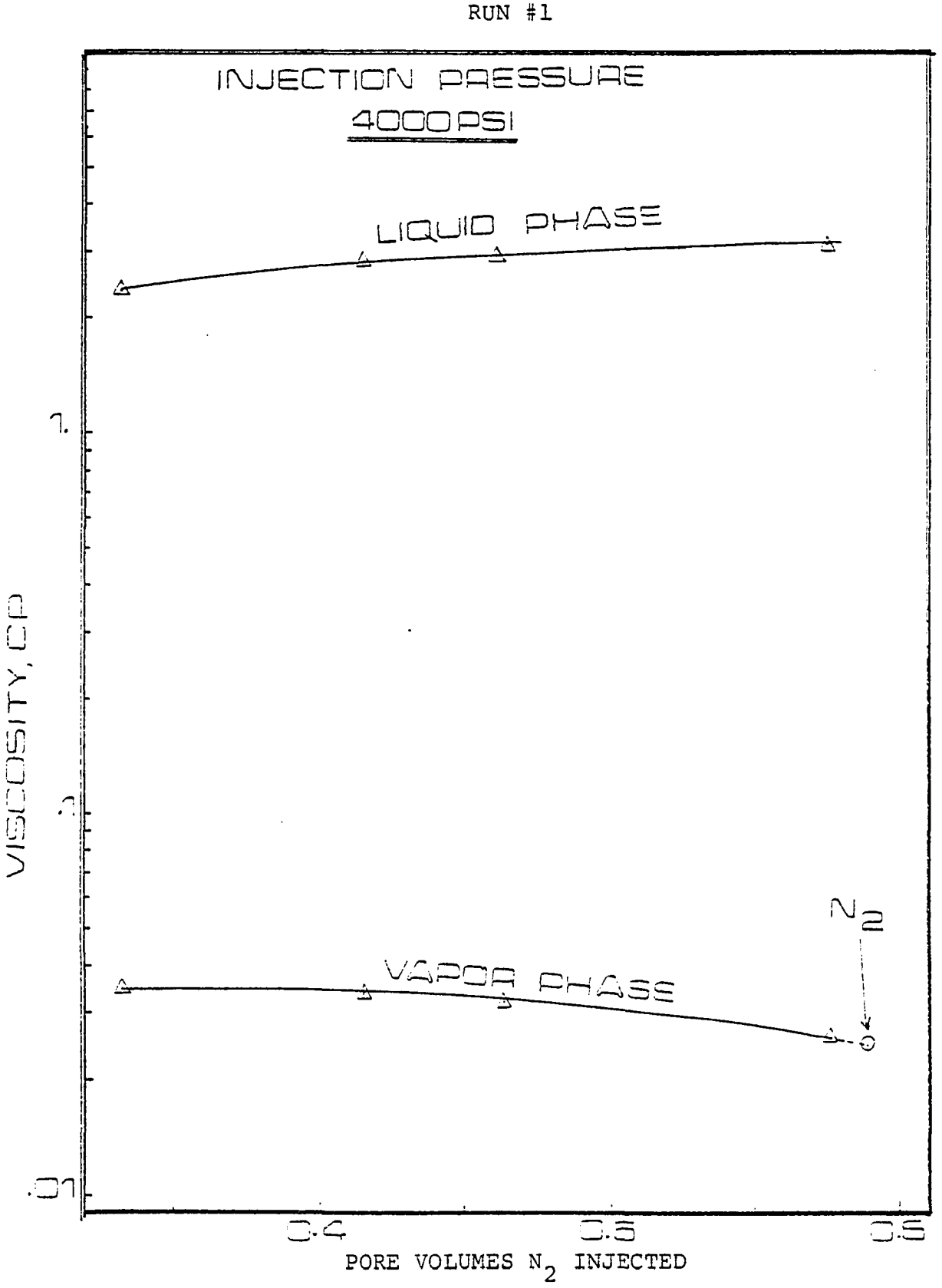

Figure 9-19. Calculated liquid and vapor phase viscosity of samples taken from sampling point "B" vs. pore volumes N_2 injected

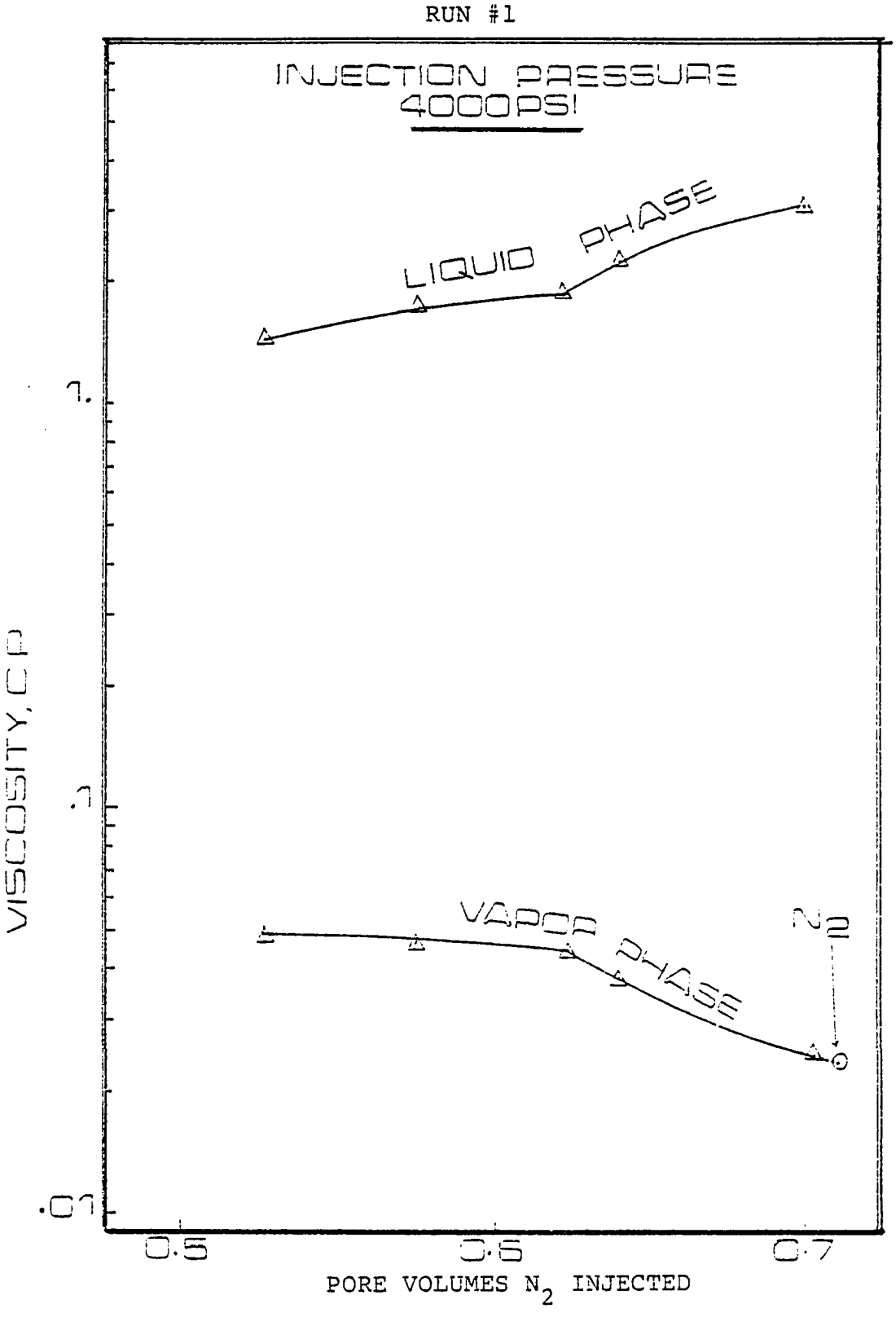

Figure 9-20. Calculated liquid and vapor phase viscosity of samples taken from sampling point "C" vs. pore volumes N_2 injected

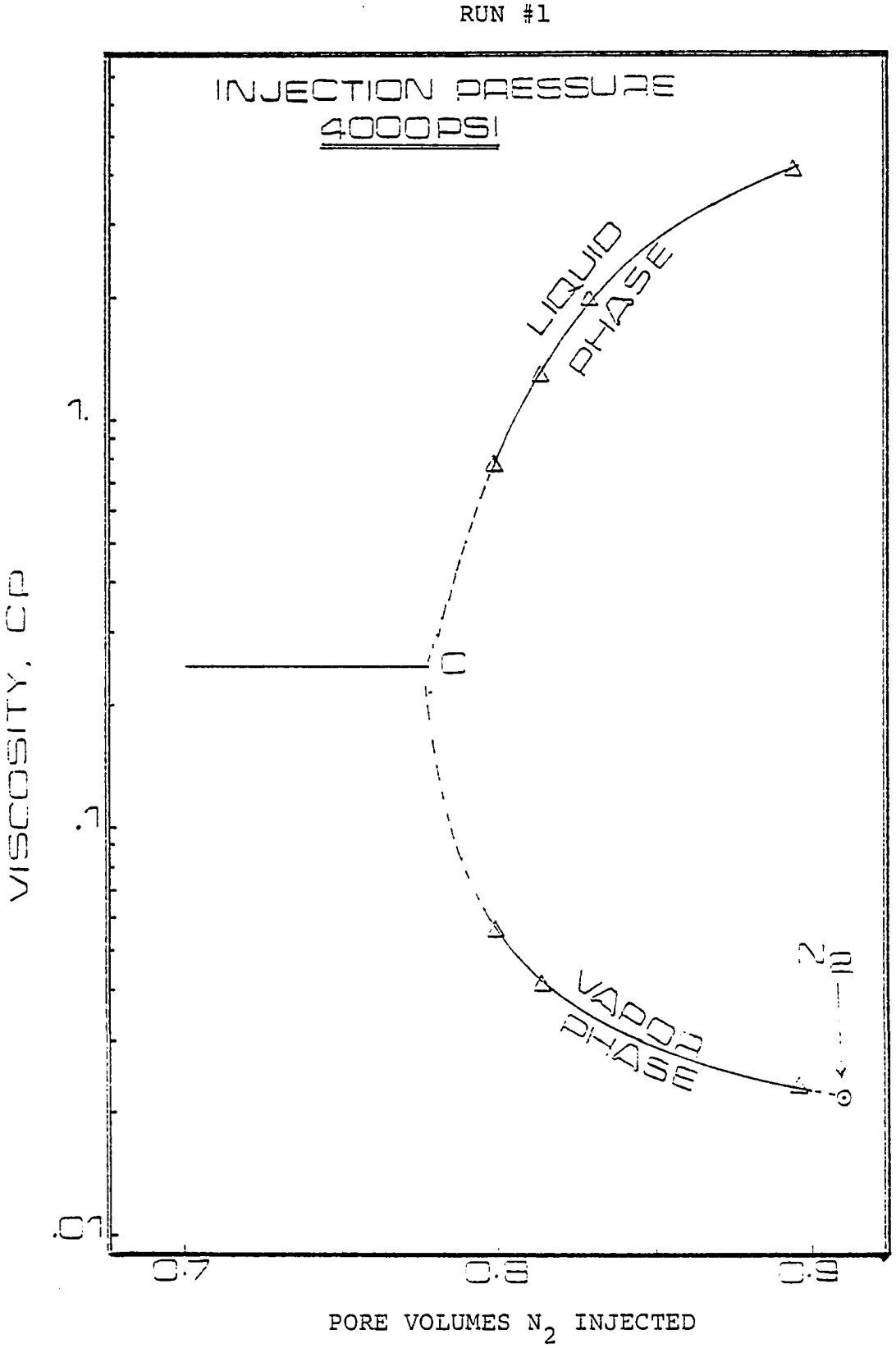

Figure 9-21. Calculated liquid and vapor phase viscosity of samples taken from injection point "D" vs. pore volumes N_2 injected

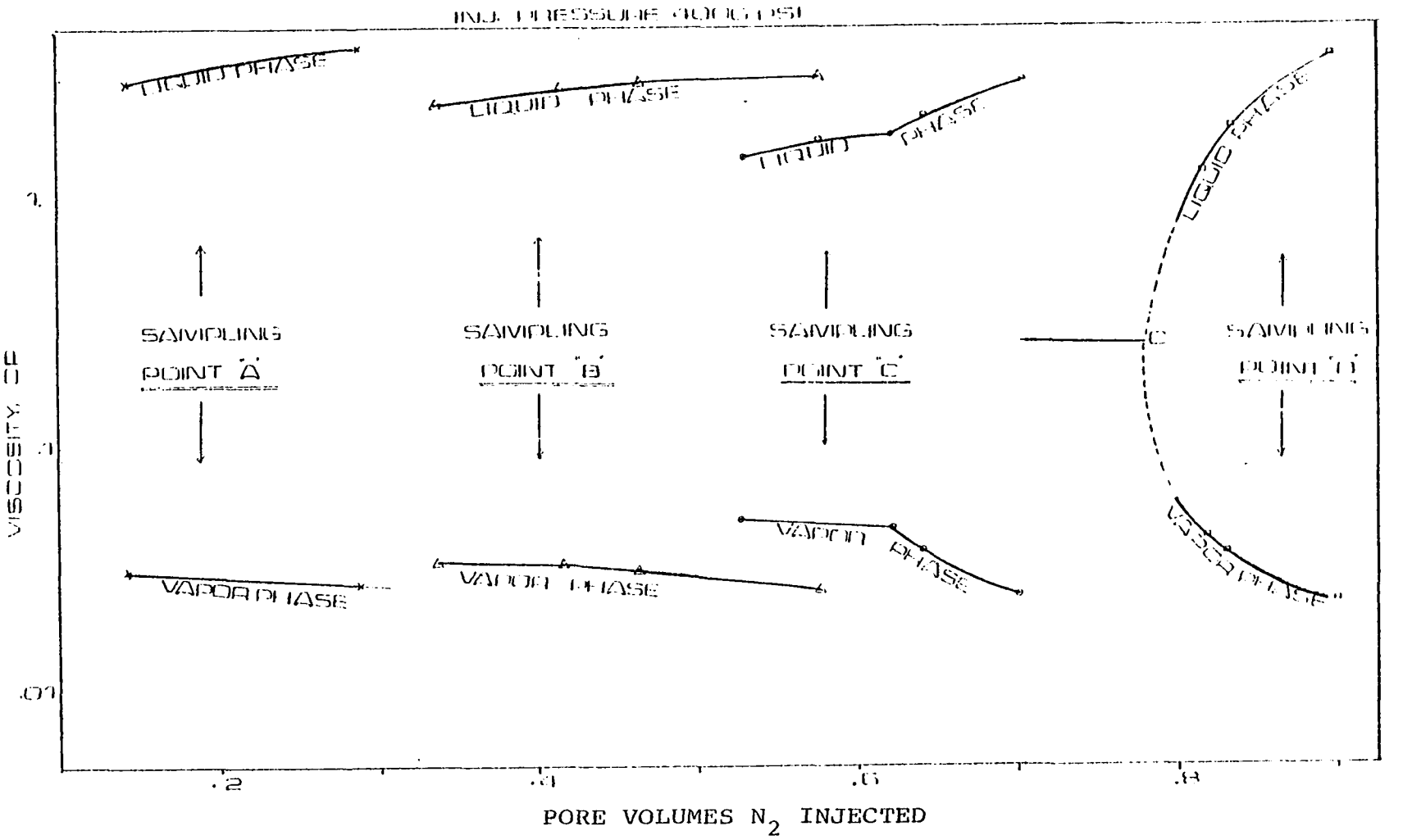

Figure 9-22. Calculated liquid and vapor viscosity distribution throughout the core vs. pore volumes N_2 injected

Finally, an attempt was made to calculate and monitor the magnitude of the surface tension between the fluids involved in the displacing process. The importance and effect of the surface tension on the ultimate oil recovery by gas injection was investigated by many research workers.[53,60] They agreed that the unrecoverable oil during any immiscible flooding is retained (or trapped) in the porous media by the capillary forces (which is a function of surface tension).

In this study, the results of the surface tension calculations by the available correlations (discussed in Chapter 5) are shown in Figure 9-23, while a summary of these calculations is given in tables A-55 through A-58, Appendix A.

Second Run

The decision was made to perform another run under higher pressure (5000 psi) to further the study of miscible displacement by nitrogen injection and to investigate the effect of pressure on the:

(a) size of the generated slug,

(b) critical composition of the formed rich gas slug,

(c) compositional profiles of the displacing phase, and

(d) distance from the injection point at which the miscibility will be achieved.

Following the same analysis procedure used in the first run, samples of the displacing phase were taken regularly from the sampling points (A, B, C, D, and E) and recorded as a function of pressure and cumulative volume injected. Analysis

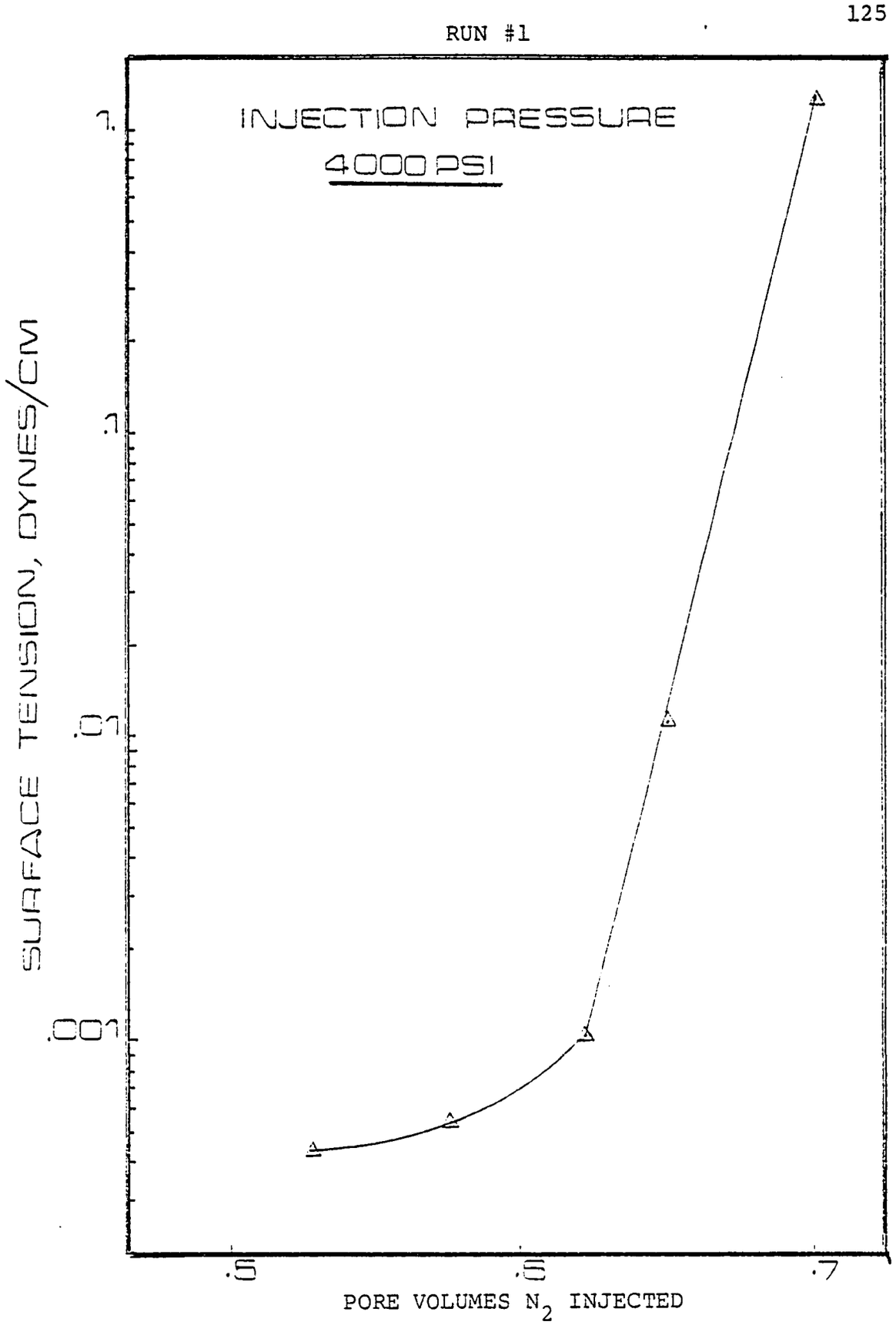

Figure 9-23. Calculated surface tension of samples taken from sampling point "C" vs. pore volumes N_2 injected

of the vapor samples were used to construct the ternary diagrams and to study the changes in the compositions and properties of the displacing and displaced phase.

The experimentally determined compositional profiles are shown in figures 9-24 through 9-28, while a summary of the vapor phase analysis is given in Table 9-5. Notice that the compositional profiles are similar to those of run number one.

At this point of the study significant observations should be mentioned:

(a) The author proposes that an increase in the pressure, above that of the minimum miscibility pressure, will not produce any substantial increases in the cumulative vaporization. Table 9-6, which summarizes the results of the first and second runs, shows no tangible changes in the critical compositions of the generated slug as the pressure was increased from 4000 to 5000 psi.

(b) For the pressure ranges studied, an increase in pressure resulted in substantial decreases in the generated rich gas slug size. This occurrence can be justified by the fact that the increase in pressure accounts for increased retrograde evaporation* which in turn leads to a rapid buildup of the slug's critical composition.

(c) Concentration of the intermediate components behind the slug decreases more rapidly as the injection pressure

---

*Retrograde evaporation can be defined by the process in which vapor is formed upon increasing the pressure at constant temperature.

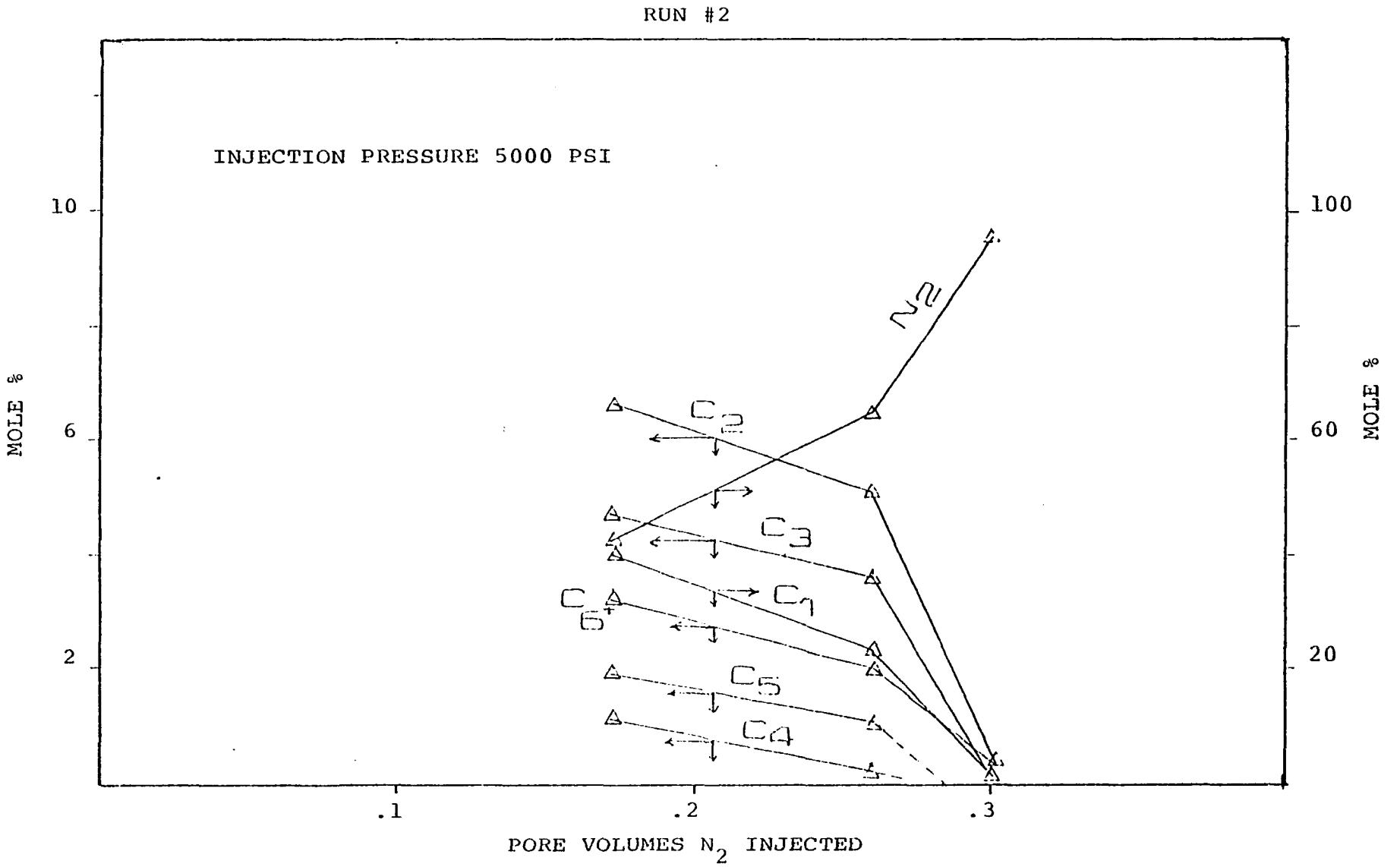

Figure 9-24. Composition of vapor phase samples taken from sampling point "A" vs. pore volumes N_2 injected

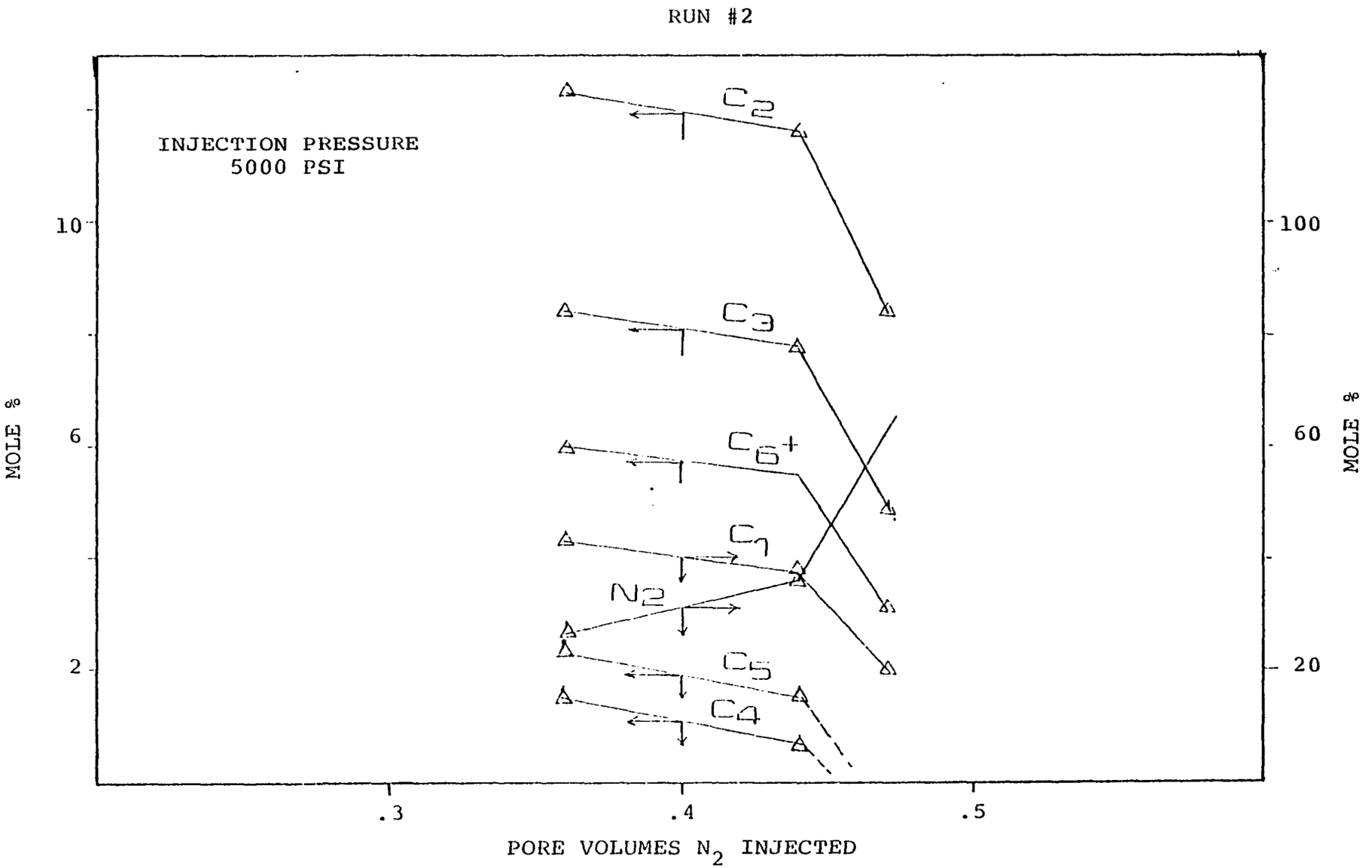

Figure 9-25. Composition of vapor phase samples taken from sampling point "B" vs. pore volumes N_2 injected

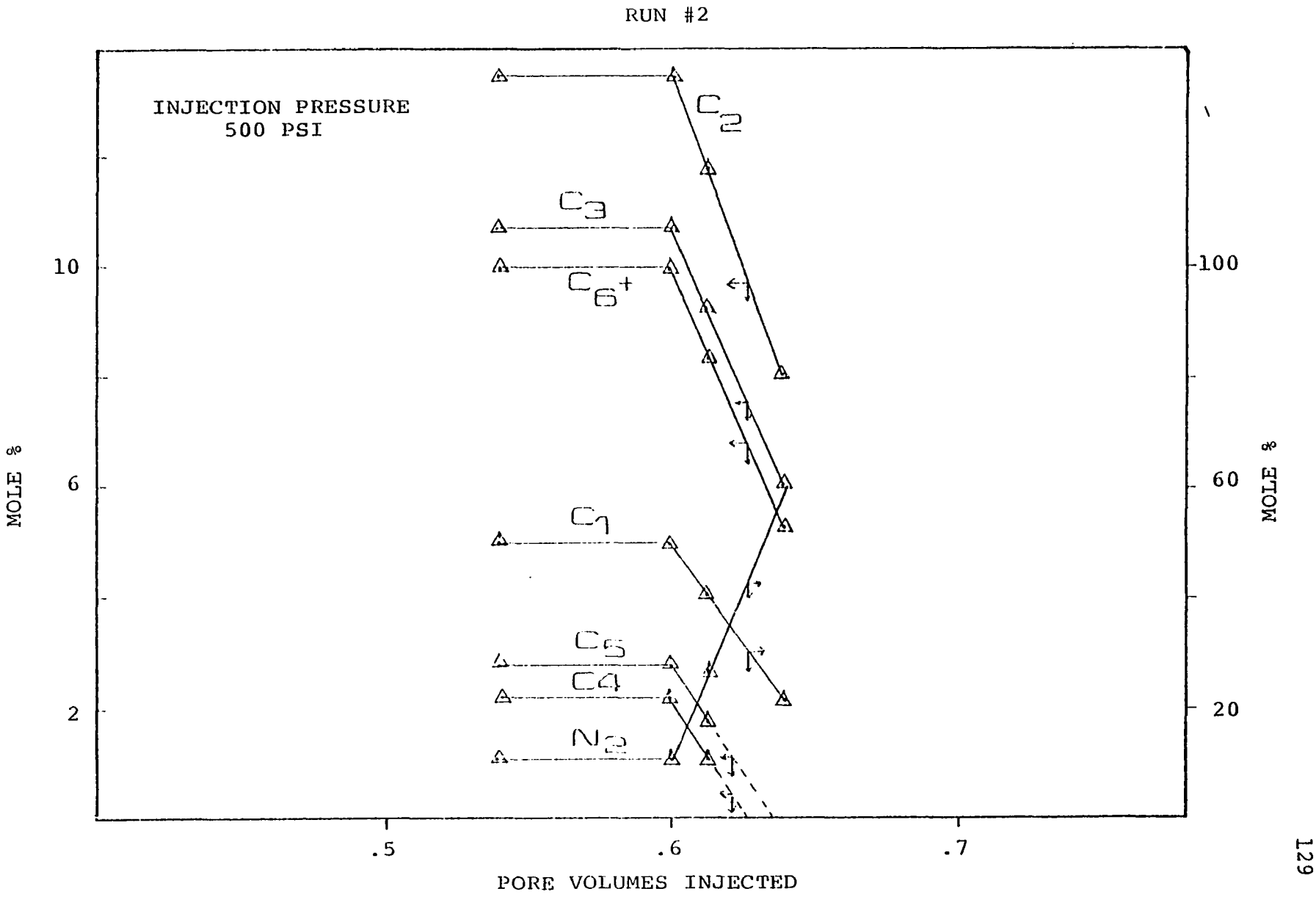

Figure 9-26. Composition of vapor phase samples taken from sampling point "C" vs. pore volumes N_2 injected

RUN #2

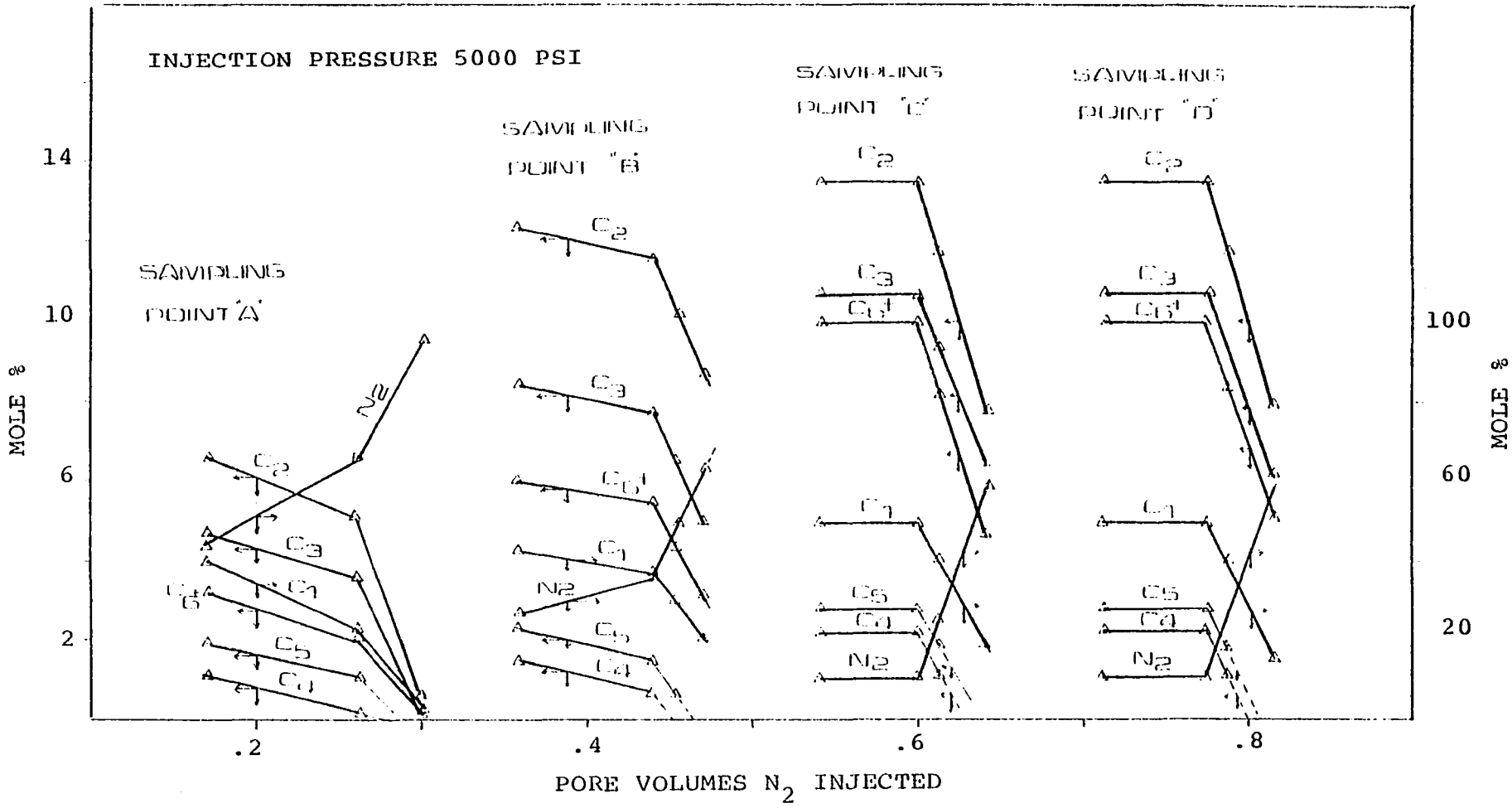

Figure 9-27. Compositional distribution of vapor phase throughout the core vs. pore volumes N_2 injected

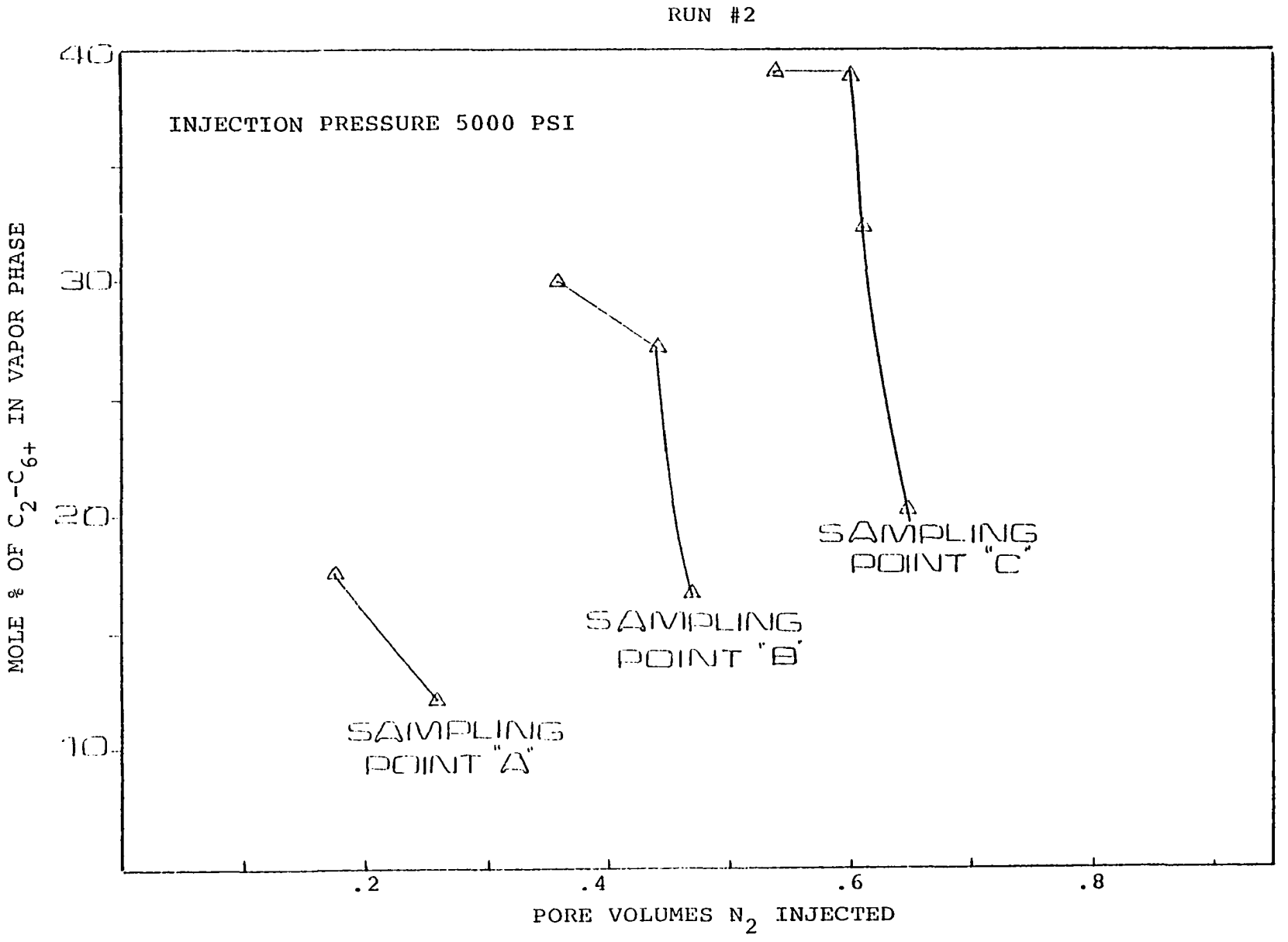

Figure 9-28. Overall composition of C_2-C_{6+} in vapor phase throughout the core vs. pore volumes N_2 injected

TABLE 9-5

MOLAR COMPOSITION OF THE COLLECTED SAMPLES

P.V.N_2 inj → / Comp.	Sampling Point A			Sampling Point B				Sampling Point C				Sampling Point D			
	.172	.26	.3	.359	.44	.454	.47	.5391	.6	.612	.638	.711	.793	.819	.839
N_2	.4245	.65	.95	.265	.359	.496	.632	.108	.108	.2765	.583	.105	.105	.395	.585
C_1	.4	.23	.04	.43	.37	.29	.2	.5	.5	.4	.22	.5	.5	.35	.24
C_2	.066	.051	.006	.123	.116	.101	.087	.135	.135	.117	.08	.137	.137	.097	.068
C_3	.047	.036	.002	.084	.078	.063	.05	.107	.107	.094	.062	.107	.107	.077	.057
C_4	.0115	.002	0	.015	.007	0	0	.022	.022	.011	0	.022	.022	.004	0
C_5	.019	.011	0	.023	.015	.006	0	.028	.028	.0185	0	.029	.029	.01	0
C_{6+}	.032	.02	.002	.06	.055	.044	.031	.100	.1	.083	.055	.10	.1	.07	.05

TABLE 9-6

SUMMARY OF THE RESULTS OF THE FIRST AND SECOND RUN

PARAMETER	FIRST RUN	SECOND RUN
Injection pressure	4000	5000
Type of displacement	Miscible	Miscible
Oil recovery at breakthrough	80%	86%
Size of the generated slug, % p.v.	8	5
Critical compositons:		
N_2	8.6%	10.9%
C_1	55.0%	50.0%
C_2	12.8%	13.4%
C_3	10.7%	10.7%
C_4	2.0%	2.2%
C_5	2.8%	2.8%
C_{6+}	8.9%	10.0%
Distance from the injection point at which miscibility was achieved, ft.	82	between 48 and 72
Solution gas-oil ratio	575 Scf/STB	575 Scf/STB
Oil gravity	43°API	43°API

increases. Ternary diagrams, as presented in figures 9-29 through 9-31, show the step-by-step procedure by which the miscible front was formed. This process can be summarized as follows: As the injected pure nitrogen vaporizes some of the intermediate components from the oil, this partially enriched nitrogen moves forward and contacts new oil and vaporizes the more intermediate components, thereby enriching the gas further. After multiple contacts, the leading edge of the gas front becomes so enriched that it is miscible with the reservoir oil (point C in Figure 9-31). When this occurs, the interface between the oil and gas disappears and fluids blend into each other.

In moving outward from the injection point, the nitrogen may travel up to 90 feet before the miscible front forms. The distance varies depending upon pressure, oil composition, and oil saturation.

Figures 9-32 through 9-38 show the calculated density and viscosity of the displacing and displaced phase. A complete summary of the calculations are given in tables B-1 through B-34, Appendix B.

There appears to be three important factors which govern and control the miscible displacement mechanism:

(i) The mutual solubility effects at the generated slug portion, which in their simplest forms can be looked upon as merely an evaporation of the oil into the gas and solubility of some light end components (N_2, C_1) into the contacted oil.

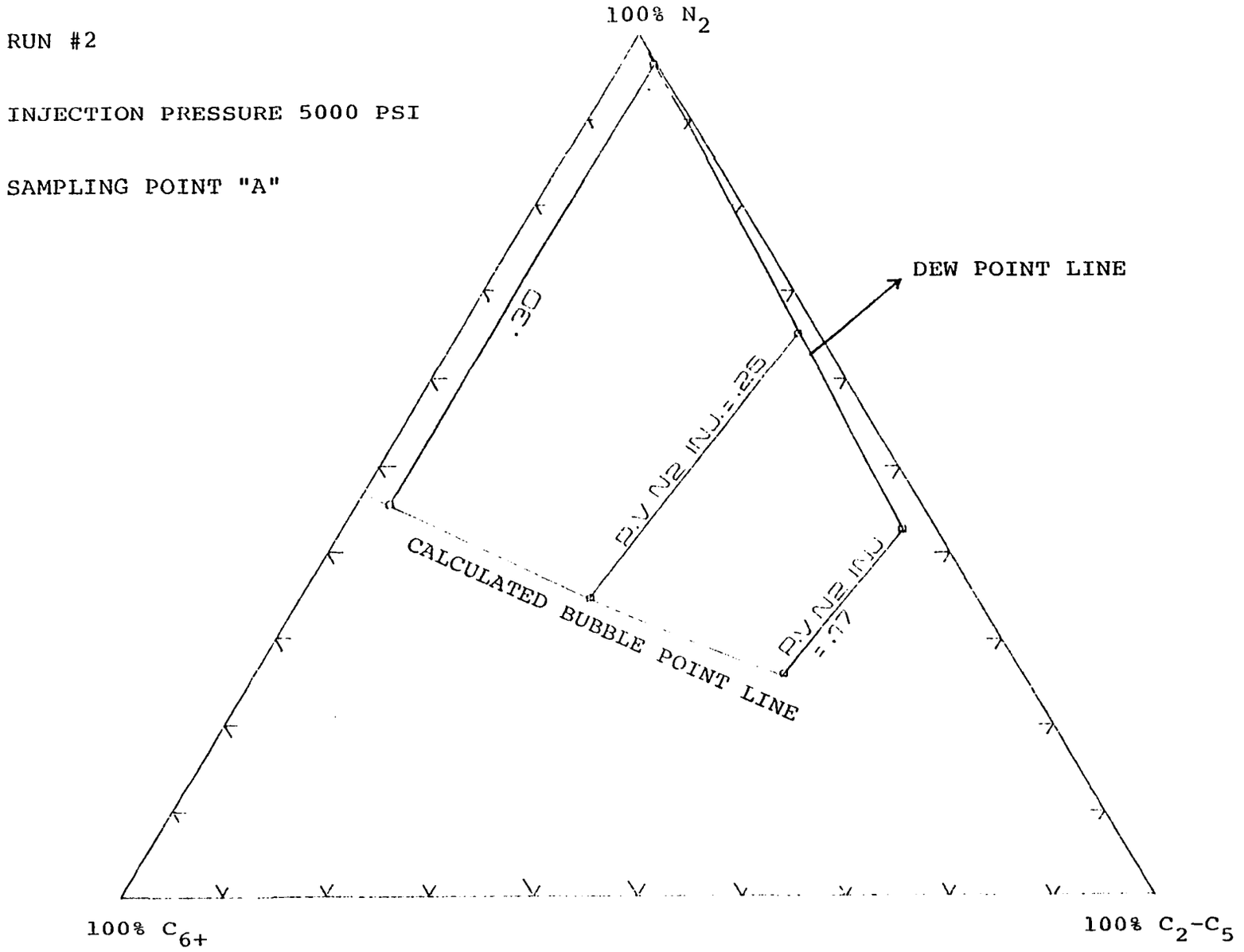

Figure 9-29. Triangular diagram showing changes in composition of vapor and liquid phase

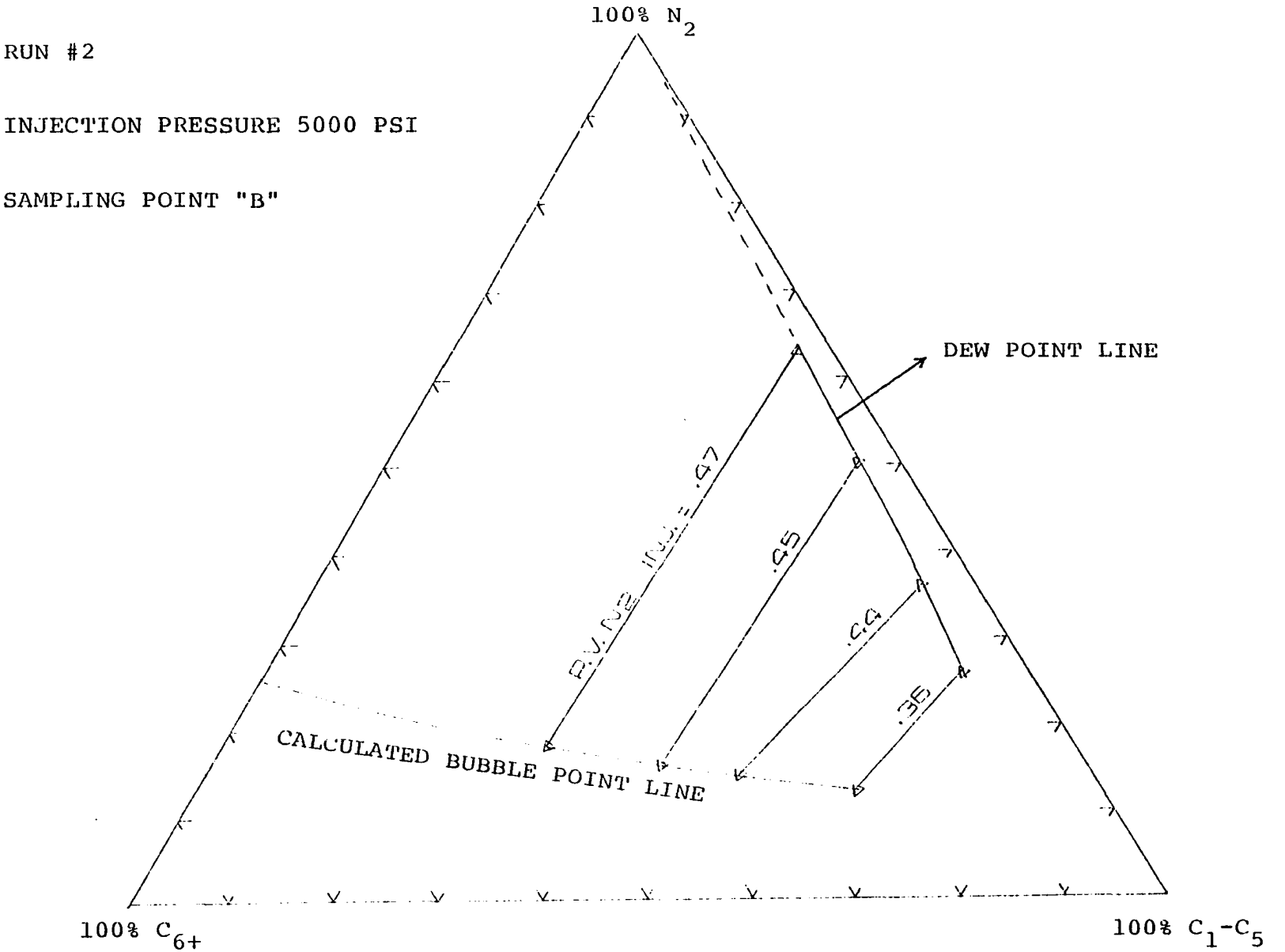

Figure 9-30. Triangular diagram showing changes in composition of vapor and liquid phase

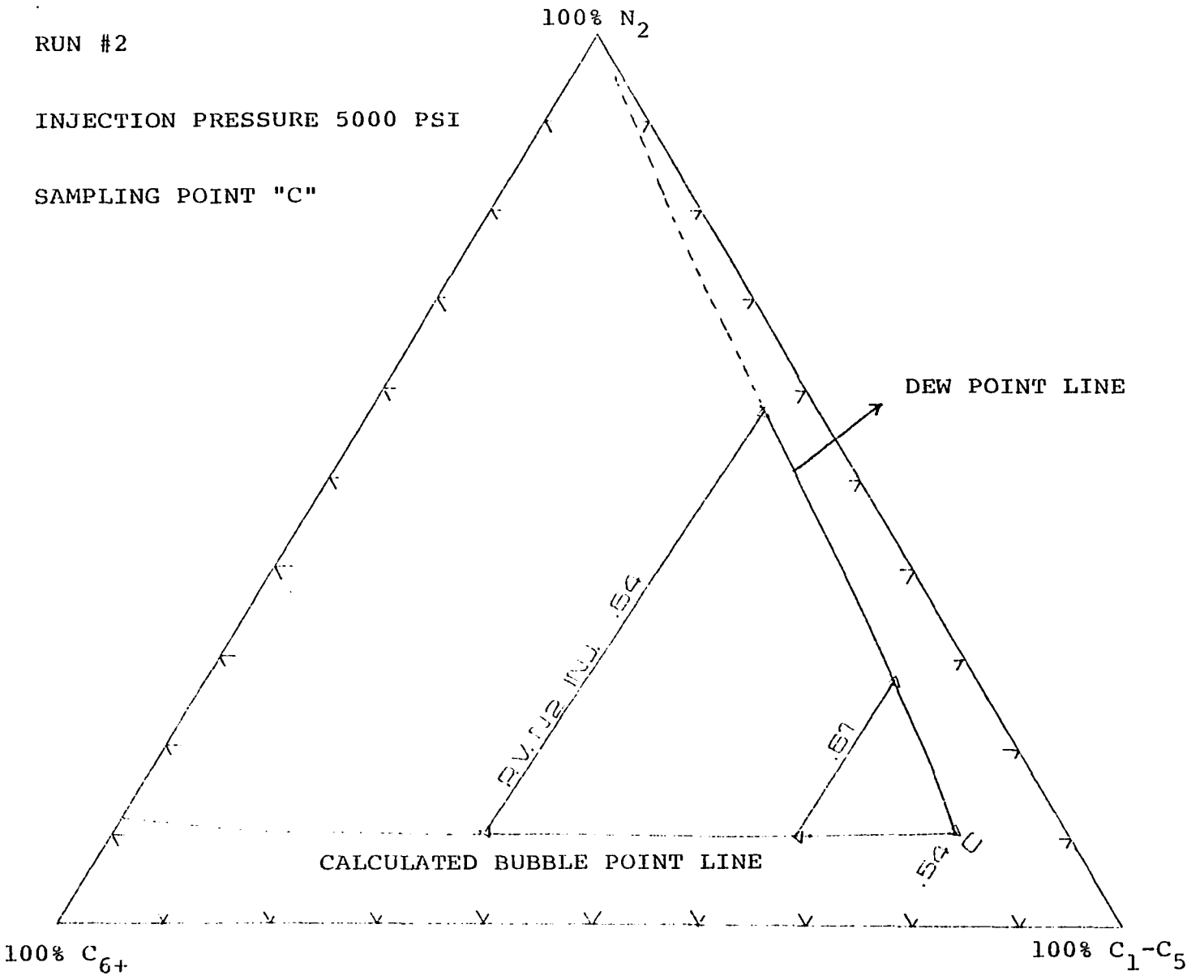

Figure 9-31. Triangular diagram showing changes in composition of vapor and liquid phase

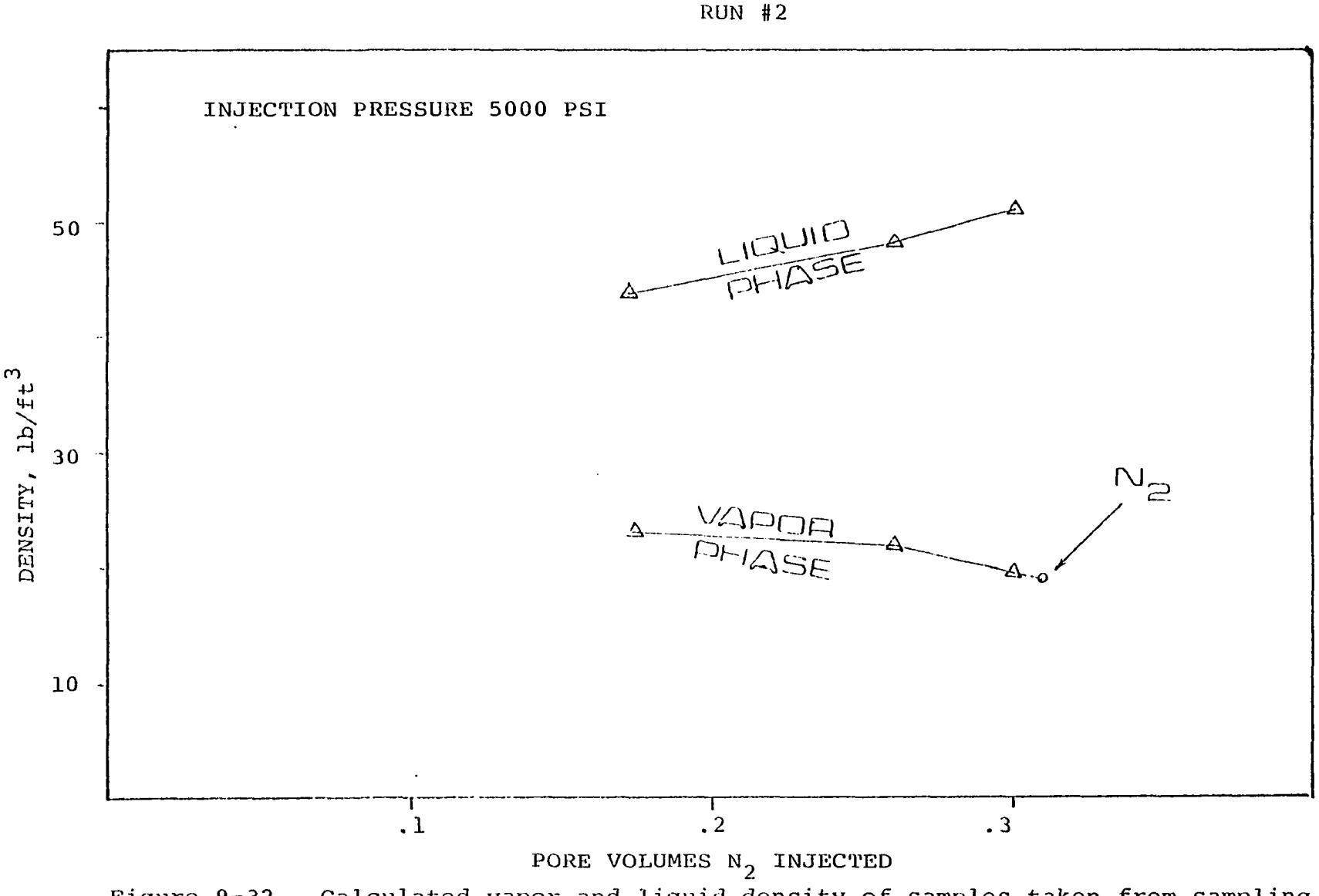

Figure 9-32. Calculated vapor and liquid density of samples taken from sampling point "A" vs. pore volumes N_2 injected

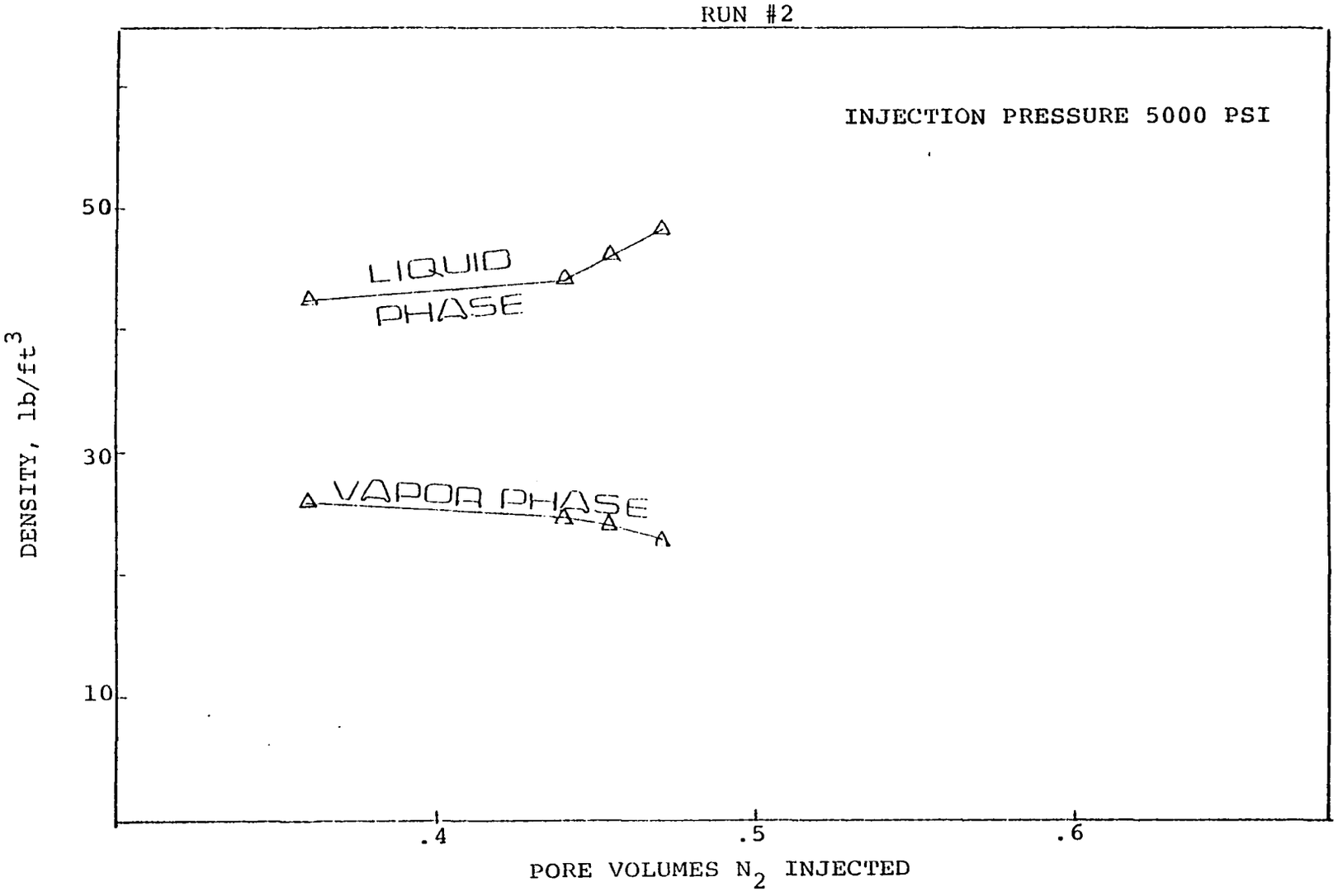

Figure 9-33. Calculated vapor and liquid density taken from sampling point "B" vs. pore volumes N_2 injected

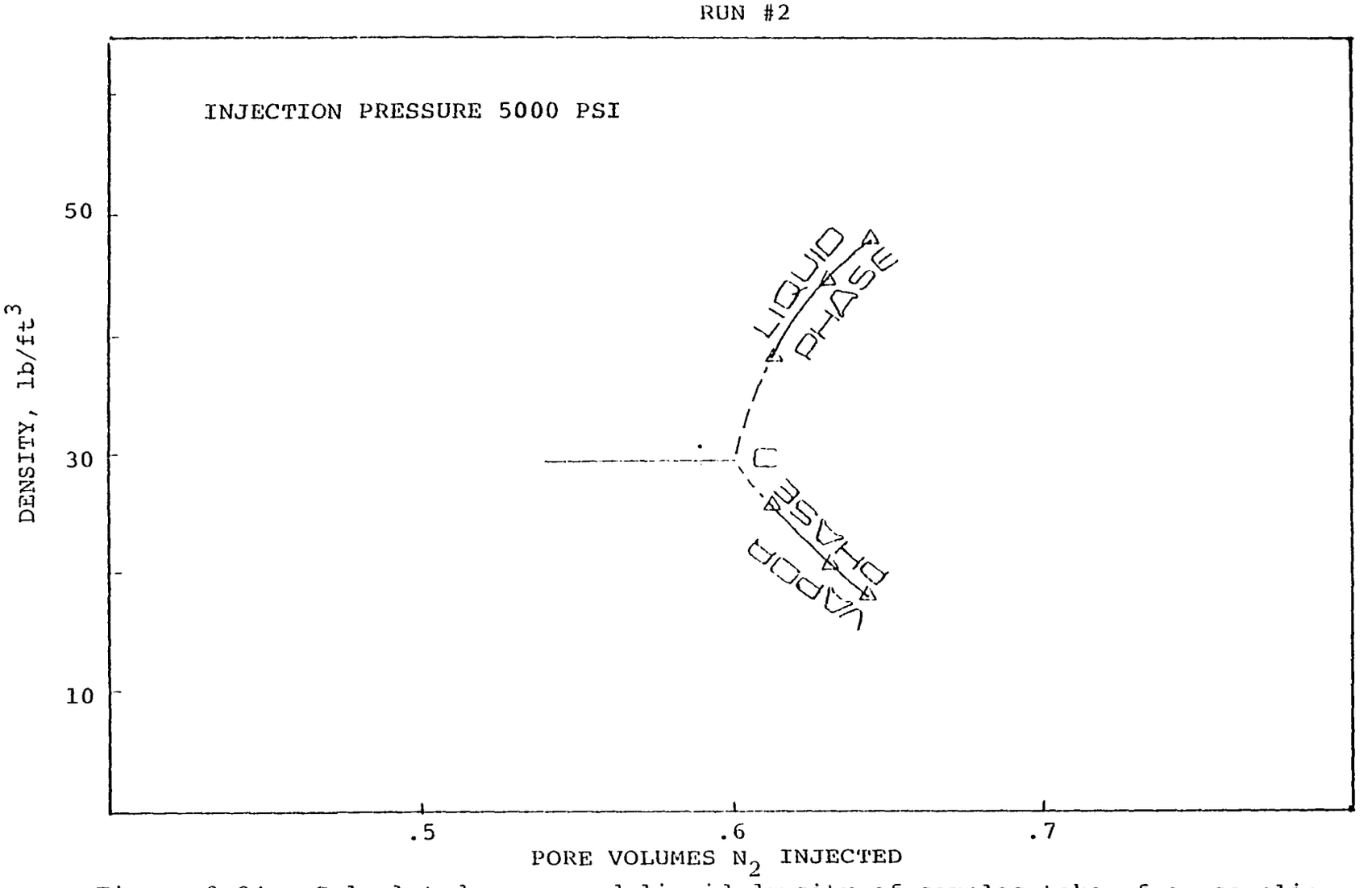

Figure 9-34. Calculated vapor and liquid density of samples taken from sampling point "C" vs. pore volumes N_2 injected

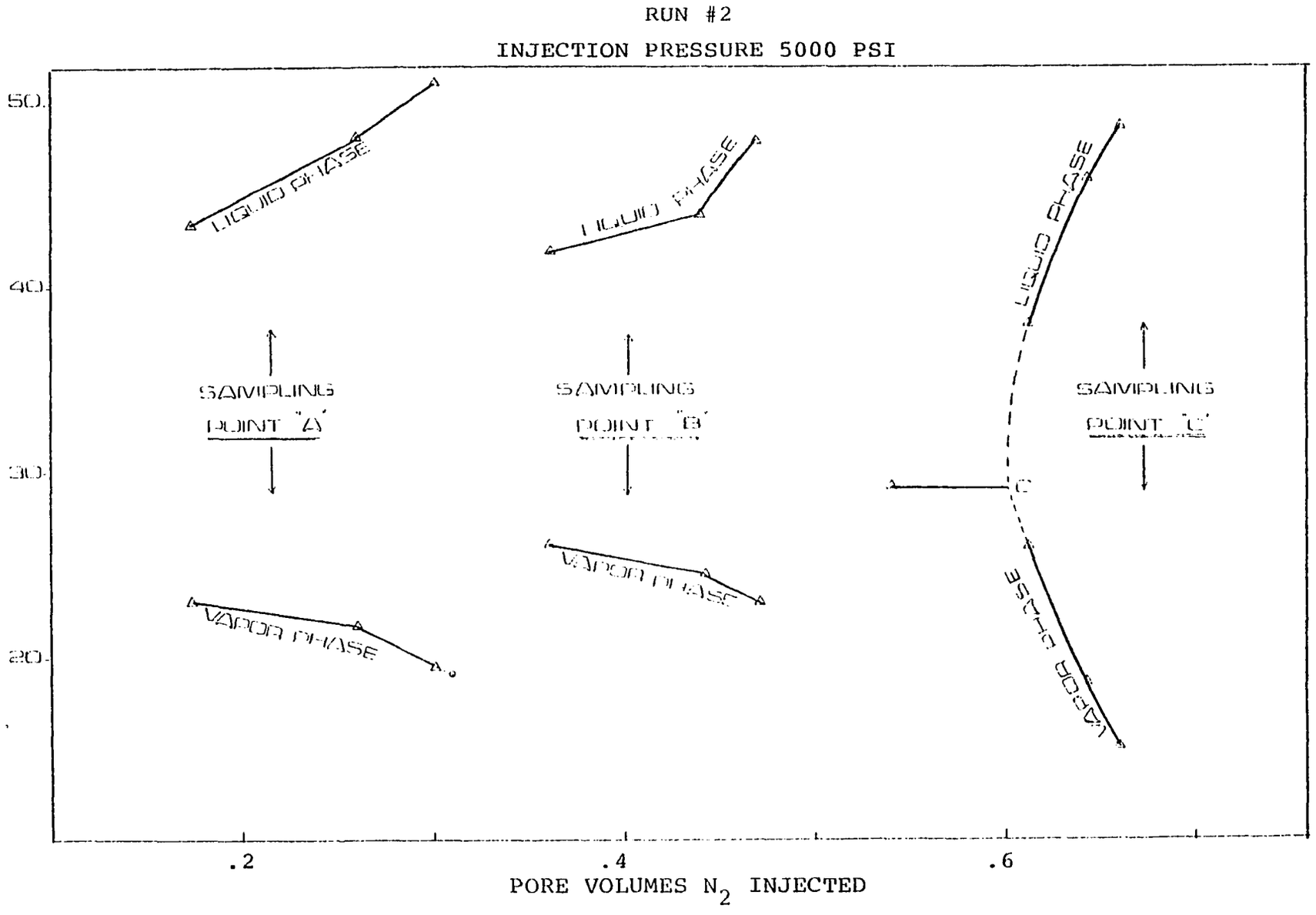

Figure 9-35. Calculated vapor phase density distribution throughout the core vs. pore volumes N_2 injected

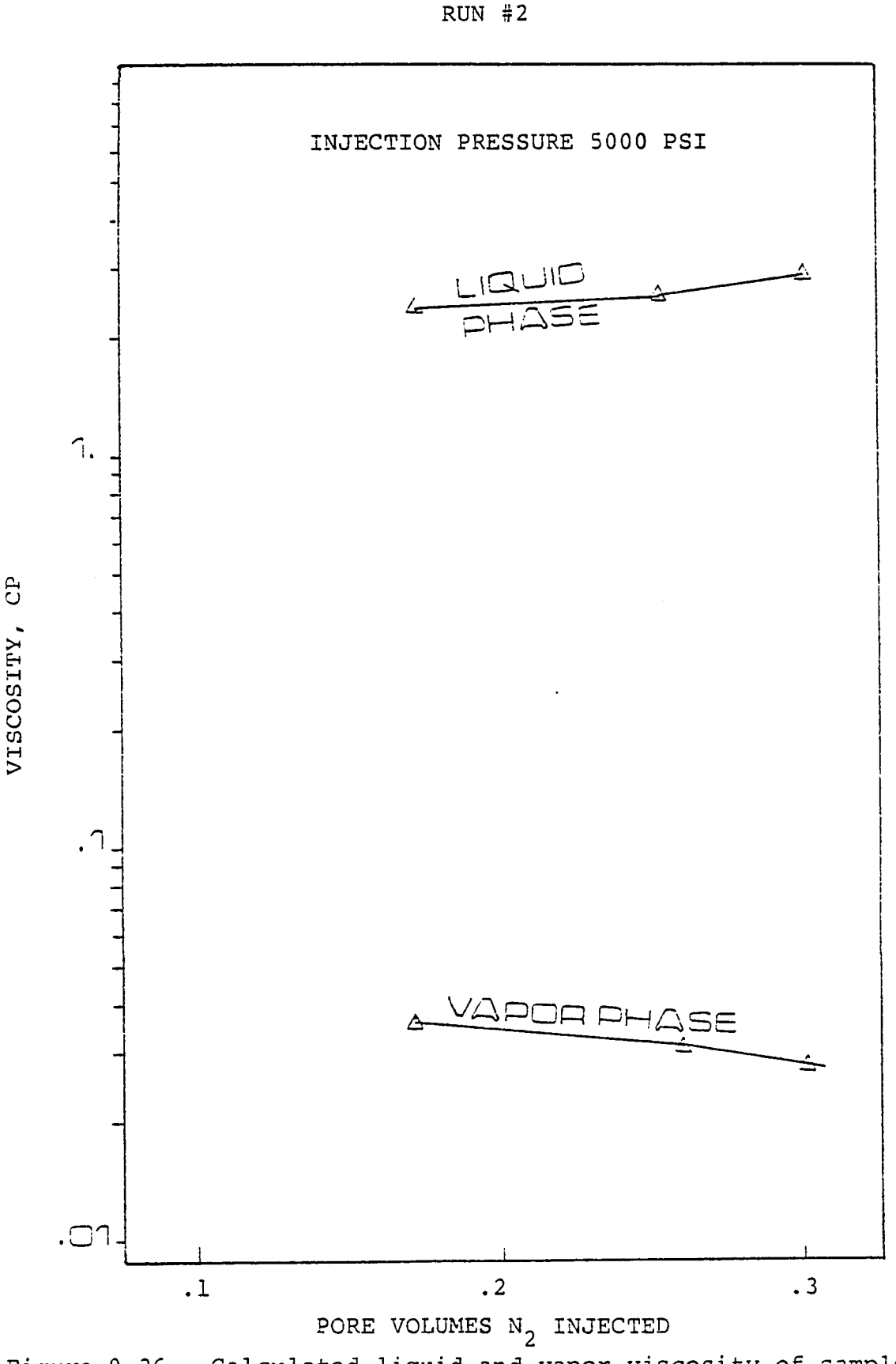

Figure 9-36. Calculated liquid and vapor viscosity of samples taken from sampling point "A" vs. pore volumes N_2 injected

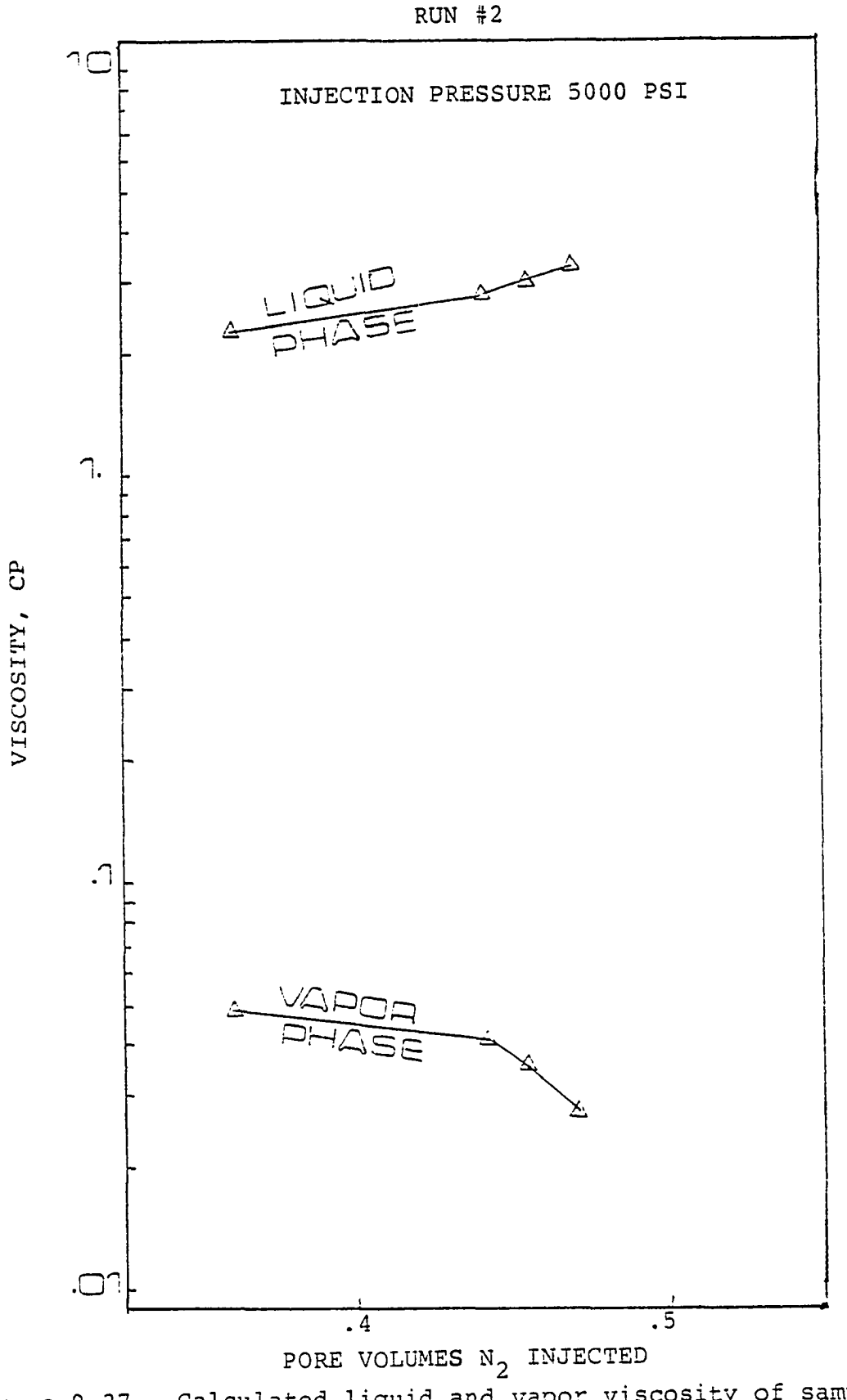

Figure 9-37. Calculated liquid and vapor viscosity of samples taken from sampling point "B" vs. pore volumes N_2 injected

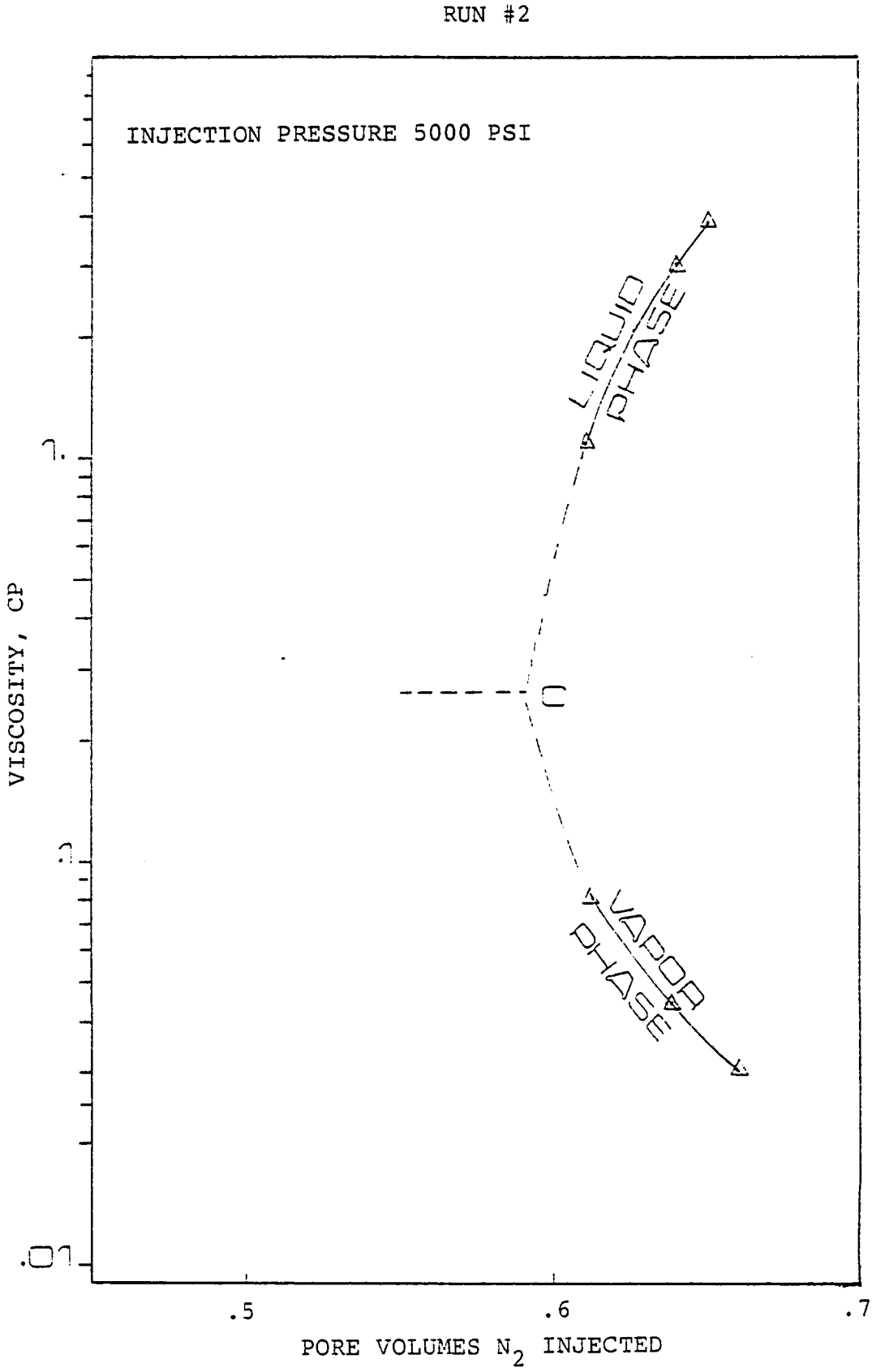

Figure 9-38. Calculated liquid and vapor viscosity of samples taken from sampling point "C" vs. pore volumes N_2 injected

(ii) A stripping process behind the formed rich gas slug

(iii) The viscosity and density effect, which would make the two phases in proportion more favorable to liquid production because of the decrease of liquid and the increase of gas viscosities.

Third Run

In order to further the understanding of the displacement mechanism by nitrogen, the decision was made to perform a run under low pressure (3000 psi). The run represented a conventional low pressure gas displacement operation.

Samples of the displacing phase were collected and analyzed as discussed before. The analysis showed traces of methane, however the (C_2-C_{6+}) components were absent. This observation led to the concept of "Minimum Evaporation Pressure" which is defined as the minimum pressure at which evaporation of intermediate components occurs.

The run was terminated at the nitrogen breakthrough which occurred at 54 percent oil recovery.

Fourth Run

This test was performed at an injection pressure of 3700 psi. A summary of the analysis results are presented in figures 9-39 to 9-43.

Following the usual procedure of analysis, the experimentally determined compositional profiles were used to

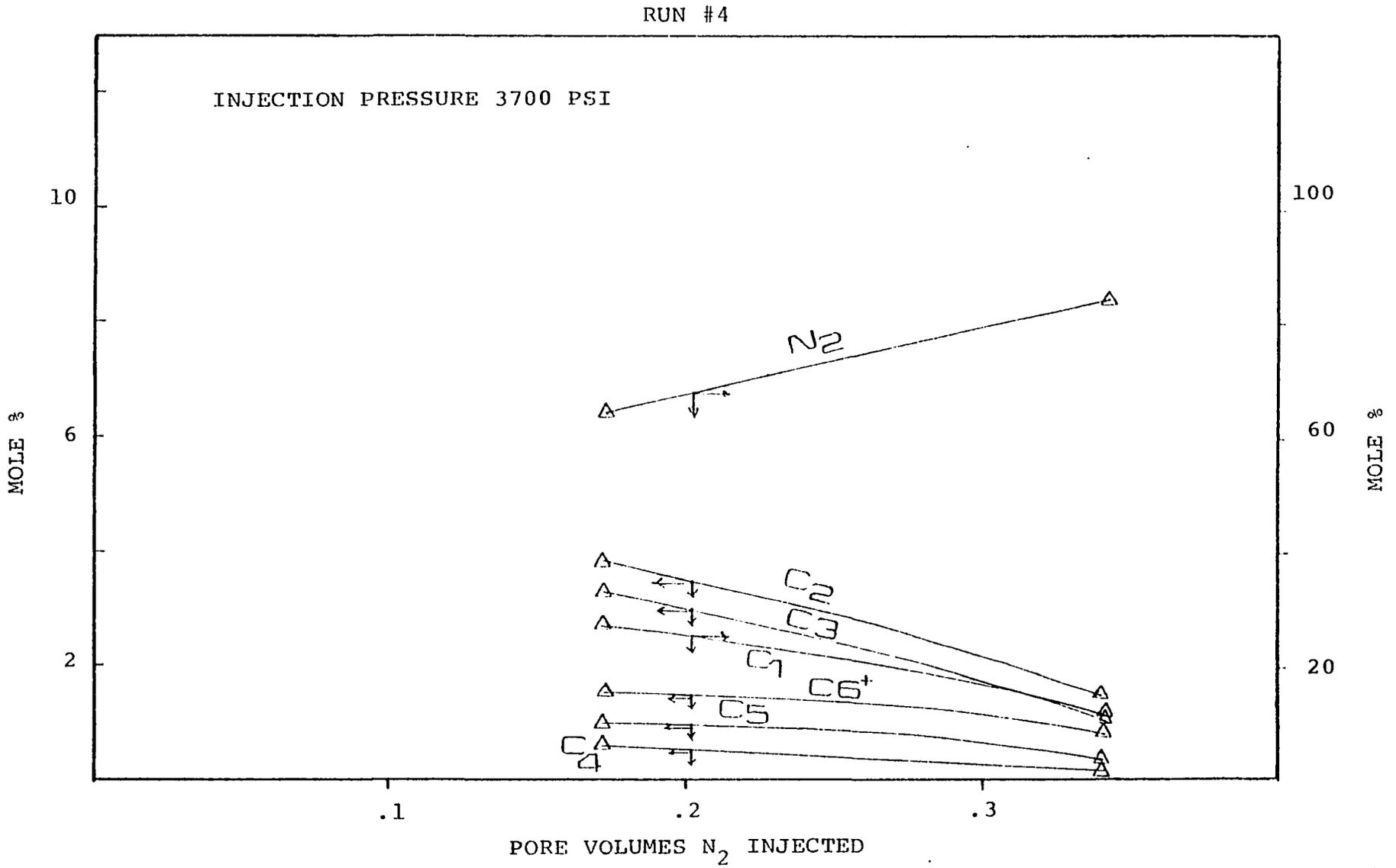

Figure 9-39. Composition of vapor samples taken from sampling point "A" vs. pore volumes N_2 injected

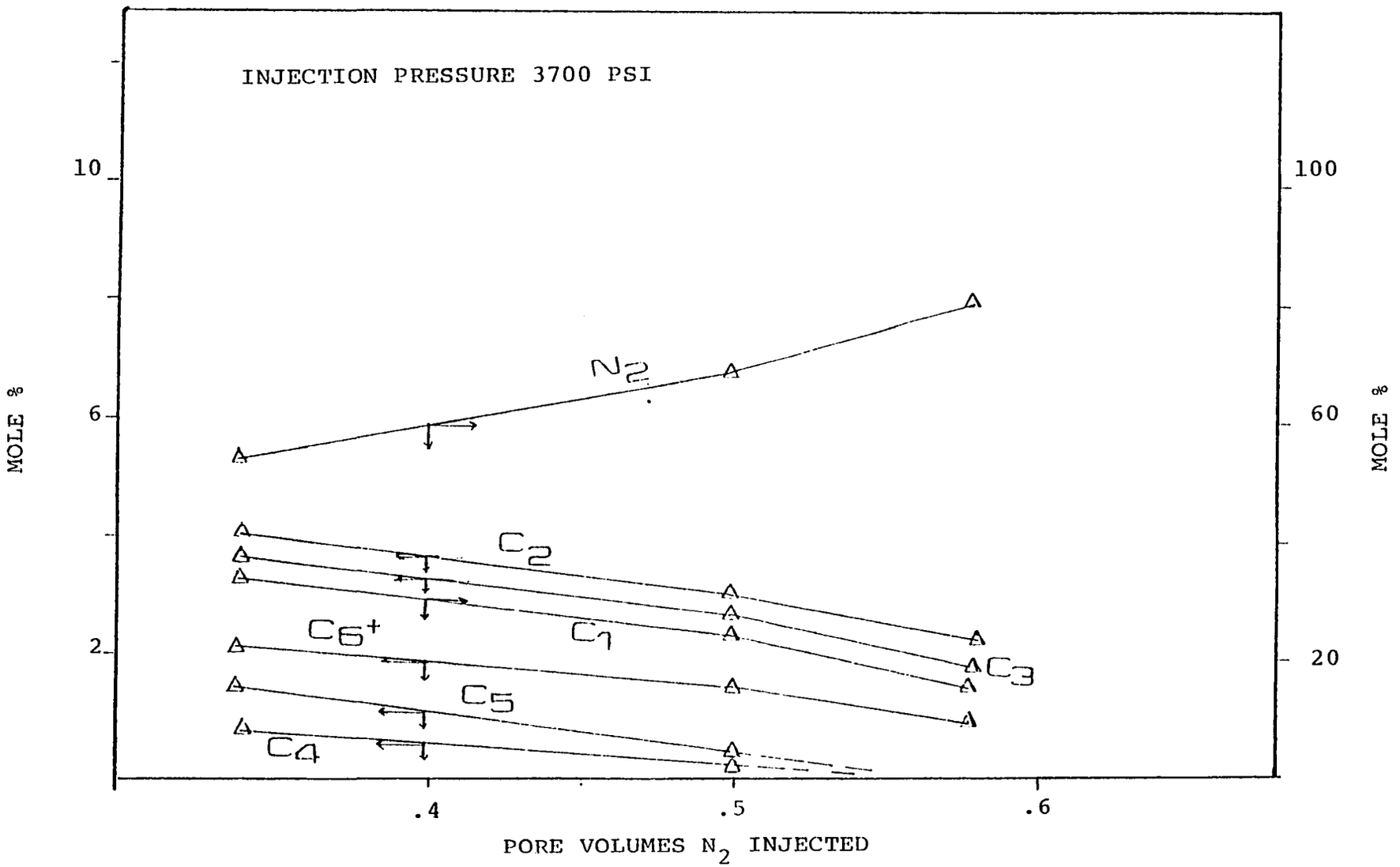

Figure 9-40. Composition of vapor phase samples taken from sampling point "B" vs pore volumes N_2 injected

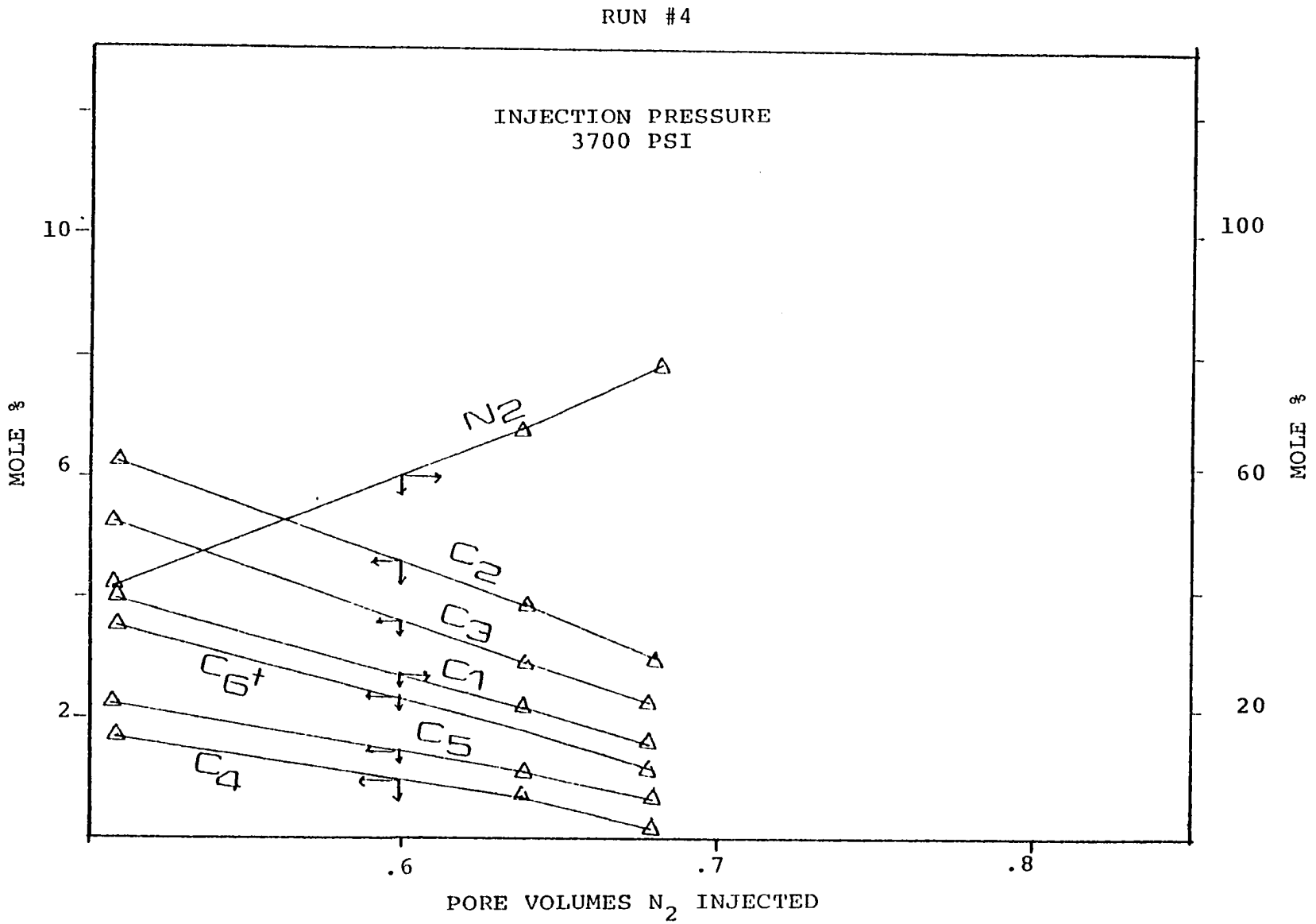

Figure 9-41. Composition of vapor phase samples taken from sampling point "C" vs. pore volumes N_2 injected

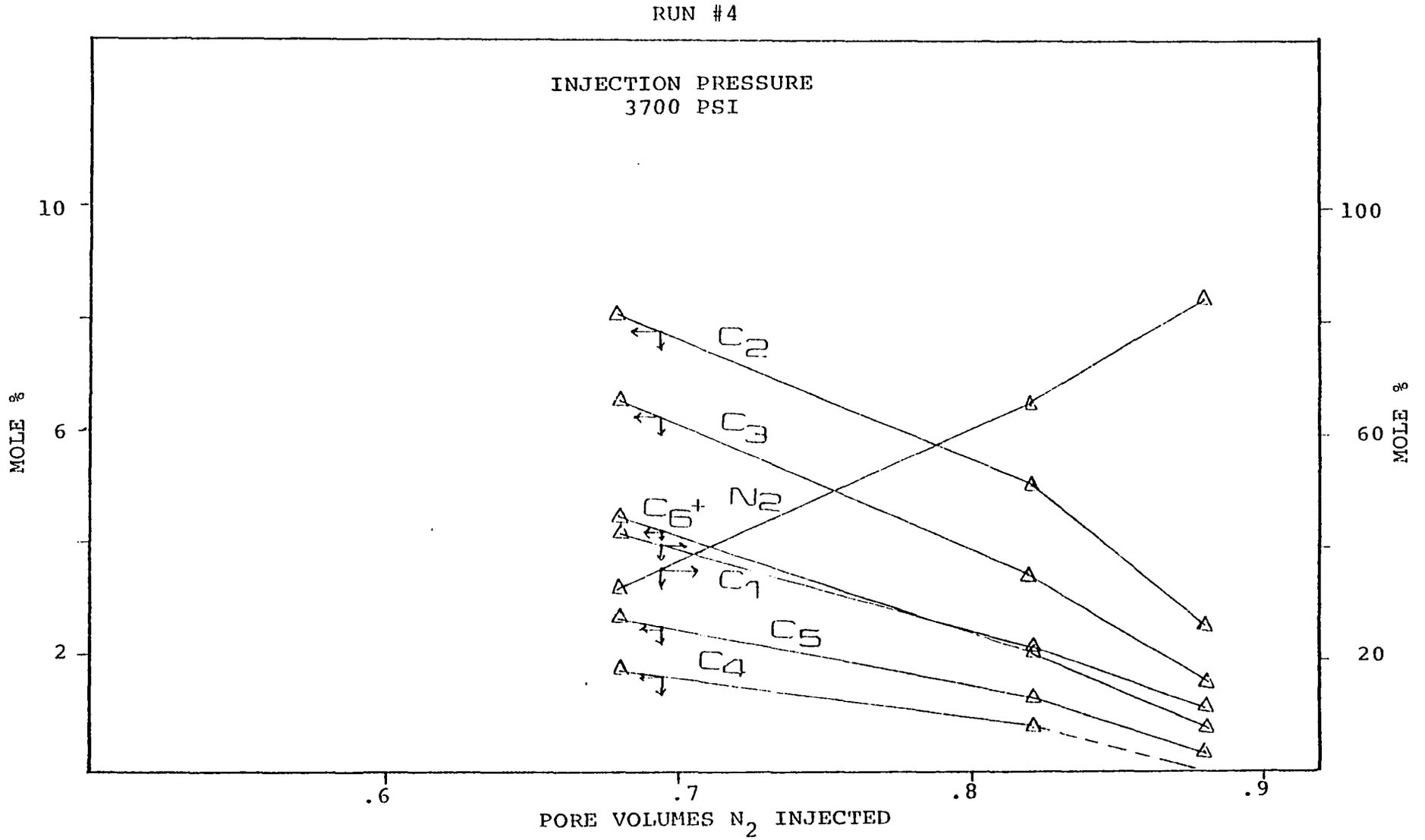

Figure 9-42. Composition of vapor phase samples taken from sampling point "D" vs. pore volumes N_2 injected

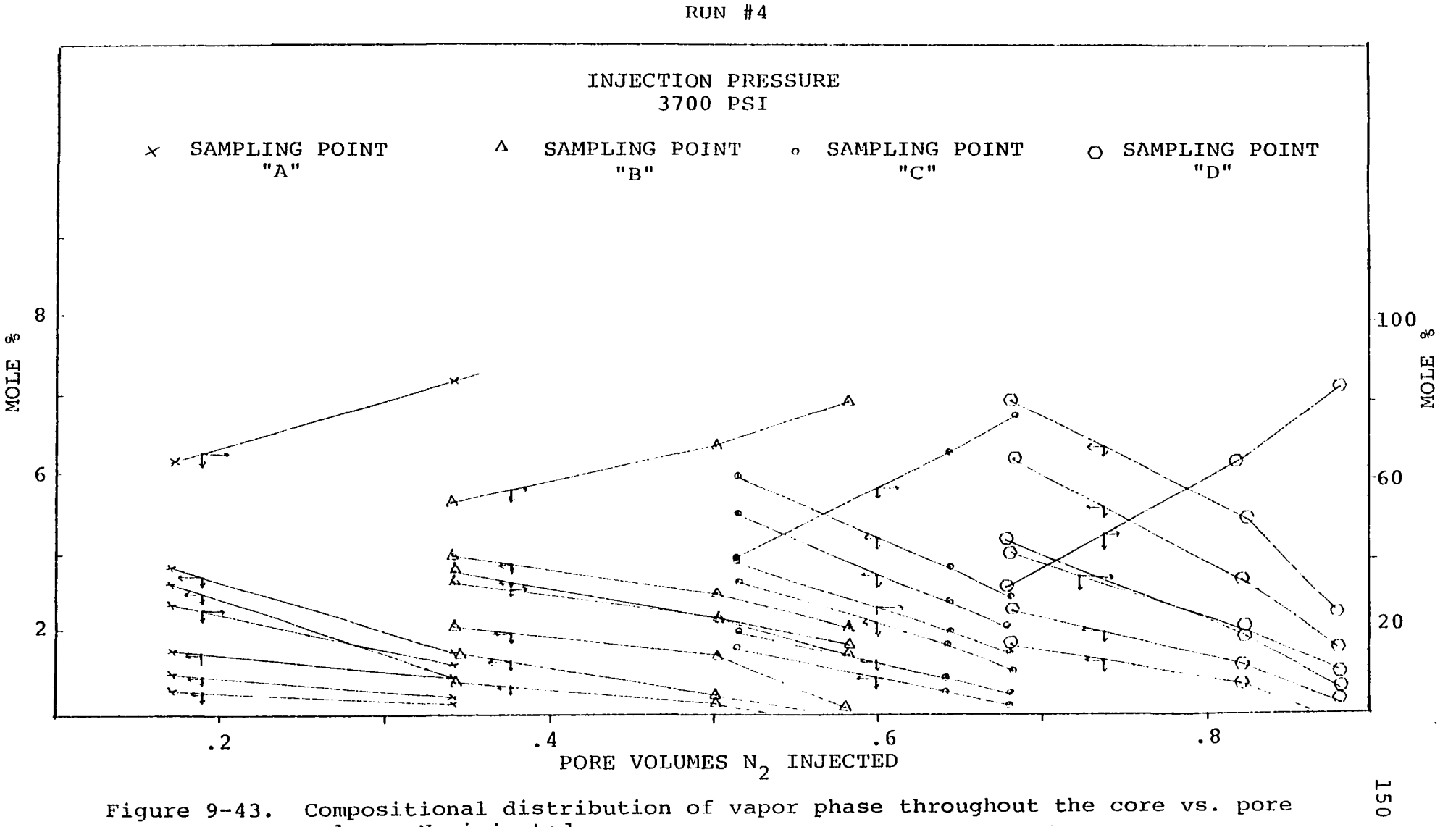

Figure 9-43. Compositional distribution of vapor phase throughout the core vs. pore volumes N_2 injected

construct the ternary diagrams and calculate the changes in both phase properties during the displacement process. Some results of the calculations are shown in figures 9-44 through 9-58, while a complete summary of the calculations is given in tables C-1 through C-48, Appendix C.

The ternary diagram in Figure 9-47 shows that the composition of the displacing phase did not approach the critical composition. This means that while the vapor compositions (dew point curve) were being enriched, the mixture lying on an equilibrium tie line was reached before miscibility (critical composition) is reached. This is in agreement with the prediction by Hutchinson and Braun[6] for an immiscible vaporization process.

The system of curves given in Figure 9-43 illustrates the stripping process of the intermediate components from the oil in place. Notice that the formed gas slug was developed at a later stage of the displacement process. This stage was recognizable by the distinct sharp break in the compositional curves.

The oil recovery obtained in this run (72 percent at B.T.) is substantially higher than that of the third run (54 percent). This improvement is the result of:

(i) A decrease in the viscosity ratio:

$$\frac{\text{viscosity of oil}}{\text{viscosity of the displacing phase}}$$

This ratio decreases largely because the displacing gas has

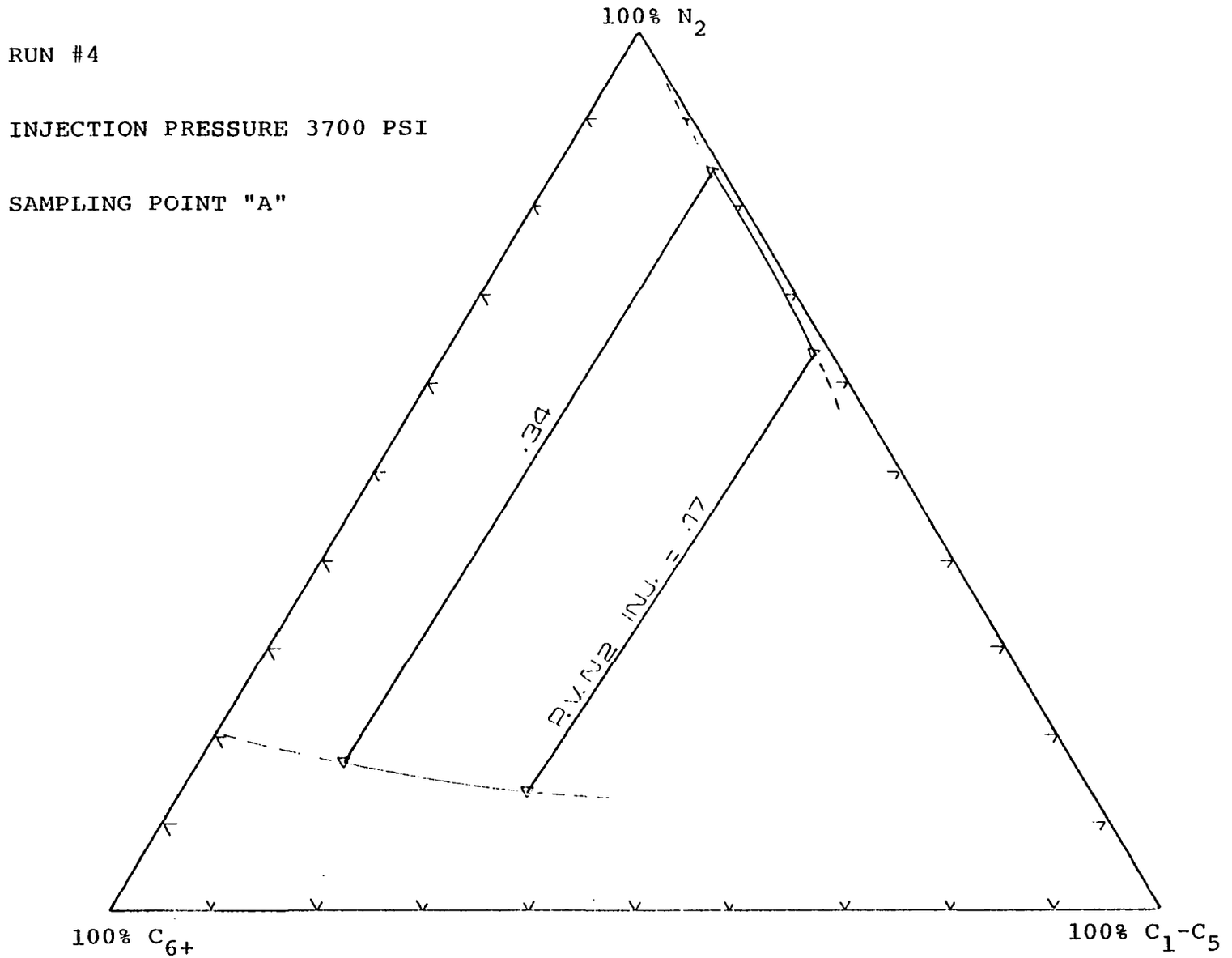

Figure 9-44. Triangular diagram showing changes in composition of vapor and liquid phase

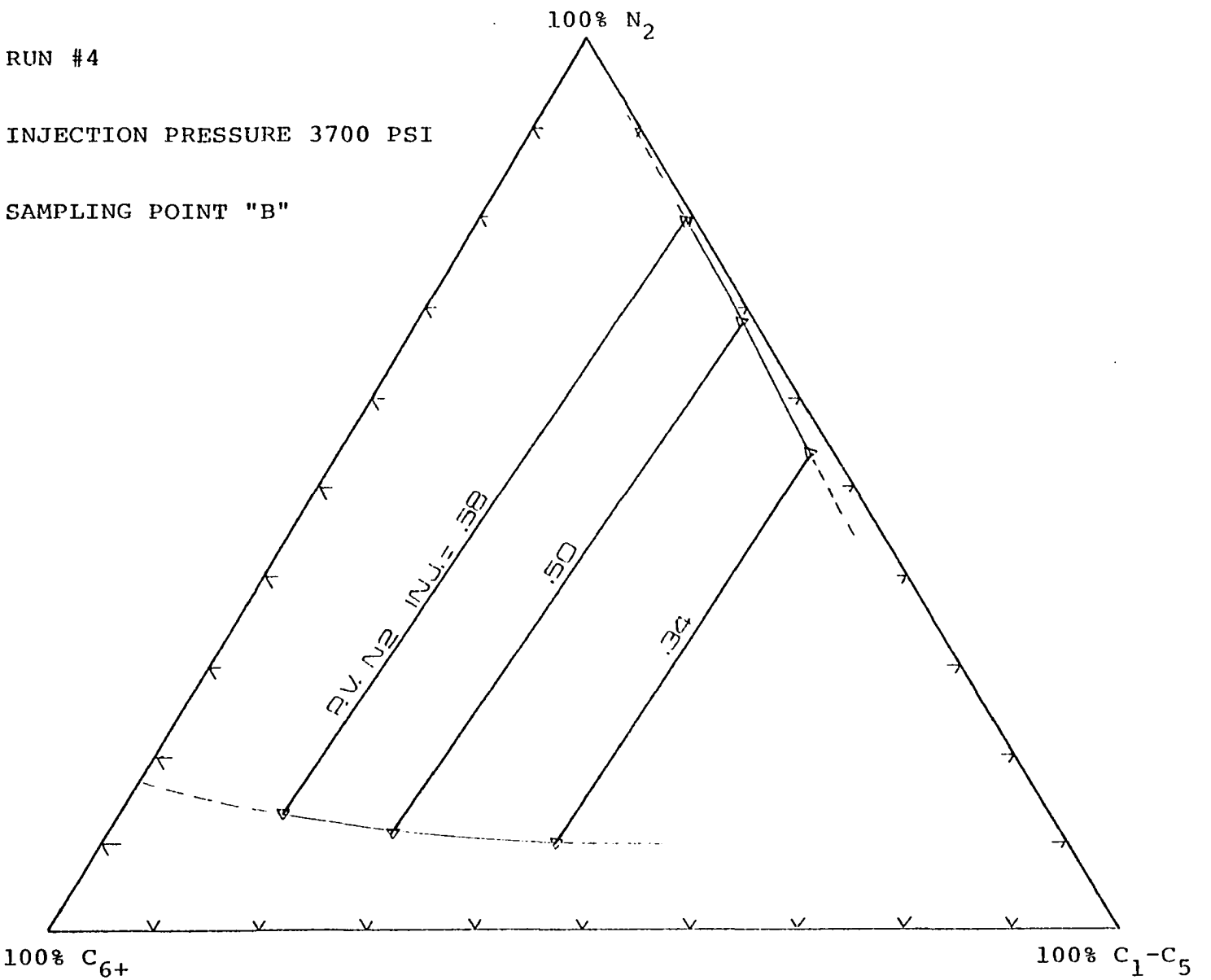

Figure 9-45. Triangular diagram showing changes in composition of vapor and liquid phase

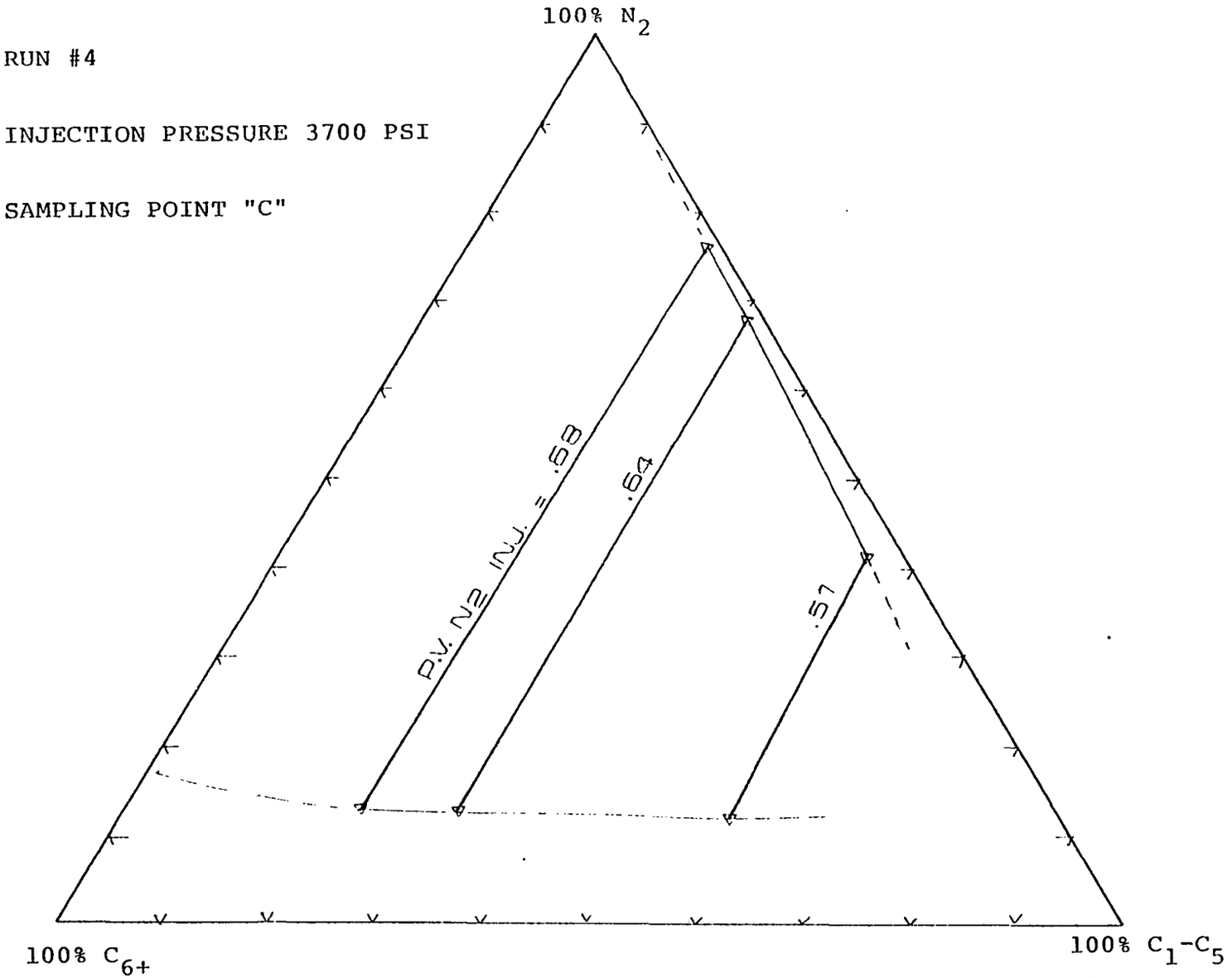

Figure 9-46. Triangular diagram showing changes in composition of vapor and liquid phase

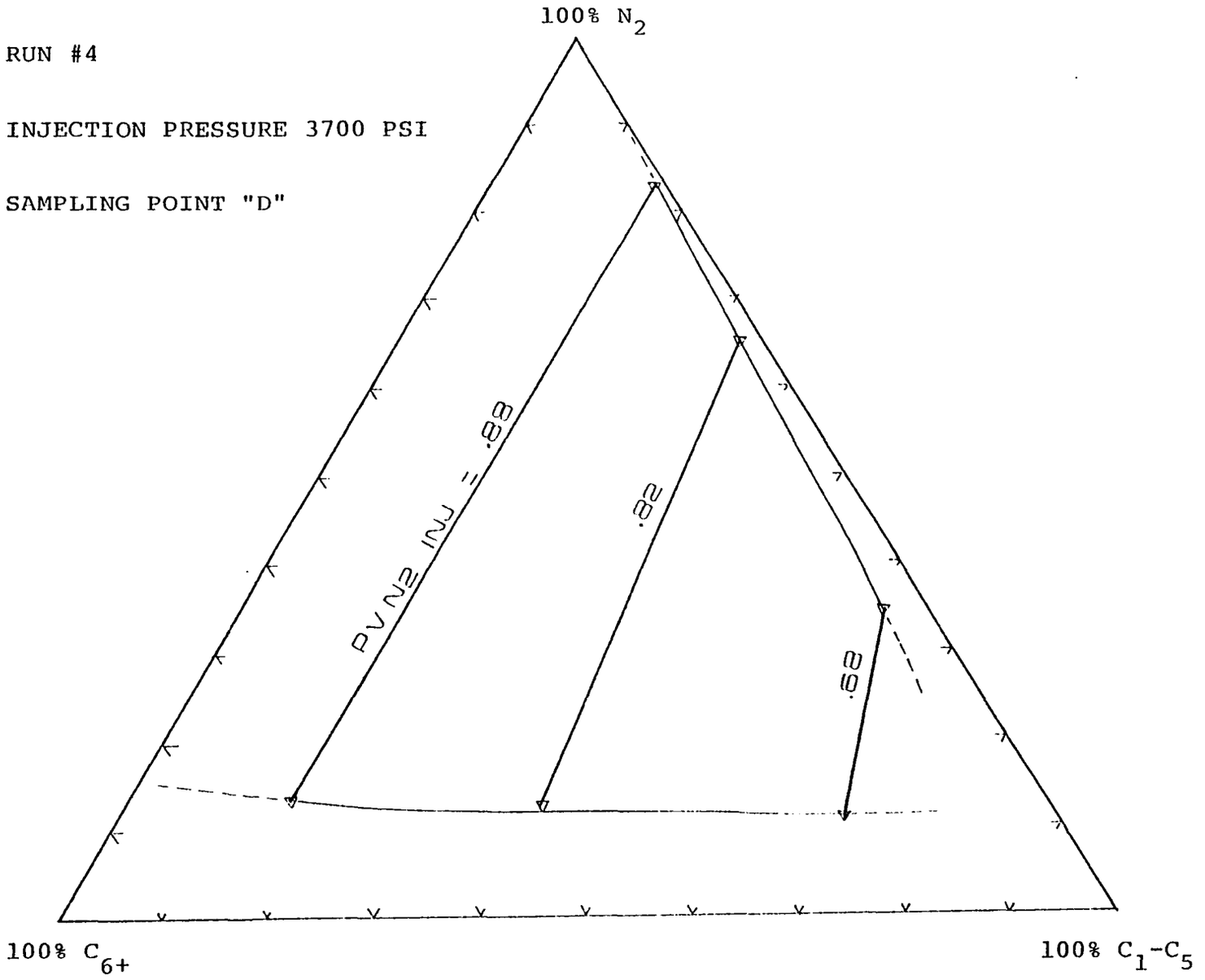

Figure 9-47. Triangular diagram showing changes in composition of vapor and liquid phase

become more viscous and, consequently, is a better displacing agent. See figures 9-48 through 9-51.

(ii) Swelling of the oil in place resulting from solution of enriched injected gas.

(iii) Improvement of the surface tension between the displacing and displaced phase (figures 9-57 and 9-58) as the injected nitrogen strips the oil from its intermediates.

Fifth and Sixth Run

The determination of the amount and distribution of the oil remaining in a reservoir is a critical prerequisite in the selection, design and evaluation of the economics of any tertiary oil method.

In the small pore spaces of the reservoir rock, oil-water interfacial tension forces tend to retain the oil, leading to the entrapment of oil by water during the immiscible water-oil displacement. Much of the oil remains distributed throughout the porous medium as isolated oil droplets. The ideal tertiary oil recovery process must reconnect or mobilize these residual oil droplets and prevent the re-entrapment of the oil before it can be flushed from the porous medium.

So, the fifth run was designed and conducted to simulate the condition for tertiary recovery process by nitrogen displacement (run number 6). The following combinations of flooding systems were used:

Run number 5 - Conventional waterflood, followed by

Run number 6 - Nitrogen displacement process at an injection pressure of 4000 psi.

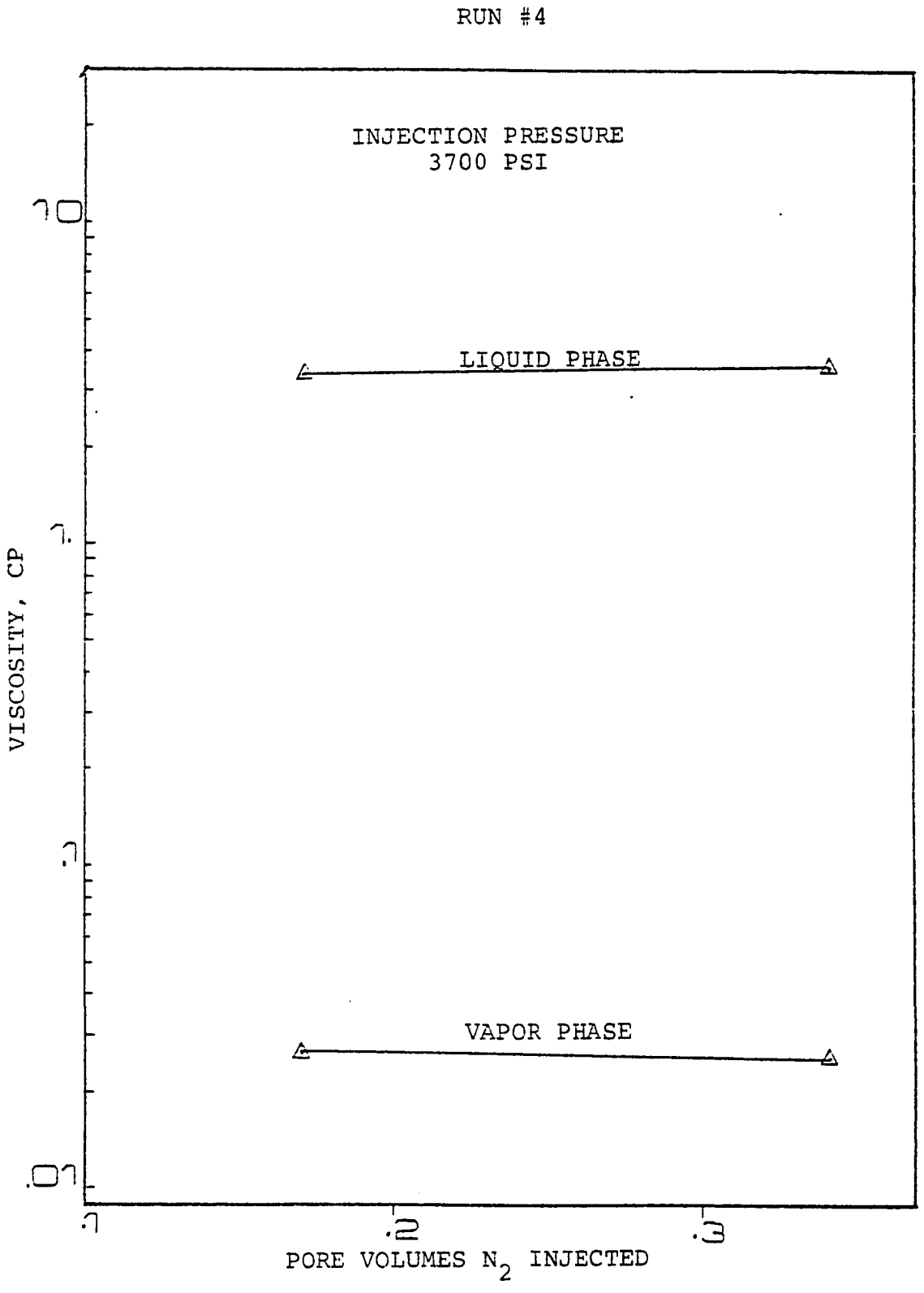

Figure 9-48. Calculated liquid and vapor phase viscosity of samples taken from sampling point "A" vs. pore volumes N_2 injected

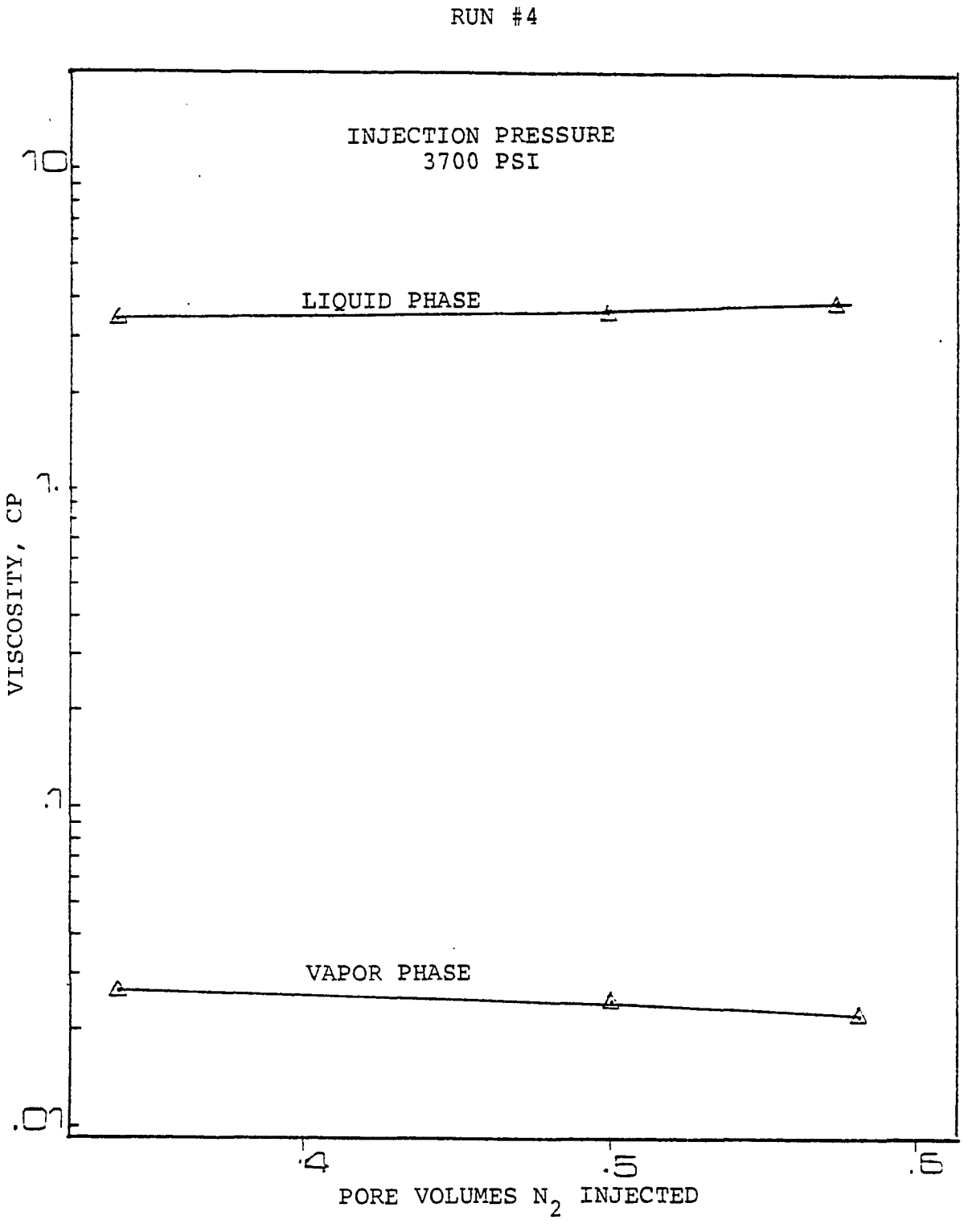

Figure 9-49. Calculated liquid and vapor phase viscosity of samples taken from sampling point "B" vs. pore volumes N_2 injected

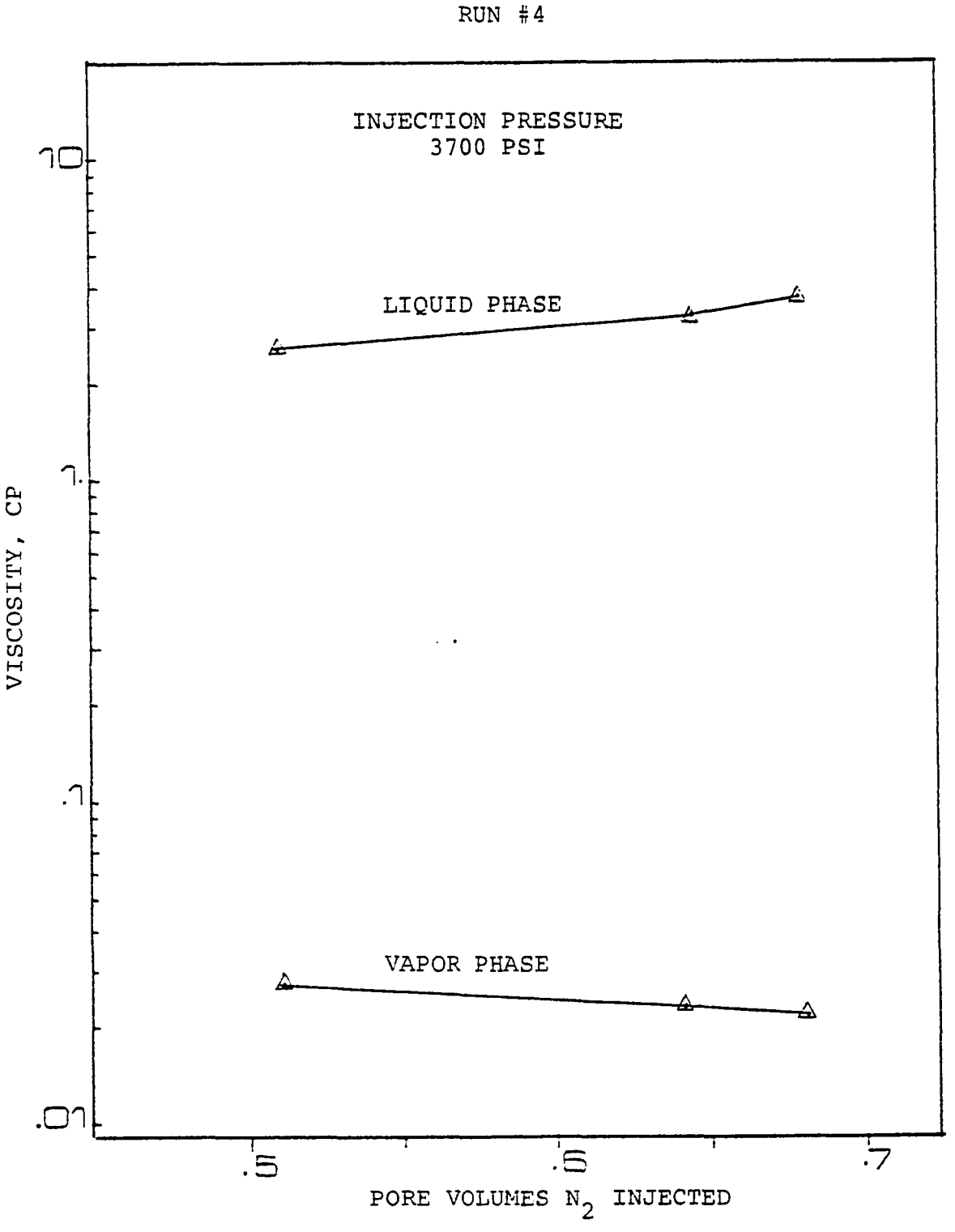

Figure 9-50. Calculated liquid and vapor phase viscosity of samples taken from sampling point "C" vs. pore volumes N_2 injected

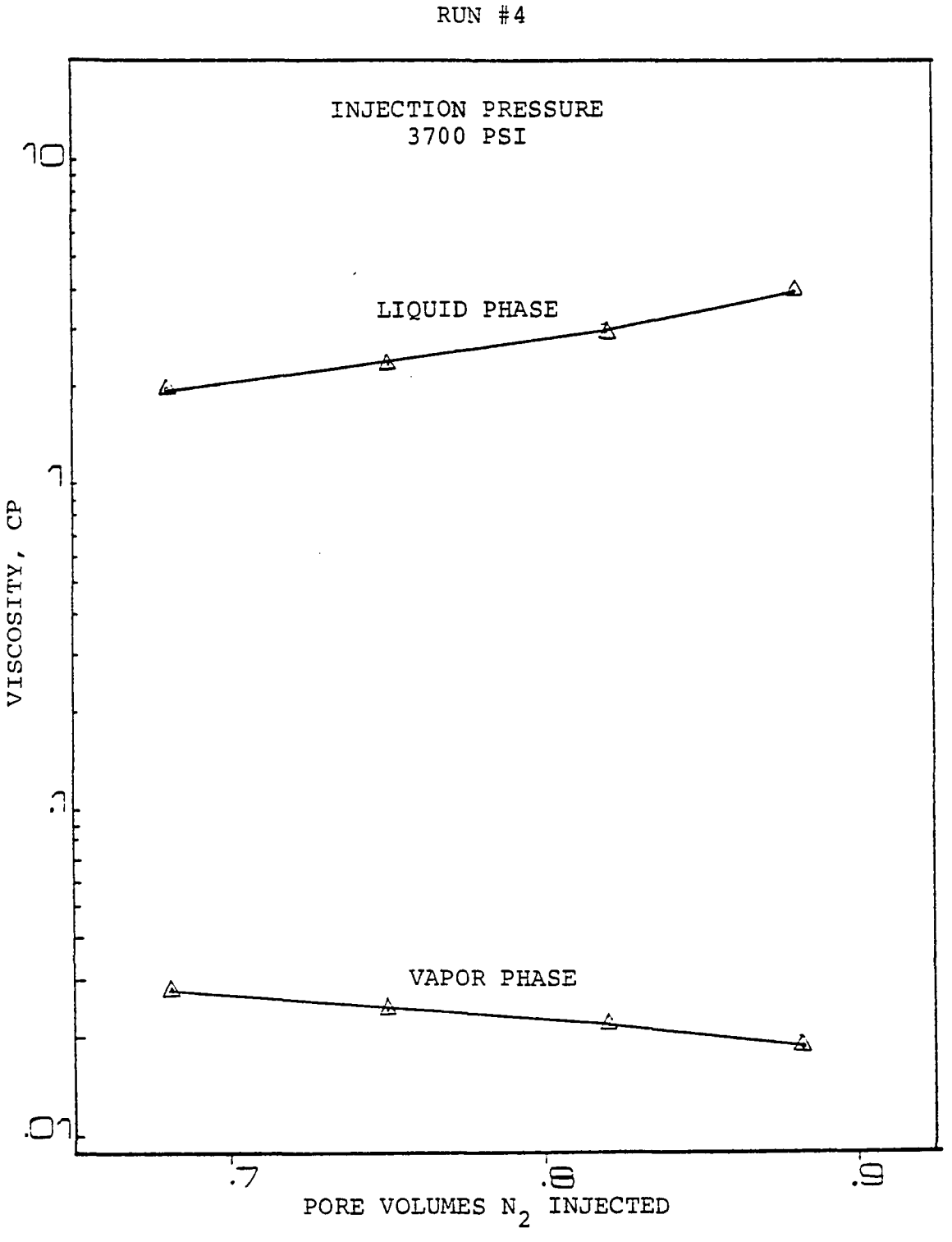

Figure 9-51. Calculated liquid and vapor viscosity of samples taken from sampling point "D" vs. pore volumes N_2 injected

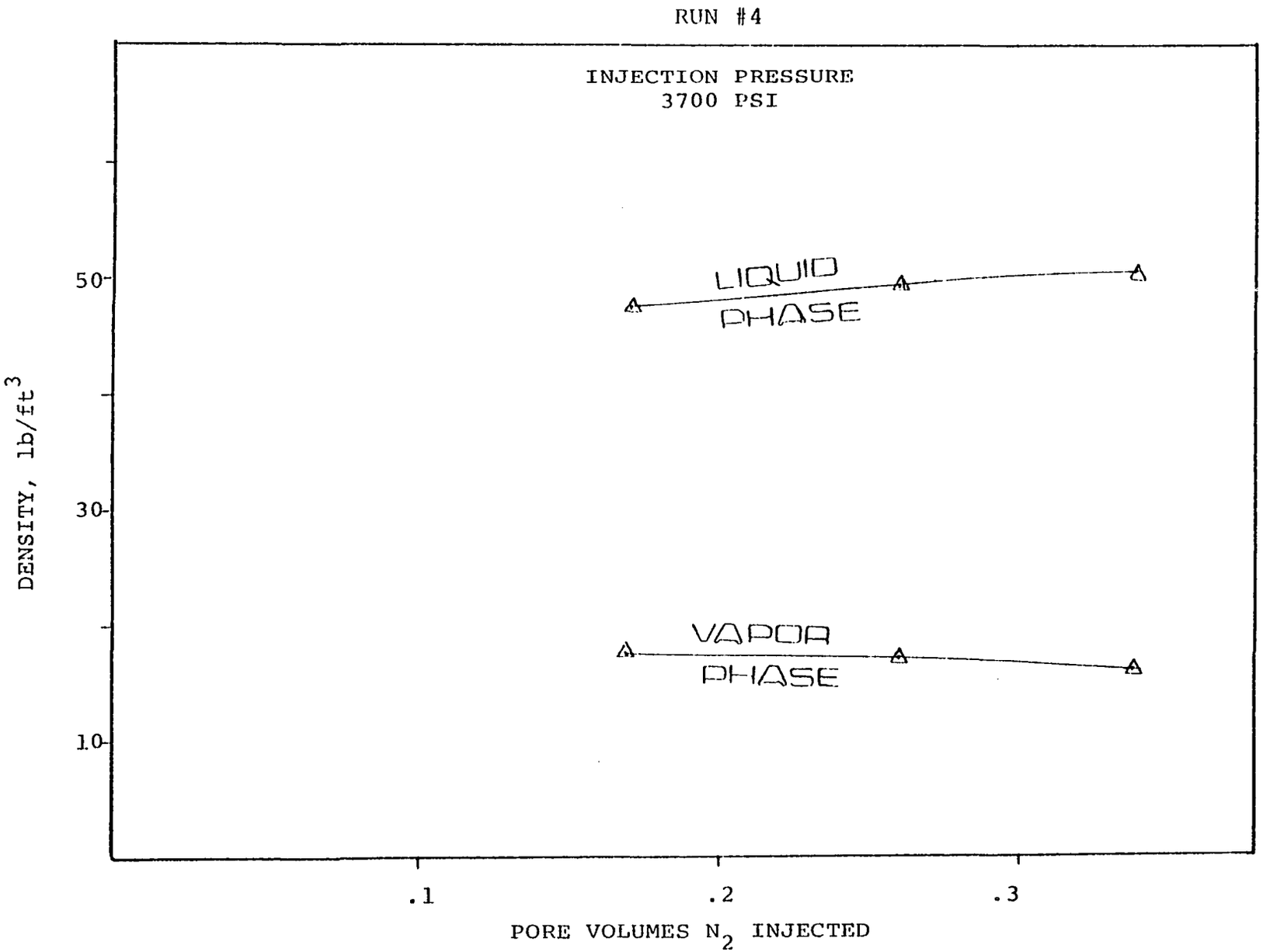

Figure 9-52. Calculated vapor and liquid density of samples taken from sampling point "A" vs. pore volumes N_2 injected

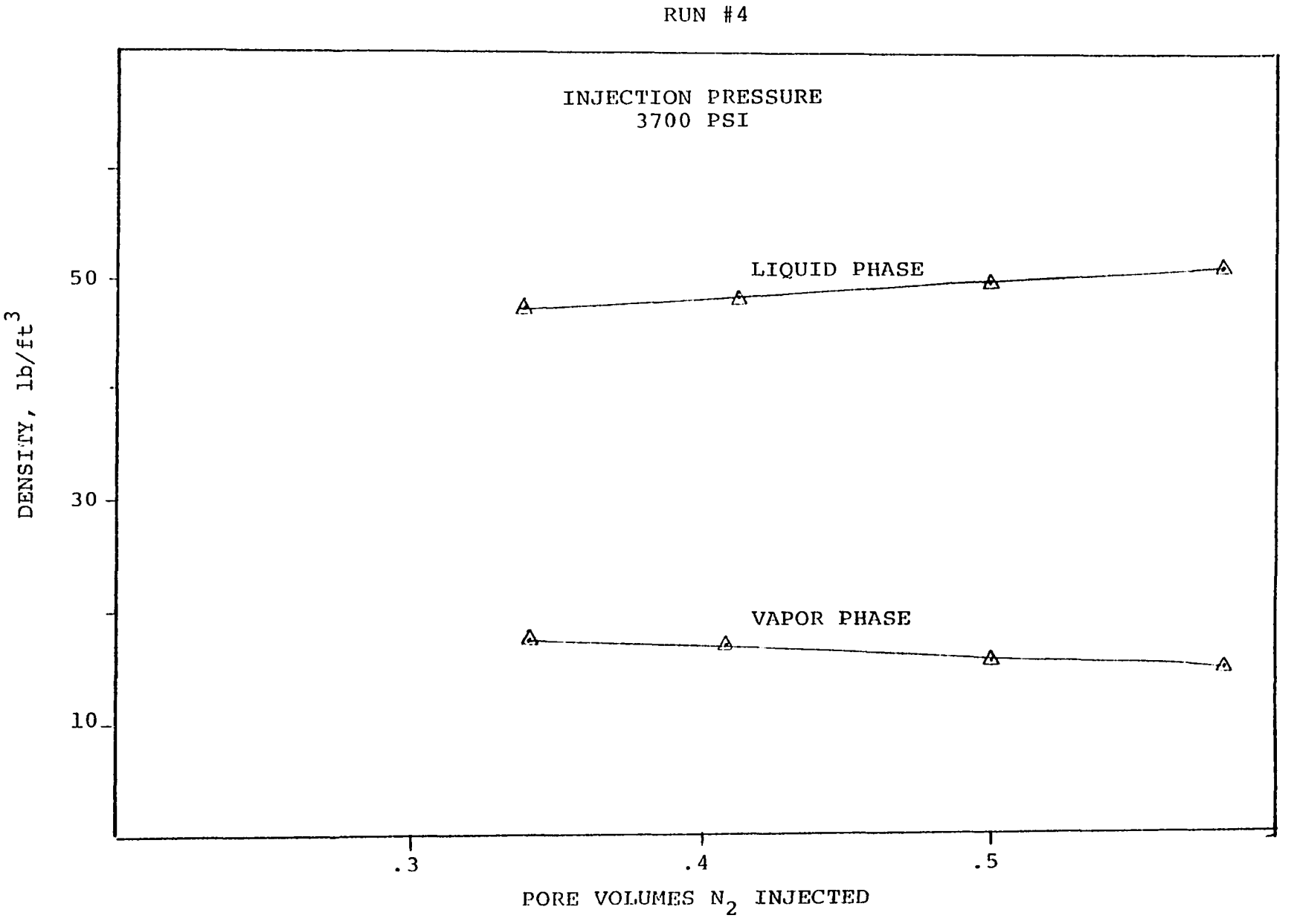

Figure 9-53. Calculated vapor and liquid density of samples taken from sampling point "B" vs. pore volumes N_2 injected

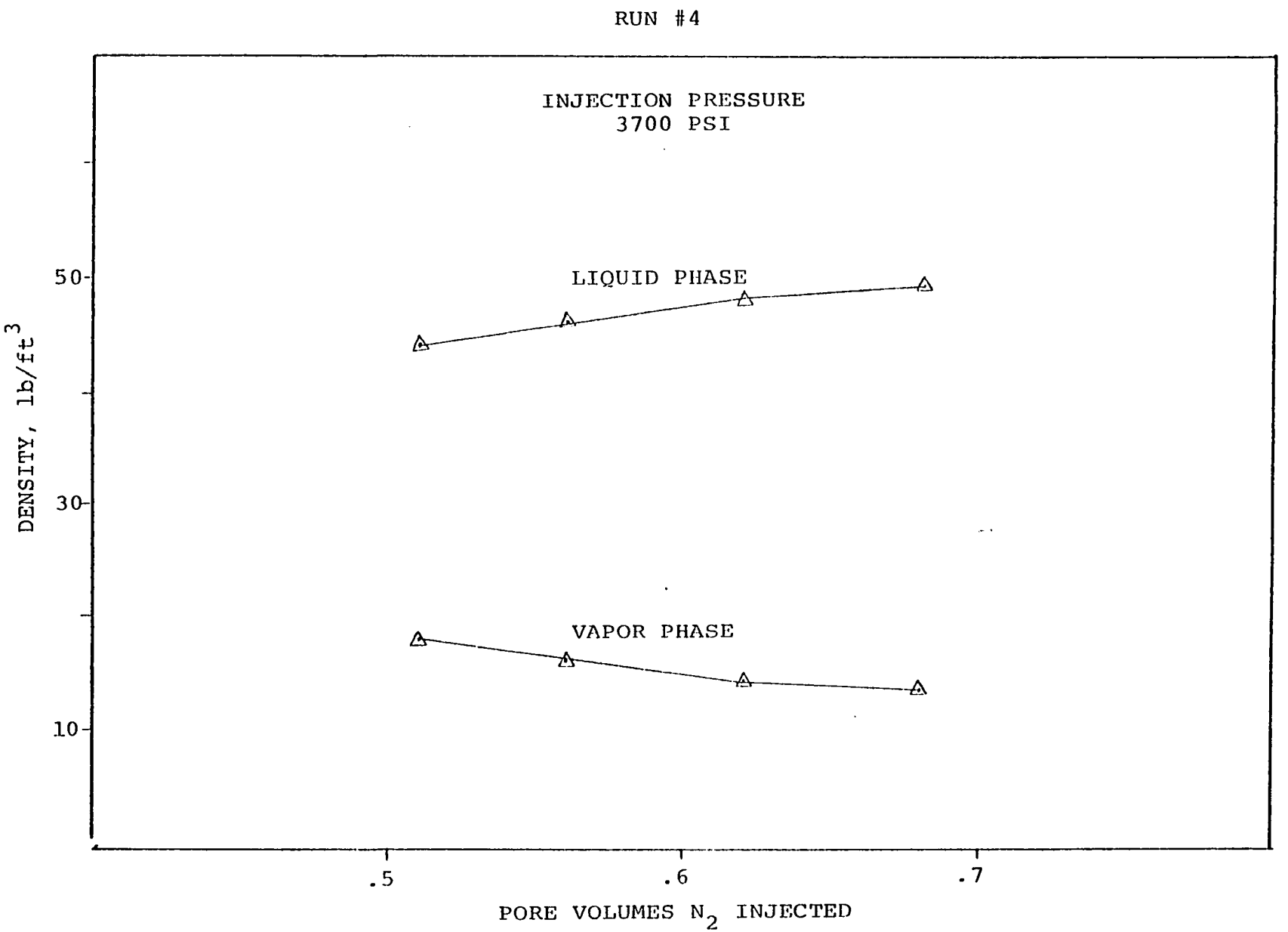

Figure 9-54. Calculated vapor and liquid density of samples taken from sampling point "C" vs. pore volumes N_2 injected

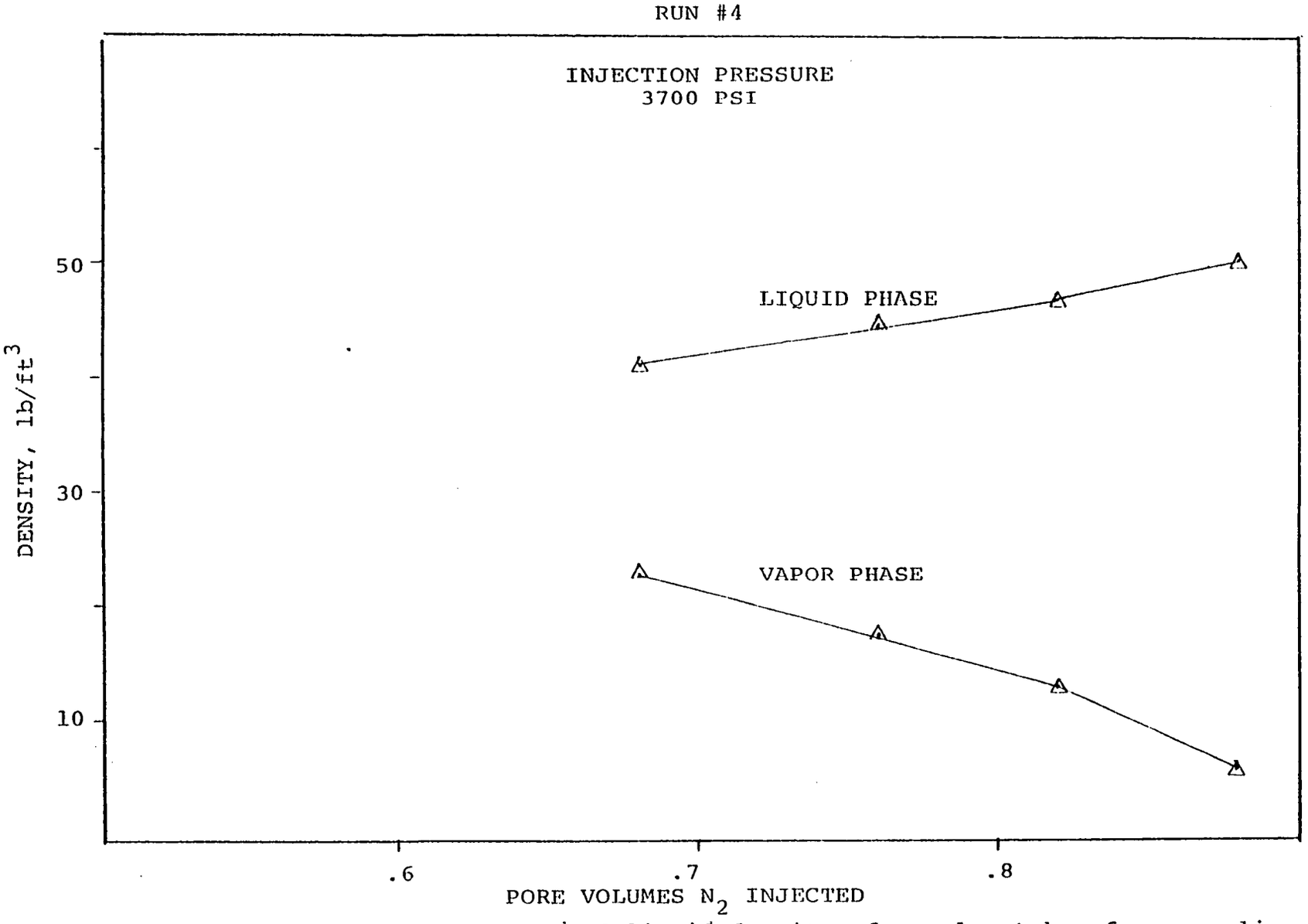

Figure 9-55. Calculated vapor and liquid density of samples taken from sampling point "D" vs. pore volumes N_2 injected

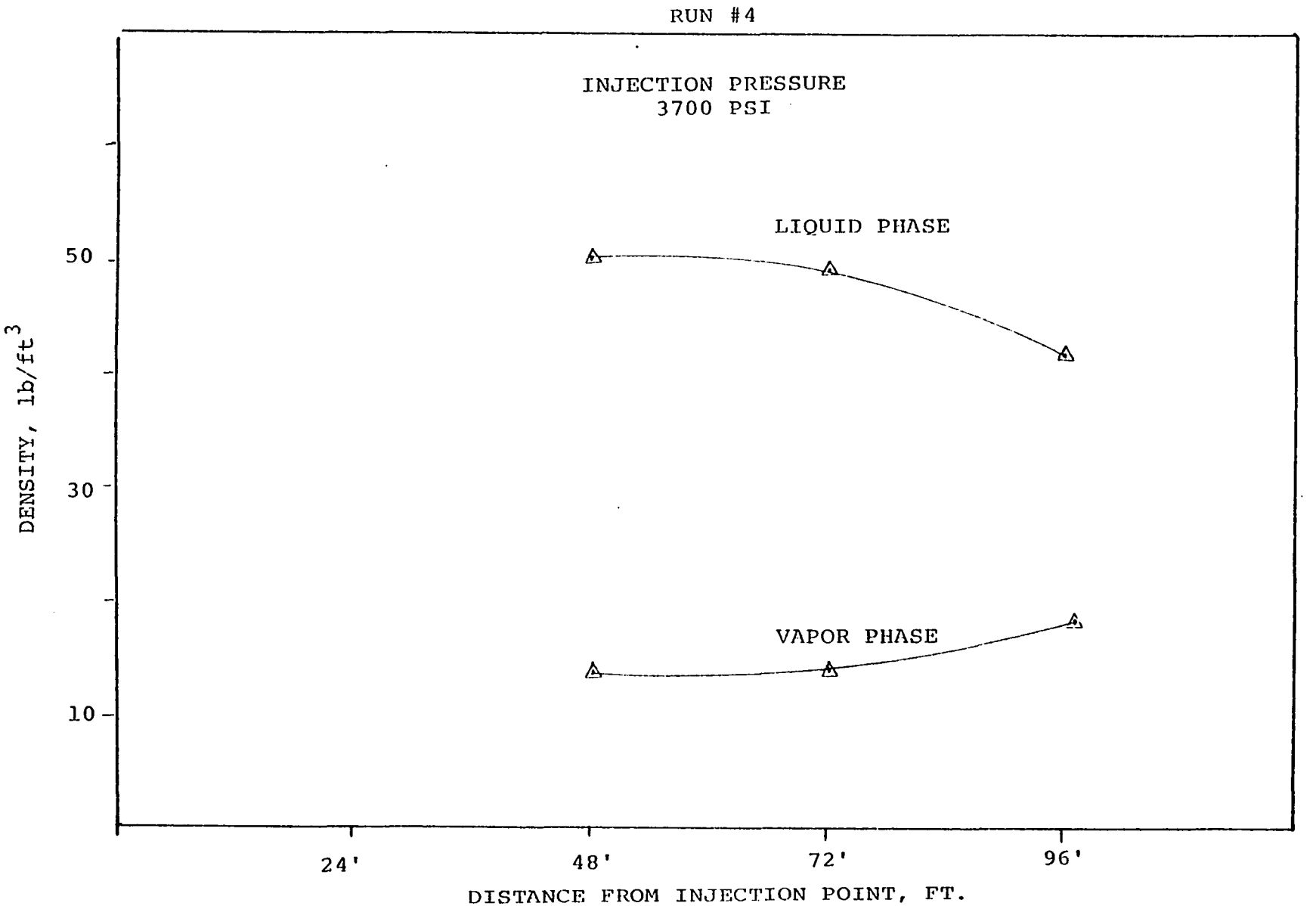

Figure 9-56. Liquid and vapor density distribution throughout the core after injection of 0.68 pore volume of N_2

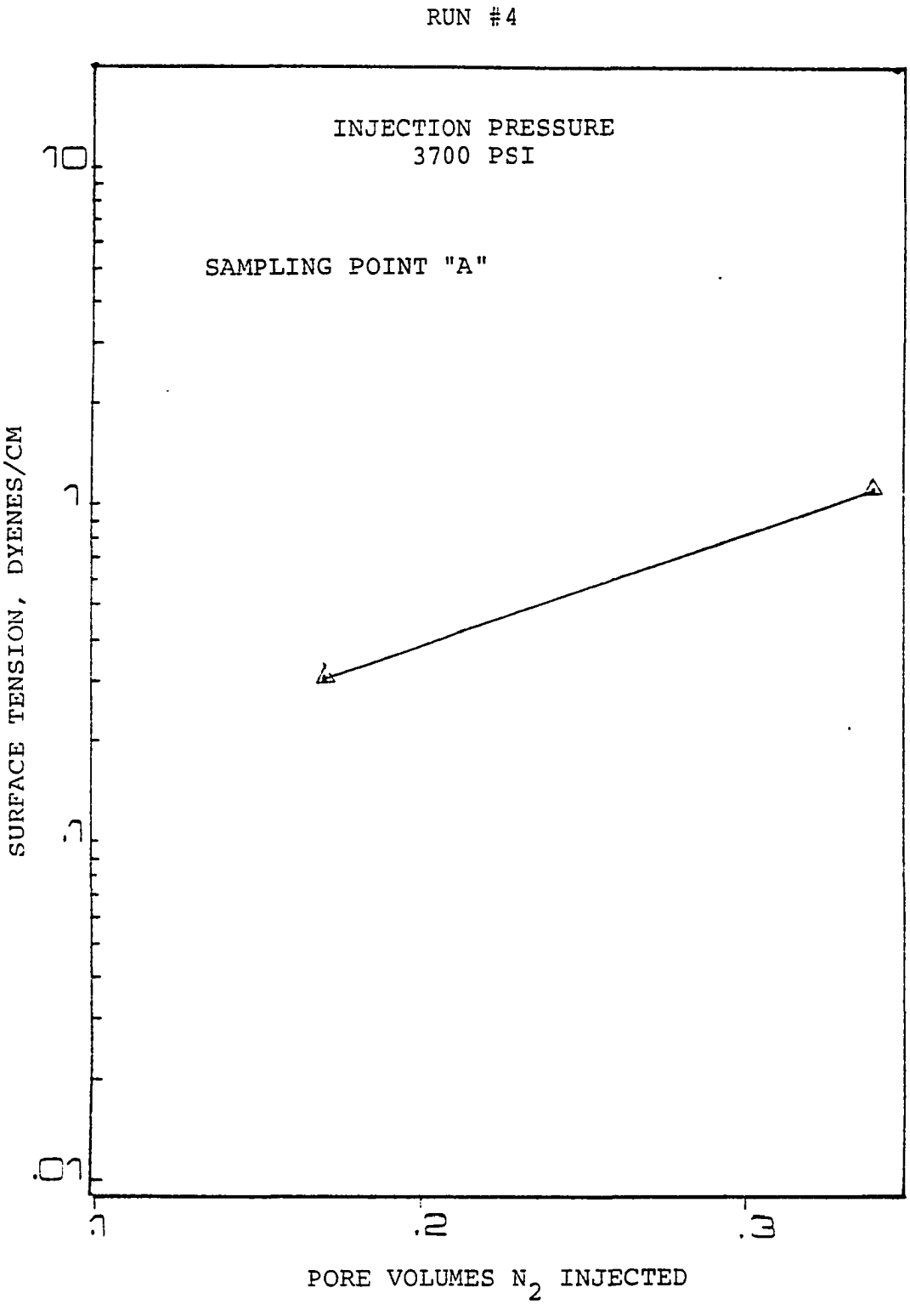

Figure 9-57. Calculated surface tension vs. pore volumes N_2 injected

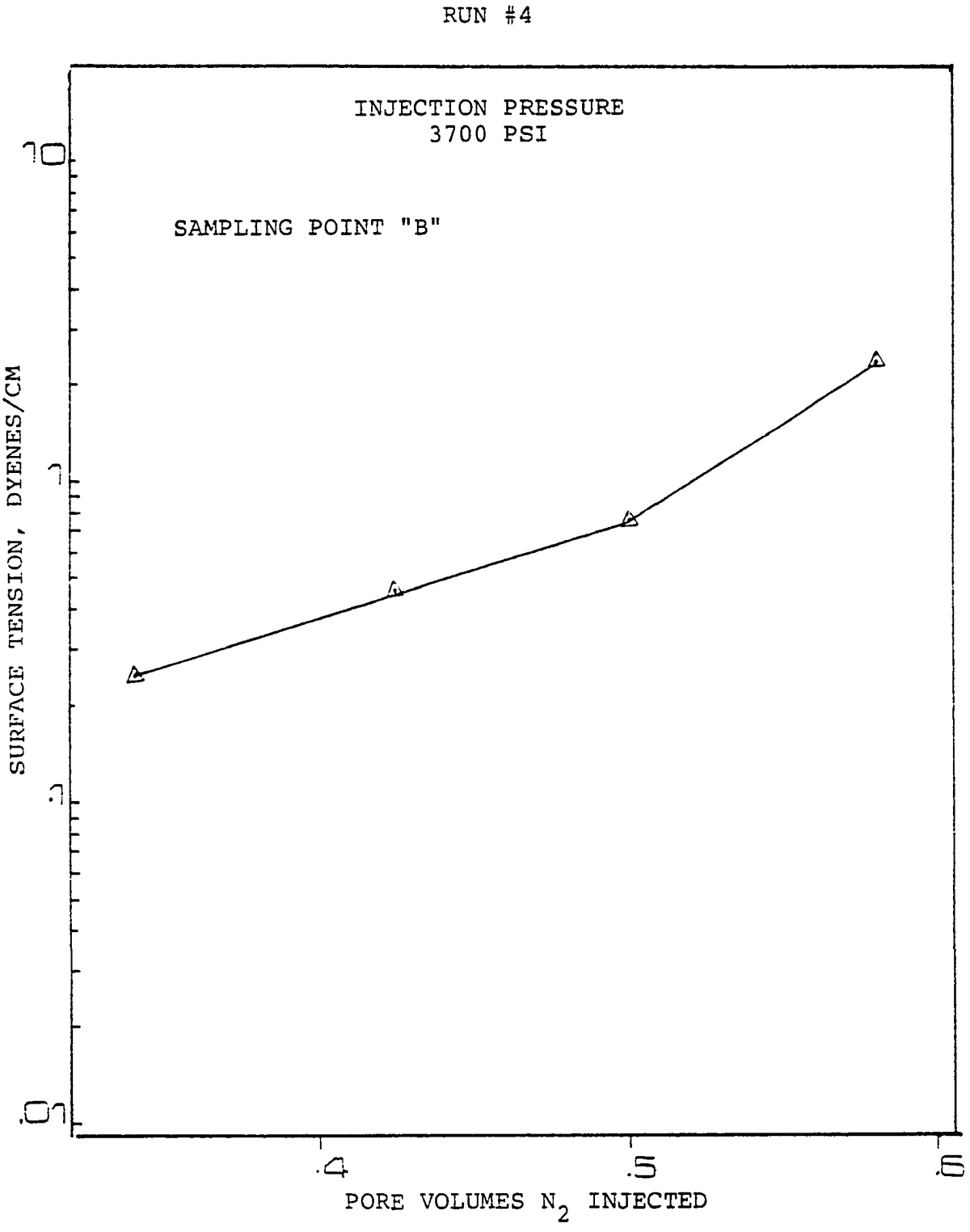

Figure 9-58. Calculated surface tension vs. pore volumes N_2 injected

A summary of the results is given in Table 9-7. Figure 9-59 shows the oil recovery results of run number 6 and 1 as a function of oil saturation. Examining Figure 9-59 leads to the conclusion that to achieve a miscible type displacement by nitrogen, a certain minimum oil saturation must exist before miscibility could occur. The low reported recovery (13 percent) shows that the type of displacement mechanism by nitrogen is a strong function of oil saturation.

Seventh Run

This run was performed on a stock tank oil (dead oil) of 43°API. The crude oil was brought into contact with natural gas to produce recombined samples whose solution gas-oil ratios were 0 and 575 Scf/STB. Figure 9-60 shows oil recovery as a function of gas-oil ratios. Displacement pressure was 5000 psi and system temperature was 70°F. Eighty-six percent recovery of oil in place was obtained for the higher gas-oil ratio run, and 59 percent was observed for the dead oil run.

It appears by examining Figure 9-60 that the resulting type of displacement mechanism is strongly related to the amount of gas in solution (G.O.R.).

Recoveries

Table 9-8 summarizes the pertinent data for all the runs described. A convenient review of the runs is presented in Figure 9-61, in which the percent recoveries are presented as a function of the operating pressures.

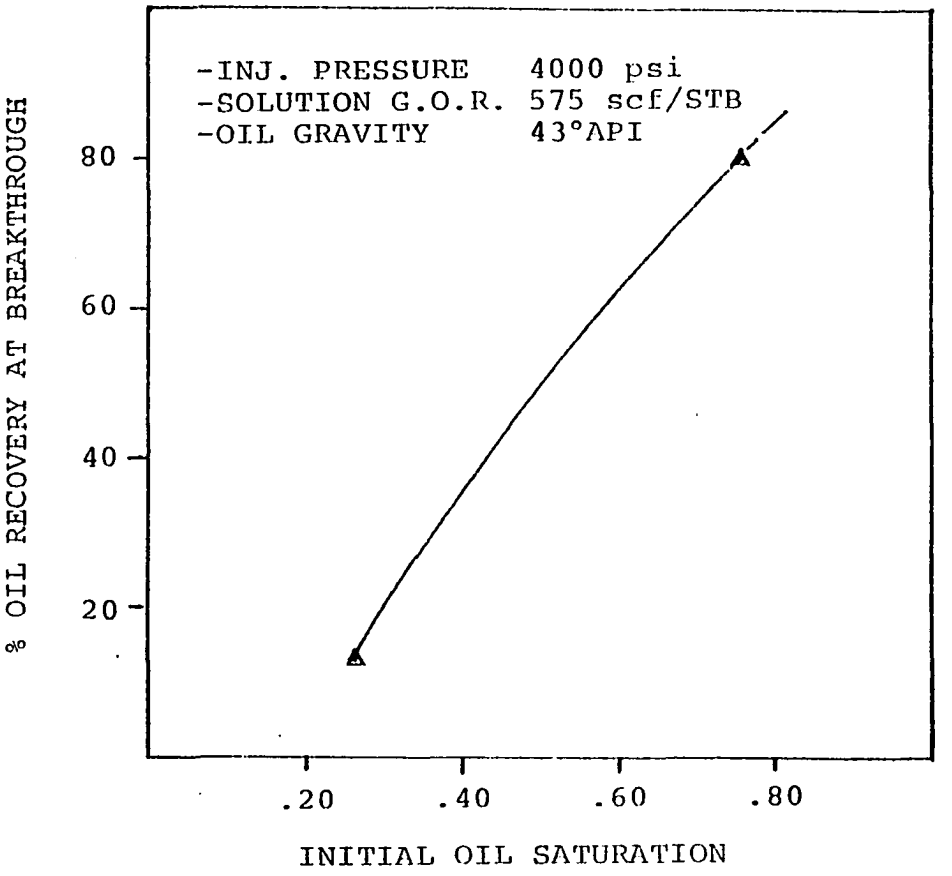

Figure 9-59. Percent of the oil recovery vs. oil saturation

TABLE 9-7

OIL DISPLACEMENT RECOVERY - RUN NUMBERS 5 AND 6

Run #	Type of Displacing Phase	Inj. Pressure psi	Initial Oil Saturation Fraction	Initial Water Saturation Fraction	Initial S.T.O. in Place CC	Oil Recovery at Breakthrough % of I.O.I.P.	Type of Displacing Mechanism
5	Water	Variable	.76	.24	702	65	Immiscible
6	Nitrogen	4000	.266	.734	246	13	Immiscible

TABLE 9-8

DATA AND RESULTS OF THE CONDUCTED RUNS

Run No.	Type of Displacing Fluid	Inj. Pressure psi	Solution G.O.R. Scf/STB	Type of Displacement	Initial Oil Saturation	Initial Water Saturation	Initial S.T.O. in Place CC	Cum. Oil Produced at B.T. CC	Oil Recovery, % of I.O.I.P.
1	N_2	4000	575	Miscible	.756	.244	698	558	80
2	N_2	5000	575	Miscible	.75	.25	692	595	86
3	N_2	3000	575	Immiscible	.732	.268	676	365	54
4	N_2	3700	575	Immiscible	.743	.257	686	494	72
5	H_2O	variable	575	Immiscible	.76	.24	702	456	65
6	N_2	4000	575	Immiscible	.266	.734	246	32	13
7	N_2	5000	0	Immiscible	.75	.25	900	531	59

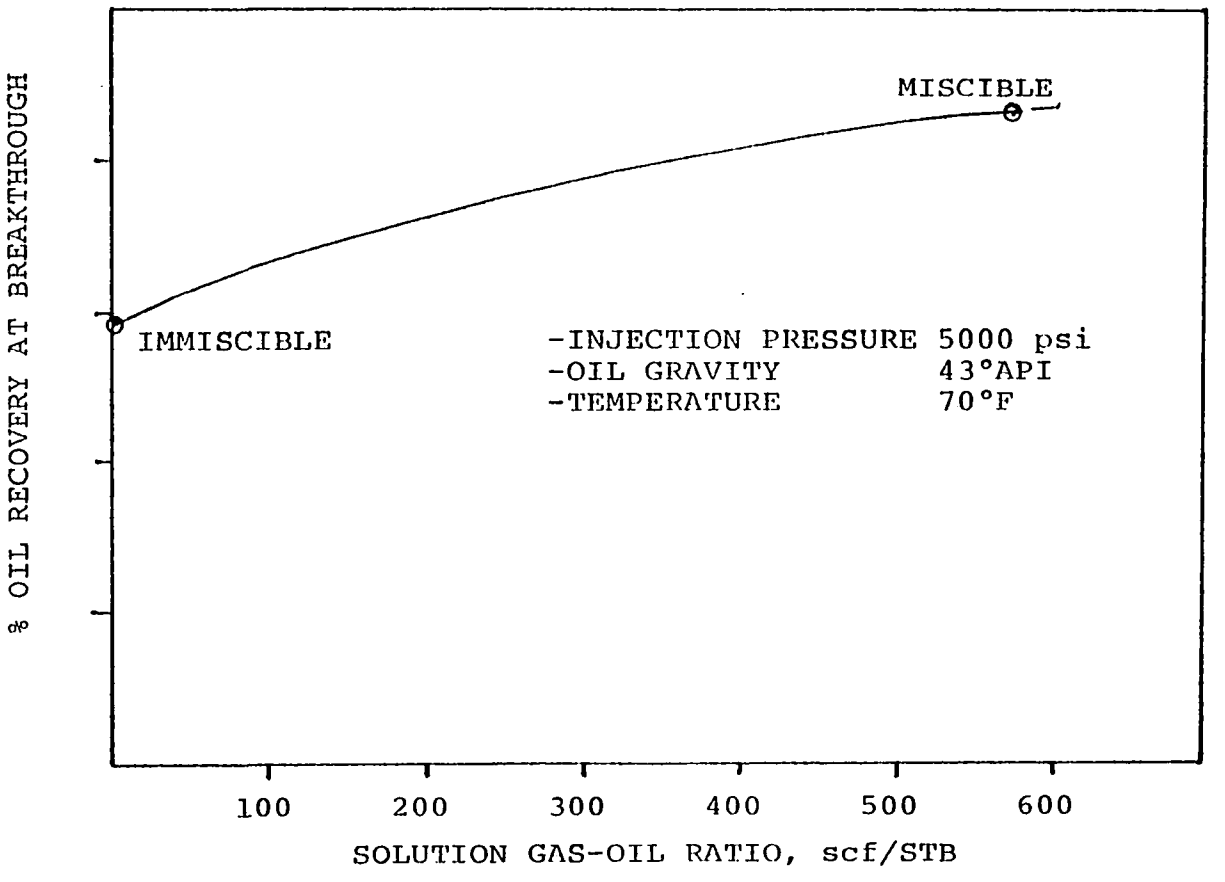

Figure 9-60. Percent of the oil recovery vs. solution G.O.R.

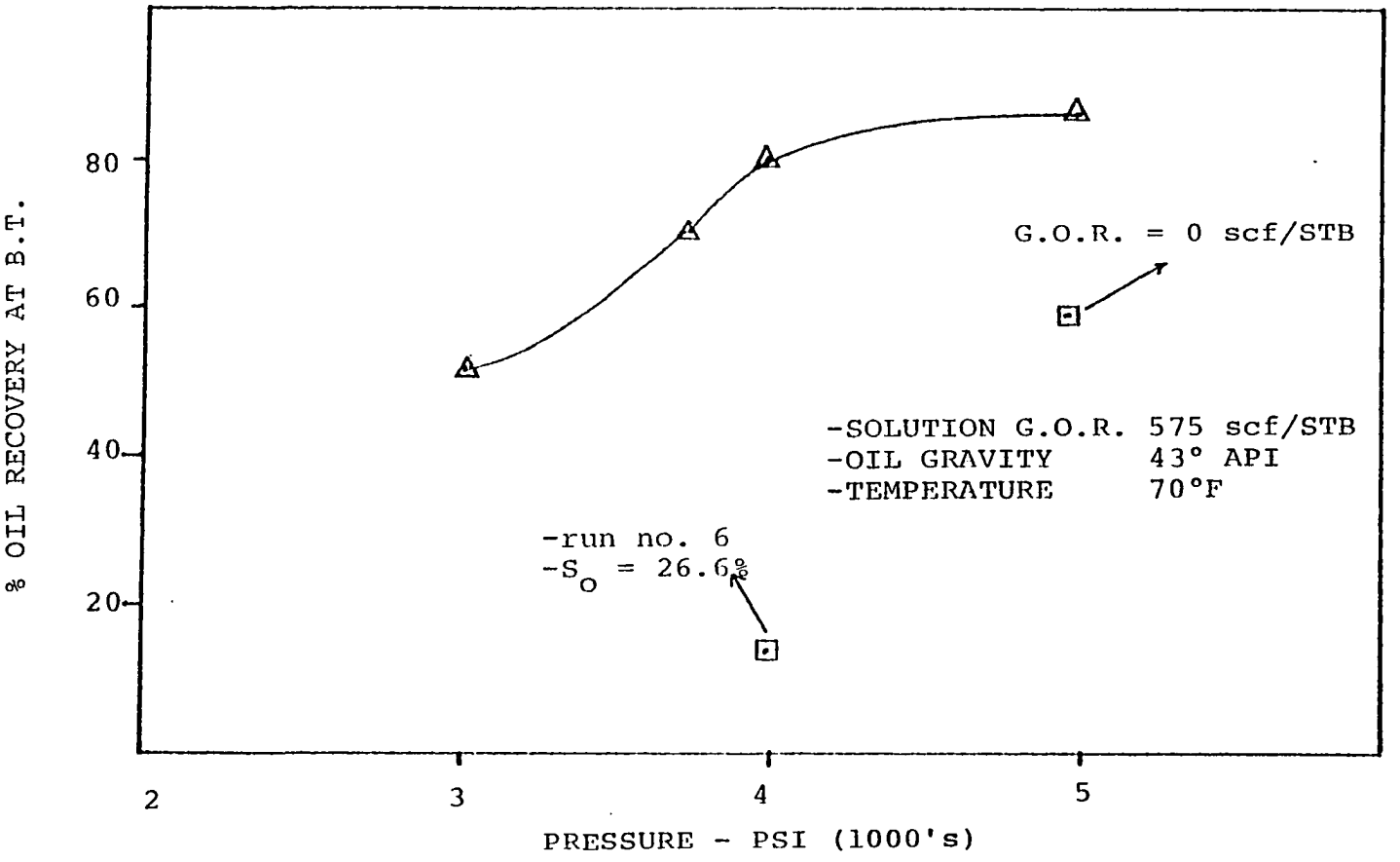

Figure 9-61. Effect of pressure on oil recovery

A miscible displacement should recover 100 percent of the oil in place. The fact that this was not quite reached in the miscible displacement runs (run numbers 1 and 2) is attributed to the fact that the gas must travel some distance through the porous medium before miscibility is achieved. Some of the reservoir liquid at the injection end of the system is unrecoverable. This is the oil that has been denuded of the intermediates by the injected nitrogen in the process of enriching it.

Figure 9-61 shows a sharp increase in recovery as the pressure is increased to 4000 psi. It appears that the minimum mescibility pressure is in the range of 3700 to 4000 psi.

Finally, figures 9-62 through 9-65 show the cumulative gas-oil ratio during displacement by nitrogen. Cumulative produced gas-oil ratios were seen to remain constant until nitrogen breakthrough. Nitrogen breakthrough was determined experimentally by observing the gas-oil ratio, the produced fluids and by continually monitoring the composition of the produced gases. A complete detailed analysis of the production history of the runs are tabulated in Appendix D.

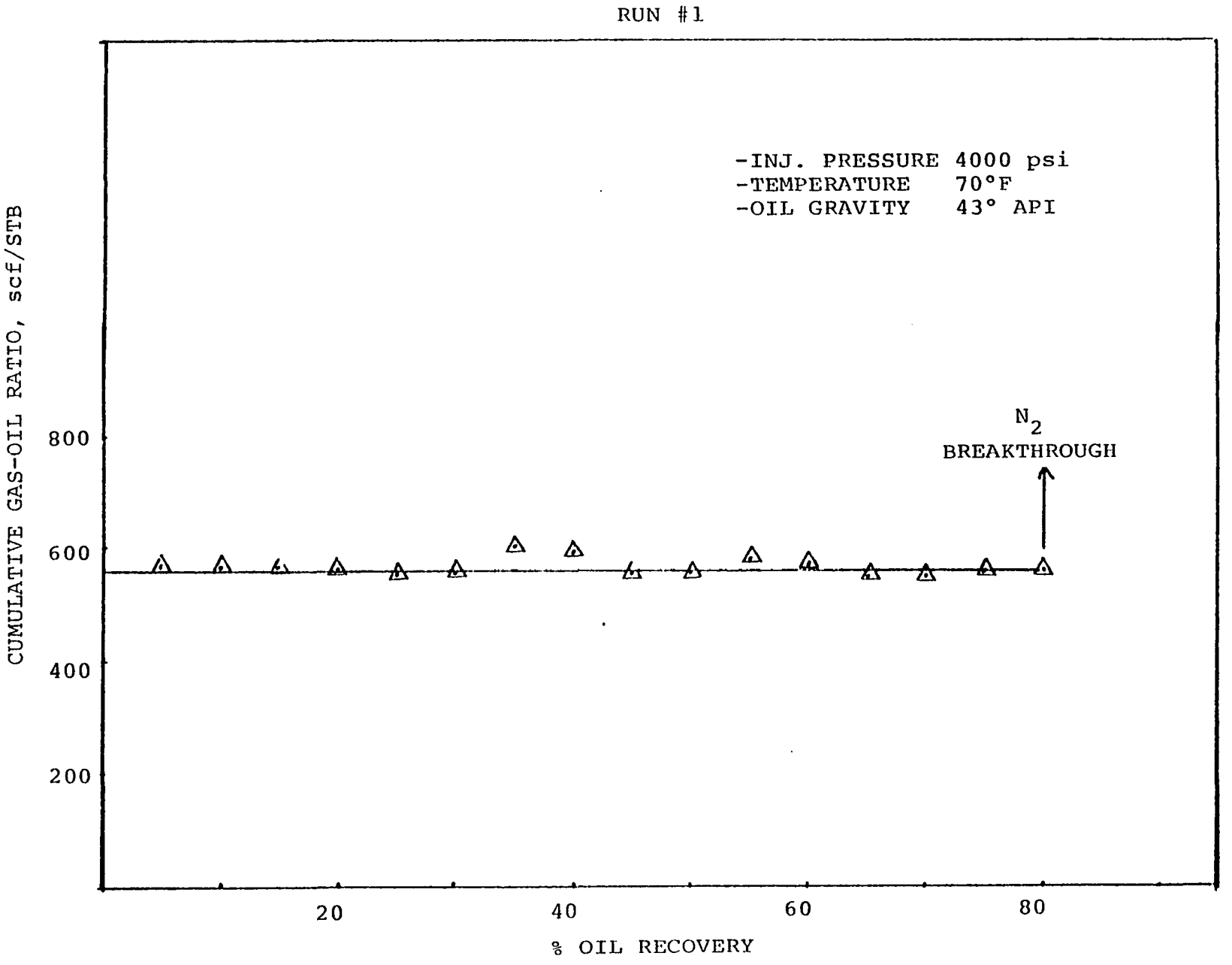

Figure 9-62. Producing G.O.R. vs. percent of the oil recovery

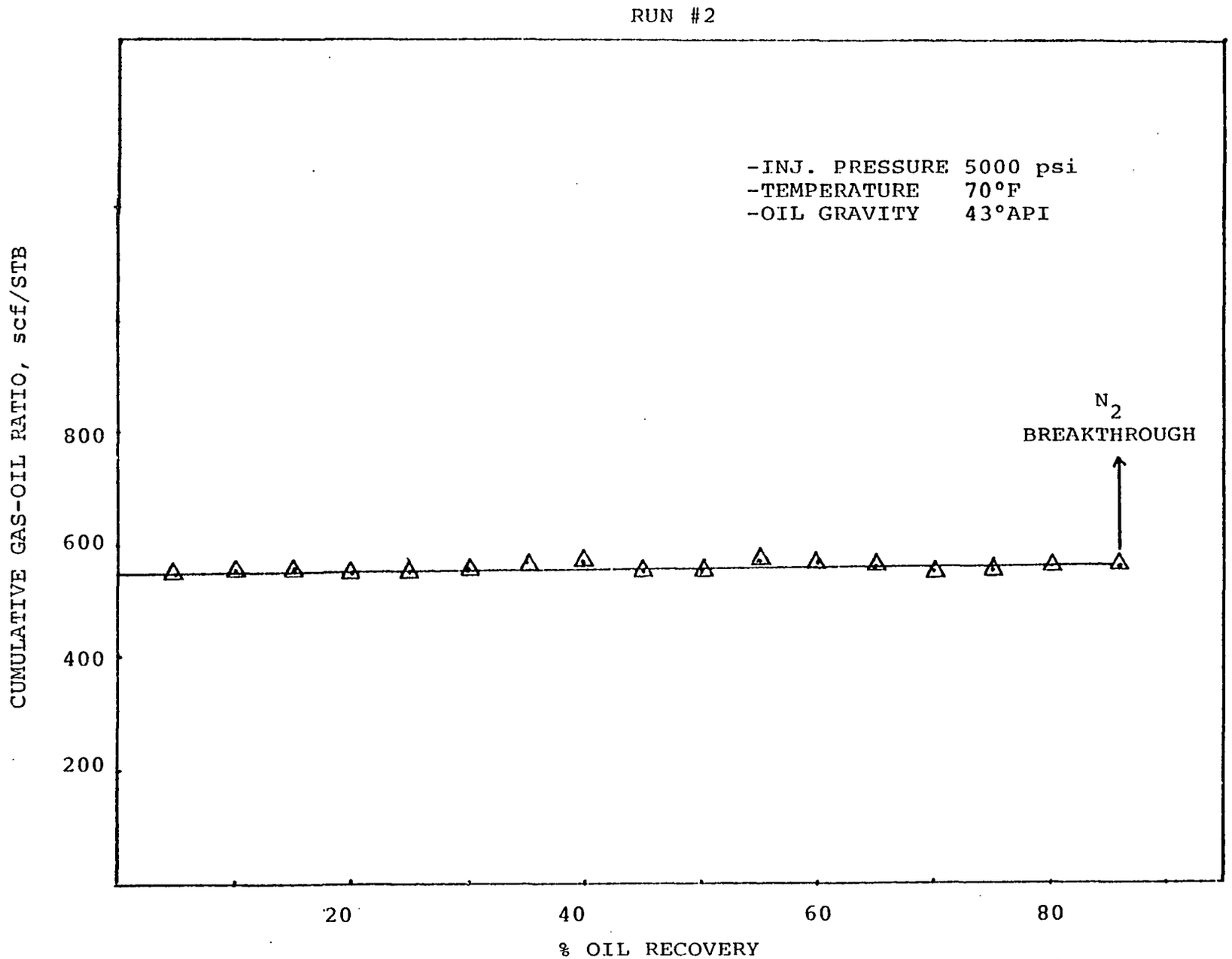

Figure 9-63. Producing G.O.R. vs. percent of the oil recovery

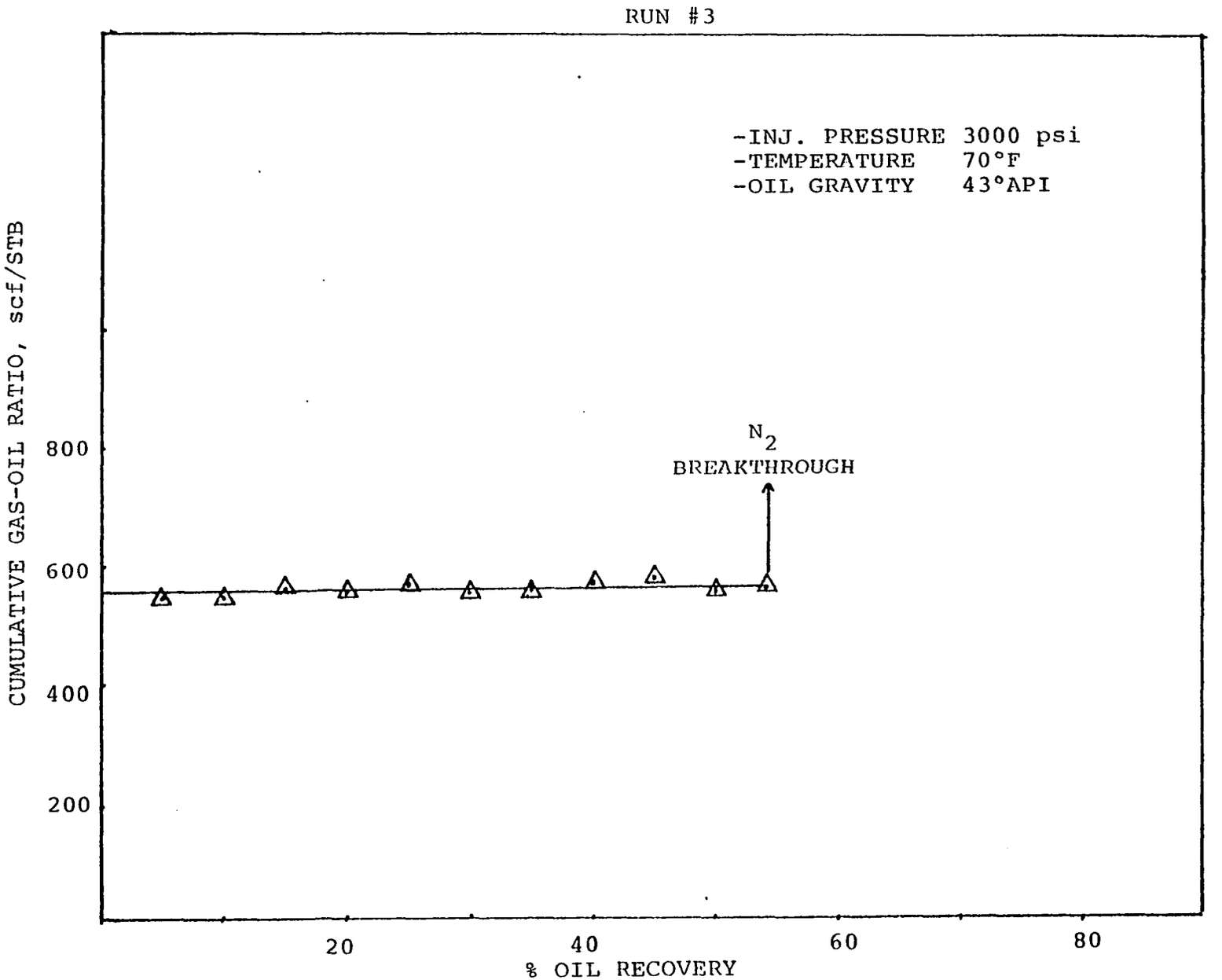

Figure 9-64. Producing G.O.R. vs. percent of the oil recovery

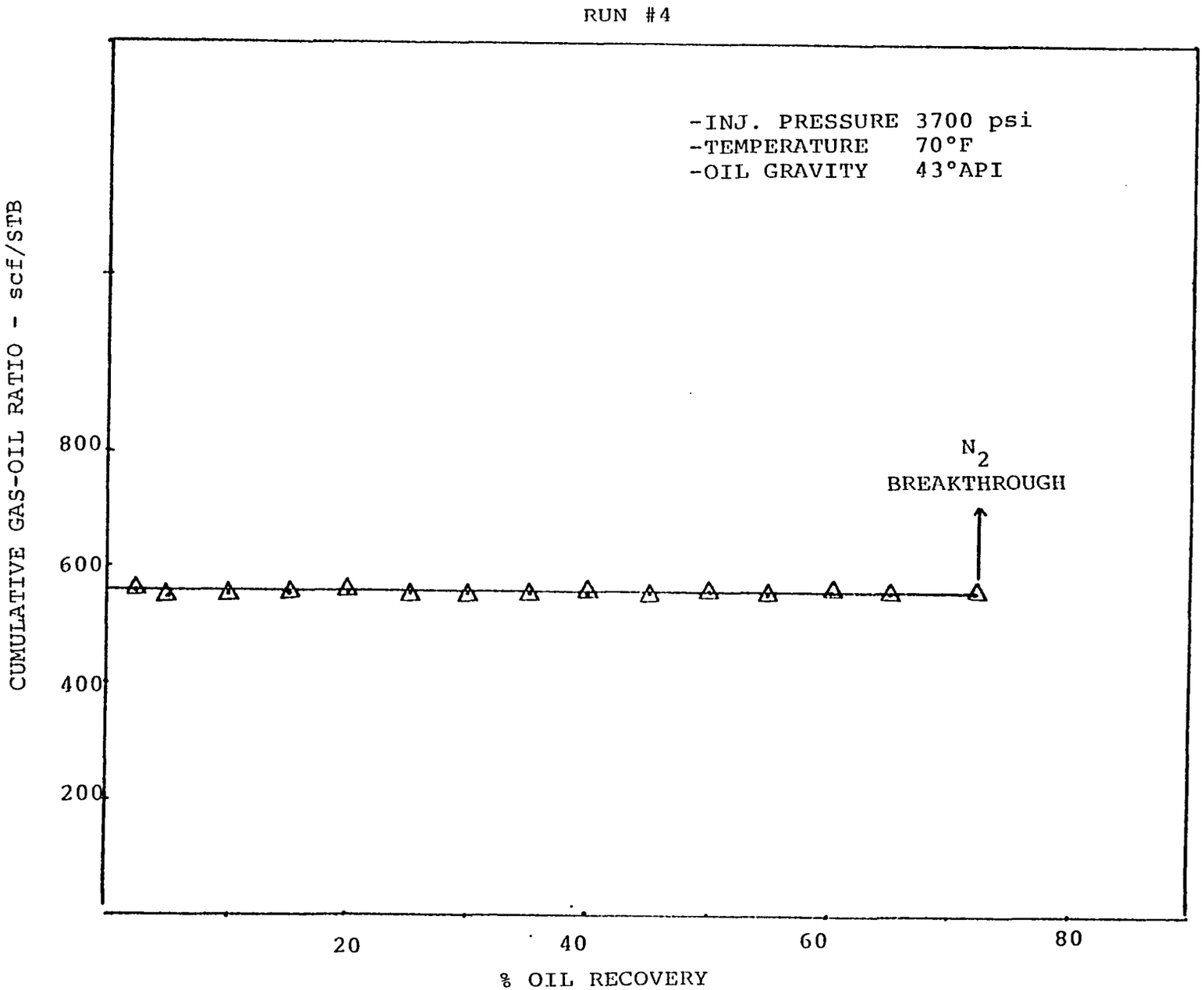

Figure 9-65. Producing G.O.R. vs. percent of the oil recovery

CHAPTER X

CONCLUSIONS

The following conclusions, while based on the data from this work and apply only to the porous medium, fluids, and displacement conditions used in this work, can be indicative of results and conclusions for a similar system.

1. An analysis of the vapor phase formed in the third run (injection pressure 3000 psi) did not show any traces of the intermediate components (C_2-C_{6+}) which led to the concept of "Minimum Evaporization Pressure."
2. The results show that a rich gas slug, followed by a transition zone, will be developed in the reservoir model (runs number 1, 2, and 4) at pressures greater than the minimum evaporization pressure.
3. An increase in the nitrogen injection pressure, above that of the minimum miscibility pressure, will not produce a substantial increase in the final mole fraction of intermediate components in the generated rich gas slug.
4. For pressure ranges studied, a decrease in the size of the formed slug occurs when the pressure increases.
5. The results indicated that two processes would occur during the nitrogen displacement:

a. In the generated slug, a mutual solubility of the phases at the higher pressure with the attendant effect of reduction in the difference in viscosity between the displaced and displacing phases.

b. Behind the generated slug (transition zone), a stripping process would occur.

6. Concentration of the intermediate components behind the generated slug decreases more rapidly as the injection pressure increases.

7. This study confirms the importance of the ternary diagram as a reliable guide for predicting the conditions required for miscibility in a flowing system of considerable complexity.

8. Surface tension at the interface between the liquid phase and the generated rich gas slug for runs 1 and 2 was far below 1.0 dynes/cm.

9. This investigation shows that the oil saturation and solution gas-oil ratio are important parameters in obtaining miscible behavior.

10. The higher the pressure the shorter the transition zone.

11. The criterion for determining miscibility is established by the shape of the compositional profiles of the displacing phase in the reservoir model. When a plateau section of the compositional profiles develops, it is a clear indication of the presence of miscibility.

CHAPTER XI

RECOMMENDATIONS FOR FURTHER WORK

1. The author would recommend that data from such experiments be employed in calibrating phase behavior models used in detailed nitrogen flooding simulations. The model can be developed as follows:
   a. Model Description: Briefly, the model should include fluid flow by Darcy's Law and mass transfer of components between phases. The mass transfer of components can be simulated through the use of the Redlich-Kwong equation of state. On the other hand, the phase properties can be simulated by using the methods described in Chapter V.
   b. Input Variables: Input to the model describes the test conditions for each displacement run. These include core properties, injection rate, fluid properties, initial system pressure, and temperature.
   c. Adjustable Variables: Only two variables can be easily adjusted if the input data are to describe a specific displacement. These are the number of grid blocks (or size of grid block) used to discretize the simulated 125 foot core and time steps.

d. Criteria for Matching: The criteria for achieving an acceptable match of a laboratory displacement by model simulation is to predict the experimentally determined oil recovery and the compositional profiles for each component as a function of pore volumes injected. Requirements for a good match of compositional profiles are the slope and shape of the predicted curves.

2. It is important to investigate the effects of oil saturation, solution gas-oil ratios, and temperatures on the behavior of the miscible displacement by nitrogen injection.

NOMENCLATURE

$\bar{M}$ = Average molecular weight

y_i = Mole fraction of ith component in vapor phase

M_i = Molecular weight of ith component

P = Absolute pressure of the system, psi

T = Absolute temperature °R

R = Gas constant = 10.72 psi ft^3/lb mole °R

Z = Gas deviation factor

P_r = Pseudo-reduced pressure, dimensionless

T_r = Pseudo-reduced temperature, dimensionless

P_{c_i} = Critical pressure of the ith component, psi

T_{c_i} = Critical temperature of the ith component, °R

ρ_v = Vapor density, lb/ft^3

x_i = Mole fraction of ith component in liquid phase

ρ_L = Liquid density, lb/ft^3

V_i = Specific volume of the ith component, ft^3/lb

$V_{c_{6+}}$ = Specific volume of hexane and heavier, ft^3/lb

EMR = Eykman Molecular Refraction

P_{chi} = Parachor of ith component

σ = Surface tension, dynes/cm

b = Constant characteristic of a particular hydrocarbon

T_b = Boiling point, °R

U_l = Viscosity of gas mixture at atmospheric pressure, cp

U_i^* = Viscosity of component i at atmospheric pressure, cp

V_{c_i} = Critical volume of i component, ft^3/lb-mole

E = Mixture viscosity parameter

ρ_r = Reduced density, dimensionless

K_i = Equilibrium vaporization ratio for an oil fraction "i"

P_k = Convergence pressure, psi

HETP = Height equivalent to a theoretical plate

N = Number of theoretical plates

RF = Response factor

A = Peak height, cm^2

B.T. = Breakthrough

P.V. = Pore volume

BIBLIOGRAPHY

1. Whorton, L. P. and Kieschnick, W. F., "A Preliminary Report on Oil Recovery by High-Pressure Gas Injection," Drilling and Production Practice, 247 (1950).
2. Clark, Norman J.; Schultz, W. P. and Shearin, H. M., "Miscible Displacement by Gas Drive," J. Petroleum Tech. (June 1958), p. 11.
3. Koch, H. A., Jr., and Slobod, R. L., Trans. Am. Inst. Mech. Engrs. (1957), p. 40.
4. Hall, H. N., and Geffen, T. M., ibid., p. 48.
5. Slobod, R. L., and Koch, H. A., Jr., "High-Pressure Gas Injection Mechanism of Recovery Increase," API Drilling and Production Practice (1953), p. 83.
6. Hutchinson, C. A., Jr., and Braun, P. H., "Phase Relation of Miscible Displacement in Oil Recovery," A. I. Ch. E. Journal, vol. 7, no. 1 (March 1961), p. 64.
7. Rushing, M. D.; Thomasson, B. C., Reynolds, B.; and Crawford, P. B., "High Pressure Air Injection," Petroleum Engineer, Nov. 1976.
8. Rushing, M. D.; Thomasson, B. C.; Reynolds, B.; and Crawford, P. B., "Miscible Displacement with Nitrogen," Petroleum Engineer, Nov. 1977.

9. Rushing, M. D.; Thomasson, B. C.; Reynolds, B.; and Crawford, P. B., "High Pressure Nitrogen or Air May be used for Miscible Displacement in Deep, Hot Oil Reservoir," 24th Annual Southwestern Petroleum Short Course Ass. Mtg. Proc. (1977), p. 119.

10. Corkeville, J.; Van Quy, N. and Simandox, P., "A Numerical and Experimental Study of Miscible or Immiscible Fluid Flow in Porous Media with Interphase Mass Transfer," Paper SPE 3481 Presented at SPE-AIME 46th Annual Fall Meeting, New Orleans.

11. Yarborough, L, and Smith, L. R., "Solvent and Driving Gas Composition for Miscible Slug Displacement," Soc. Pet. Eng. J. (Sept. 1970), pp. 298-310, Trans., AIME, vol. 249.

12. Craft, B. C., and Hawkins, M. F., Applied Petroleum Reservoir Engineering, Prentice-Hall, Inc., Englewood Cliffs, N.J. (1959), pp. 355-408.

13. Frick, T. C., Petroleum Production Handbook, vol. II, McGraw Hill Book Co., Inc., N.Y. (1962).

14. Koch, H. A., Jr., and Hutchinson, C. A., Jr., "Miscible Displacement of Reservoir Oil Using Flue Gas," Trans. AIME, vol. 231 (1958), p. 7.

15. Koch, H. A., Jr., "High Pressure Gas Injection is a Success," World Oil (Oct. 1956), p. 260.

16. Stone, H. L., and Crump, J. S., "The Effect of Gas Composition upon Oil Recovery by Gas Drive," Trans. AIME, vol. 207 (1956), p. 105.

17. Blackwell, R. J.; Rayne, J. R.; and Terry, W. M., "Factors Influencing the Efficiency of Miscible Displacement," Trans. AIME, vol. 217 p. 1.

18. Cook, Alton B.; Johnson, S. F. and Spencer, G. B., "Effects of Pressure, Temperature and Type of Oil on Vaporization of Oil During Gas Cycling," USBM RI7278 (July 1969).

19. Wilson, J. F., "Miscible Displacement - Flow and Phase Relationships for a Partially Depleted Reservoir," Trans. AIME, vol. 219 (1960), p. 223.

20. Rutherford, W. M., "Miscibility Relationships in the Displacement of Oil by Light-Hydrocarbons," Soc. Petro. Eng. Journal (Dec. 1962), p. 310.

21. Arnold, C. W.; Stone, H. L.; and Luffel, D. L., "Displacement of Oil by Rich Gas Bank," Trans. AIME (1960), vol. 219, p. 305.

22. Cook, A. B.; Walker, C. J.; and Spencer, G. B., "Realistic K-Values of C_{7+} Hydrocarbons for Calculating Oil Vaporization During Gas Cycling at High Pressures," Journal of Petroleum Tech. (July 1969), p. 901.

23. Hall, H. N., and Geffen, T. M., "A Laboratory Study of Solvent Flooding," Trans. AIME (1957), 210, p. 48.

24. Bleakley, W. B., "Miscible Flood Hikes Block 31's Oil Output," Oil and Gas Journal (Oct. 27, 1969), p. 67.

25. Herbeck, E. F., and Blanton, J. R., "Ten Years of Miscible Displacement in Block 31 Field," Journal of Petroleum Tech. (June 1961), 13, p. 543.

26. Pottier, J.; Delclaud, C.; Leduc, J.; d'Herbes, J. and Thomere, R., "Injection de Gas Miscible a Haute a Hassi-Messaoud', Proceedings of the 7th World Petroleum Congress (1967), 3, p. 517.

27. Benham, A. L.; Dowden, W. E. and Kunzman, W. J., "Miscible Fluid Displacement - Prediction of Miscibility," Trans., AIME (1960), 219, pp. 229-237.

28. Walker, J. W., and Turner, J. L., "Performance of Seeligson Zone 20B-07 Enriched-Gas Drive Project," Journal of Petroleum Tech. (April 1968), 20, p. 369.

29. Griffith, J. D.; Baiton, N. and Steffensen, R. J., "Ante Creek - A Miscible Flood Using Separator Gas and Water Injection," Journal of Petroleum Technology (Oct. 1970), 22, p. 1232.

30. Craig, F. F., and Owens, W. W., "Miscible Slug Flooding - A Review," J. Pet. Tech. (April, 1960), pp. 11-16.

31. Koch, H. A., Jr. and Slobod, R. L., "Miscible Slug Process," Trans., AIME (1957), 213, p. 7.

32. Lacey, J. W.; Faris, F. E. and Brinkman, F. H., "Effect of Bank Size on Oil Recovery in the High Pressure Gas-Driven LPG-Bank Process," Jour. Pet. Tech. (Aug. 1961), p. 806.

33. Marrs, D. G., "Field Results of Miscible-Displacement Program Using Liquid Propane Drive by Gas," J. Pet. Tech. (April 1961), pp. 327-332.

34. Holm, L. W., "CO_2 Requirements in CO_2 Slug and Carbonated Water Oil Recovery Process," Producers Monthly (Sept. 1963), 27, p. 6.

35. Simon, R., and Graue, D. J., "Generalized Correlations for Prediction Solubility, Swelling and Viscosity Behavior of CO_2 - Crude Oil Systems," Trans. AIME (1965), 234, p. 102.

36. Beeson, D. M., and Ortloff, G. D., "Laboratory Investigation of Water-Drive CO_2 Process for Oil Recovery," Trans. AIME (1959), 216, p. 388.

37. Menzie, D. E., and Nielsen, R. F., "A Study of the Vaporization of Crude Oil by Carbon Dioxide Depressuring," Trans., AIME (1963), 228, p. 1247.

38. Holm L. W., and O'Brien, L. J., "Carbon Dioxide Test at the Mead-Strawn Field," Journal of Petroleum Technology (April 1971), 23 p. 431.

39. Glasston, Samuel, Textbook of Physical Chemistry, 2ed. p. 791, Van Nostrand, N.Y. (1946).

40. McNeese, C. R., "The High Pressure Gas Process and the Use of Flue Gas," Patent no. 2,623,596.

41. Hendricks, D. R., "Gas Chromatography," Florida Gas Transmission Company, Zachary, Louisiana.

42. McNair, H. M., and Bonelli, E. J., "Basic Gas Chromatography," Varian Instrument Company.

43. Miller, A. J., "Gas Chromatography," The Oil and Gas Journal, December 17, 1936, p. 126.

44. Lederer, E., and Lederer, M., Chromatography, A Review of Principles and Applications, Elsevier Publishing Company, Houston, Texas, 1953.

45. Dewar, M. J. S., and Schroeder, J. P., J. Am. Chem. Soc., 86, 5235 (1964).

46. Bednas, M. E., and Russell, D. S., Can. J. Chem., 36, 1272 (1958).

47. Giddings, J. C., J. Chem. Ed., 39, no. 11, 569-573 (1962).

48. NGPA, "Method for Analysis of Natural Gas Liquid Mixture by Gas Chromatography," GPA Publication #2165-75.

49. Brown, G. G.; Katz, D. L.; Oberfell, G. G. and Allen, R. C., "Natural Gasoline and the Volatile Hydrocarbons," N.G.A.A., Tulsa, Oklahoma, 1948.

50. Standing, M. B., "Volumetric and Phase Behavior of Oil Field Hydrocarbon Systems," Reinhold Publishing Corp., N.Y., 1952.

51. Standing, M. B., and Katz, D. L., "Density of Natural Gases," Trans., AIME, v. 147, 140 (1942).

52. McLeod, W. R., Ph.D. Thesis, University of Oklahoma (1968).

53. Katz, D. L.; Monroe, R. R. and Trainer, R. R., "Surface Tension of Crude Oils Containing Dissolved Gases," Petroleum Technology, September 1943.

54. Sugden, J. Chem. Soc., vol. 125, 1924.

55. Herning, F., and Zipperer, L., "Calculation of the Viscosity of Technical Gas Mixtures from the Viscosity of the Individual Gases," Gas U. Wasserfoch (1936), v. 79, p. 69.

56. Carr, N. L.; Kobayashi, R. and Burrows, D. B., "Viscosity of Hydrocarbon Gases Under Pressure," Trans. AIME (1954), p. 201.

57. Lohrenz, J.; Bray, B. G., and Clark, C. R., "Calculating Viscosity of Reservoir Fluids from their Composition," J. Pet. Tech. (1964), pp. 1171-1176.

58. Clark, N. J., "Theoretical Aspects of Oil and Gas Equilibrium Calculation," J. P. T., April 1962, p. 369.

59. Engineering Data Book, Ninth Edition, N.G.P.A., 1972.

60. Katz, D. L., Monroe, R. R., and Trainer, R. R., "Surface Tension of Crude Oils Containing Dissolved Gases," Petroleum Tech., September 1943.

APPENDIX A

DATA AND RESULTS OF THE FIRST RUN

TABLE A-1

GAS DENSITY

Sampling Point A
Cum. N_2 Inj. = .14 p.v.
Pressure at sampling point = 3600 psi

Comp.	Mole fraction gas, y_i	Critical temp., T_c, °R	Critical pressure, P_c, psi	Molecular weight M_i	$y_i T_{c_i}$	$y_i P_{c_i}$	$y_i M_i$
N_2	.505	227	492.2	28.016	114.635	248.561	14.147
C_1	.352	343.2	673.1	16.068	120.806	236.931	5.647
C_2	.054	549.2	708.3	30.068	29.657	38.248	1.624
C_3	.039	666	617.4	44.094	25.974	24.079	1.72
C_4	.009	765.7	550.1	58.12	6.891	4.951	0.523
C_5	.015	846.2	489.8	72.124	12.693	7.347	1.082
C_{6+}	.026	1073+	334+	128.0	27.898	8.684	3.335
					339	569	28.077

+From Clark[58]

Gas Density = 20.03 lb/ft^3

TABLE A-2

GAS DENSITY

Sampling Point A
Cum. N_2 Inj. = .29 p.v.
Pressure at sampling point = 3600 psi

Comp.	Mole fraction gas, y_i	Critical temp., T_c, °R	Critical pressure, P_c, psi	Molecular weight M_i	$y_i T_{c_i}$	$y_i P_{c_i}$	$y_i M_i$
N_2	.85	227	492.2	28.016	192.95	418.37	23.811
C_1	.108	343.2	673.1	16.068	37.066	72.695	1.7326
C_2	.016	549.2	708.3	30.068	8.787	11.333	0.0481
C_3	.0134	666	617.4	44.094	8.924	8.273	0.5909
C_4	.001	765.7	550.1	58.12	0.766	0.5501	0.0581
C_5	.003	846.2	489.8	72.124	2.539	1.469	0.2165
C_{6+}	.009	1073+	334+	128.0	9.657	3.006	1.154
					261.0	515.7	28.045

+From Clark[58]

Gas Density = 17.42 lb/ft^3

TABLE A-3

GAS DENSITY

Sampling Point B
Cum. N_2 Inj. = .33 p.v.
Pressure at sampling point = 3200 psi

Comp.	Mole fraction gas, y_i	Critical temp., T_c, °R	Critical pressure, P_c, psi	Molecular weight M_i	$y_i T_{c_i}$	$y_i P_{c_i}$	$y_i M_i$
N_2	.358	227	492.2	28.016	81.266	176.208	10.03
C_1	.40	343.2	673.1	16.068	137.28	269.24	6.427
C_2	.102	549.2	708.3	30.068	56.0184	72.247	3.067
C_3	.0695	666	617.4	44.094	46.287	42.9093	3.065
C_4	.0115	765.7	550.1	58.12	8.806	6.326	0.668
C_5	.019	846.2	489.8	72.124	16.078	9.306	1.370
C_{6+}	.04	1073+	334+	128.0	42.92	13.36	5.12
					389	589.6	29.747

+From Clark[58]

Gas Density = 21.64 lb/ft^3

TABLE A-4

GAS DENSITY

Sampling Point B
Cum. N_2 Inj. = .42 p.v.
Pressure at sampling point = 3200 psi

Comp.	Mole fraction gas, y_i	Critical temp., T_c, °R	Critical pressure, P_c, psi	Molecular weight M_i	$y_i T_{c_i}$	$y_i P_{c_i}$	$y_i M_i$
N_2	.47	227	492.2	28.016	106.67	231.334	13.168
C_1	.306	343.2	673.1	16.068	105.019	201.969	4.917
C_2	.098	549.2	708.3	30.068	53.89	69.413	2.947
C_3	.069	666	617.4	44.094	45.954	42.601	3.042
C_4	.0069	765.7	550.1	58.12	5.283	3.796	0.401
C_5	.011	846.2	489.8	72.124	9.308	5.388	0.793
C_{6+}	.0391	1073+	334+	128.0	42.0	13.06	5.005
					368.1	571.56	30.272

+From Clark[58]

Gas Density = 21.58 lb/ft^3

TABLE A-5

GAS DENSITY

Sampling Point B
Cum. N_2 Inj. = .460 p.v.
Pressure at sampling point = 3200 psi

Comp.	Mole fraction gas, y_i	Critical temp., T_c, °R	Critical pressure, P_c, psi	Molecular weight M_i	$y_i T_{c_i}$	$y_i P_{c_i}$	$y_i M_i$
N_2	.56	227	492.2	28.016	127.12	275.632	15.689
C_1	.23	343.2	673.1	16.068	78.936	154.613	3.696
C_2	.0955	549.2	708.3	30.068	52.515	67.643	2.871
C_3	.068	666	617.4	44.094	45.288	41.983	2.998
C_4	.0025	765.7	550.1	58.12	1.914	1.375	0.1453
C_5	.005	846.2	489.8	72.124	4.231	2.449	0.361
C_{6+}	.039	1073+	334+	128.0	42	13.026	4.992
					352	556.921	30.752

+From Clark[58]

Gas Density = 21.09 lb/ft^3

TABLE A-6

GAS DENSITY

Sampling Point B
Cum. N_2 Inj. = .48 p.v.
Pressure at sampling point = 3200 psi

Comp.	Mole fraction gas, y_i	Critical temp., T_c, °R	Critical pressure, P_c, psi	Molecular weight M_i	$y_i T_{c_i}$	$y_i P_{c_i}$	$y_i M_i$
N_2	.602	227	492.2	28.016	136.654	296.304	16.866
C_1	.21	343.2	673.1	16.068	72.072	141.351	3.374
C_2	.08	549.2	708.3	30.068	43.992	56.664	2.405
C_3	.056	666	617.4	44.094	37.296	34.574	2.469
C_4	.001	765.7	550.1	58.12	0.766	0.5501	0.058
C_5	.003	846.2	489.8	72.124	2.539	1.469	0.216
C_{6+}	.034	1073+	334+	128.0	36.482	11.356	4.352
					330.08	542.268	29.74

+From Clark[58]

Gas Density = 19.14 lb/ft^3

TABLE A-7

GAS DENSITY

Sampling Point B
Cum. N_2 Inj. = .56 p.v.
Pressure at sampling point = 3200 psi

Comp.	Mole fraction gas, y_i	Critical temp., T_c, °R	Critical pressure, P_c, psi	Molecular weight M_i	$y_i T_{c_i}$	$y_i P_{c_i}$	$y_i M_i$
N_2	.881	227	492.2	28.016	199.988	433.628	24.682
C_1	.085	343.2	673.1	16.068	29.172	57.214	1.366
C_2	.0175	549.2	708.3	30.068	9.623	12.395	0.526
C_3	.01	666	617.4	44.094	6.66	6.173	0.441
C_4	0	765.7	550.1	58.12	0	0	0
C_5	0	846.2	489.8	72.124	0	0	0
C_{6+}	.0065	1073+	334+	128.0	8.255	1.658	0.832
					253.697	511.067	27.847

+From Clark[58]

Gas Density = 14.52 lb/ft^3

TABLE A-8

GAS DENSITY

Sampling Point B
Cum. N_2 Inj. = .58 p.v.
Pressure at sampling point = 3200 psi

Comp.	Mole fraction gas, y_i	Critical temp., T_c, °R	Critical pressure, P_c, psi	Molecular weight M_i	$y_i T_{c_i}$	$y_i P_{c_i}$	$y_i M_i$
N_2	.962	227	492.2	28.016	218.374	473.496	26.95
C_1	.03	343.2	673.1	16.068	20.592	40.386	0.964
C_2	.005	549.2	708.3	30.068	2.75	3.542	0.150
C_3	.001	666	617.4	44.094	0.666	0.6174	0.044
C_4	0	765.7	550.1	58.12	0	0	0
C_5	0	846.2	489.8	72.124	0	0	0
C_{6+}	.002	1073+	334+	128.0	2.54	0.51	0.256
					244.922	518.551	28.366

+From Clark[58]

Gas Density = 14.26 lb/ft^3

TABLE A-9

GAS DENSITY

Sampling Point C
Cum. N_2 Inj. = .527 p.v.
Pressure at sampling point = 2800 psi

Comp.	Mole fraction gas, y_i	Critical temp., T_c, °R	Critical pressure, P_c, psi	Molecular weight M_i	$y_i T_{c_i}$	$y_i P_{c_i}$	$y_i M_i$
N_2	.205	227	492.2	28.016	46.535	100.901	5.743
C_1	.455	343.2	673.1	16.068	156.156	306.261	7.311
C_2	.119	549.2	708.3	30.068	65.438	84.288	3.578
C_3	.0945	666	617.4	44.094	62.937	58.344	4.167
C_4	.02	765.7	550.1	58.12	15.314	11.002	1.162
C_5	.026	846.2	489.8	72.124	22.001	12.735	1.875
C_{6+}	.0805	1073+	334+	128.0	102.235	20.5275	10.304
					470.616	594.059	34.14

+From Clark[58]

Gas Density = 28.88 lb/ft^3

TABLE A-10

GAS DENSITY

Sampling Point C
Cum. N_2 Inj. = .57 p.v.
Pressure at sampling point = 2800 psi

Comp.	Mole fraction gas, y_i	Critical temp., T_c, °R	Critical pressure, P_c, psi	Molecular weight M_i	$y_i T_{c_i}$	$y_i P_{c_i}$	$y_i M_i$
N_2	.228	227	492.2	28.016	51.756	112.222	6.386
C_1	.44	343.2	673.1	16.068	151.008	296.164	7.070
C_2	.118	549.2	708.3	30.068	64.888	83.579	3.548
C_3	.0938	666	617.4	44.094	62.471	57.912	4.136
C_4	.017	765.7	550.1	58.12	13.017	9.352	0.988
C_5	.0235	846.2	489.8	72.124	19.886	11.510	1.695
C_{6+}	.0797	1073+	334+	128.0	101.219	20.324	10.202
					464.245	591.063	34.025

+From Clark[58]

Gas Density = 25.6 lb/ft^3

TABLE A-11

GAS DENSITY

Sampling Point C
Cum. N_2 Inj. = .62 p.v.
Pressure at sampling point = 2800 psi

Comp.	Mole fraction gas, y_i	Critical temp., T_c, °R	Critical pressure, P_c, psi	Molecular weight M_i	$y_i T_{c_i}$	$y_i P_{c_i}$	$y_i M_i$
N_2	.2604	227	492.2	28.016	59.111	128.169	7.295
C_1	.416	343.2	673.1	16.068	142.771	280.01	6.684
C_2	.1168	549.2	708.3	30.068	64.228	82.729	3.512
C_3	.093	666	617.4	44.094	61.938	57.418	4.1
C_4	.0142	765.7	550.1	58.12	10.873	7.811	0.825
C_5	.021	846.2	489.8	72.124	17.770	10.286	1.515
C_{6+}	.0786	1073+	334+	128.0	99.822	20.043	10.061
					446.513	586.466	33.992

+From Clark[58]

Gas Density = 25.3 lb/ft^3

TABLE A-12

GAS DENSITY

Sampling Point C
Cum. N_2 Inj. = .71 p.v.
Pressure at sampling point = 2800 psi

Comp.	Mole fraction gas, y_i	Critical temp., T_c, °R	Critical pressure, P_c, psi	Molecular weight M_i	$y_i T_{c_i}$	$y_i P_{c_i}$	$y_i M_i$
N_2	.888	227	492.2	28.016	201.576	437.074	24.818
C_1	.05	343.2	673.1	16.068	17.16	33.655	0.8034
C_2	.0375	549.2	708.3	30.068	20.621	26.561	1.128
C_3	.017	666	617.4	44.094	11.322	10.496	0.75
C_4	0	765.7	550.1	58.12	0	0	0
C_5	0	846.2	489.8	72.124	0	0	0
C_{6+}	.0075	1073+	334+	128.0	9.525	1.913	0.96
					260.204	509.699	28.519

+From Clark[58]

Gas Density = 14.49 lb/ft^3

TABLE A-13

GAS DENSITY

Sampling Point D
Cum. N_2 Inj. = .71 to .8 p.v.
Pressure at sampling point = 2400 psi

Comp.	Mole fraction gas, y_i	Critical temp., T_c, °R	Critical pressure, P_c, psi	Molecular weight M_i	$y_i T_{c_i}$	$y_i P_{c_i}$	$y_i M_i$
N_2	.072	227	492.2	28.016	16.344	35.4	2.017
C_1	.55	343.2	673.1	16.068	188.76	370.2	8.837
C_2	.13	549.2	708.3	30.068	71.396	92.08	3.9
C_3	.109	666	617.4	44.094	72.59	67.286	4.8
C_4	.021	765.7	550.1	58.12	16.1	11.552	1.2
C_5	.029	846.2	489.8	72.124	24.54	14.204	2.09
C_{6+}	.089	1073+	334+	128.0	95.5	29.72	11.39
					485.211	620.5	34.27

+From Clark[58]

Gas Density = 26.6 lb/ft^3

TABLE A-14

GAS DENSITY

Sampling Point D
Cum. N_2 Inj. = .831 p.v.
Pressure at sampling point = 2800 psi

Comp.	Mole fraction gas, y_i	Critical temp., T_c, °R	Critical pressure, P_c, psi	Molecular weight M_i	$y_i T_{c_i}$	$y_i P_{c_i}$	$y_i M_i$
N_2	.3405	227	492.2	28.016	9.539	77.294	167.594
C_1	.4	343.2	673.1	16.068	6.427	137.28	269.24
C_2	.097	549.2	708.3	30.068	2.917	53.272	68.705
C_3	.077	666	617.4	44.094	3.394	51.282	47.54
C_4	.008	765.7	550.1	58.12	0.465	6.126	4.401
C_5	.0165	846.2	489.8	72.124	1.19	13.962	8.082
C_{6+}	.061	1073+	334+	128.0	7.808	65.453	20.374
					31.74	404.669	585.936

+From Clark[58]

Gas Density = 20.1 lb/ft^3

TABLE A-15

GAS DENSITY

Sampling Point D
Cum. N_2 Inj. = .9 p.v.
Pressure at sampling point = 2800 psi

Comp.	Mole fraction gas, y_i	Critical temp., T_c, °R	Critical pressure, P_c, psi	Molecular weight M_i	$y_i T_{c_i}$	$y_i P_{c_i}$	$y_i M_i$
N_2	.8535	227	492.2	28.016	23.912	193.745	420.093
C_1	.095	343.2	673.1	16.068	1.526	32.604	63.945
C_2	.0295	549.2	708.3	30.068	0.887	16.201	20.895
C_3	.016	666	617.4	44.094	0.706	10.656	9.878
C_4	0	765.7	550.1	58.12	-	-	-
C_5	0	846.2	489.8	72.124	-	-	-
C_{6+}	.006	1073+	334+	128.0	0.768	6.438	2.004
					27.799	259.644	516.815

+From Clark[58]

Gas Density = 12.4 lb/ft^3

TABLE A-16

LIQUID DENSITY

Sampling point A
Cum. N_2 Inj. = .14 p.v.
Pressure at the sampling point = 3600 psi

Comp.	Mole fraction liquid, x_i	Molecular weight M_i	$x_i M_i$	Specific volume v_i, ft^3/lb	$x_i M_i v_i$
N_2	18.43	28.016	5.16	.01983+	0.10232
C_1	22.28	16.068	3.58	.0535	0.18725
C_2	6.43	30.068	1.93	.043	0.08299
C_3	6.34	44.094	2.81	.0316	0.08848
C_4	1.96	58.12	1.14	.0275	0.03135
C_5	4.72	72.124	3.4	.0254	0.08636
C_{6+}	39.84	214.5	85.40	.01976	1.68869
+From N.G.P.A.[59]			103.47		2.26744

Stock tank density = 45.63 lb/ft^3
Density at current pressure and temperature = 46.83 lb/ft^3

TABLE A-17

LIQUID DENSITY

Sampling point A
Cum. N_2 Inj. = .29 p.v.
Pressure at the sampling point = 3600 psi

Comp.	Mole fraction liquid, x_i	Molecular weight M_i	$x_i M_i$	Specific volume v_i, ft^3/lb	$x_i M_i v_i$
N_2	26.6	28.016	7.452	.01983+	0.14778
C_1	6.43	16.068	1.03	.0535	0.05511
C_2	1.96	30.068	0.59	.043	0.02537
C_3	2.24	44.094	0.99	.0316	0.03128
C_4	0.24	58.12	0.14	.0275	0.00385
C_5	1.07	72.124	0.77	.0254	0.01956
C_{6+}	61.46	214.5	131.8	.01976	2.604
+From N.G.P.A.[59]			142.772		2.8873

Stock tank density = 49.45 lb/ft^3
Density at current pressure and temperature = 50.28 lb/ft^3

TABLE A-18

LIQUID DENSITY

Sampling point B
Cum. N_2 Inj. = .33 p.v.
Pressure at the sampling point = 3200 psi

Comp.	Mole fraction liquid, x_i	Molecular weight M_i	$x_i M_i$	Specific volume v_i, ft^3/lb	$x_i M_i v_i$
N_2	13.26	28.016	3.715	.01983+	0.07367
C_1	25.81	16.068	4.15	.0535	0.222
C_2	12.14	30.068	3.65	.043	0.15695
C_3	11.78	44.094	5.19	.0316	0.164
C_4	2.8	58.12	1.63	.0275	0.0448
C_5	7.31	72.124	5.27	.0254	0.13386
C_{6+}	26.9	214.5	5.77	.01976	1.1401
			81.305		1.9354

+From N.G.P.A.[59]

Stock tank density = 42.01 lb/ft^3
Density at current pressure and temperature = 43.31 lb/ft^3

TABLE A-19

LIQUID DENSITY

Sampling point B
Cum. N_2 Inj. = .42 p.v.
Pressure at the sampling point = 3200 psi

Comp.	Mole fraction liquid, x_i	Molecular weight M_i	$x_i M_i$	Specific volume v_i, ft^3/lb	$x_i M_i v_i$
N_2	14.93	28.016	4.183	.01983+	0.0829
C_1	13.96	16.068	2.243	.0535	0.12
C_2	12.09	30.068	3.635	.043	0.1563
C_3	12.83	44.094	5.657	.0316	0.1788
C_4	0.68	58.12	0.395	.0275	0.0109
C_5	2.19	72.124	1.58	.0254	0.0401
C_{6+}	43.32	214.5	92.92	.01976	1.861
+From N.G.P.A.[59]			110.613		2.45

Stock tank density = 45.15 lb/ft^3
Density at current pressure and temperature = 46.2 lb/ft^3

TABLE A-20

LIQUID DENSITY

Sampling point B
Cum. N_2 Inj. = .57 p.v.
Pressure at the sampling point = 3200 psi

Comp.	Mole fraction liquid, x_i	Molecular weight M_i	$x_i M_i$	Specific volume v_i, ft^3/lb	$x_i M_i v_i$
N_2	23.18	28.016	6.49	.01983+	0.1287
C_1	3.57	16.068	0.574	.0535	0.0307
C_2	0.65	30.068	0.195	.043	0.0084
C_3	0.2	44.094	0.116	.0316	0.0037
C_4	0	58.12	0	.0275	0
C_5	0	72.124	0	.0254	0
C_{6+}	72.4	214.5	155.3	.01976	3.069
+From N.G.P.A.[59]			162.675		3.24

Stock tank density = 50.2 lb/ft^3
Density at current pressure and temperature = 51.1 lb/ft^3

TABLE A-21

LIQUID DENSITY

Sampling point C
Cum. N_2 Inj. = .53 p.v.
Pressure at the sampling point = 2800 psi

Comp.	Mole fraction liquid, x_i	Molecular weight M_i	$x_i M_i$	Specific volume v_i, ft^3/lb	$x_i M_i v_i$
N_2	7.57	28.016	2.1208	.01983+	0.042
C_1	26.8	16.068	4.62758	.0535	0.247
C_2	14.63	30.068	4.398948	.043	0.189
C_3	16.88	44.094	7.4424	.0316	0.235
C_4	5.71	58.12	3.31865	.0275	0.091
C_5	11.3	72.124	8.15	.0254	0.207
C_{6+}	15.18	214.5	32.5611	.01976	0.643
+From N.G.P.A.[59]			61.62		1.65

Stock tank density = 37.35 lb/ft^3
Density at current pressure and temperature = 38.85 lb/ft^3

TABLE A-22

LIQUID DENSITY

Sampling point C
Cum. N_2 Inj. = .57 p.v.
Pressure at the sampling point = 2800 psi

Comp.	Mole fraction liquid, x_i	Molecular weight M_i	$x_i M_i$	Specific volume v_i, ft^3/lb	$x_i M_i v_i$
N_2	8.44	28.016	2.365	.01983+	0.0469
C_1	27.85	16.068	4.475	.0535	0.2394
C_2	14.57	30.068	4.381	.043	0.1884
C_3	16.75	44.094	7.385	.0316	0.2334
C_4	4.86	58.12	2.825	.0275	0.0777
C_5	10.22	72.124	7.371	.0254	0.1872
C_{6+}	17.49	214.5	37.516	.01976	0.7413
+From N.G.P.A.[59]			66.318		1.714

Stock tank density = 38.69 lb/ft^3
Density at current pressure and temperature = 40.14 lb/ft^3

TABLE A-23

LIQUID DENSITY

Sampling point C
Cum. N_2 Inj. = .62 p.v.
Pressure at the sampling point = 2800 psi

Comp.	Mole fraction liquid, x_i	Molecular weight M_i	$x_i M_i$	Specific volume v_i, ft^3/lb	$x_i M_i v_i$
N_2	8.83	28.016	2.474	.01983+	0.0491
C_1	25.68	16.068	4.126	.0535	0.2207
C_2	14.46	30.068	4.348	.043	0.187
C_3	17.03	44.094	7.509	.0316	0.2373
C_4	4.18	58.12	2.429	.0275	0.0668
C_5	9.68	72.124	6.982	.0254	0.17734
C_{6+}	20.14	214.5	43.2	.01976	0.8536
+From N.G.P.A.[59]			71.0683		1.79184

Stock tank density = 39.662 lb/ft^3
Density at current pressure and temperature = 60.96 lb/ft^3

TABLE A-24

LIQUID DENSITY

Sampling point C
Cum. N_2 Inj. = .64 p.v.
Pressure at the sampling point = 2800 psi

Comp.	Mole fraction liquid, x_i	Molecular weight M_i	$x_i M_i$	Specific volume v_i, ft^3/lb	$x_i M_i v_i$
N_2	10.42	28.016	2.919	.01983+	0.0579
C_1	20.2	16.068	3.246	.0535	0.1737
C_2	12.63	30.068	3.798	.043	0.1633
C_3	15.25	44.094	6.724	.0316	0.2125
C_4	2.2	58.12	0.97	.0275	0.0267
C_5	7.49	72.124	5.402	.0254	0.1372
C_{6+}	31.81	214.5	68.232	.01976	1.3483
+From N.G.P.A.[59]			91.291		2.1196

Stock tank density = 43.07 lb/ft^3
Density at current pressure and temperature = 44.17 lb/ft^3

TABLE A-25

LIQUID DENSITY

Sampling point C
Cum. N_2 Inj. = .70 p.v.
Pressure at the sampling point = 2800 psi

Comp.	Mole fraction liquid, x_i	Molecular weight M_i	$x_i M_i$	Specific volume v_i, ft^3/lb	$x_i M_i v_i$
N_2	19.67	28.016	5.455	.01983+	0.1082
C_1	2.78	16.068	0.4467	.0535	0.0239
C_2	4.99	30.068	1.5	.043	0.0645
C_3	3.57	44.094	1.574	.0316	0.0497
C_4	0	58.12	0	.0275	0
C_5	0	72.124	0	.0254	0
C_{6+}	69.19	214.5	148.412	.01976	2.9326
+From N.G.P.A.[59]			157.3877		3.1789

Stock tank density = 49.51 lb/ft^3
Density at current pressure and temperature = 50.51 lb/ft^3

TABLE A-26

LIQUID DENSITY

Sampling point D
Cum. N_2 Inj. = .815 p.v.
Pressure at the sampling point = 2400 psi

Comp.	Mole fraction liquid, x_i	Molecular weight M_i	$x_i M_i$	Specific volume v_i, ft^3/lb	$x_i M_i v_i$
N_2	.068	28.016	1.90	.01983+	.038
C_1	.2764	16.068	4.44	.0535	.238
C_2	.1487	30.068	4.5	.043	.192
C_3	.1927	44.094	8.497	.0316	.269
C_4	.0518	58.12	3.01	.0275	.083
C_5	.1437	72.124	10.36	.0254	.263
C_{6+}	.1187	214.5	25.46	.01976	.503
+From N.G.P.A.[59]			58.15		1.585

Stock tank density = 36.68 lb/ft^3
Density at current pressure and temperature = 38.08 lb/ft^3

TABLE A-27

LIQUID DENSITY

Sampling point D
Cum. N_2 Inj. = .830 p.v.
Pressure at the sampling point = 2400 psi

Comp.	Mole fraction liquid, x_i	Molecular weight M_i	$x_i M_i$	Specific volume v_i, ft^3/lb	$x_i M_i v_i$
N_2	.1427	28.016	3.9979	.01983+	.079
C_1	.0447	16.068	.718	.0535	.038
C_2	.0407	30.068	1.22	.043	.053
C_3	.0399	44.094	1.76	.0316	.056
C_4	0	58.12	0	.0275	0
C_5	0	72.124	0	.0254	0
C_{6+}	.732	214.5	157.01	.01976	3.102
+From N.G.P.A.[59]			164.7		3.33

Stock tank density = 49.48 lb/ft^3
Density at current pressure and temperature = 50.18 lb/ft^3

TABLE A-28

GAS VISCOSITY

Sampling point A
Cum. N_2 Inj. = .14 p.v.
Pressure at sampling point = 3600 psi

Comp.	Mole fraction gas, y_i	Molecular weight M_i	$M_i^{\frac{1}{2}}$	$y_i M_i^{\frac{1}{2}}$	Atmospheric viscosity u_i^*, cp	$u_i^* y_i M_i^{\frac{1}{2}}$
N_2	0.505	28.016	5.29	2.673	.0176+	0.0470
C_1	0.352	16.068	4.01	1.411	.0108	0.01524
C_2	0.054	30.068	5.48	0.2961	.0102	0.00302
C_3	0.039	44.094	6.64	0.2589	.0082	0.00212
C_4	0.009	58.12	7.62	0.06861	.0073	0.0005
C_5	0.015	72.124	8.5	0.1374	.0065	0.00083
C_{6+}	0.026	128	11.31	0.2942	.005	0.0015
From Carr et al.[56]				5.12921		0.07021

Mixture atmospheric viscosity = u^* = .013 cp
Mixture viscosity at the system temperature and pressure = u = .031 cp

TABLE A-29

GAS VISCOSITY

Sampling point A
Cum. N_2 Inj. = .29 p.v.
Pressure at sampling point = 3600 psi

Comp.	Mole fraction gas, y_i	Molecular weight M_i	$M_i^{1/2}$	$y_i M_i^{1/2}$	Atmospheric viscosity u_i^*, cp	$u_i^* y_i M_i^{1/2}$
N_2	0.85	28.016	5.29	4.4991	.0176+	0.07918
C_1	0.108	16.068	4.01	0.43292	.0108	0.00468
C_2	0.010	30.068	5.48	0.08773	.0102	0.000895
C_3	0.0134	44.094	6.64	0.08895	.0082	0.000729
C_4	0.001	58.12	7.62	0.006638	.0073	0.0000485
C_5	0.003	72.124	8.5	0.02548	.0065	0.000166
C_{6+}	0.009	128	11.31	0.10182	.005	0.0005091
From Carr et al.[56]				5.242638		0.08621

Mixture atmospheric viscosity = u* = .016 cp
Mixture viscosity at the system temperature and pressure = u = .026 cp

TABLE A-30

GAS VISCOSITY

Sampling point B
Cum. N_2 Inj. = .33 p.v.
Pressure at sampling point = 3200 psi

Comp.	Mole fraction gas, y_i	Molecular weight M_i	$M_i^{1/2}$	$y_i M_i^{1/2}$	Atmospheric viscosity u_i^*, cp	$u_i^* y_i M_i^{1/2}$
N_2	0.358	28.016	5.29	1.895	.0176+	0.03335
C_1	0.4	16.068	4.01	1.603	.0108	0.01731
C_2	0.102	30.068	5.48	0.5593	.0102	0.0057
C_3	0.0695	44.094	6.64	0.4614	.0082	0.00378
C_4	0.0115	58.12	7.62	0.08767	.0073	0.00064
C_5	0.019	72.124	8.5	0.16136	.0065	0.0010
C_{6+}	0.04	128	11.31	0.4525	.005	0.00226
From Carr et al.[56]				5.2202		0.06404

Mixture atmospheric viscosity = u* = .012 cp
Mixture viscosity at the system temperature and pressure = u = .034 cp

TABLE A-31

GAS VISCOSITY

Sampling point B
Cum. N_2 Inj. = .42 p.v.
Pressure at sampling point = 3200 psi

Comp.	Mole fraction gas, y_i	Molecular weight M_i	$M_i^{1/2}$	$y_i M_i^{1/2}$	Atmospheric viscosity u_i^*, cp	$u_i^* y_i M_i^{1/2}$
N_2	0.47	28.016	5.29	2.48772	.0176+	0.043784
C_1	0.306	16.068	4.01	1.2266	.0108	0.01325
C_2	0.098	30.068	5.48	0.53738	.0102	0.00548
C_3	0.069	44.094	6.64	0.45805	.0082	0.003756
C_4	0.0069	58.12	7.62	0.052603	.0073	0.000384
C_5	0.01	72.124	8.5	0.0849	.0065	0.000552
C_{6+}	0.0391	128	11.31	0.44237	.005	0.002212
From Carr et al.[56]				5.2901		0.069418

Mixture atmospheric viscosity = u* = .0131 cp
Mixture viscosity at the system temperature and pressure = u = .0335 cp

TABLE A-32

GAS VISCOSITY

Sampling point B
Cum. N_2 Inj. = .46 p.v.
Pressure at sampling point = 3200 psi

Comp.	Mole fraction gas, y_i	Molecular weight M_i	$M_i^{1/2}$	$y_i M_i^{1/2}$	Atmospheric viscosity u_i^*, cp	$u_i^* y_i M_i^{1/2}$
N_2	.56	28.016	5.29	2.9641	.0176+	0.0522
C_1	.23	16.068	4.01	0.922	.0108	0.00996
C_2	.0955	30.068	5.48	0.5237	.0102	0.0053
C_3	.068	44.094	6.64	0.4514	.0082	0.0037
C_4	.0025	58.12	7.62	0.01906	.0073	0.00014
C_5	0.005	72.124	8.5	0.0425	.0065	0.00028
C_{6+}	0.039	128	11.31	0.4412	.005	0.00221
From Carr et al.[56]				5.36396		0.07379

Mixture atmospheric viscosity = u* = .0137 cp
Mixture viscosity at the system temperature and pressure = u = .0316 cp

TABLE A-33

GAS VISCOSITY

Sampling point B
Cum. N_2 Inj. = .57 p.v.
Pressure at sampling point = 3200 psi

Comp.	Mole fraction gas, y_i	Molecular weight M_i	$M_i^{1/2}$	$y_i M_i^{1/2}$	Atmospheric viscosity u_i^*, cp	$u_i^* y_i M_i^{1/2}$
N_2	0.962	28.016	5.29	5.0919	.0176+	0.08962
C_1	0.06	16.068	4.01	0.24051	.0108	0.0025975
C_2	0.005	30.068	5.48	0.02742	.0102	0.0002797
C_3	0.001	44.094	6.64	0.006638	.0082	0.0000544
C_4	0	58.12	7.62	0	.0073	0
C_5	0	72.124	8.5	0	.0065	0
C_{6+}	0.002	128	11.31	0.02263	.005	0.0001132
				5.3891		0.092665

From Carr et al.[56]

Mixture atmospheric viscosity = u* = .0172 cp
Mixture viscosity at the system temperature and pressure = u = .026 cp

TABLE A-34

GAS VISCOSITY

Sampling point C
Cum. N_2 Inj. = .57 p.v.
Pressure at sampling point = 2800 psi

Comp.	Mole fraction gas, y_i	Molecular weight M_i	$M_i^{\frac{1}{2}}$	$y_i M_i^{\frac{1}{2}}$	Atmospheric viscosity u_i^*, cp	$u_i^* y_i M_i^{\frac{1}{2}}$
N_2	0.228	28.016	5.29	1.20681	.0176+	0.02124
C_1	0.44	16.068	4.01	1.76374	.0108	0.01905
C_2	0.118	30.068	5.48	0.6470	.0102	0.0066
C_3	0.0938	44.094	6.64	0.6228	.0082	0.00511
C_4	0.017	58.12	7.62	0.1296	.0073	0.000946
C_5	0.0235	72.124	8.5	0.19958	.0065	0.0013
C_{6+}	0.0797	128	11.31	0.90170	.005	0.00451
From Carr et al.[56]				5.47123		0.04876

Mixture atmospheric viscosity = u* = .0089 cp
Mixture viscosity at the system temperature and pressure = u = .039 cp

TABLE A-35

GAS VISCOSITY

Sampling point C
Cum. N_2 Inj. = .62 p.v.
Pressure at sampling point = 2800 psi

Comp.	Mole fraction gas, y_i	Molecular weight M_i	$M_i^{1/2}$	$y_i M_i^{1/2}$	Atmospheric viscosity u_i^*, cp	$u_i^* y_i M_i^{1/2}$
N_2	0.2604	28.016	5.29	1.3783	.0176+	0.0242581
C_1	0.416	16.068	4.01	1.66753	.0108	0.0180093
C_2	0.1168	30.068	5.48	0.640465	.0102	0.0065327
C_3	0.093	44.094	6.64	0.6175228	.0082	0.0050637
C_4	0.0142	58.12	7.62	0.1082558	.0073	0.00079027
C_5	0.021	72.124	8.5	0.1783443	.0065	0.00115924
C_{6+}	0.0780	128	11.31	0.8892575	.005	0.00444629
From Carr et al.[56]				5.47968		0.0602596

Mixture atmospheric viscosity = u* = .011 cp
Mixture viscosity at the system temperature and pressure = u = .046 cp

TABLE A-36

GAS VISCOSITY

Sampling point C
Cum. N_2 Inj. = .64 p.v.
Pressure at sampling point = 2800 psi

Comp.	Mole fraction gas, y_i	Molecular weight M_i	$M_i^{1/2}$	$y_i M_i^{1/2}$	Atmospheric viscosity u_i^*, cp	$u_i^* y_i M_i^{1/2}$
N_2	0.388	28.016	5.29	2.05369	.0176+	0.036145
C_1	0.35	16.068	4.01	1.402972	.0108	0.0151521
C_2	0.099	30.068	5.48	0.54286	.0102	0.0055372
C_3	0.077	44.094	6.64	0.511282	.0082	0.004193
C_4	0.007	58.12	7.62	0.0533655	.0073	0.00039
C_5	0.014	72.124	8.5	0.1189	.0065	0.000773
C_{6+}	0.065	128	11.31	0.735391	.005	0.003677
From Carr et al.[56]				5.4185		0.0658673

Mixture atmospheric viscosity = u* = .012 cp
Mixture viscosity at the system temperature and pressure = u = .038 cp

TABLE A-37

GAS VISCOSITY

Sampling point C
Cum. N_2 Inj. = .7 p.v.
Pressure at sampling point = 2800 psi

Comp.	Mole fraction gas, y_i	Molecular weight M_i	$M_i^{1/2}$	$y_i M_i^{1/2}$	Atmospheric viscosity u_i^*, cp	$u_i^* y_i M_i^{1/2}$
N_2	0.888	28.016	5.29	4.7002	.0176+	0.082723
C_1	0.05	16.068	4.01	0.200425	.0108	0.002165
C_2	0.0375	30.068	5.48	0.205629	.0102	0.00297
C_3	0.017	44.094	6.64	0.1128805	.0082	0.0009256
C_4	0	58.12	7.62	0	.0073	0
C_5	0	72.124	8.5	0	.0065	0
C_{6+}	0.0075	128	11.31	0.084853	.005	0.0004243
From Carr et al.[56]				5.30399		0.0892079

Mixture atmospheric viscosity = u* = .017 cp
Mixture viscosity at the system temperature and pressure = u = .024 cp

TABLE A-38

GAS VISCOSITY

Sampling point D
Cum. N_2 Inj. = .815 p.v.
Pressure at sampling point = 2400 psi

Comp.	Mole fraction gas, y_i	Molecular weight M_i	$M_i^{1/2}$	$y_i M_i^{1/2}$	Atmospheric viscosity u_i^*, cp	$u_i^* y_i M_i^{1/2}$
N_2	.21	28.016	5.29	1.11153	.0176+	.0195
C_1	.47	16.068	4.01	1.88	.0108	.0204
C_2	.1145	30.068	5.48	.628	.0102	.006
C_3	.0925	44.094	6.64	.614	.0082	.005
C_4	.0145	58.12	7.62	.1105	.0073	.0008
C_5	.023	72.124	8.5	.195	.0065	.0013
C_{6+}	.0755	128	11.31	.854	.005	.004
From Carr et al.[56]				5.397		.0577

Mixture atmospheric viscosity = u^* = .0107 cp
Mixture viscosity at the system temperature and pressure = u = .041 cp

TABLE A-39

GAS VISCOSITY

Sampling point D
Cum. N_2 Inj. = .83 p.v.
Pressure at sampling point = 2400 psi

Comp.	Mole fraction gas, y_i	Molecular weight M_i	$M_i^{1/2}$	$y_i M_i^{1/2}$	Atmospheric viscosity u_i^*, cp	$u_i^* y_i M_i^{1/2}$
N_2	.3405	28.016	5.29	1.62	.0176+	.028
C_1	.4	16.068	4.01	1.63	.0108	.017
C_2	.097	30.068	5.48	.532	.0102	.0054
C_3	.077	44.094	6.64	.511	.0082	.0042
C_4	.008	58.12	7.62	.061	.0073	.00044
C_5	.0165	72.124	8.5	.140	.0065	.0009
C_{6+}	.061	128	11.31	.69	.005	.0035
From Carr et al.[56]				5.14		.05994

Mixture atmospheric viscosity = u* = .01166 cp
Mixture viscosity at the system temperature and pressure = u = .0455 cp

TABLE A-40

GAS VISCOSITY

Sampling point D
Cum. N_2 Inj. = .9 p.v.
Pressure at sampling point = 2400 psi

Comp.	Mole fraction gas, y_i	Molecular weight M_i	$M_i^{1/2}$	$y_i M_i^{1/2}$	Atmospheric viscosity u_i^*, cp	$u_i^* y_i M_i^{1/2}$
N_2	.8535	28.016	5.29	4.517	.0176+	.0795
C_1	.095	16.068	4.01	.381	.0108	.004
C_2	.0295	30.068	5.48	.162	.0102	.0017
C_3	.016	44.094	6.64	.106	.0082	.0009
C_4	0	58.12	7.62	0	.0073	0
C_5	0	72.124	8.5	0	.0065	0
C_{6+}	.006	128	11.31	.068	.005	.00034
From Carr et al.[56]				5.23425		.08648

Mixture atmospheric viscosity = u* = .0165 cp
Mixture viscosity at the system temperature and pressure = u = .0231 cp

TABLE A-41

LIQUID VISCOSITY

Sampling Point A
Cum. N_2 Inj. = .14 p.v.
Pressure at sampling point = 3600 psi

Comp.	x_i	M_i	$M_i^{1/2}$	u_i^* cp	$x_i M_i^{1/2}$	$x_i u_i^* M_i^{1/2}$	Critical volume v_{c_i} gm/cm^3	$x_i v_{c_i}$	$x_i M_i$	T_{c_m} °K	P_c, atm	$x_i T_{c_i}$	$x_i P_{c_i}$
N_2	.1843	28.016	5.29	.0176	.9755	.01717	3.215+	.5925	5.1633	126.2	33.5	23.2587	6.1741
C_1	.2228	16.068	4.01	.0108	.8931	.0096	6.173	1.375	3.58	191.1	45.8	42.5771	10.204
C_2	.0643	30.068	5.48	.0102	.3526	.0036	4.926	.3167	1.9334	305.5	48.2	19.6437	3.0993
C_3	.0634	44.094	6.64	.0082	.421	.00345	4.545	.2882	2.7956	370	42.	23.458	2.663
C_4	.0196	58.12	7.62	.0073	.1494	.00109	4.386	.086	1.1392	425.2	37.5	8.334	.735
C_5	.0472	72.124	8.49	.0065	.401	.00261	4.31	.2034	3.4043	469.8	33.3	22.1746	1.5718
C_{6+}	.3984	214.5	14.65	3.0	5.835	17.505	3.551	1.415	85.4568	705.4	17.347	281.0314	6.911
+From N.G.P.A.[59]					9.0276	17.5425		4.277	103.4726			420.478	31.358

u = 3.12 cp

TABLE A-42

LIQUID VISCOSITY

Sampling Point A
Cum. N_2 Inj. = .29 p.v.
Pressure at sampling point = 3600 psi

Comp.	x_i	M_i	$M_i^{\frac{1}{2}}$	u_i^* cp	$x_i M_i^{\frac{1}{2}}$	$x_i u_i^* M_i^{\frac{1}{2}}$	Critical volume v_{c_i} gm/cm^3	$x_i v_{c_i}$	$x_i M_i$	T_{c_i} °K	P_c, atm	$x_i T_{c_i}$	$x_i P_{c_i}$
N_2	.266	28.016	5.29	.0176	1.408	.02478	3.215+	.8552	7.452	126.2	33.5	33.569	8.911
C_1	.0643	16.068	4.01	.0108	.2577	.00278	6.173	.3969	1.033	191.1	45.8	12.288	2.945
C_2	.0196	30.068	5.48	.0102	.1075	.0011	4.926	.0965	.589	305.5	48.2	5.988	.945
C_3	.00224	44.094	6.64	.0082	.1487	.00122	4.545	.1018	.988	370	42.	8.288	.941
C_4	.0024	58.12	7.62	.0073	.0183	.00013	4.386	.0105	.139	425.2	37.5	1.020	.09
C_5	.0107	72.124	8.49	.0065	.0909	.00059	4.31	.0461	.772	469.8	33.3	5.027	.356
C_{6+}	.6146	214.5	14.65	3.0	9.0013	27.004	3.551	2.1824	131.83	705.4	17.347	433.54	10.661
+From N.G.P.A.[59]					11.0324	27.0340		3.6894	142.803			449.72	24.849

$u = 2.79$ cp

TABLE A-43

LIQUID VISCOSITY

Sampling Point B
Cum. N_2 Inj. = .33 p.v.
Pressure at sampling point = 3200 psi

Comp.	x_i	M_i	$M_i^{\frac{1}{2}}$	u_i^* cp	$x_i M_i^{\frac{1}{2}}$	$x_i u_i^* M_i^{\frac{1}{2}}$	Critical volume v_{c_i} gm/cm^3	$x_i v_{c_i}$	$x_i M_i$	T_{c_m} °K	P_c, atm	$x_i T_{c_i}$	$x_i P_{c_i}$
N_2	.1326	28.016	5.29	.0176	.7019	.0124	3.215+	.426	3.715	126.2	33.5	16.734	4.442
C_1	.2581	16.068	4.01	.0108	1.035	.0112	6.173	1.593	4.147	191.1	45.8	49.323	11.821
C_2	.1214	30.068	5.48	.0102	.6657	.0068	4.926	.598	3.650	305.5	48.2	37.088	5.851
C_3	.1178	44.094	6.64	.0082	.7822	.0064	4.545	.535	5.194	370	42.	43.586	4.948
C_4	.028	58.12	7.62	.0073	.2135	.0016	4.386	.123	1.627	425.2	37.5	11.906	1.05
C_5	.0731	72.124	8.49	.0065	.6208	.0040	4.31	.315	5.272	469.8	33.3	34.342	2.434
C_{6+}	.269	214.5	14.65	3.0	3.94	11.819	3.551	.955	57.7	705.4	17.347	189.753	4.666
+From N.G.P.A.[59]					7.9591	11.8614		4.545	81.305			382.732	35.212

$u = 2.36$ cp

TABLE A-44

LIQUID VISCOSITY

Sampling Point B
Cum. N_2 Inj. = .42 p.v.
Pressure at sampling point = 3200 psi

Comp.	x_i	M_i	$M_i^{1/2}$	u_i^* cp	$x_i M_i^{1/2}$	$x_i u_i^* M_i^{1/2}$	Critical volume V_{c_i} gm/cm^3	$x_i V_{c_i}$	$x_i M_i$	T_cm °K	P_c, atm	$x_i T_{c_i}$	$x_i P_{c_i}$
N_2	.1446	28.016	5.29	.0176	.765	.0135	3.215+	.465	4.051	126.2	33.5	18.249	4.844
C_1	.1913	16.068	4.01	.0108	.7668	.0083	6.173	1.181	3.074	191.1	45.8	36.557	8.762
C_2	.121	30.068	5.48	.0102	.663	.0068	4.926	.596	5.335	305.5	48.2	36.966	5.832
C_3	.1234	44.094	6.64	.0082	.819	.0067	4.545	.561	5.441	370	42.	45.658	5.183
C_4	.018	58.12	7.62	.0073	.137	.001	4.386	.079	1.046	425.2	37.5	7.654	0.675
C_5	.0482	72.124	8.49	.0065	.4093	.0027	4.31	.208	3.476	469.8	33.3	22.644	1.605
C_{6+}	.3555	214.5	14.65	3.0	5.207	15.62	3.551	1.262	76.255	705.4	17.347	250.770	6.167
+From N.G.P.A.[59]					8.7671	15.659		4.352	98.678			418.498	33.068

u = 2.5

TABLE A-45

LIQUID VISCOSITY

Sampling Point B
Cum. N_2 Inj. = .46 p.v.
Pressure at sampling point = 3200 psi

Comp.	x_i	M_i	$M_i^{1/2}$	u_i^* cp	$x_i M_i^{1/2}$	$x_i u_i^* M_i^{1/2}$	Critical volume v_{cj} gm/cm^3	$x_i v_{c_i}$	$x_i M_i$	T_cm °K	P_c, atm	$x_i T_{c_i}$	$x_i P_{c_i}$
N_2	.1493	28.016	5.29	.0176	.7902	.0139	3.215+	.4800	4.183	126.2	33.5	18.842	5.002
C_1	.1396	16.068	4.01	.0108	.5596	.006	6.173	.8618	2.243	191.1	45.8	26.678	6.394
C_2	.1209	30.068	5.48	.0102	.6629	.0068	4.926	.5956	3.635	305.5	48.2	36.935	5.827
C_3	.1283	44.094	6.64	.0082	.852	.007	4.545	.5831	5.657	370	42.	47.471	5.389
C_4	.0068	58.12	7.62	.0073	.0518	.0004	4.386	.0298	.3952	425.2	37.5	2.891	0.255
C_5	.0219	72.124	8.49	.0065	.186	.0012	4.31	.0944	1.5795	469.8	33.3	10.289	0.729
C_{6+}	.4332	214.5	14.65	3.0	6.345	19.034	3.551	1.5383	92.9214	705.4	17.347	305.579	7.515
+From N.G.P.A.[59]					9.4475	19.0693		4.183	110.6141			448.685	31.111

u = 2.827 cp

TABLE A-46

LIQUID VISCOSITY

Sampling Point B
Cum. N_2 Inj. = .57 p.v.
Pressure at sampling point = 3200 psi

Comp.	x_i	M_i	$M_i^{1/2}$	u_i^* cp	$x_i M_i^{1/2}$	$x_i u_i^* M_i^{1/2}$	Critical volume v_{c_i} gm/cm^3	$x_i v_{c_i}$	$x_i M_i$	T_{c_m} °K	P_c, atm	$x_i T_{c_i}$	$x_i P_{c_i}$
N_2	.2318	28.016	5.29	.0176	1.2269	.0216	3.215+	.7452	6.494	126.2	33.5	29.25	7.765
C_1	.0357	16.068	4.01	.0108	.1431	.0015	6.173	.2204	.574	191.1	45.8	6.822	1.635
C_2	.0065	30.068	5.48	.0102	.0356	.0004	4.926	.0320	.195	305.5	48.2	1.986	.313
C_3	.002	44.094	6.64	.0082	.0133	.0001	4.545	.0091	.088	370	42.	0.74	.084
C_4	0	58.12	7.62	.0073	0	0	4.386	0	0	425.2	37.5	0	0
C_5	0	72.124	8.49	.0065	0	0	4.31	0	0	469.8	33.3	0	0
C_{6+}	.724	214.5	14.65	3.0	10.604	31.811	3.551	2.5709	155.298	705.4	17.347	510.71	12.559
+From N.G.P.A.[59]					12.0229	31.8346		3.5776	162.649			549.508	22.356

u = 3.09 cp

TABLE A-47

LIQUID VISCOSITY

Sampling Point C
Cum. N_2 Inj. = .53 p.v.
Pressure at sampling point = 2800 psi

Comp.	x_i	M_i	$M_i^{\frac{1}{2}}$	u_i^* cp	$x_i M_i^{\frac{1}{2}}$	$x_i u_i^* M_i^{\frac{1}{2}}$	Critical volume V_{c_i} gm/cm^3	$x_i V_{c_i}$	$x_i M_i$	T_{c_m} °K	P_c, atm	$x_i T_{c_i}$	$x_i P_{c_i}$
N_2	.0759	28.016	5.29	.0176	.4017	.0071	3.215+	.2440	2.126	126.2	33.5	9.5786	2.543
C_1	.288	16.068	4.01	.0108	1.1544	.0125	6.173	1.7778	4.628	191.1	45.8	55.037	13.190
C_2	.1463	30.068	5.48	.0102	.8022	.0082	4.926	.7207	4.4	305.5	48.2	44.695	7.052
C_3	.1688	44.094	6.64	.0082	1.1209	.0092	4.545	.7672	7.443	370	42.	62.450	7.09
C_4	.0571	58.12	7.62	.0073	.4353	.0032	4.386	.2504	3.319	425.2	37.5	24.279	2.141
C_5	.113	72.124	8.49	.0065	.9597	.0062	4.31	.4870	8.15	469.8	33.3	53.0874	3.763
C_{6+}	.1518	214.5	14.65	3.0	2.2232	6.6697	3.551	.539	32.561	705.4	17.347	107.08	2.633
+From N.G.P.A.[59]					7.0974	6.7161		4.7861	62.627			356.207	38.412

u = 1.44 cp

TABLE A-48

LIQUID VISCOSITY

Sampling Point C
Cum. N_2 Inj. = .57 p.v.
Pressure at sampling point = 2800 psi

Comp.	x_i	M_i	$M_i^{1/2}$	u_i^* cp	$x_i M_i^{1/2}$	$x_i u_i^* M_i^{1/2}$	Critical volume v_{c_i} gm/cm^3	$x_i v_{c_i}$	$x_i M_i$	T_c in °K	P_c, atm	$x_i T_{c_i}$	$x_i P_{c_i}$
N_2	.844	28.016	5.29	.0176	.4467	.0079	3.215+	.2713	2.36	126.2	33.5	10.65	2.83
C_1	.2785	16.068	4.01	.0108	1.1164	.0121	6.173	1.719	4.47	191.1	45.8	53.22	12.76
C_2	.1457	30.068	5.48	.0102	.7989	.0081	4.926	.7177	4.38	305.5	48.2	44.51	7.02
C_3	.1675	44.094	6.64	.0082	1.1122	.0091	4.545	.7613	7.39	370	42.	61.98	7.04
C_4	.0486	58.12	7.62	.0073	.3705	.0027	4.386	.2132	2.82	425.2	37.5	20.66	1.82
C_5	.1022	72.124	8.49	.0065	.8679	.0056	4.31	.4405	7.37	469.8	33.3	48.01	3.40
C_{6+}	.1749	214.5	14.65	3.0	2.562	7.685	3.551	.6211	37.52	705.4	17.347	123.37	3.03
+From N.G.P.A.[59]					7.2746	7.7305		4.7441	66.31			362.4	37.9

$u = 1.7$ cp

TABLE A-49

LIQUID VISCOSITY

Sampling Point C
Cum. N_2 Inj. = .62 p.v.
Pressure at sampling point = 2800 psi

Comp.	x_i	M_i	$M_i^{1/2}$	u_i^* cp	$x_i M_i^{1/2}$	$x_i u_i^* M_i^{1/2}$	Critical volume v_{c_i} gm/cm^3	$x_i v_{c_i}$	$x_i M_i$	T_{c_m} °K	P_c, atm	$x_i T_{c_i}$	$x_i P_{c_i}$
N_2	.0883	28.016	5.29	.0176	.4674	.0082	3.215+	.2839	2.47	126.2	33.5	11.143	2.96
C_1	.2568	16.068	4.01	.0108	1.029	.0111	6.173	1.585	4.13	191.1	45.8	49.07	11.76
C_2	.1446	30.068	5.48	.0102	.7929	.0081	4.926	.712	4.35	305.5	48.2	44.18	6.97
C_3	.1703	44.094	6.64	.0082	1.1308	.0093	4.545	.774	7.51	370	42.	63.01	7.15
C_4	.0481	58.12	7.62	.0073	.3187	.0023	4.386	.183	2.43	425.2	37.5	17.77	1.57
C_5	.0968	72.124	8.49	.0065	.8221	.0053	4.31	.417	6.98	469.8	33.3	45.48	3.22
C_{6+}	.2014	214.5	14.65	3.0	2.95	8.849	3.551	.715	43.2	705.4	17.347	142.07	3.49
+From N.G.P.A.[59]					7.5109	8.8933		4.6699	71.07			372.723	37.12

$u = 1.86$ cp

TABLE A-50

LIQUID VISCOSITY

Sampling Point C
Cum. N_2 Inj. = .64 p.v.
Pressure at sampling point = 2800 psi

Comp.	x_i	M_i	$M_i^{1/2}$	u_i^* cp	$x_i M_i^{1/2}$	$x_i u_i^* M_i^{1/2}$	Critical volume V_{c_i} gm/cm^3	$x_i V_{c_i}$	$x_i M_i$	T_cm °K	P_c, atm	$x_i T_{c_i}$	$x_i P_{c_i}$
N_2	.1042	28.016	5.29	.0176	.5515	.0097	3.215+	.335	2.919	126.2	33.5	13.15	3.49
C_1	.202	16.068	4.01	.0108	.8097	.0143	6.173	1.247	3.246	191.1	45.8	38.6	9.25
C_2	.1263	30.068	5.48	.0102	.6926	.0071	4.926	.622	3.798	305.5	48.2	38.58	6.09
C_3	.1525	44.094	6.64	.0082	1.013	.0083	4.545	.693	6.724	370	42.	56.43	6.4
C_4	.022	58.12	7.62	.0073	.1677	.0012	4.386	.096	1.279	425.2	37.5	9.35	.825
C_5	.0749	72.124	8.49	.0065	.6361	.0041	4.31	.323	5.402	469.8	33.3	35.19	2.49
C_{6+}	.3181	214.5	14.65	3.0	4.6588	13.9765	3.551	1.13	68.23	705.4	17.347	224.39	5.518
+From N.G.P.A.[59]					8.2294	14.0212		4.446	91.598			415.69	34.063

u = 2.643 cp

TABLE A-51

LIQUID VISCOSITY

Sampling Point C
Cum. N_2 Inj. = .7 p.v.
Pressure at sampling point = 2800 psi

Comp.	x_i	M_i	$M_i^{1/2}$	u_i^* cp	$x_i M_i^{1/2}$	$x_i u_i^* M_i^{1/2}$	Critical volume V_{ci} gm/cm^3	$x_i V_{c_i}$	$x_i M_i$	T_cm °K	P_c, atm	$x_i T_{c_i}$	$x_i P_{c_i}$
N_2	.1947	28.016	5.29	.0176	1.031	.0181	3.215+	.626	5.454	126.2	33.5	24.57	6.52
C_1	.278	16.068	4.01	.0108	.1114	.0012	6.173	.1716	.447	191.1	45.8	5.31	1.27
C_2	.0499	30.068	5.48	.0102	.2736	.0028	4.926	.246	1.5	305.5	48.2	15.24	2.41
C_3	.0357	44.094	6.64	.0082	.2371	.0019	4.545	.1623	1.57	370	42.	13.31	1.5
C_4	0	58.12	7.62	.0073	0	0	4.386	0	0	425.2	37.5	0	0
C_5	0	72.124	8.49	.0065	0	0	4.31	0	0	469.8	33.3	0	0
C_{6+}	.6919	214.5	14.65	3.0	10.1334	30.4	3.551	2.4569	148.41	705.4	17.347	488.07	12.00
+From N.G.P.A.[59]					11.7865	30.424		3.6628	157.381			546.4	23.7

u = 3.088 cp

TABLE A-52

LIQUID VISCOSITY

Sampling Point D
Cum. N_2 Inj. = .815 p.v.
Pressure at sampling point = 2400 psi

Comp.	x_i	M_i	$M_i^{1/2}$	u_i^* cp	$x_i M_i^{1/2}$	$x_i u_i^* M_i^{1/2}$	Critical volume v_{c_i} gm/cm^3	$x_i v_{c_i}$	$x_i M_i$	T_{c_m} °K	P_c, atm	$x_i T_{c_i}$	$x_i P_{c_i}$
N_2	.068	28.016	5.29	.0176	.36	.0063	3.215+	.2186	1.905	126.2	33.5	8.58	2.28
C_1	.2764	16.068	4.01	.0108	1.108	.012	6.173	1.7062	4.44	191.1	45.8	52.85	12.66
C_2	.1487	30.068	5.48	.0102	.8154	.0083	4.926	.7325	4.47	305.5	48.2	45.43	7.17
C_3	.1927	44.094	6.64	.0082	1.28	.0105	4.545	.8758	8.5	370	42.	55.02	8.09
C_4	.0518	58.12	7.62	.0073	.3949	.0029	4.386	.2272	3.01	425.2	37.5	22.03	1.94
C_5	.1437	72.124	8.49	.0065	1.220	.0079	4.31	.6193	10.36	469.8	33.3	67.51	4.79
C_{6+}	.1187	214.5	14.65	3.0	1.7384	5.2154	3.551	.4215	25.46	705.4	17.347	83.73	2.06
+From N.G.P.A.[59]					6.9167	5.2633		4.8011	58.145			335.12	38.99

u = 1.065 cp

TABLE A-53

LIQUID VISCOSITY

Sampling Point D
Cum. N_2 Inj. = .83 p.v.
Pressure at sampling point = 2400 psi

Comp.	x_i	M_i	$M_i^{1/2}$	u_i^* cp	$x_i M_i^{1/2}$	$x_i u_i^* M_i^{1/2}$	Critical volume v_{c_i} gm/cm^3	$x_i v_{c_i}$	$x_i M_i$	T_{c_m} °K	P_c, atm	$x_i T_{c_i}$	$x_i P_{c_i}$
N_2	.0782	28.016	5.29	.0176	.4139	.0073	3.215+	.2514	2.191	126.2	33.5	9.87	2.62
C_1	.2162	16.068	4.01	.0108	.8666	.0094	6.173	1.3346	3.474	191.1	45.8	41.32	9.9
C_2	.1276	30.068	5.48	.0102	.7	.0071	4.926	.6286	3.837	305.5	48.2	38.98	6.15
C_3	.1711	44.094	6.64	.0082	1.1753	.0096	4.545	.7776	7.544	370	42.	63.31	7.19
C_4	.031	58.12	7.62	.0073	.2363	.0017	4.386	.136	1.801	425.2	37.5	13.18	1.16
C_5	.1222	72.124	8.49	.0065	1.038	.0067	4.31	.5267	8.81	469.8	33.3	57.41	4.07
C_{6+}	.2537	214.5	14.65	3.0	3.716	11.147	3.551	.901	54.42	705.4	17.347	178.96	4.4
+From N.G.P.A.[59]					8.1461	11.1888		4.5559	82.077			403.03	35.49

$u = 1.983$ cp

TABLE A-54

LIQUID VISCOSITY

Sampling Point D
Cum. N_2 Inj. = .9 p.v.
Pressure at sampling point = 2400 psi

Comp.	x_i	M_i	$M_i^{1/2}$	u_i^* cp	$x_i M_i^{1/2}$	$x_i u_i^* M_i^{1/2}$	Critical volume v_{c_i} gm/cm^3	$x_i v_{c_i}$	$x_i M_i$	T_{c_m} °K	P_c, atm	$x_i T_{c_i}$	$x_i P_{c_i}$
N_2	.1427	28.016	5.29	.0176	.7553	.0133	3.215+	.4588	4.00	126.2	33.5	18.01	4.78
C_1	.0447	16.068	4.01	.0108	.1792	.0019	6.173	.276	.718	191.1	45.8	8.54	2.05
C_2	.0497	30.068	5.48	.0102	.2232	.0023	4.926	.2005	1.224	305.5	48.2	12.45	1.96
C_3	.0399	44.094	6.64	.0082	.2649	.0022	4.545	.1813	1.759	370	42.	14.763	1.68
C_4	0	58.12	7.62	.0073	0	0	4.386	0	0	425.2	37.5	0	0
C_5	0	72.124	8.49	.0065	0	0	4.31	0	0	469.8	33.3	0	0
C_{6+}	.732	214.5	14.65	3.0	10.721	32.162	3.551	2.599	157.01	705.4	17.347	516.35	12.7
+From N.G.P.A.[59]					12.1436	32.1817		3.7156	164.711			570.093	23.17

$u = 3.12$ cp

TABLE A-55

SURFACE TENSION

Sampling point C
Cum. N_2 Inj. = .53 p.v.
Pressure at sampling point = 2800 psi

(1) Comp.	(2) x_i	(3) y_i	(4) $x_i \frac{\rho_L}{M_L}$	(5) $y_i \frac{\rho_v}{M_v}$	(6) (4) - (5)	(7) Parachor P_{chi}	(8) (6) x (7)
N_2	.0759	.205	.0005	.6023	-.0018	41+	-.0752
C_1	.288	.455	.002	.0052	-.003	77	-.249
C_2	.1463	.1185	.001	.0014	-.00036	108	-.0388
C_3	.1688	.0945	.0011	.0011	.000068	150	.0102
C_4	.0571	.02	.0003	.00023	.000016	190	.0304
C_5	.113	.026	.00077	.000297	.00047	232	.11
C_{6+}	.1539	.0805	.0010	.0009	.00013	548.2	.07
							.144

+From Katz et al.[53]

Surface tension = .0004 dynes/cm.

TABLE A-56

SURFACE TENSION

Sampling point C
Cum. N_2 Inj. = .62 p.v.
Pressure at sampling point = 2800 psi

(1) Comp.	(2) x_i	(3) y_i	(4) $x_i \frac{\rho_L}{M_L}$	(5) $y_i \frac{\rho_v}{M_v}$	(6) (4) - (5)	(7) Parachor P_{chi}	(8) (6) x (7)
N_2	.0883	.2604	.00058	.003	-.0024	41+	-.0996
C_1	.2568	.416	.00016	.005	-.003	77	-.24
C_2	.1446	.1168	.001	.0013	-.0004	108	-.043
C_3	.1703	.093	.0011	.001	-.00004	150	.0064
C_4	.0418	.0142	.00027	.0002	.00011	190	.021
C_5	.0968	.021	.0006	.0002	.0004	232	.091
C_{6+}	.2014	.0786	.0013	.001	.00041	548.2	.227
							.1817

+From Katz et al.[53]

Surface tension = .001 dynes/cm.

TABLE A-57

SURFACE TENSION

Sampling point C
Cum. N_2 Inj. = .64 p.v.
Pressure at sampling point = 2800 psi

(1) Comp.	(2) x_i	(3) y_i	(4) $x_i \frac{\rho_L}{M_L}$	(5) $y_i \frac{\rho_V}{M_V}$	(6) (4) - (5)	(7) Parachor P_{chi}	(8) (6) x (7)
N_2	.1176	.388	.0007	.0042	-.0035	41+	-.1429
C_1	.2059	.35	.0012	.0038	-.00256	77	-.1968
C_2	.1238	.099	.0007	.0011	-.00034	108	-.0363
C_3	.1481	.077	.00087	.00083	.00004	150	.00657
C_4	.0215	.007	.00013	.000075	.00005	190	.00976
C_5	.0718	.014	.00042	.00015	.0003	232	.006322
C_{6+}	.3113	.065	.0018	.0007	.00114	548.2	.6223
							.3257

+From Katz et al.[53]

Surface tension = .0113 dynes/cm.

TABLE A-58

SURFACE TENSION

Sampling point C
Cum. N_2 Inj. = .7 p.v.
Pressure at sampling point = 2800 psi

(1) Comp.	(2) x_i	(3) y_i	(4) $x_i \frac{\rho_L}{M_L}$	(5) $y_i \frac{\rho_V}{M_V}$	(6) (4) - (5)	(7) Parachor P_{chi}	(8) (6) x (7)
N_2	.1947	.888	.00072	.007	-.0063	41+	-.2577
C_1	.0278	.05	.0001	.00039	-.00029	77	-.0225
C_2	.0499	.0375	.00018	.000295	-.00011	108	-.01211
C_3	.0357	.017	.000131	.00013	-.000027	150	-.00042
C_4	0	0	0	0	0	190	0
C_5	0	0	0	0	0	232	0
C_{6+}	.6919	.0075	.00254	.000059	.002485	548.2	1.3625
							1.0742

+From Katz et al.[53]

Surface tension = 1.332 dynes/cm.

TABLE A-59

K-VALUES

Sampling point A
Cum. N_2 Inj. = .14 p.v. P_K = 6000 psi
Pressure at sampling point = 3600 psi

Comp.	MW_i	b	T_c	P_c	y_i	K_i	x_i	$x_i \cdot MW_i$	$T_c(x_i \cdot MW_i)$	$P_c(x_i \cdot MW_i)$
N_2	28.016	552.05	-	-	50.5	-	18.63	-	-	-
C_1	16.068	808	-116.7	667.8	35.2	1.58	22.28	3.58	-417.79	667.8
C_2	30.068	1415	90.09	707.8	5.4	.840	6.43	1.93	173.87	1366.054
C_3	44.096	1792	206	616.3	3.9	.615	6.34	2.8	576.8	1725.64
C_4	58.12	2129	305.65	550.7	0.9	.46	1.96	1.14	348.44	627.798
C_5	72.124	2473	385.7	488.6	1.5	.318	4.72	3.4	1311.38	1661.24
C_{6+}	214.5	4428	810	255	2.6	.6653	39.84	85.46	69222.6	21792.3
								98.31	71215.3	27840.832

TABLE A-60

K-VALUES

Sampling point A
Cum. N_2 Inj. = .29 p.v. P_K = 7000 psi
Pressure at sampling point = 3600 psi

Comp.	MW_i	b	T_c	P_c	y_i	K_i	x_i	$x_i \cdot MW_i$	$T_c(x_i \cdot MW_i)$	$P_c(x_i \cdot MW_i)$
N_2	28.016	552.05	-	-	85.0	-	26.6	-	-	-
C_1	16.068	808	-116.7	667.8	10.8	1.68	6.43	1.03	-120.20	687.834
C_2	30.068	1415	90.09	707.8	1.6	.817	1.96	0.59	53.15	417.602
C_3	44.096	1792	206	616.3	1.3	.58	2.24	0.99	203.94	610.137
C_4	58.12	2129	305.65	550.7	.1	.418	.24	.14	42.79	77.098
C_5	72.124	2473	385.7	488.6	.3	.28	1.07	.77	297	376.222
C_{6+}	214.5	4428	810	255	.9	.015	61.46	131.8	106758	33609
								135.32	107234.7	35777.893

TABLE A-61

K-VALUES

Sampling point B
Cum. N_2 Inj. = .33 p.v. P_K = 5000 psi
Pressure at sampling point = 3200 psi

Comp.	MW_i	b	T_c	P_c	y_i	K_i	x_i	$x_i \cdot MW_i$	$T_c(x_i \cdot MW_i)$	$P_c(x_i \cdot MW_i)$
N_2	28.016	552.05	-	-	35.8	2.7	13.26	-	-	-
C_1	16.068	808	-116.7	667.8	40	1.55	25.81	4.15	-484.31	2771.37
C_2	30.068	1415	90.09	707.8	10.2	.84	12.14	3.65	328.83	2583.47
C_3	44.096	1792	206	616.3	6.95	.59	11.78	5.19	1069.14	3198.6
C_4	58.12	2129	305.65	550.7	1.15	.41	2.8	1.63	498.21	897.64
C_5	72.124	2473	385.7	488.6	1.9	.26	7.31	5.27	2032.64	2574.92
C_{6+}	214.5	4428	810	255	4	.1487	26.9	57.7	46737	14713.5
								77.59	50181.51	26739.5

TABLE A-62

K-VALUES

Sampling point B
Cum. N_2 Inj. = .42 p.v. P_K = 6000 psi
Pressure at sampling point = 3200 psi

Comp.	MW_i	b	T_c	P_c	y_i	K_i	x_i	$x_i \cdot MW_i$	$T_c(x_i \cdot MW_i)$	$P_c(x_i \cdot MW_i)$
N_2	28.016	552.05	-	-	47	3.25	14.46	-	-	-
C_1	16.068	808	-116.7	667.8	30.6	1.6	19.13	3.07	-358.27	2050.15
C_2	30.068	1415	90.09	707.8	9.8	.81	12.1	3.64	327.93	2576.39
C_3	44.096	1792	206	616.3	6.9	.559	12.34	5.44	1120.64	3352.67
C_4	58.12	2129	305.65	550.7	.69	.383	1.8	1.05	320.93	578.24
C_5	72.124	2473	385.7	488.6	1.1	.238	4.62	3.33	1284.38	1627.04
C_{6+}	214.5	4428	810	255	3.91	.11	35.55	76.25	61762.5	19443.75
								92.78	64458	29628

TABLE A-63

K-VALUES

Sampling point D
Cum. N_2 Inj. = .83 p.v. P_K = 5000 psi
Pressure at sampling point = 2400 psi

Comp.	MW_i	b	T_c	P_c	y_i	K_i	x_i	$x_i \cdot MW_i$	$T_c(x_i \cdot MW_i)$	$P_c(x_i \cdot MW_i)$
N_2	28.016	552.05	-	-	.3405	4.3	0.0782	-	-	-
C_1	16.068	808	-116.7	667.8	.40	1.85	.2162	3.47	-404.95	2317.27
C_2	30.068	1415	90.09	707.8	0.097	.76	.1276	3.837	345.68	2715.83
C_3	44.096	1792	206	616.3	.077	.45	.1711	7.544	1554.06	4649.37
C_4	58.12	2129	305.65	550.7	.008	.26	0.031	1.802	550.78	992.36
C_5	72.124	2473	385.7	488.6	.0165	.135	.1222	8.814	3399.56	4306.52
C_{6+}	214.5	4428	810	255	0.061	-	.2537	54.419	44079.39	13876.84
								79.886	49524.52	28858.19

TABLE A-64

K-VALUES

Sampling point D
Cum. N_2 Inj. = .9 p.v. P_K = 7000 psi
Pressure at sampling point = 2400 psi

Comp.	MW_i	b	T_c	P_c	y_i	K_i	x_i	$x_i \cdot MW_i$	$T_c(x_i \cdot MW_i)$	$P_c(x_i \cdot MW_i)$
N_2	28.016	552.05	-	-	.8535	-	.1427	-	-	-
C_1	16.068	808	-116.7	667.8	.095	2.125	.0447	0.718	-83.791	479.48
C_2	30.068	1415	90.09	707.8	.0295	.725	0.0407	1.224	110.27	866.367
C_3	44.096	1792	206	616.3	0.016	.401	0.0399	1.759	362.354	1084.072
C_4	58.12	2129	305.65	550.7	0	.235	0	0	0	0
C_5	72.124	2473	385.7	488.6	0	.125	0	0	0	0
C_{6+}	214.5	4428	810	255	0.006	0.0082	.732	157.014	127181.34	40038.57
								160.715	127570.173	42468.469

APPENDIX B

DATA AND RESULTS OF THE SECOND RUN

TABLE B-1

GAS DENSITY

Sampling Point A
Cum. N_2 Inj. = .172 p.v.
Pressure at sampling point = 4400 psi

Comp.	Mole fraction gas, y_i	Critical temp., T_c, °R	Critical pressure, P_c, psi	Molecular weight M_i	$y_i T_{c_i}$	$y_i P_{c_i}$	$y_i M_i$
N_2	.4245	227	492.2	28.016	96.3615	208.939	11.893
C_1	.40	343.2	673.1	16.068	137.28	269.24	6.4272
C_2	.066	549.2	708.3	30.068	36.247	46.7478	1.9845
C_3	.047	666	617.4	44.094	31.302	29.018	2.0724
C_4	.0115	765.7	550.1	58.12	8.8056	6.326	.6684
C_5	.019	846.2	489.8	72.124	16.078	9.306	1.3704
C_{6+}	.032	1073+	334+	128.0	34.336	10.688	4.096
					360.4	580.26	28.5119

+From Clark[58]

Gas Density = 23 lb/ft^3

TABLE B-2

GAS DENSITY

Sampling Point A
Cum. N_2 Inj. = .26 p.v.
Pressure at sampling point = 4400 psi

Comp.	Mole fraction gas, y_i	Critical temp., T_c, °R	Critical pressure, P_c, psi	Molecular weight M_i	$y_i T_{c_i}$	$y_i P_{c_i}$	$y_i M_i$
N_2	.65	227	492.2	28.016	147.55	319.93	18.2104
C_1	.23	343.2	673.1	16.068	79.936	154.813	3.696
C_2	.051	549.2	708.3	30.068	28.009	36.123	1.533
C_3	.036	666	617.4	44.094	23.976	22.226	1.587
C_4	.002	765.7	550.1	58.12	1.531	1.10	.116
C_5	.011	846.2	489.8	72.124	9.308	5.388	.793
C_{6+}	.02	1073+	334+	128.0	21.46	6.65	2.56
					311.77	546.23	28.4954

+From Clark[58]

Gas Density = 21.63 lb/ft^3

TABLE B-3

GAS DENSITY

Sampling Point A
Cum. N_2 Inj. = .3 p.v.
Pressure at sampling point = 4400 psi

Comp.	Mole fraction gas, y_i	Critical temp., T_c, °R	Critical pressure, P_c, psi	Molecular weight M_i	$y_i T_{c_i}$	$y_i P_{c_i}$	$y_i M_i$
N_2	.95	227	492.2	28.016	215.05	467.59	26.615
C_1	.04	343.2	673.1	16.068	13.728	26.924	.6427
C_2	.006	549.2	708.3	30.068	3.295	4.25	0.1804
C_3	.002	666	617.4	44.094	1.332	1.235	.0882
C_4	0	765.7	550.1	58.12	0	0	0
C_5	0	846.2	489.8	72.124	0	0	0
C_{6+}	.002	1073+	334+	128.0	2.146	0.668	.256
					236.151	501	27.7823

+From Clark[58]

Gas Density = 19.47 lb/ft^3

TABLE B-4

GAS DENSITY

Sampling Point B
Cum. N_2 Inj. = .359 p.v.
Pressure at sampling point = 3800 psi

Comp.	Mole fraction gas, y_i	Critical temp., T_c, °R	Critical pressure, P_c, psi	Molecular weight M_i	$y_i T_{c_i}$	$y_i P_{c_i}$	$y_i M_i$
N_2	.265	227	492.2	28.016	97.61	130.433	7.424
C_1	.43	343.2	673.1	16.068	147.576	289.433	6.909
C_2	.123	549.2	708.3	30.068	67.552	87.121	3.698
C_3	.084	666	617.4	44.094	55.944	51.862	3.704
C_4	.015	765.7	550.1	58.12	11.486	8.252	.8718
C_5	.023	846.2	489.8	72.124	19.463	11.265	1.659
C_{6+}	.06	1073+	334+	128.0	64.38	20.04	7.68
					464	598.4	31.9458

+From Clark[58]

Gas Density = 25.9 lb/ft^3

TABLE B-5

GAS DENSITY

Sampling Point B
Cum. N_2 Inj. = .44 p.v.
Pressure at sampling point = 3800 psi

Comp.	Mole fraction gas, y_i	Critical temp., T_c, °R	Critical pressure, P_c, psi	Molecular weight M_i	$y_i T_{c_i}$	$y_i P_{c_i}$	$y_i M_i$
N_2	.359	227	492.2	28.016	81.493	176.7	10.058
C_1	.37	343.2	673.1	16.068	126.984	249.047	5.945
C_2	.116	549.2	708.3	30.068	63.707	82.163	3.488
C_3	.078	666	617.4	44.094	51.948	48.157	3.439
C_4	.007	765.7	550.1	58.12	5.36	3.651	0.407
C_5	.015	846.2	489.8	72.124	12.693	7.347	1.082
C_{6+}	.055	1073+	334+	128.0	59.015	18.37	7.04
					401.2	585.6	31.459

+From Clark[58]

Gas Density = 24.69 lb/ft^3

TABLE B-6

GAS DENSITY

Sampling Point B
Cum. N_2 Inj. = .454 p.v.
Pressure at sampling point = 3800 psi

Comp.	Mole fraction gas, y_i	Critical temp., T_c, °R	Critical pressure, P_c, psi	Molecular weight M_i	$y_i T_{c_i}$	$y_i P_{c_i}$	$y_i M_i$
N_2	.496	227	492.2	28.016	112.592	244.13	13.896
C_1	.29	343.2	673.1	16.068	99.528	195.2	4.66
C_2	.101	549.2	708.3	30.068	55.47	71.54	3.037
C_3	.063	666	617.4	44.094	41.958	38.9	2.778
C_4	0	765.7	550.1	58.12	0	0	0
C_5	0.006	846.2	489.8	72.124	5.077	2.939	0.433
C_{6+}	0.044	1073+	334+	128.0	47.212	14.696	5.632
					361.8	567.4	30.436

+From Clark[58]

Gas Density = 24.09 lb/ft^3

TABLE B-7

GAS DENSITY

Sampling Point B
Cum. N_2 Inj. = .47 p.v.
Pressure at sampling point = 3800 psi

Comp.	Mole fraction gas, y_i	Critical temp., T_c, °R	Critical pressure, P_c, psi	Molecular weight M_i	$y_i T_{c_i}$	$y_i P_{c_i}$	$y_i M_i$
N_2	.632	227	492.2	28.016	143.46	458.7	17.706
C_1	.2	343.2	673.1	16.068	68.64	134.62	3.2136
C_2	.087	549.2	708.3	30.068	47.78	61.622	2.616
C_3	.05	666	617.4	44.094	33.3	30.87	2.205
C_4	0	765.7	550.1	58.12	0	0	0
C_5	0	846.2	489.8	72.124	0	0	0
C_{6+}	.031	1073+	334+	128.0	33.263	10.354	3.968
					326.4	696.2	29.7086

+From Clark[58]

Gas Density = 22.97 lb/ft^3

TABLE B-8

GAS DENSITY

Sampling Point C
Cum. N_2 Inj. = .612 p.v.
Pressure at sampling point = 3200 psi

Comp.	Mole fraction gas, y_i	Critical temp., T_c, °R	Critical pressure, P_c, psi	Molecular weight M_i	$y_i T_{c_i}$	$y_i P_{c_i}$	$y_i M_i$
N_2	.2765	227	492.2	28.016	62.766	136.09	7.746
C_1	.4	343.2	673.1	16.068	137.28	269.24	6.427
C_2	.117	549.2	708.3	30.068	64.26	82.87	3.518
C_3	.094	666	617.4	44.094	62.604	58.04	4.145
C_4	.011	765.7	550.1	58.12	8.423	6.051	0.639
C_5	.0185	846.2	489.8	72.124	15.655	9.061	1.334
C_{6+}	.083	1073+	334+	128.0	89.06	27.722	10.624
					440.0	589.1	34.433

+From Clark[58]

Gas Density = 26.24 lb/ft^3

TABLE B-9

GAS DENSITY

Sampling Point C
Cum. N_2 Inj. = .647 p.v.
Pressure at sampling point = 3200 psi

Comp.	Mole fraction gas, y_i	Critical temp., T_c, °R	Critical pressure, P_c, psi	Molecular weight M_i	$y_i T_{c_i}$	$y_i P_{c_i}$	$y_i M_i$
N_2	.583	227	492.2	28.016	188.41	286.95	16.333
C_1	.22	343.2	673.1	16.068	75.504	148.082	3.535
C_2	.08	549.2	708.3	30.068	43.936	56.664	3.528
C_3	.062	666	617.4	44.094	41.292	38.28	2.734
C_4	0	765.7	550.1	58.12	0	0	0
C_5	0	846.2	489.8	72.124	0	0	0
C_{6+}	0.055	1073+	334+	128.0	59.015	18.37	7.04
					408.15	548.3	33.17

+From Clark[58]

Gas Density = 23.64 lb/ft^3

TABLE B-10

LIQUID DENSITY

Sampling point A
Cum. N_2 Inj. = .172 p.v.
Pressure at the sampling point = 4400 psi

Comp.	Mole fraction liquid, x_i	Molecular weight M_i	$x_i M_i$	Specific volume v_i, ft^3/lb	$x_i M_i v_i$
N_2	.257	28.016	7.2	.01983+	.1428
C_1	.329	16.068	5.286	.0535	.2828
C_2	.073	30.068	2.195	.043	.0944
C_3	.06	44.094	2.6456	.0316	.0836
C_4	.017	58.12	.988	.0275	.0272
C_5	.032	72.124	2.308	.0254	.0586
C_{6+}	.232	214.5	49.764	.01976	.9833
			70.3866		1.6727

+From N.G.P.A.[59]

Stock tank density = 42.08 lb/ft^3
Density at current pressure and temperature = 43.78 lb/ft^3

TABLE B-11

LIQUID DENSITY

Sampling point A
Cum. N_2 Inj. = .26 p.v.
Pressure at the sampling point = 4400 psi

Comp.	Mole fraction liquid, x_i	Molecular weight M_i	$x_i M_i$	Specific volume v_i, ft^3/lb	$x_i M_i v_i$
N_2	.342	28.016	9.5815	.01983+	.19
C_1	.153	16.068	2.4584	.0535	.1315
C_2	.0593	30.068	1.783	.043	.07667
C_3	.05	44.094	2.2047	.0316	.06967
C_4	.003	58.12	.1744	.0275	.0048
C_5	.022	72.124	1.5867	.0254	.0403
C_{6+}	.3707	214.5	79.515	.01976	1.5712
			97.3037		2.08414

+From N.G.P.A.[59]

Stock tank density = 46.687 lb/ft^3
Density at current pressure and temperature = 48.287 lb/ft^3

TABLE B-12

LIQUID DENSITY

Sampling point A
Cum. N_2 Inj. = .3 p.v.
Pressure at the sampling point = 4400 psi

Comp.	Mole fraction liquid, x_i	Molecular weight M_i	$x_i M_i$	Specific volume v_i, ft^3/lb	$x_i M_i v_i$
N_2	.452	28.016	12.663	.01983+	.2511
C_1	.025	16.068	.4017	.0535	.0215
C_2	.007	30.068	.2105	.043	.0091
C_3	.003	44.094	.1323	.0316	.0042
C_4	0	58.12	0	.0275	0
C_5	0	72.124	0	.0254	0
C_{6+}	.513	214.5	110.04	.01976	2.1744
+From N.G.P.A.[59]			123.4475		2.4603

Stock tank density = 50.176 lb/ft^3
Density at current pressure and temperature = 51.18 lb/ft^3

TABLE B-13

LIQUID DENSITY

Sampling point B
Cum. N_2 Inj. = .359 p.v.
Pressure at the sampling point = 3800 psi

Comp.	Mole fraction liquid, x_i	Molecular weight M_i	$x_i M_i$	Specific volume v_i, ft^3/lb	$x_i M_i v_i$
N_2	0.1325	28.016	3.712	.01983+	.0736
C_1	.307	16.068	4.9329	.0535	.26391
C_2	.14	30.068	4.2095	.043	.181
C_3	.115	44.094	5.071	.0316	.16024
C_4	.026	58.12	1.5111	.0275	.0416
C_5	.055	72.124	3.967	.0254	.1008
C_{6+}	.2245	214.5	48.155	.01976	.9515
			71.5585		1.77265

+From N.G.P.A.[59]

Stock tank density = 40.37 lb/ft^3
Density at current pressure and temperature = 42.088 lb/ft^3

TABLE B-14

LIQUID DENSITY

Sampling point B
Cum. N_2 Inj. = .44 p.v.
Pressure at the sampling point = 3800 psi

Comp.	Mole fraction liquid, x_i	Molecular weight M_i	$x_i M_i$	Specific volume v_i, ft^3/lb	$x_i M_i v_i$
N_2	.138	28.016	3.866	.01983+	.07667
C_1	.255	16.068	4.097	.0535	.2192
C_2	.136	30.068	4.089	.043	.1758
C_3	.117	44.094	5.159	.0316	.1630
C_4	.013	58.12	.7556	.0275	.0208
C_5	.042	72.124	3.029	.0254	.07694
C_{6+}	.299	214.5	64.136	.01976	1.2673
+From N.G.P.A.[59]			85.1316		1.99971

Stock tank density = 42.57 lb/ft^3
Density at current pressure and temperature = 44.172 lb/ft^3

TABLE B-15

LIQUID DENSITY

Sampling point B
Cum. N_2 Inj. = .454 p.v.
Pressure at the sampling point = 3800 psi

Comp.	Mole fraction liquid, x_i	Molecular weight M_i	$x_i M_i$	Specific volume v_i, ft^3/lb	$x_i M_i v_i$
N_2	.16	28.016	4.483	.01983+	.0889
C_1	.193	16.068	3.101	.0535	.1659
C_2	.123	30.068	3.6984	.043	.1590
C_3	.102	44.094	4.4976	.0316	.14212
C_4	0	58.12	0	.0275	0
C_5	.019	72.124	1.3704	.0254	.03481
C_{6+}	.403	214.5	86.444	.01976	1.7081
+From N.G.P.A.[59]			103.5944		2.29883

Stock tank density = 45.06 lb/ft^3
Density at current pressure and temperature = 46.354 lb/ft^3

TABLE B-16

LIQUID DENSITY

Sampling point B
Cum. N_2 Inj. = .47 p.v.
Pressure at the sampling point = 3800 psi

Comp.	Mole fraction liquid, x_i	Molecular weight M_i	$x_i M_i$	Specific volume v_i, ft^3/lb	$x_i M_i v_i$
N_2	.178	28.016	4.9868	.01983+	.09889
C_1	.13	16.068	2.0888	.0535	.11175
C_2	.109	30.068	3.2774	.043	.1409
C_3	.086	44.094	3.7921	.0316	.11983
C_4	0	58.12	0	.0275	0
C_5	0	72.124	0	.0254	0
C_{6+}	.507	214.5	108.75	.01976	2.62027
+From N.G.P.A.[59]			122.8951		2.62027

Stock tank density = 46.90 lb/ft^3
Density at current pressure and temperature = 48 lb/ft^3

TABLE B-17

LIQUID DENSITY

Sampling point C
Cum. N_2 Inj. = .612 p.v.
Pressure at the sampling point = 3200 psi

Comp.	Mole fraction liquid, x_i	Molecular weight M_i	$x_i M_i$	Specific volume v_i, ft^3/lb	$x_i M_i v_i$
N_2	.102	28.016	2.8576	.01983+	.05667
C_1	.258	16.068	4.1455	.0535	.2218
C_2	.139	30.068	4.1795	.043	.1797
C_3	.157	44.094	6.9228	.0316	.21876
C_4	.026	58.12	1.5111	.0275	.04156
C_5	.071	72.124	5.1208	.0254	.13007
C_{6+}	.247	214.5	52.982	.01976	1.0469
+From N.G.P.A.[59]			77.7173		1.89546

Stock tank density = 41.0 lb/ft^3
Density at current pressure and temperature = 42.4 lb/ft^3

TABLE B-18

LIQUID DENSITY

Sampling point C
Cum. N_2 Inj. = .638 p.v.
Pressure at the sampling point = 3200 psi

Comp.	Mole fraction liquid, x_i	Molecular weight M_i	$x_i M_i$	Specific volume v_i, ft^3/lb	$x_i M_i v_i$
N_2	.106	28.016	2.9697	.01983+	.05889
C_1	.134	16.068	2.1531	.0535	.1152
C_2	.101	30.068	3.0369	.043	.1306
C_3	.115	44.094	5.0708	.0316	.1602
C_4	0	58.12	0	.0275	0
C_5	0	72.124	0	.0254	0
C_{6+}	.544	214.5	116.688	.01976	2.3058
			129.9185		2.77069

+From N.G.P.A.[59]

Stock tank density = 46.9 lb/ft^3
Density at current pressure and temperature = 47.94 lb/ft^3

TABLE B-19

GAS VISCOSITY

Sampling point A
Cum. N_2 Inj. = .172 p.v.
Pressure at sampling point = 4400 psi

Comp.	Mole fraction gas, y_i	Molecular weight M_i	$M_i^{\frac{1}{2}}$	$y_i M_i^{\frac{1}{2}}$	Atmospheric viscosity u_i^*, cp	$u_i^* y_i M_i^{\frac{1}{2}}$
N_2	.4245	28.016	5.29	2.2469	.0176+	.0395
C_1	.4	16.068	4.01	1.6034	.0108	.01732
C_2	.066	30.068	5.48	.3619	.0102	.00369
C_3	.047	44.094	6.64	.3121	.0082	.00256
C_4	0.0115	58.12	7.62	.08767	.0073	.00064
C_5	.019	72.124	8.5	.1614	.0065	.00105
C_{6+}	.032	128	11.31	.3620	.005	.0018
From Carr et al.[56]				5.13537		.06656

Mixture atmospheric viscosity = u* = .013 cp
Mixture viscosity at the system temperature and pressure = u = .0364 cp

TABLE B-20

GAS VISCOSITY

Sampling point A
Cum. N_2 Inj. = .26 p.v.
Pressure at sampling point = 4400 psi

Comp.	Mole fraction gas, y_i	Molecular weight M_i	$M_i^{\frac{1}{2}}$	$y_i M_i^{\frac{1}{2}}$	Atmospheric viscosity u_i^*, cp	$u_i^* y_i M_i^{\frac{1}{2}}$
N_2	.65	28.016	5.29	3.4405	.0176+	.06055
C_1	.23	16.068	4.01	.92195	.0108	.00996
C_2	.051	30.068	5.48	.2797	.0102	.0029
C_3	.036	44.094	6.64	.23905	.0082	.00196
C_4	.002	58.12	7.62	.01525	.0073	.00011
C_5	.011	72.124	8.5	.09342	.0065	.00061
C_{6+}	.02	128	11.31	.2263	.005	.00113
				5.21617		.07722

From Carr et al.[56]

Mixture atmospheric viscosity = u* = .0148 cp
Mixture viscosity at the system temperature and pressure = u = .03182 cp

TABLE B-21

GAS VISCOSITY

Sampling point A
Cum. N_2 Inj. = .3 p.v.
Pressure at sampling point = 4400 psi

Comp.	Mole fraction gas, y_i	Molecular weight M_i	$M_i^{1/2}$	$y_i M_i^{1/2}$	Atmospheric viscosity u_i^*, cp	$u_i^* y_i M_i^{1/2}$
N_2	.95	28.016	5.29	5.0284	.0176+	.0885
C_1	.04	16.068	4.01	.16034	.0108	.00173
C_2	.006	30.068	5.48	.0329	.0102	.60034
C_3	.002	44.094	6.64	.01328	.0082	.00011
C_4	0	58.12	7.62	0	.0073	0
C_5	0	72.124	8.5	0	.0065	0
C_{6+}	.002	128	11.31	.02263	.005	.000113
From Carr et al.[56]				5.25755		.090793

Mixture atmospheric viscosity = u* = .0173 cp
Mixture viscosity at the system temperature and pressure = u = .027 cp

TABLE B-22

GAS VISCOSITY

Sampling point B
Cum. N_2 Inj. = .359 p.v.
Pressure at sampling point = 3800 psi

Comp.	Mole fraction gas, y_i	Molecular weight M_i	$M_i^{1/2}$	$y_i M_i^{1/2}$	Atmospheric viscosity u_i^*, cp	$u_i^* y_i M_i^{1/2}$
N_2	.265	28.016	5.29	1.4026	.0176+	.02469
C_1	.43	16.068	4.01	1.72365	.0108	.018615
C_2	.123	30.068	5.48	.67446	.0102	.00688
C_3	.084	44.094	6.64	.55779	.0082	.00457
C_4	.015	58.12	7.62	.11435	.0073	.00083
C_5	.023	72.124	8.5	.19533	.0065	.00127
C_{6+}	.06	128	11.31	.67882	.005	.00339
From Carr et al.[56]				5.347		.060245

Mixture atmospheric viscosity = u* = .0113 cp
Mixture viscosity at the system temperature and pressure = u = .0486 cp

TABLE B-23

GAS VISCOSITY

Sampling point B
Cum. N_2 Inj. = .44 p.v.
Pressure at sampling point = 3800 psi

Comp.	Mole fraction gas, y_i	Molecular weight M_i	$M_i^{1/2}$	$y_i M_i^{1/2}$	Atmospheric viscosity u_i^*, cp	$u_i^* y_i M_i^{1/2}$
N_2	.359	28.016	5.29	1.9002	.0176+	.03344
C_1	.37	16.068	4.01	1.4831	.0108	.01602
C_2	.116	30.068	5.48	.6361	.0102	.0065
C_3	.078	44.094	6.64	.51795	.0082	.00425
C_4	.007	58.12	7.62	.05337	.0073	.00039
C_5	.015	72.124	8.5	.1274	.0065	.00083
C_{6+}	.055	128	11.31	.6223	.005	.00311
				5.34042		.06454

From Carr et al.[56]

Mixture atmospheric viscosity = u* = .0121 cp
Mixture viscosity at the system temperature and pressure = u = .0411 cp

TABLE B-24

GAS VISCOSITY

Sampling point B
Cum. N_2 Inj. = .454 p.v.
Pressure at sampling point = 3800 psi

Comp.	Mole fraction gas, y_i	Molecular weight M_i	$M_i^{1/2}$	$y_i M_i^{1/2}$	Atmospheric viscosity u_i^*, cp	$u_i^* y_i M_i^{1/2}$
N_2	.496	28.016	5.29	2.625	.0176+	.04621
C_1	.29	16.068	4.01	1.1625	.0108	.01255
C_2	.101	30.068	5.48	.5538	.0102	.00565
C_3	.063	44.094	6.64	.4183	.0082	.00343
C_4	0	58.12	7.62	0	.0073	0
C_5	.006	72.124	8.5	0.051	.0065	.00033
C_{6+}	.044	128	11.31	.4978	.005	.0025
From Carr et al.[56]				5.3084		.07067

Mixture atmospheric viscosity = u* = .0133 cp
Mixture viscosity at the system temperature and pressure = u = .0353 cp

TABLE B-25

GAS VISCOSITY

Sampling point B
Cum. N_2 Inj. = .47 p.v.
Pressure at sampling point = 3800 psi

Comp.	Mole fraction gas, y_i	Molecular weight M_i	$M_i^{1/2}$	$y_i M_i^{1/2}$	Atmospheric viscosity u_i^*, cp	$u_i^* y_i M_i^{1/2}$
N_2	.632	28.016	5.29	3.3452	.0176+	.05888
C_1	.2	16.068	4.01	.8017	.0108	.60866
C_2	.087	30.068	5.48	.4771	.0102	.00487
C_3	.05	44.094	6.64	.33202	.0082	.0027
C_4	0	58.12	7.62	0	.0073	0
C_5	0	72.124	8.5	0	.0065	0
C_{6+}	.031	128	11.31	.3507	.005	.00175
				5.30672		.07686

From Carr et al.[56]

Mixture atmospheric viscosity = u* = .01448 cp
Mixture viscosity at the system temperature and pressure = u = .0268 cp

TABLE B-26

GAS VISCOSITY

Sampling point C
Cum. N_2 Inj. = .612 p.v.
Pressure at sampling point = 3200 psi

Comp.	Mole fraction gas, y_i	Molecular weight M_i	$M_i^{1/2}$	$y_i M_i^{1/2}$	Atmospheric viscosity u_i^*, cp	$u_i^* y_i M_i^{1/2}$
N_2	.2765	28.016	5.29	1.4635	.0176+	.02576
C_1	.4	16.068	4.01	1.6034	.0108	.01732
C_2	.117	30.068	5.48	.64156	.0102	.0065
C_3	.094	44.094	6.64	.6242	.0082	.0051
C_4	.011	58.12	7.62	.0839	.0073	.00061
C_5	.0185	72.124	8.5	.15711	.0065	.00102
C_{6+}	.083	128	11.31	.93904	.005	.0047
From Carr et al.[56]				5.51271		.06101

Mixture atmospheric viscosity = u* = .0111 cp
Mixture viscosity at the system temperature and pressure = u = .0454 cp

TABLE B-27

GAS VISCOSITY

Sampling point C
Cum. N_2 Inj. = .638 p.v.
Pressure at sampling point = 3200 psi

Comp.	Mole fraction gas, y_i	Molecular weight M_i	$M_i^{1/2}$	$y_i M_i^{1/2}$	Atmospheric viscosity u_i^*, cp	$u_i^* y_i M_i^{1/2}$
N_2	.583	28.016	5.29	3.08583	.0176+	.05431
C_1	.22	16.068	4.01	.8819	.0108	.0095
C_2	.08	30.068	5.48	.4387	.0102	.0045
C_3	.062	44.094	6.64	.4117	.0082	.00338
C_4	0	58.12	7.62	0	.0073	0
C_5	0	72.124	8.5	0	.0065	0
C_{6+}	.055	128	11.31	.6223	.005	.00311
From Carr et al.[56]				5.4404		0.0748

Mixture atmospheric viscosity = u* = .0137 cp
Mixture viscosity at the system temperature and pressure = u = .0467 cp

TABLE B-28

LIQUID VISCOSITY

Sampling Point A
Cum. N_2 Inj. = .172 p.v.
Pressure at sampling point = 4400 psi

Comp.	x_i	M_i	$M_i^{1/2}$	u_i^* cp	$x_i M_i^{1/2}$	$x_i u_i^* M_i^{1/2}$	Critical volume v_{ci} gm/cm^3	$x_i v_{c_i}$	$x_i M_i$	T_cm °K	P_c, atm	$x_i T_{c_i}$	$x_i P_{c_i}$
N_2	.257	28.016	5.29	.0176	1.3603	.0239	3.215+	.8263	7.2	126.2	33.5	32.43	8.61
C_1	.329	16.068	4.01	.0108	1.3188	.0124	6.173	2.0319	5.2864	191.1	45.8	62.9	15.1
C_2	.073	30.068	5.48	.0102	.4003	.0041	4.926	.3596	2.195	305.5	48.2	22.3	3.5
C_3	.06	44.094	6.64	.0082	.3984	.0033	4.545	.2727	2.6456	370	42.	22.2	2.52
C_4	.017	58.12	7.62	.0073	.1296	.0009	4.386	.0746	.988	425.2	37.5	7.228	.630
C_5	.032	72.124	8.49	.0065	.2718	.0018	4.31	.1379	2.308	469.8	33.3	15.03	1.07
C_{6+}	.232	214.5	14.65	3.0	3.398	10.193	3.551	.8238	49.764	705.4	17.347	163.65	4.02
+From N.G.P.A.[59]					7.2772	10.2394		4.5258	70.387			325.648	35.458

$u = 2.374$ cp

TABLE B-29

LIQUID VISCOSITY

Sampling Point A
Cum. N_2 Inj. = .26 p.v.
Pressure at sampling point = 4400 psi

Comp.	x_i	M_i	$M_i^{1/2}$	u_i^* cp	$x_i M_i^{1/2}$	$x_i u_i^* M_i^{1/2}$	Critical volume V_{ci} gm/cm^3	$x_i V_{c_i}$	$x_i M_i$	T_{cm} °K	P_c, atm	$x_i T_{c_i}$	$x_i P_{c_i}$
N_2	.342	28.016	5.29	.0176	1.81	.0319	3.215+	1.042	9.581	126.2	33.5	43.1604	11.457
C_1	.153	16.068	4.01	.0108	.6133	.0066	6.173	.9445	2.458	191.1	45.8	29.238	7.01
C_2	.0593	30.068	5.48	.0102	.3252	.0033	4.926	.2921	1.783	305.5	48.2	18.116	2.858
C_3	.05	44.094	6.64	.0082	.3320	.0027	4.545	.2273	2.205	370	42.	18.5	2.1
C_4	.003	58.12	7.62	.0073	.0229	.0002	4.386	.0132	.1744	425.2	37.5	1.276	.1125
C_5	.022	72.124	8.49	.0065	.1868	.0012	4.31	.0948	1.5867	469.8	33.3	10.336	.7326
C_{6+}	.3707	214.5	14.65	3.0	5.4292	16.288	3.551	1.3164	79.515	705.4	17.347	261.49	6.431
+From N.G.P.A.[59]					8.7194	16.3339		3.9303	97.3031			382.1164	30.7011

$u = 2.5165$ cp

TABLE B-30

LIQUID VISCOSITY

Sampling Point A
Cum. N_2 Inj. = .3 p.v.
Pressure at sampling point = 4400 psi

Comp.	x_i	M_i	$M_i^{1/2}$	u_i^* cp	$x_i M_i^{1/2}$	$x_i u_i^* M_i^{1/2}$	Critical volume V_{c_i} gm/cm^3	$x_i V_{c_i}$	$x_i M_i$	T_cm °K	P_c, atm	$x_i T_{c_i}$	$x_i P_{c_i}$
N_2	.452	28.016	5.29	.0176	2.392	.0421	3.215+	1.453	12.663	126.2	33.5	57.04	15.142
C_1	.025	16.068	4.01	.0108	.1002	.00108	6.173	.1543	.4017	191.1	45.8	4.78	1.145
C_2	.007	30.068	5.48	.0102	.0384	.0004	4.926	.0345	.2105	305.5	48.2	2.139	.3374
C_3	.003	44.094	6.64	.0082	.020	.0002	4.545	.0136	.1323	370	42.	1.11	.126
C_4	0	58.12	7.62	.0073	0	0	4.386	0	0	425.2	37.5	0	0
C_5	0	72.124	8.49	.0065	0	0	4.31	0	0	469.8	33.3	0	0
C_{6+}	.513	214.5	14.65	3.0	7.5133	22.54	3.551	1.822	110.04	705.4	17.347	361.87	8.9
+From N.G.P.A.[59]					10.0639	22.58378		3.4774	123.4475			426.939	25.6504

u = 2.594 cp

TABLE B-31

LIQUID VISCOSITY

Sampling Point B
Cum. N_2 Inj. = .44 p.v.
Pressure at sampling point = 3800 psi

Comp.	x_i	M_i	$M_i^{1/2}$	u_i^* cp	$x_i M_i^{1/2}$	$x_i u_i^* M_i^{1/2}$	Critical volume v_{c_i} gm/cm^3	$x_i v_{c_i}$	$x_i M_i$	T_{c_m} °K	P_c, atm	$x_i T_{c_i}$	$x_i P_{c_i}$
N_2	.138	28.016	5.29	.0176	.7304	.0129	3.215+	.4437	3.87	126.2	33.5	17.42	4.62
C_1	.255	16.068	4.01	.0108	1.022	.011	6.173	1.514	4.1	191.1	45.8	48.73	11.68
C_2	.136	30.068	5.48	.0102	.7457	.0076	4.926	.67	4.1	305.5	48.2	41.55	6.56
C_3	.117	44.094	6.64	.0082	.7769	.0064	4.545	.5318	5.16	370	42.	43.29	4.91
C_4	.013	58.12	7.62	.0073	.0991	.0007	4.386	.057	.76	425.2	37.5	5.53	.49
C_5	.042	72.124	8.49	.0065	.3567	.0023	4.31	.181	.181	469.8	33.3	19.73	1.4
C_{6+}	.299	214.5	14.65	3.0	4.379	13.137	3.551	1.0617	64.14	705.4	17.347	210.9	5.19
+From N.G.P.A.[59]					8.1098	13.1779		4.5192	82.311			387.15	34.85

$u = 2.722$ cp

TABLE B-32

LIQUID VISCOSITY

Sampling Point B
Cum. N_2 Inj. = .47 p.v.
Pressure at sampling point = 3800 psi

Comp.	x_i	M_i	$M_i^{1/2}$	u_i^* cp	$x_i M_i^{1/2}$	$x_i u_i^* M_i^{1/2}$	Critical volume v_{c_i} gm/cm^3	$x_i v_{c_i}$	$x_i M_i$	T_c m °K	P_c, atm	$x_i T_{c_i}$	$x_i P_{c_i}$
N_2	.178	28.016	5.29	.0176	.942	.0166	3.215+	.572	4.99	126.2	33.5	22.46	5.96
C_1	.13	16.068	4.01	.0108	.5211	.0056	6.173	.802	2.09	191.1	45.8	24.84	5.95
C_2	.109	30.068	5.48	.0102	.5977	.0061	4.926	.537	3.28	305.5	48.2	33.3	5.25
C_3	.086	44.094	6.64	.0082	.5711	.0047	4.545	.391	3.79	370	42.	31.82	3.61
C_4	0	58.12	7.62	.0073	0	0	4.386	0	0	425.2	37.5	0	0
C_5	0	72.124	8.49	.0065	0	0	4.31	0	0	469.8	33.3	0	0
C_{6+}	.507	214.5	14.65	3.0	7.425	22.28	3.551	1.8	108.75	705.4	17.347	357.64	8.79
+From N.G.P.A.[59]					10.0569	22.313		4.102	122.9			470.06	29.56

$u = 3.217$ cp

TABLE B-33

LIQUID VISCOSITY

Sampling Point C
Cum. N_2 Inj. = .612 p.v.
Pressure at sampling point = 3200 psi

Comp.	x_i	M_i	$M_i^{\frac{1}{2}}$	u_i^* cp	$x_i M_i^{\frac{1}{2}}$	$x_i u_i^* M_i^{\frac{1}{2}}$	Critical volume v_{c_i} gm/cm^3	$x_i v_{c_i}$	$x_i M_i$	T_{c_m} °K	P_c, atm	$x_i T_{c_i}$	$x_i P_{c_i}$
N_2	.102	28.016	5.29	.0176	.5399	.0095	3.215+	.328	2.86	126.2	33.5	12.87	3.417
C_1	.258	16.068	4.01	.0108	1.034	.0112	6.173	1.593	4.15	191.1	45.8	49.3	11.82
C_2	.139	30.068	5.48	.0102	.7622	.0078	4.926	.685	4.18	305.5	48.2	42.46	6.7
C_3	.157	44.094	6.64	.0082	1.043	.0085	4.545	.714	6.92	370	42.	58.09	6.59
C_4	.026	58.12	7.62	.0073	.1982	.0014	4.386	.114	1.51	425.2	37.5	11.06	.98
C_5	.071	72.124	8.49	.0065	.603	.0039	4.31	.306	5.12	469.8	33.3	33.36	2.36
C_{6+}	.247	214.5	14.65	3.0	3.618	10.853	3.551	.8771	52.98	705.4	17.347	174.23	4.28
+From N.G.P.A.[59]					7.7983	10.8953		4.6171	77.72			381.37	36.147

$u = 2.28$ cp

TABLE B-34

LIQUID VISCOSITY

Sampling Point C
Cum. N_2 Inj. = .638 p.v.
Pressure at sampling point = 3200 psi

Comp.	x_i	M_i	$M_i^{1/2}$	u_i^* cp	$x_i M_i^{1/2}$	$x_i u_i^* M_i^{1/2}$	Critical volume v_{c_i} gm/cm^3	$x_i v_{c_i}$	$x_i M_i$	T_cm °K	P_c, atm	$x_i T_{c_i}$	$x_i P_{c_i}$
N_2	.106	28.016	5.29	.0176	.561	.01	3.2154	.341	2.97	126.2	33.5	13.38	3.55
C_1	.134	16.068	4.01	.0108	.537	.006	6.173	.827	2.153	191.1	45.8	25.61	6.14
C_2	.101	30.068	5.48	.0102	.554	.0056	4.926	.498	3.037	305.5	48.2	30.86	4.87
C_3	.115	44.094	6.64	.0082	.7636	.0063	4.545	.523	5.071	370	42.	42.55	4.83
C_4	0	58.12	7.62	.0073	0	0	4.386	0	0	425.2	37.5	0	0
C_5	0	72.124	8.49	.0065	0	0	4.31	0	0	469.8	33.3	0	0
C_{6+}	.544	214.5	14.65	3.0	7.967	23.90	3.551	1.932	116.69	705.4	17.347	383.74	9.44
+From N.G.P.A.[59]					10.3826	23.9279		4.121	129.921			496.14	28.83

u = 3.343 cp

APPENDIX C

DATA AND RESULTS OF THE FOURTH RUN

TABLE C-1

GAS DENSITY

Sampling Point A
Cum. N_2 Inj. = .17 p.v.
Pressure at sampling point = 3360 psi

Comp.	Mole fraction gas, y_i	Critical temp., T_c, °R	Critical pressure, P_c, psi	Molecular weight M_i	$y_i T_{c_i}$	$y_i P_{c_i}$	$y_i M_i$
N_2	.631	227	492.2	28.016	143	311	17.678
C_1	.27	343.2	673.1	16.068	93	182	4.338
C_2	.037	549.2	708.3	30.068	20	26	1.113
C_3	.033	666	617.4	44.094	22	20	1.455
C_4	.005	765.7	550.1	58.12	4	3	.291
C_5	.009	846.2	489.8	72.124	8	4	.649
C_{6+}	.015	1073+	334+	128.0	16	5	2.048
					306	551	27.572

+From Clark[58]

Gas Density = 17.53 lb/ft^3

TABLE C-2

GAS DENSITY

Sampling Point A
Cum. N_2 Inj. = .34 p.v.
Pressure at sampling point = 3360 psi

Comp.	Mole fraction gas, y_i	Critical temp., T_c, °R	Critical pressure, P_c, psi	Molecular weight M_i	$y_i T_{c_i}$	$y_i P_{c_i}$	$y_i M_i$
N_2	.841	227	492.2	28.016	191	413.9	23.561
C_1	.12	343.2	673.1	16.068	41	80.8	1.928
C_2	.015	549.2	708.3	30.068	8	10.6	.451
C_3	.009	666	617.4	44.094	6	5.6	.397
C_4	.002	765.7	550.1	58.12	1.5	1.1	.116
C_5	.004	846.2	489.8	72.124	3.4	2.0	.288
C_{6+}	.009	1073+	334+	128.0	9.7	3.0	1.152
				260.6	517		27.893

+From Clark[58]

Gas Density = 16.46 lb/ft^3

TABLE C-3

GAS DENSITY

Sampling Point B
Cum. N_2 Inj. = .34 p.v.
Pressure at sampling point = 3020 psi

Comp.	Mole fraction gas, y_i	Critical temp., T_c, °R	Critical pressure, P_c, psi	Molecular weight M_i	$y_i T_{c_i}$	$y_i P_{c_i}$	$y_i M_i$
N_2	.5365	227	492.2	28.016	121.8	264.1	15.031
C_1	.34	343.2	673.1	16.068	116.7	228.9	5.463
C_2	.041	549.2	708.3	30.068	25.5	29.0	1.233
C_3	.0375	666	617.4	44.094	25	23.2	1.654
C_4	.008	765.7	550.1	58.12	6.1	4.4	.465
C_5	.015	846.2	489.8	72.124	12.7	7.3	1.082
C_{6+}	.022	1073+	334+	128.0	23.6	7.3	2.816
					331.4	564.2	27.744

+From Clark[58]

Gas Density = 17.575 lb/ft^3

TABLE C-4

GAS DENSITY

Sampling Point B
Cum. N_2 Inj. = .5 p.v.
Pressure at sampling point = 3020 psi

Comp.	Mole fraction gas, y_i	Critical temp., T_c, °R	Critical pressure, P_c, psi	Molecular weight M_i	$y_i T_{c_i}$	$y_i P_{c_i}$	$y_i M_i$
N_2	.682	227	492.2	28.016	154.8	335.7	19.107
C_1	.24	343.2	673.1	16.068	82.4	161.5	3.856
C_2	.031	549.2	708.3	30.068	17.0	22	.932
C_3	.024	666	617.4	44.094	16	14.8	1.058
C_4	.003	765.7	550.1	58.12	2.3	1.7	.174
C_5	.005	846.2	489.8	72.124	4.2	2.4	.361
C_{6+}	.015	1073+	334+	128.0	16.1	5.0	1.92
					292.8	543.1	27.408

+From Clark[58]

Gas Density = 15.663 lb/ft^3

TABLE C-5

GAS DENSITY

Sampling Point B
Cum. N_2 Inj. = .58 p.v.
Pressure at sampling point = 3020 psi

Comp.	Mole fraction gas, y_i	Critical temp., T_c, °R	Critical pressure, P_c, psi	Molecular weight M_i	$y_i T_{c_i}$	$y_i P_{c_i}$	$y_i M_i$
N_2	.799	227	492.2	28.016	181.4	393.3	22.385
C_1	.15	343.2	673.1	16.068	51.5	101	2.410
C_2	.023	549.2	708.3	30.068	12.6	16.3	.692
C_3	.018	666	617.4	44.094	12	11.1	.794
C_4	0	765.7	550.1	58.12	0	0	0
C_5	0	846.2	489.8	72.124	0	0	0
C_{6+}	.01	1073+	334+	128.0	10.73	3.3	1.28
					256.23	525	27.561

+From Clark[58]

Gas Density = 14.871 lb/ft^3

TABLE C-6

GAS DENSITY

Sampling Point C
Cum. N_2 Inj. = .51 p.v.
Pressure at sampling point = 2680 psi

Comp.	Mole fraction gas, y_i	Critical temp., T_c, °R	Critical pressure, P_c, psi	Molecular weight M_i	$y_i T_{c_i}$	$y_i P_{c_i}$	$y_i M_i$
N_2	.412	227	492.2	28.016	93.5	202.8	11.543
C_1	.4	343.2	673.1	16.068	137.3	269.2	6.427
C_2	.062	549.2	708.3	30.068	34.1	43.9	1.864
C_3	.052	666	617.4	44.094	34.6	32.1	2.293
C_4	.017	765.7	550.1	58.12	13.0	9.4	.988
C_5	.022	846.2	489.8	72.124	18.6	10.8	1.587
C_{6+}	.035	1073+	334+	128.0	37.6	11.7	4.48
					368.7	579.9	29.182

+From Clark[58]

Gas Density = 17.992 lb/ft^3

TABLE C-7

GAS DENSITY

Sampling Point C
Cum. N_2 Inj. = .64 p.v.
Pressure at sampling point = 2680 psi

Comp.	Mole fraction gas, y_i	Critical temp., T_c, °R	Critical pressure, P_c, psi	Molecular weight M_i	$y_i T_{c_i}$	$y_i P_{c_i}$	$y_i M_i$
N_2	.678	227	492.2	28.016	153.9	333.7	18.995
C_1	.22	343.2	673.1	16.068	75.5	148.1	3.535
C_2	.0385	549.2	708.3	30.068	21.1	27.3	1.158
C_3	.029	666	617.4	44.094	19.3	17.9	1.279
C_4	.0065	765.7	550.1	58.12	5.0	3.6	.378
C_5	.01	846.2	489.8	72.124	8.5	4.9	.721
C_{6+}	.98	1073+	334+	128.0	19.3	6.0	2.304
					302.6	541.5	28.37

+From Clark[58]

Gas Density = 14.704 lb/ft^3

TABLE C-8

GAS DENSITY

Sampling Point C
Cum. N_2 Inj. = .68 p.v.
Pressure at sampling point = 2680 psi

Comp.	Mole fraction gas, y_i	Critical temp., T_c, °R	Critical pressure, P_c, psi	Molecular weight M_i	$y_i T_{c_i}$	$y_i P_{c_i}$	$y_i M_i$
N_2	.7635	227	492.2	28.016	173.3	375.8	21.390
C_1	.162	343.2	673.1	16.068	55.6	109	2.603
C_2	.0305	549.2	708.3	30.068	16.8	21.6	.917
C_3	.023	666	617.4	44.094	15.3	14.2	1.014
C_4	.002	765.7	550.1	58.12	1.5	1.1	.116
C_5	.007	846.2	489.8	72.124	5.9	3.4	.505
C_{6+}	.012	1073+	334+	128.0	12.9	4.1	1.536
					281.3	529.2	28.081

+From Clark[58]

Gas Density = 14.16 lb/ft^3

TABLE C-9

GAS DENSITY

Sampling Point D
Cum. N_2 Inj. = .68 p.v.
Pressure at sampling point = 2340 psi

Comp.	Mole fraction gas, y_i	Critical temp., T_c, °R	Critical pressure, P_c, psi	Molecular weight M_i	$y_i T_{c_i}$	$y_i P_{c_i}$	$y_i M_i$
N_2	.344	227	492.2	28.016	78.1	169.3	9.638
C_1	.42	343.2	673.1	16.068	144.1	282.7	6.749
C_2	.081	549.2	708.3	30.068	44.5	57.4	2.436
C_3	.066	666	617.4	44.094	44.0	40.7	2.910
C_4	.017	765.7	550.1	58.12	13.0	9.4	.988
C_5	.027	846.2	489.8	72.124	22.8	13.2	1.947
C_{6+}	.045	1073+	334+	128.0	48.3	15.0	5.76
					394.8	58.77	30.328

+From Clark[58]

Gas Density = 18.233 lb/ft^3

TABLE C-10

GAS DENSITY

Sampling Point D
Cum. N_2 Inj. = .82 p.v.
Pressure at sampling point = 2340 psi

Comp.	Mole fraction gas, y_i	Critical temp., T_c, °R	Critical pressure, P_c, psi	Molecular weight M_i	$y_i T_{c_i}$	$y_i P_{c_i}$	$y_i M_i$
N_2	.652	227	492.2	28.016	148	320.9	18.266
C_1	.22	343.2	673.1	16.068	75.5	148.1	3.545
C_2	.051	549.2	708.3	30.068	28	36.1	1.533
C_3	.035	666	617.4	44.094	23.3	21.6	1.543
C_4	.008	765.7	550.1	58.12	6.1	4.4	.465
C_5	.013	846.2	489.8	72.124	11	6.4	.938
C_{6+}	.021	1073+	334+	128.0	22.5	7.0	2.688
					314.4	544.5	28.978

+From Clark[58]

Gas Density = 28.978 lb/ft^3

TABLE C-11

GAS DENSITY

Sampling Point D
Cum. N_2 Inj. = .88 p.v.
Pressure at sampling point = 2340 psi

Comp.	Mole fraction gas, y_i	Critical temp., T_c, °R	Critical pressure, P_c, psi	Molecular weight M_i	$y_i T_{c_i}$	$y_i P_{c_i}$	$y_i M_i$
N_2	.838	227	492.2	28.016	190.2	412.5	23.477
C_1	.11	343.2	673.1	16.068	37.8	74.0	2.767
C_2	.026	549.2	708.3	30.068	14.3	18.4	.782
C_3	.016	666	617.4	44.094	10.7	9.9	.706
C_4	0.0	765.7	550.1	58.12	0	0	0
C_5	.003	846.2	489.8	72.124	2.5	1.5	.216
C_{6+}	.007	1073+	334+	128.0	7.5	2.3	.896
					263	518.6	27.844

+From Clark[58]

Gas Density = 12.07 lb/ft^3

TABLE C-12

LIQUID DENSITY

Sampling point A
Cum. N_2 Inj. = .17 p.v.
Pressure at the sampling point = 3360 psi

Comp.	Mole fraction liquid, x_i	Molecular weight M_i	$x_i M_i$	Specific volume v_i, ft^3/lb	$x_i M_i v_i$
N_2	.1353	28.016	3.7906	.01983+	.07517
C_1	.174	16.068	2.79583	.0535	.14958
C_2	.046	30.068	1.383	.043	.05947
C_3	.058	44.094	2.557	.0316	.08082
C_4	.013	58.12	.756	.0275	.02078
C_5	.0367	72.124	2.647	.0254	.06723
C_{6+}	.536	214.5	114.972	.01976	2.272
+From N.G.P.A.[59]			128.901		2.725

Stock tank density = 47.303 lb/ft^3
Density at current pressure and temperature = 48.253 lb/ft^3

TABLE C-13

LIQUID DENSITY

Sampling point A
Cum. N_2 Inj. = .34 p.v.
Pressure at the sampling point = 3360 psi

Comp.	Mole fraction liquid, x_i	Molecular weight M_i	$x_i M_i$	Specific volume v_i, ft^3/lb	$x_i M_i v_i$
N_2	.3202	28.016	8.971	.01983+	.1779
C_1	.075	16.068	1.205	.0535	.0645
C_2	.0192	30.068	.577	.043	.0248
C_3	.0167	44.094	.736	.0316	.023
C_4	.0057	58.12	.331	.0275	.0091
C_5	.0182	72.124	1.313	.0254	.0333
C_{6+}	.692	214.5	148.434	.01976	2.9331
			161.567		3.2657

+From N.G.P.A.[59]

Stock tank density = 49.474 lb/ft^3
Density at current pressure and temperature = 50.474 lb/ft^3

TABLE C-14

LIQUID DENSITY

Sampling point B
Cum. N_2 Inj. = .34 p.v.
Pressure at the sampling point = 3020 psi

Comp.	Mole fraction liquid, x_i	Molecular weight M_i	$x_i M_i$	Specific volume v_i, ft^3/lb	$x_i M_i v_i$
N_2	.099	28.016	2.774	.01983+	.055
C_1	.206	16.068	3.31	.0535	.1771
C_2	.052	30.068	1.564	.043	.0672
C_3	.071	44.094	3.131	.0316	.0989
C_4	.023	58.12	1.337	.0275	.0368
C_5	.071	72.124	5.121	.0254	.1301
C_{6+}	.478	214.5	102.531	.01976	2.026
+From N.G.P.A.[59]			119.768		2.5911

Stock tank density = 46.223 lb/ft^3
Density at current pressure and temperature = 47.153 lb/ft^3

TABLE C-15

LIQUID DENSITY

Sampling point B
Cum. N_2 Inj. = .5 p.v.
Pressure at the sampling point = 3020 psi

Comp.	Mole fraction liquid, x_i	Molecular weight M_i	$x_i M_i$	Specific volume v_i, ft^3/lb	$x_i M_i v_i$
N_2	.112	28.016	3.138	.01983+	.0622
C_1	.141	16.068	2.266	.0535	.1212
C_2	.04	30.068	1.203	.043	.0517
C_3	.047	44.094	2.072	.0316	.065
C_4	.009	58.12	.523	.0275	.0144
C_5	.026	72.124	1.875	.0254	.0476
C_{6+}	.625	214.5	134.063	.01976	2.6491
+From N.G.P.A.[59]			145.14		3.0112

Stock tank density = 48.2 lb/ft^3
Density at current pressure and temperature = 49.1 lb/ft^3

TABLE C-16

LIQUID DENSITY

Sampling point B
Cum. N_2 Inj. = .58 p.v.
Pressure at the sampling point = 3020 psi

Comp.	Mole fraction liquid, x_i	Molecular weight M_i	$x_i M_i$	Specific volume v_i, ft^3/lb	$x_i M_i v_i$
N_2	.132	28.016	3.698	.01983+	.0733
C_1	.087	16.068	1.398	.0535	.0748
C_2	.03	30.068	.902	.043	.0388
C_3	.037	44.094	1.631	.0316	.0516
C_4	0	58.12	0	.0275	0
C_5	0	72.124	0	.0254	0
C_{6+}	.714	214.5	153.153	.01976	3.0263
			160.782		3.2648

+From N.G.P.A.[59]

Stock tank density = 49.247 lb/ft^3
Density at current pressure and temperature = 50.137 lb/ft^3

TABLE C-17

LIQUID DENSITY

Sampling point C
Cum. N_2 Inj. = .51 p.v.
Pressure at the sampling point = 2680 psi

Comp.	Mole fraction liquid, x_i	Molecular weight M_i	$x_i M_i$	Specific volume v_i, ft^3/lb	$x_i M_i v_i$
N_2	.116	28.016	3.25	.01983+	.0644
C_1	.229	16.068	3.68	.0535	.1969
C_2	.078	30.068	2.345	.043	.1009
C_3	.104	44.094	4.586	.0316	.1449
C_4	.055	58.12	3.197	.0275	.0879
C_5	.116	72.124	8.366	.0254	.213
C_{6+}	.302	214.5	64.779	.01976	1.28
+From N.G.P.A.[59]			90.203		2.088

Stock tank density = 43.2007 lb/ft^3
Density at current pressure and temperature = 44.3507 lb/ft^3

TABLE C-18

LIQUID DENSITY

Sampling point C
Cum. N_2 Inj. = .64 p.v.
Pressure at the sampling point = 2680 psi

Comp.	Mole fraction liquid, x_i	Molecular weight M_i	$x_i M_i$	Specific volume v_i, ft^3/lb	$x_i M_i v_i$
N_2	.125	28.016	3.502	.01983+	.0694
C_1	.121	16.068	1.944	.0535	.104
C_2	.05	30.068	1.503	.043	.0647
C_3	.062	44.094	2.734	.0316	.0864
C_4	.023	58.12	1.337	.0275	.0368
C_5	.059	72.124	4.255	.0254	.1081
C_{6+}	.56	214.5	120.12	.01976	2.3736
			135.395		2.843

+From N.G.P.A.[59]

Stock tank density = 47.624 lb/ft^3
Density at current pressure and temperature = 48.524 lb/ft^3

TABLE C-19

LIQUID DENSITY

Sampling point C
Cum. N_2 Inj. = .68 p.v.
Pressure at the sampling point = 2680 psi

Comp.	Mole fraction liquid, x_i	Molecular weight M_i	$x_i M_i$	Specific volume v_i, ft^3/lb	$x_i M_i v_i$
N_2	.125	28.016	3.502	.01983+	.0694
C_1	.087	16.068	1.398	.0535	.0748
C_2	.041	30.068	1.233	.043	.053
C_3	.051	44.094	2.249	.0316	.071
C_4	.007	58.12	.407	.0275	.0112
C_5	.044	72.124	3.173	.0254	.0806
C_{6+}	.645	214.5	138.353	.01976	2.734
+From N.G.P.A.[59]			150.315		3.094

Stock tank density = 48.5827 lb/ft^3
Density at current pressure and temperature = 49.432 lb/ft^3

TABLE C-20

LIQUID DENSITY

Sampling point D
Cum. N_2 Inj. = .68 p.v.
Pressure at the sampling point = 2340 psi

Comp.	Mole fraction liquid, x_i	Molecular weight M_i	$x_i M_i$	Specific volume v_i, ft^3/lb	$x_i M_i v_i$
N_2	.101	28.016	2.83	.01983+	.0561
C_1	.233	16.068	3.744	.0535	.2003
C_2	.104	30.068	3.127	.043	.1345
C_3	.137	44.094	6.041	.0316	.1909
C_4	.059	58.12	3.429	.0275	.0943
C_5	.15	72.124	10.819	.0254	.2748
C_{6+}	.216	214.5	46.332	.01976	.9155
			76.322		1.8664

+From N.G.P.A.[59]

Stock tank density = 40.8926 lb/ft^3
Density at current pressure and temperature = 41.89 lb/ft^3

TABLE C-21

LIQUID DENSITY

Sampling point D
Cum. N_2 Inj. = .82 p.v.
Pressure at the sampling point = 2340 psi

Comp.	Mole fraction liquid, x_i	Molecular weight M_i	$x_i M_i$	Specific volume v_i, ft^3/lb	$x_i M_i v_i$
N_2	.125	28.016	3.502	.01983+	.0694
C_1	.113	16.068	1.816	.0535	.0971
C_2	.068	30.068	2.045	.043	.0879
C_3	.081	44.094	3.572	.0316	.1129
C_4	.033	58.12	1.918	.0275	.0527
C_5	.1	72.124	7.212	.0254	.1832
C_{6+}	.68	214.5	102.96	.01976	2.0345
+From N.G.P.A.[59]			123.025		2.6377

Stock tank density = 46.64 lb/ft^3
Density at current pressure and temperature = 47.49 lb/ft^3

TABLE C-22

LIQUID DENSITY

Sampling point D
Cum. N_2 Inj. = .88 p.v.
Pressure at the sampling point = 2340 psi

Comp.	Mole fraction liquid, x_i	Molecular weight M_i	$x_i M_i$	Specific volume v_i, ft^3/lb	$x_i M_i v_i$
N_2	.139	28.016	3.894	.01983+	.0772
C_1	.055	16.068	.884	.0535	.0473
C_2	.035	30.068	1.052	.043	.0453
C_3	.038	44.094	1.676	.0316	.053
C_4	0	58.12	0	.0275	0
C_5	.024	72.124	1.731	.0254	.044
C_{6+}	.709	214.5	152.081	.01976	3.0051
			161.318		3.2719

+From N.G.P.A.[59]

Stock tank density = 49.304 lb/ft^3
Density at current pressure and temperature = 50.004 lb/ft^3

Sampling p[redacted]23
Cum. N_2 I[redacted]
Pressure[redacted]

(1) Comp.				(7) Parachor P_{chi}	(8) (6) x (7)
N_2	[redacted]	[redacted]	[redacted]	41+	-.24
C_1	[redacted]	[redacted]	[redacted]	77	-.15514
C_2	[redacted]	[redacted]	[redacted]	108	-.01971
C_3	[redacted]	[redacted]	[redacted]	150	-.013695
C_4	.01[redacted]	[redacted]	[redacted]	190	.00076
C_5	.0367	[redacted]	063	232	.0147
C_{6+}	.536	.01[redacted]	.002111	548.2	1.1573
					.7442

+From Katz et al.[53]

Surface tension = .306 dynes/cm.

TABLE C-23

SURFACE TENSION

Sampling point A
Cum. N_2 Inj. = .17 p.v.
Pressure at sampling point = 3360 psi

(1) Comp.	(2) x_i	(3) y_i	(4) $x_i \frac{\rho_L}{M_L}$	(5) $y_i \frac{\rho_v}{M_v}$	(6) (4) - (5)	(7) Parachor P_{chi}	(8) (6) x (7)
N_2	.1353	.631	.0005714	.006426	-.00585	41+	-.24
C_1	.174	.27	.000735	.00275	-.00201	77	-.15514
C_2	.046	.037	.000194	.000377	-.0001825	108	-.01971
C_3	.058	.033	.000245	.00034	-.00009	150	-.013695
C_4	.013	.005	.000055	.000051	0.000004	190	.00076
C_5	.0367	.009	.000155	.000092	0.000063	232	.0147
C_{6+}	.536	.015	.002264	.000153	.002111	548.2	1.1573
							.7442

+From Katz et al.[53]

Surface tension = .306 dynes/cm.

TABLE C-24

SURFACE TENSION

Sampling point A
Cum. N_2 Inj. = .34 p.v.
Pressure at sampling point = 3360 psi

(1) Comp.	(2) x_i	(3) y_i	(4) $x_i \frac{\rho_L}{M_L}$	(5) $y_i \frac{\rho_v}{M_v}$	(6) (4) - (5)	(7) Parachor P_{chi}	(8) (6) x (7)
N_2	.3202	.841	.00119	.00795	-.00676	41+	.2771
C_1	.075	.12	.00028	.00113	-.00085	77	-.0658
C_2	.0192	.015	.00007	.000142	-.00007	108	-.00759
C_3	.0167	.009	.00006	.000085	-.000023	150	-.00344
C_4	.0057	.002	.000021	.00002	.00000233	190	.000443
C_5	.0182	.004	.0000678	.000038	.00003	232	.00696
C_{6+}	.692	.009	.00258	.000085	.00249	548.2	1.3668
							1.020273

+From Katz et al.[53]

Surface tension = 1.084 dynes/cm.

TABLE C-25

SURFACE TENSION

Sampling point B
Cum. N_2 Inj. = .5 p.v.
Pressure at sampling point = 3020 psi

(1) Comp.	(2) x_i	(3) y_i	(4) $x_i \frac{\rho_L}{M_L}$	(5) $y_i \frac{\rho_v}{M_v}$	(6) (4) - (5)	(7) Parachor P_{chi}	(8) (6) x (7)
N_2	.112	.682	.00045	.00624	-.0058	41+	-.2375
C_1	.141	.24	.00057	.0022	-.00163	77	-.1256
C_2	.04	.031	.00016	.000284	-.00012	108	-.0133
C_3	.047	.024	.00019	.00022	-.000031	150	-.00467
C_4	.009	.003	.000036	.00003	.000009	190	.00164
C_5	.026	.005	.0001	.0000457	.000059	232	.01359
C_{6+}	.625	.015	.00251	.000137	.00237	548.2	1.2996
							.93376

+From Katz et al.[53]

Surface tension = .76 dynes/ cm.

TABLE C-26

SURFACE TENSION

Sampling point B
Cum. N_2 Inj. = .58 p.v.
Pressure at sampling point = 3020 psi

(1) Comp.	(2) x_i	(3) y_i	(4) $x_i \frac{\rho_L}{M_L}$	(5) $y_i \frac{\rho_v}{M_v}$	(6) (4) - (5)	(7) Parachor P_{chi}	(8) (6) x (7)
N_2	.132	.799	.0005	.003448	-.002947	41+	-.1208
C_1	.087	.15	.00033	.0013	.00097	77	-.0744
C_2	.03	.023	.000114	.000199	-.000085	108	-.0092
C_3	.037	.018	.00014	.000156	-.000015	150	-.0023
C_4	0	0	0	0	0	190	0
C_5	0	0	0	0	0	232	0
C_{6+}	.714	.01	.002711	.1000086	.002625	548.2	1.439
							1.2323

+From Katz et al.[53]

Surface tension = 2.31 dynes/ cm.

TABLE C-27

GAS VISCOSITY

Sampling point A
Cum. N_2 Inj. = .17 p.v.
Pressure at sampling point = 3360 psi

Comp.	Mole fraction gas, y_i	Molecular weight M_i	$M_i^{1/2}$	$y_i M_i^{1/2}$	Atmospheric viscosity u_i^*, cp	$u_i^* y_i M_i^{1/2}$
N_2	.631	28.016	5.29	3.3399	.0176+	.0588
C_1	.27	16.068	4.01	1.0823	.0108	.0117
C_2	.037	30.068	5.48	.2029	.0102	.0021
C_3	.033	44.094	6.64	.2191	.0082	.0018
C_4	.005	58.12	7.62	.0381	.0073	.0003
C_5	.009	72.124	8.5	.0764	.0065	.0005
C_{6+}	.015	128	11.31	.1697	.005	.0008
From Carr et al.[56]				5.1284		.076

Mixture atmospheric viscosity = u* = .0148 cp
Mixture viscosity at the system temperature and pressure = u = .0265 cp

TABLE C-28

GAS VISCOSITY

Sampling point A
Cum. N_2 Inj. = .34 p.v.
Pressure at sampling point = 3360 psi

Comp.	Mole fraction gas, y_i	Molecular weight M_i	$M_i^{1/2}$	$y_i M_i^{1/2}$	Atmospheric viscosity u_i^*, cp	$u_i^* y_i M_i^{1/2}$
N_2	.841	28.016	5.29	4.4514	.0176+	.0783
C_1	.12	16.068	4.01	.4810	.0108	.0052
C_2	.015	30.068	5.48	.0823	.0102	.0008
C_3	.009	44.094	6.64	.0598	.0082	.0005
C_4	.002	58.12	7.62	.0152	.0073	.0001
C_5	.004	72.124	8.5	.034	.0065	.0002
C_{6+}	.009	128	11.31	.1018	.005	.0005
				5.2255		.0856

From Carr et al.[56]

Mixture atmospheric viscosity = u* = .0164 cp
Mixture viscosity at the system temperature and pressure = u = .0254 cp

TABLE C-29

GAS VISCOSITY

Sampling point B
Cum. N_2 Inj. = .34 p.v.
Pressure at sampling point = 3020 psi

Comp.	Mole fraction gas, y_i	Molecular weight M_i	$M_i^{1/2}$	$y_i M_i^{1/2}$	Atmospheric viscosity u_i^*, cp	$u_i^* y_i M_i^{1/2}$
N_2	.5365	28.016	5.29	2.8397	.0176+	.05
C_1	.34	16.068	4.01	1.3629	.0108	.0147
C_2	.041	30.068	5.48	.2248	.0102	.0023
C_3	.0375	44.094	6.64	.249	.0082	.002
C_4	.008	58.12	7.62	.061	.0073	.0004
C_5	.015	72.124	8.5	.1274	.0065	.0008
C_{6+}	.022	128	11.31	.2489	.005	.0012
From Carr et al.[56]				5.1137		.0714

Mixture atmospheric viscosity = u* = .014 cp
Mixture viscosity at the system temperature and pressure = u = .0266 cp

TABLE C-30

GAS VISCOSITY

Sampling point B
Cum. N_2 Inj. = .5 p.v.
Pressure at sampling point = 3020 psi

Comp.	Mole fraction gas, y_i	Molecular weight M_i	$M_i^{1/2}$	$y_i M_i^{1/2}$	Atmospheric viscosity u_i^*, cp	$u_i^* y_i M_i^{1/2}$
N_2	.682	28.016	5.29	3.6098	.0176+	.0635
C_1	.24	16.068	4.01	.962	.0108	.0104
C_2	.031	30.068	5.48	.1700	.0102	.0017
C_3	.024	44.094	6.64	.1594	.0082	.0013
C_4	.003	58.12	7.62	.0229	.0073	.0002
C_5	.005	72.124	8.5	.0425	.0065	.0003
C_{6+}	.015	128	11.31	.1697	.005	.0008
				5.1363		.0782

From Carr et al.[56]

Mixture atmospheric viscosity = u* = .0152 cp
Mixture viscosity at the system temperature and pressure = u = .0243 cp

TABLE C-31

GAS VISCOSITY

Sampling point B
Cum. N_2 Inj. = .58 p.v.
Pressure at sampling point = 3020 psi

Comp.	Mole fraction gas, y_i	Molecular weight M_i	$M_i^{1/2}$	$y_i M_i^{1/2}$	Atmospheric viscosity u_i^*, cp	$u_i^* y_i M_i^{1/2}$
N_2	.799	28.016	5.29	4.2291	.0176+	.0744
C_1	.15	16.068	4.01	.6013	.0108	.0065
C_2	.023	30.068	5.48	.1261	.0102	.0013
C_3	.018	44.094	6.64	.1195	.0082	.0010
C_4	0	58.12	7.62	0	.0073	0
C_5	0	72.124	8.5	0	.0065	0
C_{6+}	.01	128	11.31	.1131	.005	.0006
				5.1891		.0838

From Carr et al.[56]

Mixture atmospheric viscosity = u* = .0161 cp
Mixture viscosity at the system temperature and pressure = u = .02254 cp

TABLE C-32

GAS VISCOSITY

Sampling point C
Cum. N_2 Inj. = .51 p.v.
Pressure at sampling point = 2680 psi

Comp.	Mole fraction gas, y_i	Molecular weight M_i	$M_i^{1/2}$	$y_i M_i^{1/2}$	Atmospheric viscosity u_i^*, cp	$u_i^* y_i M_i^{1/2}$
N_2	.412	28.016	5.29	2.1807	.0176+	.0384
C_1	.4	16.068	4.01	1.6034	.0108	.0173
C_2	.062	30.068	5.48	.34	.0102	.0035
C_3	.052	44.094	6.64	.3453	.0082	.0028
C_4	.017	58.12	7.62	.1296	.0073	.0009
C_5	.022	72.124	8.5	.1868	.0065	.0012
C_{6+}	.035	128	11.31	.396	.005	.002
From Carr et al.[56]				5.1818		.0661

Mixture atmospheric viscosity = u* = .0128 cp
Mixture viscosity at the system temperature and pressure = u = .0273 cp

TABLE C-33

GAS VISCOSITY

Sampling point C
Cum. N_2 Inj. = .64 p.v.
Pressure at sampling point = 2680 psi

Comp.	Mole fraction gas, y_i	Molecular weight M_i	$M_i^{1/2}$	$y_i M_i^{1/2}$	Atmospheric viscosity u_i^*, cp	$u_i^* y_i M_i^{1/2}$
N_2	.678	28.016	5.29	3.5887	.0176+	.0632
C_1	.22	16.068	4.01	.8819	.0108	.0095
C_2	.0385	30.068	5.48	.2111	.0102	.0022
C_3	.029	44.094	6.64	.1926	.0082	.0016
C_4	.0065	58.12	7.62	.0496	.0073	.0004
C_5	.01	72.124	8.5	.0849	.0065	.0006
C_{6+}	.018	128	11.31	.636	.005	.001
				5.2124		.0785

From Carr et al.[56]

Mixture atmospheric viscosity = u* = .015 cp
Mixture viscosity at the system temperature and pressure = u = .023 cp

TABLE C-34

GAS VISCOSITY

Sampling point C
Cum. N_2 Inj. = .68 p.v.
Pressure at sampling point = 2680 psi

Comp.	Mole fraction gas, y_i	Molecular weight M_i	$M_i^{1/2}$	$y_i M_i^{1/2}$	Atmospheric viscosity u_i^*, cp	$u_i^* y_i M_i^{1/2}$
N_2	.7635	28.016	5.29	4.0412	.0176+	.0711
C_1	.162	16.068	4.01	.6494	.0108	.007
C_2	.0305	30.068	5.48	.1672	.0102	.0017
C_3	.023	44.094	6.64	.1527	.0082	.0013
C_4	.002	58.12	7.62	.0152	.0073	.0001
C_5	.007	72.124	8.5	.0594	.0065	.0004
C_{6+}	.012	128	11.31	.1358	.005	.0007
					5.2209	.0823

From Carr et al.[56]

Mixture atmospheric viscosity = u* = .0158 cp
Mixture viscosity at the system temperature and pressure = u = .023 cp

TABLE C-35

GAS VISCOSITY

Sampling point D
Cum. N_2 Inj. = .68 p.v.
Pressure at sampling point = 2340 psi

Comp.	Mole fraction gas, y_i	Molecular weight M_i	$M_i^{1/2}$	$y_i M_i^{1/2}$	Atmospheric viscosity u_i^*, cp	$u_i^* y_i M_i^{1/2}$
N_2	.344	28.016	5.29	1.8208	.0176+	.0320
C_1	.42	16.068	4.01	1.6836	.0108	.0182
C_2	.081	30.068	5.48	.4442	.0102	.0045
C_3	.066	44.094	6.64	.4383	.0082	.0036
C_4	.017	58.12	7.62	.1296	.0073	.0009
C_5	.027	72.124	8.5	.2293	.0065	.0015
C_{6+}	.045	128	11.31	.5091	.005	.0025
				5.2549		.0632

From Carr et al.[56]

Mixture atmospheric viscosity = u* = .012 cp
Mixture viscosity at the system temperature and pressure = u = .0282 cp

TABLE C-36

GAS VISCOSITY

Sampling point D
Cum. N_2 Inj. = .82 p.v.
Pressure at sampling point = 2340 psi

Comp.	Mole fraction gas, y_i	Molecular weight M_i	$M_i^{\frac{1}{2}}$	$y_i M_i^{\frac{1}{2}}$	Atmospheric viscosity u_i^*, cp	$u_i^* y_i M_i^{\frac{1}{2}}$
N_2	.652	28.016	5.29	3.451	.0176+	.0607
C_1	.22	16.068	4.01	.8819	.0108	.0095
C_2	.051	30.068	5.48	.2797	.0102	.0029
C_3	.035	44.094	6.64	.2324	.0082	.0019
C_4	.008	58.12	7.62	.0610	.0073	.0004
C_5	.013	72.124	8.5	.1104	.0065	.0007
C_{6+}	.021	128	11.31	.2376	.005	.0012
				5.254		.0773

From Carr et al.[56]

Mixture atmospheric viscosity = u* = .0147 cp
Mixture viscosity at the system temperature and pressure = u = .022 cp

TABLE C-37

GAS VISCOSITY

Sampling point D
Cum. N_2 Inj. = .88 p.v.
Pressure at sampling point = 2340 psi

Comp.	Mole fraction gas, y_i	Molecular weight M_i	$M_i^{1/2}$	$y_i M_i^{1/2}$	Atmospheric viscosity u_i^*, cp	$u_i^* y_i M_i^{1/2}$
N_2	.838	28.016	5.29	4.4355	.0176+	.0781
C_1	.11	16.068	4.01	.4409	.0108	.0048
C_2	.026	30.068	5.48	.1426	.0102	.0015
C_3	.016	44.094	6.64	.1062	.0082	.0009
C_4	0.0	58.12	7.62	0	.0073	0
C_5	.003	72.124	8.5	.0255	.0065	.0002
C_{6+}	.007	128	11.31	.0792	.005	.0004
				5.2299		.0859

From Carr et al.[56]

Mixture atmospheric viscosity = u* = .0164 cp
Mixture viscosity at the system temperature and pressure = u = .022 cp

TABLE C-38

LIQUID VISCOSITY

Sampling Point A
Cum. N_2 Inj. = .17p.v.
Pressure at sampling point = 4400psi

Comp.	x_i	M_i	$M_i^{1/2}$	u_i^* cp	$x_i M_i^{1/2}$	$x_i u_i^* M_i^{1/2}$	Critical volume V_{ci} gm/cm^3	$x_i V_{c_i}$	$x_i M_i$	T_cm °K	P_c, atm	$x_i T_{c_i}$	$x_i P_{c_i}$
N_2	.1353	28.016	5.29	.0176	.7156	.0126	3.215+	.4350	3.7906	126.2	33.5	17.1	4.5
C_1	.174	16.068	4.01	.0108	.6975	.0075	6.173	1.0741	2.7958	191.1	45.8	33.3	8.0
C_2	.046	30.068	5.48	.0102	.2522	.0026	4.926	.2266	1.3831	305.5	48.2	14.1	2.2
C_3	.058	44.094	6.64	.0082	.3851	.0032	4.545	.2636	2.557	370	42.	21.5	2.4
C_4	.013	58.12	7.62	.0073	.0991	.0007	4.386	.057	.7556	425.2	37.5	5.5	.49
C_5	.0368	72.124	8.49	.0065	.3125	.002	4.31	.1586	2.647	469.8	33.3	17.3	1.2
C_{6+}	.536	214.5	14.65	3.0	7.8502	23.5505	3.551	1.9033	114.972	705.4	17.347	378.1	9.3
+From N.G.P.A.[59]					10.3122	23.5791		4.1182	128.9011			486.9	28.09

u = 3.37 cp

TABLE C-39

LIQUID VISCOSITY

Sampling Point A
Cum. N_2 Inj. = .34 p.v.
Pressure at sampling point = 4400 psi

Comp.	x_i	M_i	$M_i^{1/2}$	u_i^* cp	$x_i M_i^{1/2}$	$x_i u_i^* M_i^{1/2}$	Critical volume v_{c_i} gm/cm^3	$x_i v_{c_i}$	$x_i M_i$	T_c °K	P_c, atm	$x_i T_{c_i}$	$x_i P_{c_i}$
N_2	.3202	28.016	5.29	.0176	1.6948	.0298	3.215+	1.0294	8.971	126.2	33.5	40.4	10.7
C_1	.075	16.068	4.01	.0108	.3006	.0032	6.173	.463	1.2051	191.1	45.8	14.3	3.4
C_2	.0192	30.068	5.48	.0102	.1053	.0011	4.926	.0946	.5773	305.5	48.2	5.9	.93
C_3	.0167	44.094	6.64	.0082	.1109	.0009	4.545	.0759	.7364	370	42.	6.2	.70
C_4	.0057	58.12	7.62	.0073	.0435	.0003	4.386	.025	.3313	425.2	37.5	2.4	.21
C_5	.0182	72.124	8.49	.0065	.1546	.001	4.31	.0784	1.3127	469.8	33.3	8.6	.61
C_{6+}	.692	214.5	14.65	3.0	10.135	30.4047	3.551	2.4573	148.474	705.4	17.347	488.1	12.0
+From N.G.P.A.[59]					12.5447	30.441		4.2236	161.567			565.9	28.55

u = 3.514 cp

TABLE C-40.

LIQUID VISCOSITY

Sampling Point B
Cum. N_2 Inj. = .34 p.v.
Pressure at sampling point = 3800 psi

Comp.	x_i	M_i	$M_i^{1/2}$	u_i^* cp	$x_i M_i^{1/2}$	$x_i u_i^* M_i^{1/2}$	Critical volume v_{c_i} gm/cm^3	$x_i v_{c_i}$	$x_i M_i$	T_{c_m} °K	P_c, atm	$x_i T_{c_i}$	$x_i P_{c_i}$
N_2	.099	28.016	5.29	.0176	.524	.0092	3.215+	.3183	2.774	126.2	33.5	12.5	3.3
C_1	.206	16.068	4.01	.0108	.8257	.0089	6.173	1.2716	3.31	191.1	45.8	39.4	9.4
C_2	.056	30.068	5.48	.0102	.2851	.0029	4.926	.2562	1.5635	305.5	48.2	15.9	2.5
C_3	.071	44.094	6.64	.0082	.4715	.0039	4.545	.3227	3.1307	370	42.	26.3	3.0
C_4	.023	58.12	7.62	.0073	.1753	.0013	4.386	.1009	1.3368	425.2	37.5	9.8	.86
C_5	.071	72.124	8.49	.0065	.603	.0038	4.31	.306	5.121	469.8	33.3	33.4	2.4
C_{6+}	.478	214.5	14.65	3.0	7.0007	21.0021	3.551	1.6974	102.531	705.4	17.347	337.2	8.3
+From N.G.P.A.[59]					9.8853	21.0321		4.2731	119.767			474.5	29.76

u = 3.41 cp

TABLE C-41

LIQUID VISCOSITY

Sampling Point B
Cum. N_2 Inj. = .5 p.v.
Pressure at sampling point = 3800 psi

Comp.	x_i	M_i	$M_i^{1/2}$	u_i^* cp	$x_i M_i^{1/2}$	$x_i u_i^* M_i^{1/2}$	Critical volume v_{ci} gm/cm^3	$x_i v_{c_i}$	$x_i M_i$	T_c m °K	P_c, atm	$x_i T_{c_i}$	$x_i P_{c_i}$
N_2	.112	28.016	5.29	.0176	.5928	.0104	3.215+	.3601	3.138	126.2	33.5	14.1	3.8
C_1	.141	16.068	4.01	.0108	.5652	.0061	6.173	.8704	2.2656	191.1	45.8	26.9	6.5
C_2	.04	30.068	5.48	.0102	.2193	.0022	4.926	.197	1.2027	305.5	48.2	12.2	1.9
C_3	.047	44.094	6.64	.0082	.3121	.0026	4.545	.2136	2.0724	370	42.	17.4	2.0
C_4	.009	58.12	7.62	.0073	.0686	.0005	4.386	.0395	.52308	425.2	37.5	3.80	.34
C_5	.026	72.124	8.49	.0065	.2208	.0014	4.31	.1121	1.8752	469.8	33.3	12.2	.87
C_{6+}	.625	214.5	14.65	3.0	9.1536	27.461	3.551	2.2194	134.063	705.4	17.347	440.9	10.8
+From N.G.P.A.[59]					11.1324	27.4842		4.0121	145.139			527.5	26.21

u = 3.46 cp

TABLE C-42

LIQUID VISCOSITY

Sampling Point B
Cum. N_2 Inj. = .58 p.v.
Pressure at sampling point = 3800 psi

Comp.	x_i	M_i	$M_i^{\frac{1}{2}}$	u_i^* cp	$x_i M_i^{\frac{1}{2}}$	$x_i u_i^* M_i^{\frac{1}{2}}$	Critical volume V_{c_i} gm/cm^3	$x_i V_{c_i}$	$x_i M_i$	T_cm °K	P_c, atm	$x_i T_{c_i}$	$x_i P_{c_i}$
N_2	.132	28.016	5.29	.0176	.6987	.0003	3.215+	.4244	3.698	126.2	33.5	16.7	4.4
C_1	.087	16.060	4.01	.0108	.3487	.0038	6.173	.5371	1.3979	191.1	45.8	16.6	4.0
C_2	.03	30.068	5.48	.0102	.1645	.0017	4.926	.1478	.90204	305.5	48.2	9.2	1.4
C_3	.037	44.094	6.64	.0082	.2457	.002	4.545	.1682	1.6315	370	42.	13.7	1.6
C_4	0	58.12	7.62	.0073	0	0	4.386	0	0	425.2	37.5	0	0
C_5	0	72.124	8.49	.0065	0	0	4.31	0	0	469.8	33.3	0	0
C_{6+}	.714	214.5	14.65	3.0	10.4571	31.3713	3.551	2.5354	153.153	705.4	17.347	503.7	12.4
+From N.G.P.A.[59]					11.9147	31.3791		3.8129	160.7824			529.9	23.8

u = 3.64 cp

TABLE C-43

LIQUID VISCOSITY

Sampling Point C
Cum. N_2 Inj. = .51 p.v.
Pressure at sampling point = 3200 psi

Comp.	x_i	M_i	$M_i^{1/2}$	u_i^* cp	$x_i M_i^{1/2}$	$x_i u_i^* M_i^{1/2}$	Critical volume V_{c_i} gm/cm^3	$x_i V_{c_i}$	$x_i M_i$	T_{c_m} °K	P_c, atm	$x_i T_{c_i}$	$x_i P_{c_i}$
N_2	.116	28.016	5.29	.0176	.614	.0108	3.2154	.3729	3.25	126.2	33.5	14.6	3.9
C_1	.229	16.068	4.01	.0108	.9179	.0094	6.173	1.4136	3.6796	191.1	45.8	43.8	10.5
C_2	.078	30.068	5.48	.0102	.4277	.0044	4.926	.3842	2.3453	305.5	48.2	23.8	3.8
C_3	.104	44.094	6.64	.0082	.6906	.0057	4.545	.4727	4.5858	370	42.	38.5	4.4
C_4	.055	58.12	7.62	.0073	.4193	.0031	4.386	.2412	3.1966	425.2	37.5	23.4	2.1
C_5	.116	72.124	8.49	.0065	.9851	.0062	4.31	.5	8.3664	469.8	33.3	54.5	3.9
C_{6+}	.302	214.5	14.65	3.0	4.423	13.2691	3.551	1.0724	64.779	705.4	17.347	213.0	5.2
+From N.G.P.A.[59]					8.4776	13.3087	4.457	90.2027				411.6	33.8

$u = 2.568$ cp

TABLE C-44

LIQUID VISCOSITY

Sampling Point C
Cum. N_2 Inj. = .64 p.v.
Pressure at sampling point = 3200 psi

Comp.	x_i	M_i	$M_i^{1/2}$	u_i^* cp	$x_i M_i^{1/2}$	$x_i u_i^* M_i^{1/2}$	Critical volume v_{c_i} gm/cm^3	$x_i v_{c_i}$	$x_i M_i$	T_{cm} °K	P_c, atm	$x_i T_{c_i}$	$x_i P_{c_i}$
N_2	.125	28.016	5.29	.0176	.6616	.0116	3.215+	.4019	3.502	126.2	33.5	15.8	4.2
C_1	.121	16.068	4.01	.0108	.485	.0052	6.173	.7469	1.9442	191.1	45.8	23.1	7.1
C_2	.05	30.068	5.48	.0102	.2742	.0028	4.926	.2463	1.5034	305.5	48.2	15.3	2.4
C_3	.062	44.094	6.64	.0082	.4117	.0034	4.545	.2818	2.7338	370	42.	22.9	2.6
C_4	.023	58.12	7.62	.0073	.1753	.0013	4.386	.1009	1.3368	425.2	37.5	9.8	.86
C_5	.059	72.124	8.49	.0065	.5011	.0032	4.31	.2543	4.255	469.8	33.3	27.7	2.0
C_{6+}	.56	214.5	14.65	3.0	8.2017	24.605	3.551	1.9886	120.12	705.4	17.347	395	9.7
+From N.G.P.A.[59]					10.7106	24.6325		4.0207	135.3952			509.6	28.86

u = 3.22 cp

TABLE C-45

LIQUID VISCOSITY

Sampling Point C
Cum. N_2 Inj. = .68 p.v.
Pressure at sampling point = 3200 psi

Comp.	x_i	M_i	$M_i^{1/2}$	u_i^* cp	$x_i M_i^{1/2}$	$x_i u_i^* M_i^{1/2}$	Critical volume v_{c_i} gm/cm^3	$x_i v_{c_i}$	$x_i M_i$	T_cm °K	P_c, atm	$x_i T_{c_i}$	$x_i P_{c_i}$
N_2	.125	28.016	5.29	.0176	.6616	.0116	3.215+	.4019	3.502	126.2	33.5	15.8	4.2
C_1	.087	16.068	4.01	.0108	.3487	.0038	6.173	.5371	1.39792	191.1	45.8	16.6	4.0
C_2	.041	30.068	5.48	.0102	.2248	.0023	4.926	.2020	1.2328	305.5	48.2	12.5	2.0
C_3	.051	44.094	6.64	.0082	.3387	.0028	4.545	.2318	2.2488	370	42.	18.9	2.1
C_4	.007	58.12	7.62	.0073	.0534	.0004	4.386	.0307	.40684	425.2	37.5	3	.26
C_5	.044	72.124	8.49	.0065	.3737	.0024	4.31	.1896	3.1735	469.8	33.3	20.7	1.5
C_{6+}	.645	214.5	14.65	3.0	9.4466	28.3397	3.551	2.2904	138.353	705.4	17.347	455	11.9
+From N.G.P.A.[59]					11.4475	28.363		3.8835	150.3144			542.5	25.96

u = 3.23 cp

TABLE C-46

LIQUID VISCOSITY

Sampling Point D
Cum. N_2 Inj. = .68 p.v.
Pressure at sampling point = 2600 psi

Comp.	x_i	M_i	$M_i^{1/2}$	u_i^* cp	$x_i M_i^{1/2}$	$x_i u_i^* M_i^{1/2}$	Critical volume v_{c_i} gm/cm^3	$x_i v_{c_i}$	$x_i M_i$	T_{cm} °K	P_c, atm	$x_i T_{c_i}$	$x_i P_{c_i}$
N_2	.101	28.016	5.29	.0176	.5346	.0094	3.215+	.3247	2.83	126.2	33.5	12.7	3.4
C_1	.233	16.068	4.01	.0108	.934	.0101	6.173	1.4383	3.7438	191.1	45.8	44.5	10.7
C_2	.104	30.068	5.48	.0102	.5703	.0058	4.926	.5123	3.1271	305.5	48.2	31.8	5.0
C_3	.137	44.094	6.64	.0082	.9097	.0075	4.545	.6227	6.0409	370	42.	50.7	9.9
C_4	.059	58.12	7.62	.0073	.4498	.0033	4.386	.2588	3.836	425.2	37.5	25.1	2.2
C_5	.15	72.124	8.49	.0065	1.2739	.008	4.31	.6465	10.8186	469.8	33.3	70.5	5.0
C_{6+}	.216	214.5	14.65	3.0	3.1635	9.4905	3.551	.767	46.332	705.4	17.347	152.4	3.7
+From N.G.P.A.[59]					7.8358	9.6255		4.5703	76.7284			387.7	39.9

$u = 1.97$ cp

TABLE C-47

LIQUID VISCOSITY

Sampling Point D
Cum. N_2 Inj. = .82 p.v.
Pressure at sampling point = 2660 psi

Comp.	x_i	M_i	$M_i^{\frac{1}{2}}$	u_i^* cp	$x_i M_i^{\frac{1}{2}}$	$x_i u_i^* M_i^{\frac{1}{2}}$	Critical volume v_{c_i} gm/cm^3	$x_i v_{c_i}$	$x_i M_i$	T_cm °K	P_c, atm	$x_i T_{c_i}$	$x_i P_{c_i}$
N_2	.125	28.016	5.29	.0176	.6616	.0116	3.215+	.4019	3.502	126.2	33.5	15.8	4.2
C_1	.113	16.068	4.01	.0108	.453	.0049	6.173	.6975	1.8157	191.1	45.8	21.6	5.2
C_2	.068	30.068	5.48	.0102	.3729	.0038	4.926	.335	2.0446	305.5	48.2	20.8	3.3
C_3	.081	44.094	6.64	.0082	.5379	.004	4.545	.3681	3.5716	370	42.	30	3.4
C_4	.033	58.12	7.62	.0073	.2516	.0018	4.386	.1447	1.918	425.2	37.5	14.0	1.2
C_5	.1	72.124	8.49	.0065	.8493	.0054	4.31	.431	7.2124	469.8	33.3	46.98	3.33
C_{6+}	.48	214.5	14.65	3.0	7.03	21.09	3.551	1.7045	102.96	705.4	17.347	338.6	8.3
+From N.G.P.A.[59]					10.1563	21.1219		4.0827	123.022			487.78	28.93

u = 2.909 cp

TABLE C-48

LIQUID VISCOSITY

Sampling Point D
Cum. N_2 Inj. = .88 p.v.
Pressure at sampling point = 2600 psi

Comp.	x_i	M_i	$M_i^{1/2}$	u_i^* cp	$x_i M_i^{1/2}$	$x_i u_i^* M_i^{1/2}$	Critical volume V_{ci} gm/cm^3	$x_i V_{c_i}$	$x_i M_i$	T_{cm} °K	P_c, atm	$x_i T_{c_i}$	$x_i P_{c_i}$
N_2	.139	28.016	5.29	.0176	.7357	.0129	3.215+	.4469	3.894	126.2	33.5	17.5	4.7
C_1	.055	16.068	4.01	.0108	.2205	.0024	6.173	.3395	.88374	191.1	45.8	10.5	2.5
C_2	.035	30.068	5.48	.0102	.1919	.002	4.926	.1724	1.0524	305.5	48.2	10.7	1.7
C_3	.038	44.094	6.64	.0082	.2523	.0021	4.545	.1727	1.67557	370	42.	14.1	1.6
C_4	0	58.12	7.62	.0073	0	0	4.386	0	0	425.2	37.5	0	0
C_5	.024	72.124	8.49	.0065	.2038	.0013	4.31	.1034	1.731	469.8	33.3	11.3	.8
C_{6+}	.709	214.5	14.65	3.0	10.3839	31.1517	3.551	2.5177	152.081	705.4	17.347	500.1	12.3
+From N.G.P.A.[59]					11.9881	31.1724		3.7526	161.317			564.2	23.6

u = 3.18 cp

APPENDIX D

OIL DISPLACEMENT TESTS

DATA AND RESULTS

TABLE D-1

RUN NUMBER 1

Barometric Pressure	29.92" Hg	Oil Saturation	.756
Room Temperature	70°F	Water Saturation	.244
Injection Pressure	4000 psi	Stock Tank Oil-in-Place	698cc
Solution G.O.R.	575 scf/STB	Oil Gravity	43°API
Rate of Advance	.068 cm/sec		

Time Min.	Cumulative Oil Prod. cc	Recovery % I.O.I.P.	Cum. Gas Prod. scf	Back Pressure, psi
15	17	2.4	.06	2000
30	34	4.8	.12	1870
45	40	5.7	.13	2000
60	53	7.6	.14	2100
75	70	10.02	.21	2000
90	75	10.7	.28	2000
105	95	13.6	.34	2000
120	110	15.7	.39	1920
135	123	17.6	.40	1980
150	125	17.9	.48	2000
180	143	20.5	.52	2000
200	170	24.3	.66	2100
220	185	26.5	.67	2000
240	203	29.1	.78	1990
260	222	31.8	.8	2200
280	243	34.8	.87	2100
300	262	37.5	.95	2000
320	283	40.5	1.0	2000
350	310	44.4	1.1	2000
380	340	48.7	1.2	2000
410	368	52.7	1.3	1890
430	381	54.5	1.4	1900
450	403	57.7	1.5	1950
510	458	65.6	1.6	2000
530	478	68.5	1.7	2115
550	496	71.1	1.8	2050
570	510	73.1	1.8	2000
590	532	.762	1.9	2000
611	558	.8	2.0	2000

TABLE D-2

RUN NUMBER 2

Barometric Pressure	29.09" Hg	Oil Saturation	.75
Room Temperature	72°F	Water Saturation	.25
Injection Pressure	5000 psi	Stock Tank Oil-in-Place	595cc
Solution G.O.R.	575 scf/STB	Oil Gravity	43°API
Rate of Advance	.12 cm/sec		

Time Min.	Cumulative Oil Prod. cc	Recovery % I.O.I.P.	Cum. Gas Prod. scf	Back Pressure, psi
10	15	2.2	.05	2000
20	25	3.6	.09	2000
25	30	4.3	.11	1920
30	32	4.6	.12	1900
40	45	6.5	.13	1950
50	55	7.9	.15	2000
70	75	10.8	.28	2000
90	80	11.6	.3	2110
110	112	16.2	.41	2000
125	127	18.3	.43	2000
150	155	22.4	.58	2050
180	189	27.3	.61	2000
195	207	29.9	.69	1955
210	225	32.5	.81	2000
220	230	33.2	.83	2000
235	255	36.8	.92	2000
245	265	38.3	.96	2200
255	280	40.5	1.00	2000
310	350	50.6	1.10	2000
330	370	53.5	1.40	2060
345	390	56.3	1.50	1950
400	450	65.0	1.60	2000
420	475	68.6	1.70	2000
430	485	70.0	1.90	2000
445	500	72.3	1.90	2000
500	570	82.6	2.10	2000
529	595	86.0	2.20	2000

TABLE D-3

RUN NUMBER 3

Barometric Pressure	28.89" Hg	Oil Saturation	.732
Room Temperature	70°F	Water Saturation	.268
Injection Pressure	3000 psi	Stock Tank Oil-in-Place	676cc
Solution G.O.R.	575 scf/STB	Oil Gravity	43°API
Rate of Advance	.068 cm/sec		

Time Min.	Cumulative Oil Prod. cc	Recovery % I.O.I.P.	Cum. Gas Prod. scf	Back Pressure, psi
30	8	1.2	.03	2000
60	25	3.7	.11	2000
80	32	4.7	.13	2050
90	38	5.6	.17	2050
120	45	6.6	.17	1950
140	53	7.8	.21	1940
180	65	9.6	.22	1870
200	75	11.1	.25	2000
225	83	12.3	.30	2000
250	92	13.6	.40	2000
270	103	15.2	.40	2000
300	115	17.0	.45	2010
330	124	18.3	.50	2000
350	130	19.2	.50	2000
360	140	20.7	.60	2050
390	150	22.2	.60	2000
430	164	24.3	.65	2000
470	181	26.8	.71	2010
500	192	28.4	.80	1990
540	210	31.1	.83	1980
590	230	34.0	.90	1990
650	254	37.6	1.00	2000
730	283	41.9	1.10	2000
750	290	42.9	1.10	2000
810	312	46.2	1.20	2000
840	323	47.8	1.30	2010
900	350	51.8	1.40	2000
915	355	52.5	1.40	2000
934	365	54.0	1.40	2100

TABLE D-4

RUN NUMBER 4

Barometric Pressure	28.95" Hg	Oil Saturation	.743
Room Temperature	71°F	Water Saturation	.257
Injection Pressure	3700 psi	Stock Tank Oil-in-Place	686cc
Solution G.O.R.	575 scf/STB	Oil Gravity	43°API
Rate of Advance	.097 cm/sec		

Time Min.	Cumulative Oil Prod. cc	Recovery % I.O.I.P.	Cum. Gas Prod. scf	Back Pressure, psi
20	13	1.9	.05	2000
40	27	3.9	.06	2000
60	38	5.5	.14	1990
100	65	9.5	.23	1980
130	86	12.5	.30	1990
155	105	15.3	.30	2000
190	130	18.9	.40	2000
230	160	23.3	.49	2010
250	175	25.5	.63	2030
320	238	34.7	.86	2000
350	250	36.4	.90	2000
370	270	39.4	.97	1870
395	290	42.3	1.00	1870
420	307	44.7	1.00	1990
445	325	47.4	1.20	2000
470	345	50.3	1.20	2000
500	378	55.1	1.30	2000
515	380	55.4	1.40	2000
530	395	57.6	1.40	2110
545	407	59.3	1.50	2110
570	425	61.9	1.50	2050
590	440	64.1	1.60	2000
610	450	65.6	1.60	2000
630	470	68.5	1.70	2010
658	494	72.0	1.80	2000

TABLE D-5

RUN NUMBER 7

Barometric Pressure	28.9" Hg	Oil Saturation	.75
Room Temperature	70°F	Water Saturation	.25
Injection Pressure	5000 psi	Stock Tank Oil-in-Place	900cc
Solution G.O.R.	0 scf/STB	Oil Gravity	43°API

Rate of Advance .11 cm/sec

Time Min.	Cumulative Oil Prod. cc	Recovery % I.O.I.P.	Back Pressure psi
15	16	1.8	2000
30	26	2.9	2000
45	40	4.4	2000
60	54	6.0	2010
80	70	7.7	2000
100	90	7.7	2000
130	115	10.0	2000
160	145	16.1	1990
180	165	18.3	2000
200	185	20.5	1990
225	207	23.0	2000
240	221	24.6	2000
260	244	27.1	2000
280	260	28.9	2000
300	280	31.1	2015
320	319	35.4	2015
350	320	35.6	2000
380	350	38.9	1980
400	355	39.4	2000
415	380	42.2	2000
430	392	43.5	1990
460	423	47.0	1980
490	449	49.9	1990
510	466	51.8	2000
525	480	53.3	2000
540	495	55.0	1985
577	531	59.0	2000